Endoplasmic Reticulum H_2O_2: Ero1-driven Generation and GPx-mediated Detoxification

Inauguraldissertation

zur

Erlangung der Würde eines Doktors der Philosophie

vorgelegt der

Philosophisch-Naturwissenschaftlichen Fakultät

der Universität Basel

von

Thomas Ramming,

aus Schweinfurt, Deutschland

Basel, 2014

Genehmigt von der Philosophisch-Naturwissenschaftlichen Fakultät

auf Antrag von:

Prof. Dr. Alex Odermatt

(Fakultätsverantwortlicher)

_____

Prof. Dr. Alex Odermatt

Dr. Christian Appenzeller-Herzog

(Dissertationsleiter/Referent)

_____

Dr. Christian Appenzeller-Herzog

Prof. Dr. Fabio Martinon

(Co-Referent)

_____

Prof. Dr. Fabio Martinon

Basel, den 24. Juni 2014

_____

Dekan

Prof. Dr. Jörg Schibler

Acknowledgements

First and foremost, I would like to express my deep gratitude to my supervisor Dr. Christian Appenzeller-Herzog and his initial funding efforts, which made this thesis possible in the first place. His contagious enthusiasm and dedication for science together with his excellence guidance formed the cornerstones of this work. I will always be thankful for the lively discussions, his remarkable patience and the technical and theoretical knowledge he has passed on to me.

My sincere thanks also go to Prof. Dr. Alex Odermatt, who has been a generous host and provided an excellent scientific environment for this thesis. Smooth integration to his research group allowed access to established structures and enabled me to profit from a harmonious atmosphere, which went way beyond the daily lab routine.

I would also like to thank Prof. Dr. Fabio Martinon for investing his time to complement my thesis committee by acting as co-referee.

I am thankful for the generous financial support of Böhringer Ingelheim Fonds and Freiwillige Akademische Gesellschaft, who made this work possible.

Additionally, I would like to acknowledge the help of Dr. Julia Birk, who always had an open ear and taught me a great deal while being exceptionally patient. She facilitated my first steps here in the lab and without her this thesis would not appear in its present form.

Special thanks also to all members, present and alumni, of the MolSysTox group, who provided a cheerful and stimulating environment and helped me to get back on my feet when things were not going as planned.

Furthermore, I would like to highlight Katharina Wagner, whose continues support and patience were of invaluable significance and cannot be rated high enough. Throughout the last years, she has covered my back in countless situations and thereby made a major contribution to this thesis. I don’t know how I would have managed without you and I am looking forward to our exciting summer!

Last but not least, I would like to express my sincere gratitude to my parents, Eva and Gerhard Ramming, for years and years of infinite support and for one or two shoves in the right moments.

Table of Contents

I. Abbreviations:

ΔG	difference in Gibbs free energy
3D	three dimensional
ALS	amyotrophic lateral sclerosis
ARE	antioxidant responsive element
ATF6	activating transcription factor 6
BAK	Bcl-2 homologous antagonist killer
BAX	Bcl-2-associated X protein
Bcl-2	B-cell lymphoma 2
BCNU	glutathione reductase inhibitor carmustine
BH3	Bcl-2 homology 3
BID	BH3-interacting domain death agonist
BiFC	bi-molecular fluorescence complementation
BiP	immunoglobulin binding protein
BPTI	bovine pancreatic trypsin inhibitor
BSO	buthionine-sulfoximine
CHOP	C/EBP-homologous protein
CHX	cycloheximide
CICR	calcium-induced calcium release
CJD	Creutzfeld-Jakob disease
CNX	calnexin
COP1	coat protein 1
C_P	peroxidatic cysteine
C_R	resolving cysteine
CRT	calreticulin
Cys	cysteine
Dia	Diamide
Dox	doxycycline
DRMs	detergent-resistant membranes
DTT	dithiothreitol
EDEM1	ER degradation-enhancing α-mannosidase- like protein 1
EGFR	epidermal growth factor receptor
E_{GSH}	half cell reduction potential of GSH
eIF2α	eukaryotic translation initiation factor 2α
ER	endoplasmic reticulum
ERAD	ER associated degradation
ERGIC	ER-golgi intermediate compartment
Ero1	ER oxidoreductin-1
ERp	endoplasmic reticulum resident protein
ERQC	ER quality control
ESP	early secretory pathway
FAD	flavin adenine dinucleotide
FCS	fetal calf serum
GADD34	growth arrest and DNA damage-inducible 34
GlcNAc	N-acetylgucosamine
GPx	glutathione peroxidase
Grp75	glucose-regulated protein 75
Grxs	glutaredoxins
GSH	reduced glutathione
GSSG	oxidized glutathione
GST	π glutathione S-transferase
H_2O_2	hydrogen peroxide
Hb	hemoglobin
Hsp	heat shock protein
IAM	iodoacetamide
IgM	immunoglobulin M
IP_3R	inositol 1,4,5-trisphosphate receptor

IRE1	inositol-requiring protein 1
Keap1	Kelch-like ECH-associated protein 1
LPS	lipopolysaccharide
MAC	mitochondrial apoptosis-induced channel
Maf	musculoaponeurotic fibrosarcoma
MAM	mitochondria-associated membrane
MAP	mitogen-activated protein
MEM	minimum essential medium eagle
MHC	major histocompatibility complex
MOMP	mitochondrial outermembrane Permeabilization
MPTP	mitochondrial permeability transition pore
NEM	N-ethylmaleimide
NOX	nicotinamide adenine dinucleotide oxidase
Nrf2	nuclear factor erythroid 2-related factor 2
O_2	molecular oxygen
OAC	oesophageal adenocarcinoma
OST	oligosaccharyltransferase
PDI	protein disulfide isomerase
PERK	protein kinase PKR-like ER kinase
PLC	peptide loading complex
PMSF	phenylmethylsulphonylfluoride
PP1	protein phosphatase 1
PPARγ	peroxisome proliferator-activated receptor gamma
Prxs	peroxiredoxin
PTPC	permeability transition pore complex
PTPs	protein tyrosine phosphatases
QSOX	quiescin sulphydryl oxidase
Redox	reduction-oxidation
RIDD	regulated IRE1-dependent decay
roGFP	redox-sensitive GFP
ROS	reactive oxygen species
RTK	receptor tyrosine kinase
RyR	ryanodine receptor
S2P	site-2 protease
Sec	selenocysteine
SERCA	sarcoplasmic/endoplasmic reticulum Ca^{2+}-ATPase
SOD	superoxide dismutase
SRP	signal recognition particle
SUMF1	sulfatase modifying factor 1
T1/2DM	type 1 and type 2 diabetes mellitus
T4	thyroxine
T3	triiodothyronine
Tapasin	TAP-associated glycoprotein
TAP	transporter associated with antigen processing
TCA	trichloroacetic acid
TFA	trifluoro acetic acid
TG	thapsigargin
TM	tunicamycin
Trx	thioredoxin
UGGT	UDP-glucose:glycoprotein glucosyltransferase
UPR	unfolded protein response
UPS	ubiquitin-proteasome system
VDAC1	voltage-dependent anion channel 1
VEGF	vascular endothelial growth factor
VKOR	vitamin K epoxide reductase
XBP1s	spliced isoform of X-box binding protein 1

II. Summary

Endoplasmic reticulum (ER) oxidoreductin 1α (Ero1α) is an ER-resident oxidase, which utilizes molecular oxygen (O_2) as terminal electron acceptor to produce disulfide bonds and hydrogen peroxide (H_2O_2). The major target for Ero1α-derived disulfides is protein disulfide isomerase (PDI), which transfers them onto substrate proteins and plays an additional role as homeostatic regulator of Ero1α.

In this thesis, I demonstrated that PDI-mediated activation of Ero1α extends beyond the reduction of the known inhibitory disulfides Cys^{94}-Cys^{131} and Cys^{99}-Cys^{104} and involves an additional disulfide, Cys^{208}-Cys^{241}. Opening of this disulfide by PDI apparently enables diffusion of O_2 towards and of H_2O_2 away from the catalytic flavin cofactor in Ero1α. Expression of a constitutively active Ero1α mutant, which is devoid of all three regulatory disulfides, compromises cell viability. Hence, redox regulation of the O_2/H_2O_2 diffusion pathway in Ero1α emerges as critical determinant of ER homeostasis, in which PDI takes center stage by directly regulating O_2 consumption.

I also elucidated the molecular basis for the specificity of glutathione peroxidase 8 (GPx8) to detoxify Ero1α-derived H_2O_2, as this enzyme binds to the site of H_2O_2 release in Ero1α. Only depletion of GPx8 but not of the abundant ER peroxidase peroxiredoxin IV (PrxIV) exhibited an additive effect with deregulated Ero1α on ER hyperoxidation and induction of unfolded protein response and antioxidant response target genes. Furthermore, only upon GPx8 knockdown I was able to detect leakage of Ero1α-derived H_2O_2 from ER to cytosol. Therefore, GPx8 acts as a specific molecular gatekeeper to protect the cytosol from Ero1α-derived H_2O_2. The exclusion of PrxIV from this process revealed a previously unappreciated compartmentalization of electron transport pathways in the ER.

Moreover, I successfully isolated mixed-disulfide interaction partners of the ER-resident peroxidase GPx7 and of PDI. The interactome of the latter was analyzed and found to be mainly comprised of other members of the PDI family, which, in conjunction with its function as Ero1α activator, places PDI as central regulator of ER disulfide homeostasis. With regard to GPx7 interaction partners I am confident that their identification will serve as basis for future elucidation of novel cellular functions of this peroxidase.

1. General Introduction

1.1. Protein folding

Proteins within and outside of cells fulfill a plethora of different tasks, which in their entirety are essential for life. They catalyze chemical reactions by operating as enzymes; they provide structural support by serving as building units in the cytoskeleton of single cells or by crosslinking numerous cells to develop specialized tissues; in the form of hormones they transmit signals between cells; and, when acting as pathogen-scavenging antibodies, proteins are also able to protect from diseases. The underlying principle, which enables proteins to cope with this functional diversity and ensures specificity of action, is the multitude of different three dimensional (3D) structures proteins can form.

Proteins are assembled at the ribosome as polypeptide chains from amino acids, the basic building blocks of protein synthesis. Thus, by linking together amino acids in different combinations, proteins with diverse biochemical properties and functions are generated. The primary structure of a protein is defined by the linear amino acid sequence and does formally not include information on spatial orientation. However, the polypeptide backbone is rich in C=O and N-H groups, which favor the formation of hydrogen bonds. Within this first level of higher order structure, neighboring amino acids interact via hydrogen bonds to produce 3D patterns. These secondary protein structures include curled α-helices and extended β-strands, which can combine to form planar β-sheets. Subsequently, secondary structures can interact with each other to produce a complex tertiary protein structure [1]. This process of rearranging the relative orientation of residues from the protein´s primary structure into a stable tertiary structure is called protein folding and is associated with a gradual decrease in the global free energy of the macromolecule. In addition to backbone-driven interactions, the chemical properties of amino acid side chains impinge on protein folding, too. For instance, hydrophobic residues tend to concentrate within the solvent-free core of globular proteins, thereby stabilizing the native 3D structures whilst granting hydrophilic residues access to the water-based environment on the protein surface. Taken together, the 3D structure of a protein is entirely encoded in the genetic information of its primary amino acid sequence [1].

In vivo, the folding process of nascent polypeptide chains is assisted by molecular chaperones, which themselves are proteins that bind to initially exposed hydrophobic patches in order to prevent undesired aggregation [2]. When the protein reaches its native conformation, chaperone binding is dismissed.

Proteins fold along the gradient of free energy in order to gradually optimizing the environment of their functional groups until they reach the energetically favored native state [1]. The stability of a protein structure is then proportional to the difference in free energy (ΔG) between the unfolded and fully folded state and correlates with the capability to sustain physico-chemical stress. Due to their trafficking to the extracellular space, secreted and transmembrane proteins have to maintain conformational integrity throughout various conditions, like changes in pH, temperature or the surrounding ionic strength, and therefore often rely on additional stabilizing factors like disulfide bonds [3]. These covalent linkages between two sulphydryl groups can either link two cysteines residues within one protein (intramolecular disulfide) or contribute to the stability of protein complexes by connecting separate polypeptide chains (intermolecular disulfide) [4]. In the case of the former, two initially distant parts of an emerging polypeptide can be brought into proximity, thereby affecting the overall fold of the protein. In contrast to hydrogen bonds or hydrophobic interactions, disulfide bonds are covalent, which considerably increases their bond-dissociation energy and results in enhanced stability of the protein structure. In this sense, disulfide bonds actively contribute to the folding process of nascent peptides and in addition stabilize the native 3D shapes of mature proteins [3]. Indicative of their importance for protein function, missing or incorrect disulfide linkages often render the affected protein inoperative. Furthermore, this can cause protein misfolding and/or accumulation of unfolded proteins, which triggers a cellular stress cascade called unfolded protein response (UPR; see section 1.6).Therefore, elaborate enzymatic machinery has evolved to catalyze the specific introduction of disulfide bonds into newly synthesized polypeptides - a process called oxidative protein folding [3].

The significance of proper protein folding for cellular homeostasis and the deleterious effect of aggregate formation by mis- or unfolded proteins is exemplified in various medical conditions. Prominent examples are the neurodegenerative proteinopathies Alzheimer’s, Huntington’s, Parkinson’s and the Creutzfeld-Jakob disease (CJD) [5].

1.2. The endoplasmic reticulum

Newly synthesized soluble proteins, which are destined to the secretory pathway in order to function as either resident or secreted proteins, possess a cleavable N-terminal signal peptide. Upon translation at cytosolic ribosomes this signal peptide emerges from the translation complex and induces binding of the signal recognition particle (SRP) [6]. Association of signal peptide and SRP result in stalling of the translation process and recruitment of the ribosome-peptide complex to the cytosolic leaflet of the endoplasmic reticulum (ER) membrane, where SRP is bound by its cognate receptor [7,8]. Subsequently, the physical association of the translation complex with the pore-forming Sec61αβγ complex leads to the insertion of the signal peptide into the pore. After ribosomal translation is resumed, elongation of the nascent polypeptide chain then results in co-translational translocation of the protein into the lumen of the ER [9]. This highly specialized sub compartment is the starting point of the cellular secretory pathway. Furthermore, it harbors the previously mentioned enzymatic machinery for oxidative folding and a wide variety of different chaperones (see below), both of which assure proper protein folding before further passage along the secretory pathway is granted [2].

1.2.1. Glutathione and its role in oxidative protein folding

A prerequisite for oxidative folding is the establishment of a suitable reduction-oxidation (redox) environment, since disulfide bonds can only form in oxidative conditions and the stability of the bond is redox-dependent. In eukaryotic cells the ER provides this platform for oxidative protein folding, mimicking the oxidizing redox conditions prevailing in the extracellular space [10] and priming newly formed secretory and membrane-anchored proteins for their future destination. In this context, the ER stands in sharp contrast to the cytosol, where the cell invests a substantial amount of energy to maintain a reducing environment and to counteract oxidative stress (see section 1.7). These sub cellular differences in the redox conditions are mainly due to the action of the tripeptide-like compound glutathione [11], which reaches intracellular concentrations within the millimolar range [12,13] and acts as a potent redox buffer. Glutathione is synthesized in the cytosol from the amino acids glutamate, cysteine and glycine, and distributed throughout the different subcellular compartments. Since the amide bond between glutamate and cysteine

involves the γ– instead of the α–carboxyl-group of glutamate, this form of linkage differs from the classical peptide bond and is thought to correlate with an increased resistance towards proteolytic degradation [14]. Glutathione can exist in two different redox states, either in the reduced monomeric form (GSH) or in the oxidized dimeric form as glutathione disulfide (GSSG). In the cytosol, GSSG produced by the action of glutathione peroxidases or glutaredoxin (see section 1.7) will be enzymatically regenerated to GSH with the help of glutathione reductase [15]. In this reaction, NADPH acts as electron donor to reduce GSSG to two molecules of GSH. This, however, only applies to GSSG in the cytosol, since an ER-resident protein with a comparable function to glutathione reductase has not been identified [16].

The driving force for every redox reaction is the difference in the reduction potential of the two involved redox couples, for instance GSH/GSSG and $NADPH+H^+/NADP^+$. The reduction potential describes the affinity of a given redox couple to accept electrons. The more positive the potential is, the higher the species' affinity for electrons and the probability of being reduced. The reduction potential of glutathione depends on the term $[GSH]^2$ / [GSSG] and, therefore, on both the molar ratio between GSH and GSSG and on the absolute glutathione concentration ([GSH]+2[GSSG]) [17]. Since glutathione reductase constantly reduces GSSG in the cytosol, $[GSH]^2$ / [GSSG] is kept high in this compartment. This results in a cytosolic chemical half cell reduction potential of GSH (E_{GSH}(cytosol)) which ranges between -280 and -320 mV in mammalian cells [18] and resembles the findings in yeast [19]. This low E_{GSH}(cytosol) reflects the reductive environment within this compartment, which prevents the formation of disulfide bonds and keeps cysteines in a reduced state. In contrast to this, the ER reduction potential of GSH (E_{GSH}(ER)) was recently determined using a glutathione-specific redox sensor to be -208±4 mV in HeLa cells [20]. The notion that the ER constitutes a more oxidizing environment relative to the cytosol has been established earlier, when the GSH:GSSG ratio within the compartments of the secretory pathway was determined to be substantially lower compared to other compartments in the cell [12]. Initially, these findings led to the proposal of a role for GSSG in the supply of oxidative equivalents, which are needed for disulfide bond formation, and of an ER-specific import of GSSG [12]. Later, this hypothesis had to be abandoned when Banhegyi and colleagues conclusively demonstrated that only GSH can diffuse through the membranes of rat liver microsomes in an energy independent fashion, whereas GSSG diffusion was virtually absent [21]. Since the ER membrane, probably due to its high protein content and different lipid

composition compared to other endomembranes [22], shows an elevated permeability for small molecules, facilitated diffusion rather than active transport of GSH is likely to be the underlying mechanism [17]. In addition, several subsequent reports argued against a role of GSSG as source of oxidizing equivalents, most prominently the discovery of the ER oxidases ER oxidoreductin-1 (Ero1) [23,24,25] and the fact that GSH competes with other protein thiols for Ero1-driven oxidation [26]. This prompted a reevaluation of the contribution of glutathione to ER redox homeostasis and led to the idea that, like in the cytosol, glutathione rather mediates reductive processes by providing a continuously imported source of electrons [27]. Along this line, GSH-depleted cells were found to exhibit increased native and non-native disulfide bond formation [28,29]. Furthermore, direct reduction of the ER-resident ERp57 protein by GSH [30] and the previously mentioned ER half cell reduction potential of GSH, which was found to rather promote reduction of the active site cysteines within the protein disulfide isomerase (PDI) family [20], argued for opposing functions of glutathione and Ero1 activity in regulating ER redox homeostasis.

Members of the PDI family (see section 1.3) are central components of the enzymatic machinery for oxidative folding and exert their function via conserved active site CxxC-motives (where C stands for cysteine and x depicts any other amino acid). When present in an oxidized state, these motives can mediate the transfer of their disulfide bond via thiol-disulfide-exchange reaction, which results in the oxidation of two cysteine residues in the folding client and concomitant reduction of the PDI family member [31]. In order to regenerate their function and to assist subsequently imported proteins, the active site CxxC-motives of PDIs are reoxidized by donating their electrons predominantly to the oxidase Ero1 [31,32]. However, since it has been demonstrated that the formation of non-native disulfide bonds naturally occurs under physiological conditions [33], PDIs serve additional important functions besides disulfide-bond introduction. Thus, erroneously introduced disulfide linkages in folding clients can be detected and either reduced or isomerized by PDIs [20,30]. A prerequisite for this is a reduced CxxC-motif in PDIs, which, as mentioned previously, is likely mediated by a GSH to GSSG-converting reaction [20,30]. Therefore, a tightly checked redox balance between the supply of oxidative equivalents (by Ero1 and others; see section 1.4) and the delivery of electrons by the glutathione buffer has to be maintained in the ER. This redox homeostasis, if not perturbed (see section 1.6

and 1.7), allows the dual function of PDIs as oxidant and reductant, which assists the generation of a high yield of properly folded proteins [27].

The fate of GSSG produced in the ER is currently not clear. In contrast to GSH, it cannot freely equilibrate over the ER membrane [21] and is trapped in the ER as a result of Ero1 activity [13]. Even though this explains the increased concentration of total glutathione in the ER compared to the cytosol [13], it would, if not counteracted, ultimately lead to an increasing accumulation of GSSG and twist the redox balance to more oxidative conditions. Clearance from the lumen of the ER might be achieved either by the action of a so far unidentified ER to cytosol transporter, which would feed into the NADPH-driven glutathione reductase pathway, or by secretion from the cell via anterograde trafficking in secretory vesicles from the ER to the plasma membrane. Besides these possibilities, GSSG levels within the ER might also be directly buffered by the sustained import of reduced substrates for oxidative folding in the form of nascent polypeptides or by the activity of a so far unidentified ER glutathione reductase.

1.2.2. ER retrieval of resident and misfolded proteins

As stated previously, the ER marks the beginning of the cellular secretory pathway. In this sense, soluble proteins destined for the extracellular space or membrane proteins to be anchored in the plasma membrane follow this secretion route from the ER via the ER-Golgi intermediate compartment (ERGIC) to the Golgi apparatus and further on to the plasma membrane. Even though this anterograde trafficking is essential for secretory cargo to reach its final destination, ER-resident enzymatic machinery of folding factors, chaperones and oxidoreductases must be kept in place in order to assure proper function [2]. An elegant retrieval mechanism has been identified, which works at the interface between ER and Golgi apparatus and prevents undesired secretion of ER-resident proteins. These proteins are often equipped with a KDEL or KDEL-like motif within their C-terminal sequence [34,35]. The name of this motif is derived from the most common amino acid composition: lysine (K), aspartic acid (D), glutamic acid (E) and leucine (L). Due to its charged nature, these motives are sensitive to pH changes, which form the underlying mechanism for its function in ER retrieval. Three mammalian KDEL-receptors were identified to date which bind to a defined subset of the KDEL-like motives of ER-resident proteins within the ERGIC and the Golgi [35] in a pH dependent manner [36]. The pH changes throughout the route

of the secretory pathway from almost neutral conditions within the ER [37] to a more acidic environment in the Golgi apparatus [38]. Consistent with this, binding of the KDEL-receptor to KDEL motives is favored at low pH [39]. After binding in ERGIC/Golgi, the receptor-protein complex induces the formation of retrograde transport vesicles in a coat protein I (COPI) - dependent manner [40,41], which retrieves the receptor and its bound substrate back to the ER [42]. There, due to the neutral pH of the ER, dissociation of the receptor and the ER-resident protein occurs and the unbound receptor can take part in an additional round of ER retrieval by following the anterograde export route back to the ERGIC/Golgi.

Additional motives for COPI-mediated retrograde transport for ER retrieval are found in type I and type II ER-resident transmembrane proteins. Di-lysine [43] and di-arginine [44] motives within the respective cytosolic domains of these membrane spanning proteins mediate their proper localization. A prominent example of this retrieval mechanism is the ER-chaperone Calnexin (CNX), a type I transmembrane protein equipped with a C-terminal di-arginine motif [45].

It is important to note that ER-retrieval of components involved in the folding machinery of the ER fulfill two major tasks. Besides maintaining the molecular identity and composition of the ER by preventing the excretion of important folding factors it also plays a crucial role in ER quality control (ERQC) [46]. Since chaperones like CNX, PDI or the heat shock protein (Hsp) 70 family member immunoglobulin binding protein (BiP) specifically bind to only partially folded or misfolded proteins, secretion of these premature folding intermediates is efficiently prohibited by ER-retrieval [47,48]. Accordingly, they are subjected to another round of folding attempts in the lumen of the ER, which will either result in successful secretion or in targeting for ER-associated degradation (ERAD).

1.2.3. ERAD pathway in ER quality control

The most important factor, which determines the secretion efficiency of a given protein, was shown to be the stability of the folded protein structure. This was hinted from experiments in which the *in vitro* thermostability of folded mutant proteins of bovine pancreatic trypsin inhibitor (BPTI) positively correlated with the secretion efficiency of these mutants from yeast [49,50].

This phenomenon, also observed in other studies [51,52], was generalized in the following sense: the higher ΔG between misfolded and natively folded state of a secretory protein, the faster it is excreted from the cell and the lower its propensity to be degraded via the ERAD pathway [46]. Vice versa, this implies that proteins, which experience problems with folding into their native state, are specifically identified and retained within or retrieved to the ER. As stated above, this specific recognition involves the binding of ER chaperones like the abundant BiP, which predominantly recognizes exposed hydrophobic patches within non-native protein folds [2,53]. However, the cell needs to discriminate between nascent proteins in their initial folding attempts and terminally misfolded proteins, which need to be targeted to ERAD [54].

An elegant mechanism to address the period a protein has spent within the ER has been elucidated in oligosaccharide-modified glycoproteins [55] (see Figure 1). Upon translocation of these polypeptides into the ER covalent attachment of an N-linked glycan to asparagine residues within a specific consensus motif (asparagine-x/no prolin-serine/threonine) of the primary protein structure is conducted by the ER-resident enzyme oligosaccharyltransferase (OST). The glycan, a three-branched oligosaccharide originally composed of two N-acetylgucosamine (GlcNAc), nine mannose (Man) and three glucose (Glc) residues, is then further processed by the action of glucosidase I and II, which each remove one of the glucose residues. This modified oligosaccharide ($Glc_1Man_9GlcNAc_2$) is recognized and bound by ER-resident lectin chaperones, Calreticulin (CRT) and Calnexin (CNX) [56,57,58], which, together with the recruited oxidoreductase of the PDI family ERp57 [59,60,61], drive the oxidative folding of the glycoprotein. Eventually glucosidase II will remove the third and last glucose residue from the tip of the glycan (resulting in $Man_9GlcNAc_2$), which abolishes lectin binding and allows natively folded proteins to be released from the ER [62]. Non-natively folded proteins, however, are identified by the UDP-glucose:glycoprotein glucosyltransferase (UGGT), which re-glucosylates the folding intermediate on a specific mannose residue (generating $Glc_1Man_9GlcNAc_2$) in order to promote re-association with the lectins CRT/CNX for further folding attempts [63,64]. Importantly, cycling between re-glucosylation (by UGGT) and de-glucosylation (by glucosidase II) is eventually complemented by mannose trimming within the glycan when dissociated from CRT/CNX. The first mannose residue is removed by α1,2–mannosidase ($Man_8GlcNAc_2$), whereas a further demannosylation step can either be catalyzed by Golgi mannosidase I, ER degradation-enhancing α-mannosidase-like protein 1 (EDEM1) or again by α1,2–mannosidase

[65]. Upon removal of the specific mannose residue targeted by UGGT for reglucosylation, probably by α1,2–mannosidase, the folding intermediate is permanently released from the CRT/CNX cycle [66]. Further trimming exposes a α1,6-linked mannose residue, which acts as glycan-coded ERAD signal and is recognized by the lectins OS-9 or XTP3-B [65].

Even though it is known that ERAD pathway involves unfolding, retro-translocation into the cytosol, ubiquitination and subsequent proteasomal degradation of its substrates [53,54], the precise underlying mechanisms are still not well characterized. It has been suggested that the ER-resident PDI and Hsp40 family member ERdj5 plays a role in reducing disulfides in both glycosylated and non-glycosylated ERAD substrates [67,68] and that BiP association is important for targeting to the retro-translocon [68,69]. The detailed composition of this export channel from the ER back to the cytosol itself remains elusive, even though some work suggests that actually the Sec61 complex, the pore forming unit for co-translational translocation into the ER, might be involved [70,71]. Various ERAD substrates were found to be subjected to polyubiquitination catalyzed by different E3 ubiquitin ligases, which, in some cases, was shown to depend on OS-9/XTP3-B-mediated substrate delivery [65,72,73]. Interaction of these polyubiquitin tags with the cytosolic ubiquitin-binding protein p97, together with the intrinsic ATPase activity of the later are thought to provide the energy for efficient ER to cytosol extraction [74]. In the final step of ERAD, the polyubiquitinated proteins are recognized by the proteasome and, after cleavage of ubiquitin chains, proteolytically degraded.

In conclusion, the described ERQC/ERAD pathway clears terminally misfolded proteins and thereby prevents the accumulation of these non-native folding intermediates, which otherwise would trigger the unfolded protein response (UPR). ERAD involves many different proteins from different subcellular compartments, whose interconnections are still only poorly defined. ER-resident chaperones, both soluble and membrane-bound, identify the misfolded substrates and work in concert with integral membrane machinery, which, with the help of cytosolic factors, mediates retro-translocation. Subsequent degradation via the ubiquitin-proteasome system (UPS) was shown to not only target terminally misfolded but many natively folded proteins and nascent polypeptides, too [75]. Even though the objective of this, at first glance, waste of cellular resources is currently unclear, a role in immunology by mirroring the current protein biosynthesis on MHC class I molecules on the cell surface has been postulated [75].

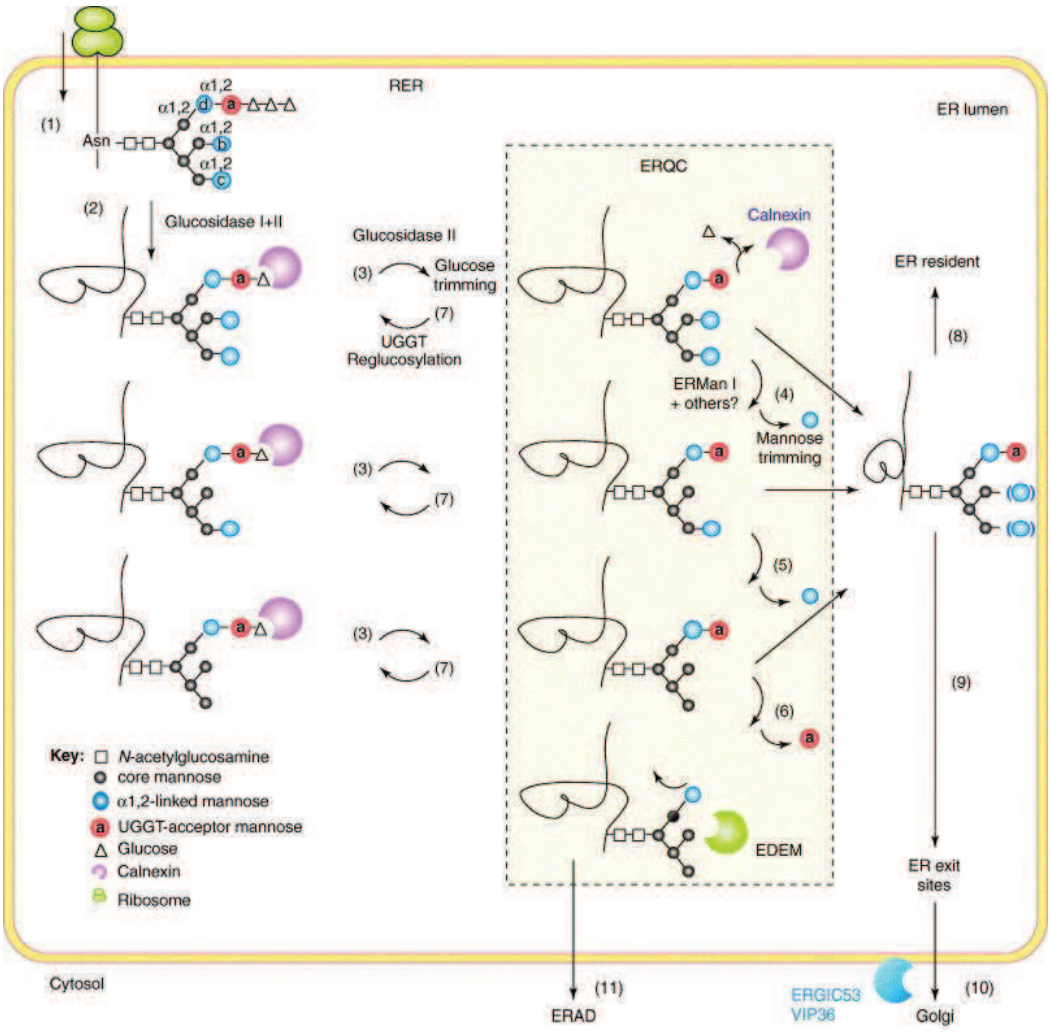

Figure 1: Endoplasmic reticulum quality control (ERQC) of glycoproteins. Following asparagine (Asn)-linked glycosylation of the nascent polypeptide upon co-translational transfer into the rough ER (RER) (1), enzymatic action of glucosidase I and II each remove one glucose residues from the glycan, which leads to association with calnexin (2) and initiates a folding cycle: glucosidase II removes the remaining glucose residue (3), which results in dissociation of calnexin; non-natively folded proteins are recognized and reglucosylated by UDPGlc:glycoprotein glucosyltransferase (UGGT) (7), which restores calnexin-mediated folding; deglucosylation and reglucosylation is complemented by mannose trimming by α1,2-mannosidases like ER mannosidase I (ERMan I) (4-6). Natively folded proteins are no longer recognized by UGGT, which results in release from the folding cycle as either mature ER resident (8) or via ER exit sites (9) and Golgi apparatus (10), as mature secreted proteins. In contrast, upon removal of the crucial UGGT-acceptor mannose (6) the immature folding intermediate is permanently released from the folding cycle. ER degradation-enhancing α-mannosidase-like protein (EDEM)-mediated exposure of α1,6-linked core mannose residues targets the folding intermediate to ER-associated degradation (ERAD)(11). This figure was reproduced from [62].

1.3. The protein disulfide isomerase (PDI) family

To prevent misfolding of nascent polypeptides and their subsequent targeting to ERAD, the ER employs elaborate enzymatic machinery composed of a variety of different folding factors to assure proper protein folding and introduction of native disulfide bonds. Within this group,

members of the protein disulfide isomerase (PDI) family play a central role, since most of them can act as chaperones and oxidoreductases. More than 20 different PDIs have been identified in the ER of mammalian cells so far, all of which exhibit at least one domain with a distinctive fold – the thioredoxin (Trx)-like fold [76]. The structure of this domain is characterized by the presence of a central four-stranded antiparallel β-sheet, which is sandwiched between three outer α-helices [77]. In order to exert their function in dithiol-disulfide transfer reactions many PDIs possess an active site CxxC motif within their Trx-like domains [78]. When the two motif cysteines form a disulfide, PDIs can transfer this disulfide bond to a substrate cysteine pair via formation of a transient mixed-disulfide complex. Upon completion of the disulfide transfer, the substrate is oxidized and the CxxC motif in PDI is in the reduced dithiol state. Since this reaction is reversible, PDIs can act both as oxidants and reductants, hence the name oxidoreductases. Furthermore, in their reduced state, they can also operate as disulfide isomerases.

However, not all PDIs possess redox active CxxC motives. For example endoplasmic reticulum resident protein 44 (ERp44) has a CxxS motif (where S is serine). Since this distinct active site enables ERp44 to form mixed-disulfide complexes with oxidized clients but prevents disulfide transfer, it plays a role in disulfide-mediated ER-retrieval via its KDEL-like motif [31]. In this context, ERp44 binds secretory folding intermediates [79] as well as peroxiredoxin IV (PrxIV) [80] and the oxidases of the Ero1 family (see section 1.4.3) [80,81] and thereby promotes ER localization by ER-retrieval from ERGIC [82,83]. Due to the fact that there are also other PDIs, like ERp27 and ERp29, which were found not to display any redox activity, it is important to stress that inclusion in the PDI family does not refer to a common protein function but is rather based on a Trx-like protein fold and on ER residency [83].

The most extensively studied and name-giving member of this family is PDI itself (also referred to as PDIA1 or prolyl 4-hydroxylase subunit beta (P4HB)). PDI possesses four Trx-like domains, two of which have redox active CxxC motives: **a-b-b'-x-a'-c,** with «**a**» and «**a'**» being the redox active and «**b**» and «**b'**» the redox inactive Trx-like domains, «**x**» being the x-linker and «**c**» a C-terminal acidic domain. Crystallographic analysis showed that these domains are aligned in a horseshoe-like shape [84]. Whereas the presence of the **c** domain is negligible for PDI function as oxidoreductase/isomerase and chaperone [85], the x-linker was proposed to confer a certain degree of flexibility of the **a'** domain relative to the remaining PDI structure [86,87]. This is highlighted by the fact that PDI undergoes redox-regulated conformational changes, which are

proposed to mirror consecutive steps in PDI oxidoreductase activity [87]. In this notion, reduced PDI (PDI^{red}) is present in a rather closed horseshoe-like state with the two active sites being in proximity to each other. However, upon disulfide formation within the two active sites in **a** and **a'**, oxidized PDI (PDI^{ox}) adopts a more open conformation with a greater distance between both active sites. Moreover, the **a'** domain rotates by approximately 45° in clockwise direction relative to the **b'** domain [87]. These redox-regulated conformational changes are thought to facilitate substrate binding by PDI^{ox}, which is mainly based on hydrophobic interactions between the unfolded polypeptide and the **b'** domain of PDI [88,89]. Whereas substrate access to the hydrophobic cleft in the **b'** domain is largely blocked in the closed conformation of PDI^{red}, in part due to interactions between **b'** and **a'** domain, dislocation of the latter upon oxidation abolishes this constraint and enables accommodation of an unfolded client protein for subsequent oxidation [87]. Following dithiol-disulfide exchange, PDI in its reduced state regains the closed conformation and needs to be re-oxidized in order to complete the catalytic cycle (for PDI oxidation see section 1.4).

First hints for catalyzed disulfide-bond formation were found in *in vitro* experiments in which the refolding of reduced and denatured ribonuclease A was accelerated upon incubation with microsomes [90]. It was 25 years later that Bulleid and Freedman showed that this microsomal effect was mainly due to PDI, since reconstitution of protein depleted microsomes with purified PDI reestablished this catalytic activity [91]. Since then lots of progress has been made regarding the *in vitro* an *in vivo* characterization of various PDI family members. Distinct roles or substrates for specific PDIs, however, were only scarcely found. Nevertheless, cross-linking/co-immunoprecipitation studies have implicated that PDI might influence the oxidative folding of fibrillins [92] and immunoglobulins [93]. Furthermore, PDI was shown to be a critical determinant in the maturation of fibrillar procollagens by acting as both, disulfide introducing oxidase [94] and stabilizer of the active form of prolyl 4-hydroxylase via representing its non-catalytic β subunit [95]. An additional client for PDI-mediated oxidative folding is thyroglobulin, the precursor protein of the thyroid hormones thyroxine (T4) and triiodothyronine (T3) [96]. Besides PDI itself, three other PDI family members have been associated with thyroglobulin folding and secretion, namely ERp29 [97], ERp72 [98] and ERp57 [96]. The latter is of special interest, since it shows more than 20% sequence identity with PDI and shares the same domain architecture (**a-b-b'-x-a'-c**) [99]. However, in contrast to PDI, ERp57 is specifically involved in

oxidative folding of glycoproteins due to its association with the lectins CNX and CRT [59,60,61]. Accordingly, the substrate spectrum of ERp57 is most probably vast due to the abundance of glycoproteins relying on oxidative folding mechanisms. Accordingly, the 26 glycoproteins co-immunoprecipitated using a trapping mutant of ERp57, which only captures substrates for reduction/isomerization, likely only represents the tip of the iceberg [100].

Besides these involvements in oxidative folding of various substrates, PDIs are also implicated in other cellular processes. Thus, PDI and ERp57 might play a role in the so-called peptide loading complex (PLC), since they were both found in mixed-disulfide complexes with Major Histocompatibility Complex (MHC) class I heavy chain [101,102]. PLC is a multimeric complex consisting of transporter associated with antigen processing (TAP), TAP-associated glycoprotein (tapasin), CRT, ERp57, PDI and a heterodimer comprised of MHC I and β2 microglobulin [102,103]. The main function of PLC is to select high-affinity peptides to be presented via MHC I molecules on the cell surface. Furthermore, ERdj5 and PDI are both thought to be involved in the reduction and retro-translocation of terminally misfolded proteins in ERAD (see above) [67,68,104]. Last but not least, ERp57 and ERp44 play opposing roles in the regulation of ER Ca^{2+} homeostasis (see section 1.6), in which the former is thought to decrease [105] and the latter to increase intraluminal Ca^{2+} concentration [106].

In conclusion, members of the PDI family, a subclass of the thioredoxin-like superfamily, are central elements in the process of oxidative folding of nascent polypeptides in the secretory pathway. Due to their mode of substrate recognition, which is primarily based on hydrophobic interactions, they operate not merely as oxidoreductases, but also as ER-resident chaperones. Their versatile involvement in an increasing number of cellular functions is notably based on a single protein fold.

1.4. *De novo* disulfide generation

Maintenance of protein synthesis is indispensable for every cell. In this context, *de novo* disulfide bond production is important to sustain oxidative folding and subsequent protein secretion. Whereas in lower eukaryotes like *Saccharomyces cerevisiae,* disulfide bond production by endoplasmic oxidoreductin 1 (Ero1p) [23,24], even though complemented by the sulfhydryl

oxidase ERV2 [25], is essential, mammalian cells utilize several distinct reaction mechanisms that can compensate for the loss of Ero1 function. Accordingly, enzymatic action of quiescin sulphydryl oxidase (QSOX) [107], vitamin K epoxide reductase (VKOR) [108], endoplasmic oxidoreductin 1 like (Ero1) [31], peroxiredoxin IV [109,110] and glutathione peroxidases 7 and 8 (GPx7 and GPx8) [111] can all contribute to the general pool of newly synthesized disulfides in human ER. With the exception of QSOX, all of these pathways were demonstrated to oxidize PDI family members rather than oxidative folding substrates directly [112].

1.4.1. Quiescin sulphydryl oxidase (QSOX)

In yeast, rescue of a non-viable Δ*ero1* deletion strain was accomplished by overexpression of ERV2 [25]. Even though a human homolog of ERV2 has not been identified, QSOX possesses a catalytically active ERV2-like domain and two intrinsic Trx-like domains [107]. ERV2 [25] and QSOX [113] both harbor a flavin adenine dinucleotide (FAD) co-factor, which enables them to couple disulfide bond production to reduction of molecular oxygen. QSOX is characterized by the presence of a disulfide generating domain (ERV2-like) and a disulfide transferring domain (Trx-like), the cooperation of which is thought to enable QSOX to interact with its substrates directly [107]. Accordingly a broad substrate specificity including GSH, DTT and various reduced proteins was determined by *in vitro* experiments [113,114]. Furthermore, since QSOX is devoid of any isomerase activity, *in vitro* collaboration with PDI was found to be essential in order to catalyze native substrate folding [115]. However, these *in vitro* observations might not mirror the *in vivo* function of QSOX, since endogenous protein primarily localized to the Golgi apparatus in various cell lines, making a contribution to ER-centered oxidative folding rather unlikely [116,117]. Accordingly, cell density-dependent secretion of endogenous QSOX1 in WI-38 fibroblasts is important for proper laminin assembly, which argues for a physiological function of secreted QSOX in extracellular matrix formation in response to cell quiescence [117]. Along this line, QSOX apparently plays a minor role in ER disulfide homeostasis of human hepatoma HepG2 cells when compared to other disulfide relays [118].

1.4.2. Vitamin K epoxide reductase (VKOR)

Vitamin K plays an important role in γ-carboxylation of glutamate residues, a posttranslation modification implicated in blood coagulation factor maturation [119]. In this process, reduced vitamin K hydroquinone is oxidized by γ-glutamyl carboxylase to vitamin K epoxide. The latter is subsequently regenerated to the reduced form with the help of the ER integral membrane protein VKOR [120]. Recently it has been demonstrated that crucial cysteine residues of VKOR are facing the ER lumen and can shuttle electrons predominantly derived from membrane-bound PDIs like TMX and TMX4 onto vitamin K epoxide, thereby recycling vitamin K hydroquinone [108]. Since the liver is the main site for coagulation factor synthesis and hence for generation of vitamin K epoxide, it does not come as surprise that disulfide bonds fed in by VKOR significantly contribute to disulfide homeostasis in the HepG2 hepatoma cell line [118]. However, to what extent this is also true for other tissues, in which these vitamin K dependent pathways are of less relevance, is so far not clear.

1.4.3. Endoplasmic oxidoreductin 1 (Ero1)

The most conserved pathway for *de novo* disulfide bond formation is represented by Ero1, which is highlighted by its essential role in yeast. Two human orthologs of yeast Ero1p have been identified: the widely expressed housekeeping isoform ERO1-like protein α (Ero1α) and the selectively expressed ERO1-like protein β (Ero1β) [31,121,122]. Like QSOX, Ero1 oxidases also rely on FAD for their catalytic activity [123]. Therefore, Ero1 generates stoichiometric amounts of hydrogen peroxide (H_2O_2) for every disulfide bond produced [124]. Furthermore, Ero1 oxidases share a common reaction mechanism, which depends on the presence of two redox active cysteine motives [125,126]. In the crystal structures of human Ero1α, the "inner" CxxC active site (comprised of Cys^{394} and Cys^{397}) is in proximity to the bound FAD moiety in the protein core [127]. Cys^{397} in its thiolate form is believed to initially form a charge transfer complex with FAD, which is subsequently replaced by formation of a covalent adduct involving C(4a) of the cofactor [127]. This C-S bond is then nucleophilically attacked by the second "inner" active site cysteine Cys^{394}, which leads to the formation of a Cys^{394} - Cys^{397} active-site disulfide bond and reduced FAD ($FADH_2$) [127]. The latter can be re-oxidized by forwarding two

electrons onto molecular oxygen [128]. The resulting "inner" active site disulfide bond is then transferred by intramolecular dithiol disulfide exchange reaction to the "outer" di-cysteine active site (in Ero1α comprised of Cys^{94} and Cys^{99}) – also called shuttle disulfide – which is located in a flexible loop on the surface of the protein [129]. This "outer" active site in the disulfide state is then preferentially attacked by PDI^{red}, which results in the formation of a mixed-disulfide intermediate [125,130,131]. Upon completion of this intermolecular dithiol disulfide exchange reaction, regenerated PDI^{ox} can again oxidize client proteins. Recently, molecular-level insights regarding this disulfide relay have been gained. These insights explained the previous findings that Ero1 recognizes PDI independently of its catalytic CxxC motives [127,132] and proposed a key-and-lock principle [133]. Accordingly, specificity of PDI as reducing substrate of human Ero1 is based on hydrophobic interactions between a protruding β-hairpin (including a critical tryptophan Trp^{272}) in Ero1 and hydrophobic residues in the **b'** domain (including phenylalanines Phe^{240} and Phe^{304}) of PDI [127,133]. In strong support of this, exchange of the respective **b'** domains between PDI and ERp57, which has a similar domain architecture, shifted their substrate preferences [127]. In addition, mutation of either Trp^{272} in Ero1 or Phe^{240} and Phe^{304} in PDI substantially reduced their catalytic efficiency as monitored by oxygen consumption [133]. Previous findings that human Ero1α preferentially oxidizes the C-terminal **a'** domain of PDI [32,134,135,136] can also be attributed to this hairpin-mediated interaction, since *in silico* modelling showed that outer active site and **a'** domain would be in proximity to each other [133]. In contrast to human Ero1α/β, yeast Ero1p lacks this tryptophan-containing β-hairpin and preferentially oxidizes the **a** domain in Pdi1p [137], thus arguing for a non-conserved recognition mechanism in this disulfide relay.

1.4.4. Hydrogen peroxide-mediated disulfide production

Since the discovery of ER-resident sulfydryl oxidases of the Ero1, QSOX or ERV2 family the need for tight enzymatic control of these flavoenzymes in order to limit concomitant H_2O_2 production has been emphasized. Indeed, elaborate intrinsic mechanisms for redox-regulated, disulfide-mediated shutdown of Ero1 oxidases have been unraveled, both in yeast and human cells (see section 1.5). However, most recent findings have also elucidated that mammalian cells harbor at least three ER-resident, H_2O_2-scavenging peroxidases, namely peroxiredoxin IV

peroxidases, namely peroxiredoxin IV (PrxIV), glutathione peroxidase 7 (GPx7) and glutathione peroxidase 8 (GPx8). These peroxidases were proposed to utilize the remaining oxidative capacity of H_2O_2 for *de novo* disulfide bond formation. This would not only constitute a potent mechanism for detoxification of this potentially deleterious side product of Ero1 activity, but also elegantly increase the efficiency of oxygen-driven disulfide production, ultimately generating two disulfide bonds from the reduction of one molecule of oxygen to water (see Figure 2).

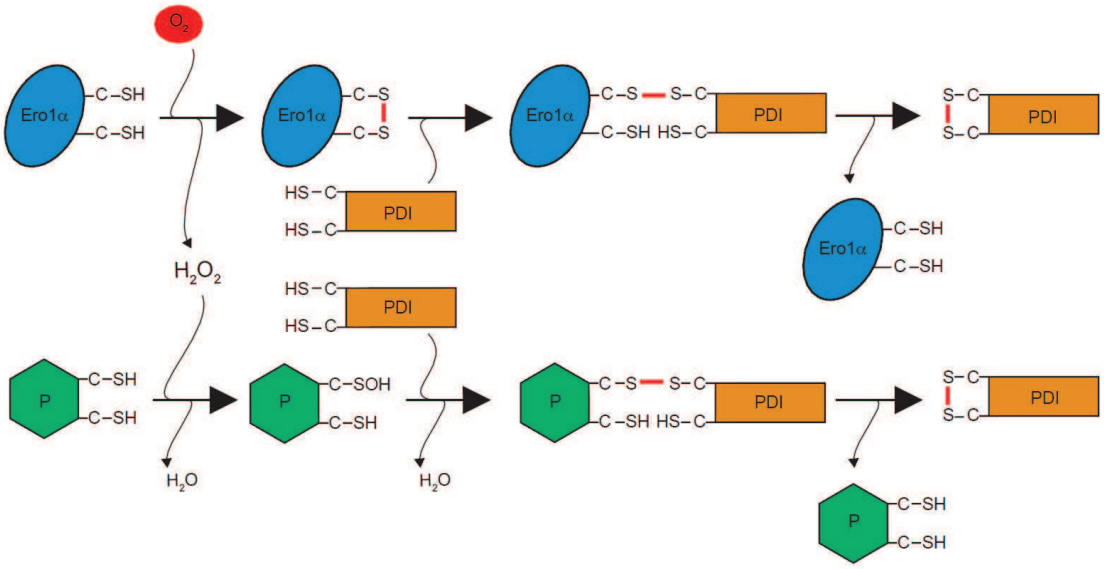

Figure 2: The two-disulfides-out-of-one-O_2 concept. O_2 (red)-mediated oxidation of endoplasmic oxidoreductin-1-like protein (Ero1α) results in the generation of one disulfide bond (red), which is transferred to reduced protein disulfide isomerase (PDI), and of one molecule of H_2O_2. ER-resident peroxidases (P) – probably exclusively of the glutathione peroxidase (GPx) family (see main text for details) – can couple the reduction of Ero1a-derived H_2O_2 to H_2O with the introduction of a second disulfide bond (red) into PDI.

1.4.4.1. Peroxiredoxin IV (PrxIV)

PrxIV is a classical 2-Cys peroxiredoxin (for details see section 1.7.3), which is equipped with an N-terminal signal sequence to promote ER translocation [138]. Instead of a classical ER-retention motif PrxIV utilizes intermolecular interactions with ERp44 and PDI in order to prevent its secretion [80]. In the ER, human PrxIV forms characteristic toroid shaped pentamers of antiparallel dimers [139]. Upon the encounter of H_2O_2, the active site peroxidatic cysteine (Cys^{124}) is oxidized exceptionally fast [140], which leads to the formation of intermolecular disulfide bonds within antiparallel dimers (Cys^{124}-Cys^{245}). This interchain disulfide bond can then be attacked by various reduced PDI family members [109,141], which results in dithiol disulfide

exchange. Various publications have argued for a role of Ero1 as candidate producer of H_2O_2 for PrxIV-mediated oxidative folding [110,142,143,144]. Even though the contribution of PrxIV to disulfide homeostasis is undisputed, several lines of evidence argue against this direct link: (1.) ectopically expressed PrxIV was identified to rescue a thermo-sensitive *ero1-1* yeast strain [110], (2.) PrxIV was shown to protect Ero1-knockout mice from H_2O_2-mediated, non-canonical scurvy [145] and (3.) combined depletion of Ero1α/β and PrxIV in HepG2 cells resulted in a more severe phenotype [118]. These three observations argue for an Ero1-independent (or at least alternative) H_2O_2 source, which fuels PrxIV-mediated disulfide production (for other H_2O_2 sources see section 1.7). Along this line, evidence from our lab clearly demonstrated that no additive effect between elevated Ero1-derived H_2O_2 levels and concomitant PrxIV depletion could be measured in living cells, except when Ero1 activity was artificially maximized by the reductant DTT (see section 2).

1.4.4.2. Glutathione peroxidases 7 and 8 (GPx7 and GPx8)

GPx7 and GPx8 are two closely related ER-resident members of the glutathione peroxidase family (for details see section 1.7.4), whose 3D structures are largely superimposable [139]. ER translocation of soluble GPx7 is mediated by a cleavable N-terminal signal sequence, whereas GPx8 relies on a transmembrane domain in its N-terminal region [111]. They both possess KDEL-like motives for ER-retention [111], which is a peculiarity for GPx8, since transmembrane proteins rather rely on cytosolic di-arginine/-lysine motives to assure ER residency (see section 1.2.2). *In vitro* characterization of both proteins showed that they readily react with H_2O_2 [111,146,147]. Additionally, it was demonstrated *in vitro* that both peroxidases preferentially use PDIs instead of glutathione as electron donors [111,147], which might be attributed to the absence of a peptide loop shown to confer glutathione specificity in other GPxs [111,148]. However, controversy still exists regarding the reaction mechanism, since neither GPx7 nor GPx8 possesses a canonical resolving cysteine normally present in cysteine GPxs (see section 1.7.4). Following peroxide-mediated oxidation of the peroxidatic cysteine (C_P; Cys^{57} in GPx7 or Cys^{79} in GPx8), sulfenylated C_P is either directly subjected to nucleophilic attack by a thiolate anion in the reducing substrate [146] or attacked by a deprotonated non-canonical resolving cysteine (C_R; Cys^{86} in GPx7 or Cys^{108} in GPx8), which results in formation of an intramolecular

disulfide bond [147,149]. Subsequently, this intrachain disulfide bond is subjected to nucleophilic attack by a reducing substrate. Irrespective of the actual involvement of a non-canonical C_R, generation of an intermediate mixed-disulfide complex comprised of GPx7/8 and PDIs is common to both reaction mechanisms [146,147]. Upon completion of the reaction cycle, reduced GPx7/8 is regenerated and oxidized PDIs can take part in oxidative folding of client proteins. Recent findings regarding the potential source of intraluminal H_2O_2 used for GPx-mediated oxidation of PDIs have pointed into a clear direction. First, Nguyen et al. could demonstrate that GPx7 addition increased Ero1 activity *in vitro* and, with the help of a bi-molecular fluorescence complementation approach, that GPx7 and GPx8 are closely associated with Ero1α in the ER of living cells [111]. This association likely place the GPxs in a privileged position to reduce Ero1-derived H_2O_2 compared to PrxIV. Second, Wang et al. confirmed the accelerating effect of GPx7 in an *in vitro* folding system comprised of Ero1, PDI and a model folding client. Furthermore, they could demonstrate a beneficial effect of overexpressed GPx7 in an *in situ* folding assay, which was clearly dependent on the presence of Ero1 [147]. Third, data from our lab demonstrated a role of GPx8 as molecular gatekeeper that confers protection against Ero1-mediated ER hyperoxidation (see section 2).

1.5. Ero1 regulation

PDI is oxidized in response to Ero1 catalysis, either by direct dithiol disulfide transfer reaction or by a H_2O_2/GPx-mediated mechanism. However, an important function of many PDIs is to resolve non-native disulfide bonds, which they can only fulfill in the reduced dithiol state. Therefore, unchecked Ero1 activity would ultimately prevent this reductase/isomerase function, twist the ER redox balance to hyperoxidizing conditions and thereby interfere with native protein maturation. Therefore, Ero1 activity has to be tightly regulated to keep a balance between disulfide-bond formation and concomitant disulfide rearrangements. In this notion, elegant mechanisms conferring feedback regulation in both Ero1p and Ero1α/β have been elucidated (see Figure 3). Even though many features of Ero1 are conserved between yeast and mammals, e.g. the protein fold, two characteristic cysteine triads and substrate specificity for PDI, the underlying principles of redox regulated inhibition are different.

Both enzymes have two active sites, the "inner" active site (Ero1p: Cys^{352}-Cys^{355}; Ero1α: Cys^{394}-Cys^{397}) and the shuttle disulfide (Ero1p: Cys^{100}-Cys^{105}; Ero1α: Cys^{94}-Cys^{99}), and a long ranging, non-catalytic disulfide bridge (Ero1p: Cys^{90}-Cys^{349}; Ero1α: Cys^{85}-Cys^{391}) (see Figure 3). However, Ero1p possesses two additional disulfides connecting Cys^{143}-Cys^{166} and Cys^{150}-Cys^{295}, which are not conserved in the human ortholog. Whereas the former was initially proposed to be of structural importance, since mutation lowered Ero1p activity *in vitro*, the latter has been implicated in activity regulation [150]. Mutation of the Cys^{150}-Cys^{295} disulfide bond substantially increased Ero1p activity both *in vitro* and *in vivo* [150]. In the same study, it was also demonstrated that mutation of the long ranging Cys^{90}-Cys^{349} disulfide lowered the previously observed lag phase in the activation of wild type Ero1p [124], arguing for a regulatory function. Therefore, a model was proposed in which reduction of Cys^{150}-Cys^{295} exerts a destabilizing effect on the long ranging disulfide, which ultimately renders this mutant constitutively active [150]. However, Heldman et al. could later show that the Cys^{143}-Cys^{166} disulfide bond is reduced at an early stage of Ero1p activation and that its stability, as observed with the long ranging disulfide, might be affected by Cys^{150}-Cys^{295} mutation [151]. In conclusion, the exact mechanism of Ero1p activation by reduction of non-catalytic, regulatory disulfide bonds is still not fully understood. Nevertheless, it is believed that inactivation of Ero1p is largely based on an increased constraint of the shuttle disulfide-harboring flexible loop, which is alleviated by reduction of the Cys^{150}-Cys^{295} disulfide [129].

In contrast, mammalian Ero1α and Ero1β rely on a different mechanism of feedback regulation, which directly involves cysteine residues of the shuttle disulfide [152] (see Figure 3). In cells, Ero1α expression is characterized by the formation of two distinct redox forms on non-reducing SDS PAGE, termed OX1 and OX2. While the OX2 redox form represents a fully oxidized, catalytically inactive form, OX1 is believed to be the active form, competent to shuttle disulfides onto PDI. Site specific mutagenesis [135] and mass spectrometry analysis [153] revealed that the OX2 form of Ero1α is characterized by a Cys^{94}-Cys^{131} disulfide bond. Since Cys^{94} is one constituent of the outer active site, Cys^{131} and reduced PDI compete for binding to the shuttle disulfide [153]. This has been elegantly proven by modulating the OX1/OX2 ratio by varying the expression levels of PDI. In this sense, overexpression of PDI lowered, whereas small interfering RNA (siRNA)-mediated depletion of PDI increased the OX1/OX2 ratio [153,154]. Interestingly, also Cys^{99}, the other constituent of the shuttle disulfide, is engaged in a disulfide bond with a

second non-active site cysteine, Cys^{104} [135,155]. Thus, *de novo* produced disulfide bonds generated by the inner active site can be stored as Cys^{94}-Cys^{131} and Cys^{99}-Cys^{104} disulfides in an oxidizing ER environment, thereby leading to the shutdown of Ero1 activity. *Vice versa*, when PDI^{red} is abundant, PDI-mediated nucleophilic attack of the Cys^{94}-Cys^{99} shuttle disulfide prevails and delivery of oxidizing equivalents onto client proteins is assured. The importance of these feedback-regulated non-catalytic disulfide bonds for general ER homeostasis has recently been demonstrated. Expression of a deregulated Ero1α mutant, which lacks the regulatory Cys^{104} and Cys^{131} residues hyperoxidized the PDI family member ERp57 and induced ER stress [155].

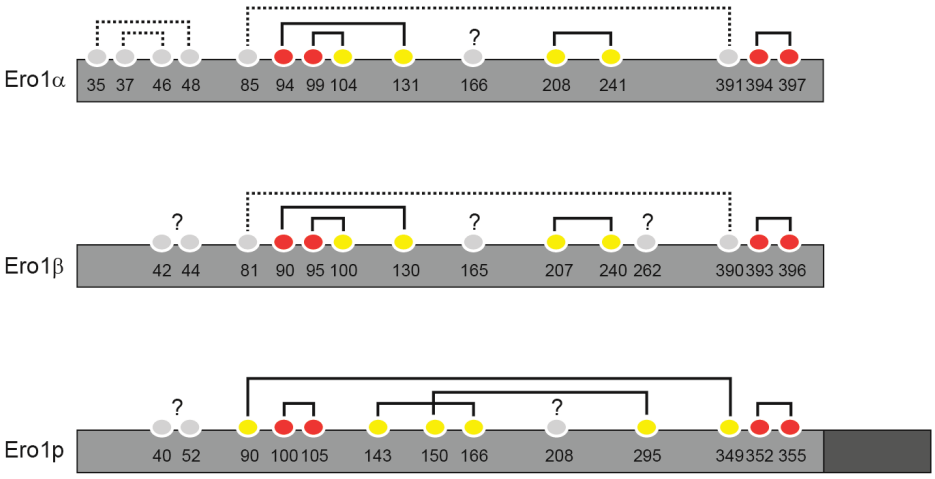

Figure 3: Cysteine connectivity of oxidatively silenced Ero1 enzymes. Ero1α, Ero1β and Ero1p polypeptides are depicted by gray bars and the additional C-terminal domain or Ero1p, which is responsible for membrane tethering, by a dark grey box. Numbered dots represent the position of cysteine residues within the respective Ero1 sequence and brackets connecting two dots show intramolecular disulfide bonds. Active site cysteines are marked in red, whereas (potential) regulatory disulfide bonds are shown in yellow. Cysteines of structural or unknow function (light grey) are connected with dotted brackets in case of disulfide-bond connection. Question marks denote that no conclusive redox state has been demonstrated. Note that the cysteine connectivity of Ero1β is speculative at the moment. For more detailed information please refer to main text and regarding the Ero1α Cys^{208}-Cys^{241} disulfide bond to section 3.

1.6. ER homeostasis, UPR and ER stress-induced apoptosis

The ER has to continuously guarantee a tight balance between the cellular demands in protein synthesis and excretion on the one side and its intrinsic standards for ERQC and protein folding capacity on the other side. Any disturbance of this balance, referred to as “ER stress”, will result in a decrease in the secretory output and a concomitant accumulation of mis-/unfolded proteins within the ER. In order to restore ER function and thereby the flow of secretion, the cell triggers

an adaptive ER-centered stress response - the UPR [156]. Thus, in an acute phase of UPR signaling, the cell decreases its overall protein load within the ER by inhibiting further protein translation and increases its folding capacity by upregulation of chaperones/oxidoreductases [156]. This adaptive UPR is an essential physiological program especially important for cells with a high secretory output like antibody-secreting plasma cells [157,158,159]. However, if these mechanisms of adaption do not alleviate the stress, but in contrast the cell experiences chronic ER dysfunction, a pro-apoptotic mode of the UPR is initiated, which results in programmed cell death/apoptosis [156,160,161]. Various triggers of the UPR have been identified so far, all having in common to disrupt ER homeostasis [162]. Among these are perturbations in redox homeostasis [155,160], interference with the physiological Ca^{2+}-distribution [163], nutrient deprivation like glucose starvation or chemical ER stressors like the N-linked glycosylation inhibitor tunicamycin [160] or the sarcoplasmic/endoplasmic reticulum Ca^{2+}-ATPase (SERCA) inhibitor thapsigargin [164].

To counteract folding dysfunctions in the ER the cell has to first transmit a distress signal from the affected ER lumen into the cytosol. This sensing of accumulated mis-/unfolded proteins has been shown to involve three ER-resident transmembrane proteins in mammalian cells, namely the inositol-requiring protein 1 (IRE1), the protein kinase PKR-like ER kinase (PERK), and the activating transcription factor 6 (ATF6) [165] (see Figure 4). Activation of these UPR-sensors is thought to involve both, common and sensor-specific principles, presumably enabling the cell to differentiate between different subroutines of ER stress and modulate the cellular response accordingly [160,166].

Since the N-terminal, ER-luminal domains of the two type 1 transmembrane proteins IRE1 and PERK show a high degree of homology [167], it is not unexpected that ER-sensing and subsequent activation of both proteins involves a common principle. In unstressed cells, both sensors are kept in a monomeric, inactive state by binding to the abundant ER chaperone BiP [168]. Upon sequestering of BiP by accumulated unfolded proteins during ER stress, this chaperone-mediated inhibition is released and IRE1 and PERK are able to homodimerize and -oligomerize [156,169]. Subsequently, this leads to sensor activation by trans-autophosphorylation of their cytosolic kinase domains, which then exert their respective downstream effects [156,169]. The contribution of direct association of their ER-luminal domains with unfolded proteins during activation, as proposed in yeast IRE1 [170], is a matter of current controversy.

In contrast to this, activation of ATF6, displays unique features when compared to the other two sensors. In unstressed cells, glycosylated ATF6 forms disulfide-linked, inactive homodimers, whose C-terminal ER-luminal domains are associated with BiP [171] and the lectin chaperones Calnexin (CNX) [172] or Calreticulin (CRT) [173]. Dismissal of chaperone binding under ER stress unmasks a Golgi-localization signal and allows passage of the reduced, monomeric form of ATF6 within the secretory pathway for further processing [171]. Upon cleavage of ATF6 within the Golgi compartment via the site-2 protease (S2P), the cytosolic fragment of ATF6 is freed (ATF6f) and can exert its downstream effector role as transcriptional regulator of predominantly pro-survival genes [174].

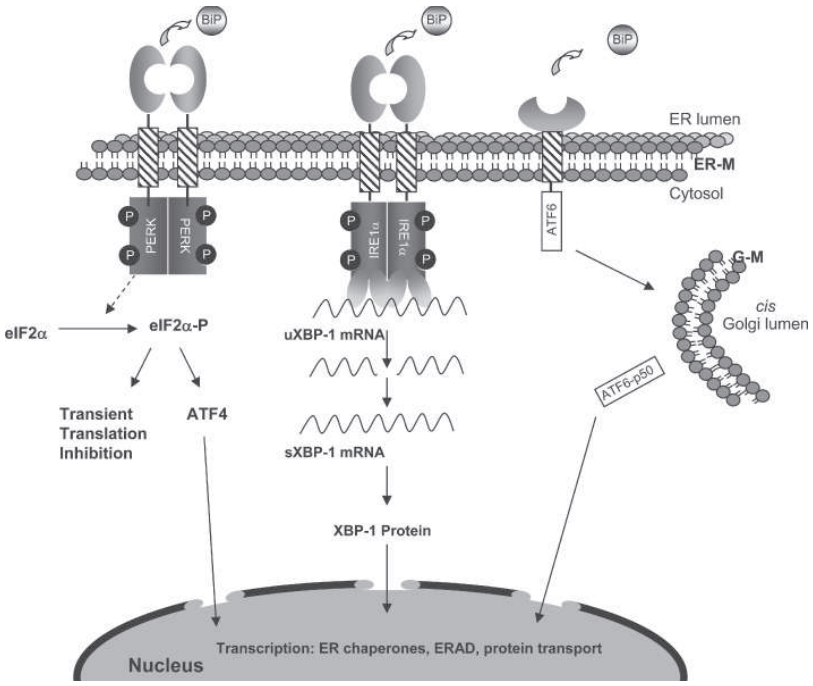

Figure 4: The three mammalian UPR sensors. The unfolded protein response (UPR) is initiated by three transmembrane proteins, namely protein kinase RNA - like ER kinase (PERK), inositol-requiring protein 1 (IRE1) and activating transcription factor 6 (ATF6), which sense the folding status of the ER via dissociation of binding immunoglobulin protein (BiP) and possibly by interacting with unfolded proteins directly (not depicted). Whereas PERK and IRE1 are activated by homodi- or oligomerization followed by trans-autophosphorylation, ATF6 is proteolytically processed in the Golgi apparatus into its active form (ATF6-p50). Once activated the senors initially aim to restore ER homeostasis by an adaptive response. This includes transient inhibition of protein synthesis by PERK-mediated eukaryotic translation initiation factor 2α (eIF2α) phosphorylation, increase in the ER folding capacity by transcriptional upregulation of ER chaperones and folding factors and increase in ER-associated degradation (ERAD). For more detailed information please refer to main text. This figure was reproduced from [175].

In conclusion, all three ER stress receptors, IRE1, PERK and ATF6, have in common to be held in an inactive state by BiP-binding [175] (see Figure 4). However, while IRE1 and PERK activation crucially depends on the formation of dimers and higher order oligomers, a requirement for trans-autophosphorylation, ATF6 needs to be present in its monomeric form prior to Golgi transport. Recent findings have highlighted a role for specific oxidoreductases of the PDI family in regulating these conversions between mono-/di- and oligomeric state of ATF6 and IRE1, respectively. In this sense, PDIA5 has been implicated in the reduction of the intermolecular disulfide bonds within the ATF6 dimer [176], a prerequisite for ER-exit and Golgi targeting [177]. Furthermore, IRE1 dimerization/oligomerization upon ER stress has been proposed to involve intermolecular disulfide bonds [166]. Resolution of these linkages and concomitant attenuation of the UPR signal critically depends on the presence of PDIA6 [166]. Since both PDI family members (in resemblance to the UPR sensors) have been shown to physically associate with BiP in unstressed conditions [166,178,179], regulatory loops between UPR signaling and PDIA5/6 activities are likely to modulate cell fate under unbalanced ER homeostasis [180].

The molecular distinctions between adaptive and fatal UPR signaling are by far not fully understood, but can be partially explained by the known signaling cascades downstream of the three UPR sensors. Adaptive UPR decreases protein influx into the ER, which is accompanied by increased expression of ERQC and ERAD components to process existent protein conglomerations. The former process is achieved by PERK-mediated phosphorylation and inactivation of the eukaryotic translation initiation factor 2α (eIF2α) [181] and by regulated IRE1-dependent mRNA decay (RIDD), an mRNA degradation pathway catalyzed by the endoribonuclease domain of activated IRE1 [182]. The transcriptional upregulation of pro-survival factors during adaptive UPR is carried out by combined action of three UPR-specific transcription factors [156], the IRE1-dependent isoform of X-box binding protein 1 (XBP1s), resulting from unconventional splicing of its mRNA [183], the cytosolic fragment of ATF6 after S2P cleavage (ATF6f) [184] and the activating transcription factor 4 (ATF4), the translation of which is paradoxically stimulated following PERK-mediated eIF2α phosphorylation [185]. Among the transcriptional targets of these effectors are proteins involved in (1.) ERAD (XBP1s, ATF6f, ATF4) [174,184,186,187,188,189] (2.) protein folding (XBP1s, ATF6f and ATF4)

[174,184,186,189,190] (3.) phospholipid synthesis and ER expansion (XBP1s) [191],and (4.) redox homeostasis and amino acid metabolism (ATF4) [186,188,192].

However, if these compensatory mechanisms fail to restore ER homeostasis, ER stress initiates apoptosis (see Figure 5). Transition to pro-apoptotic UPR signaling is thought to only happen upon exceeding a so far poorly defined ER stress threshold [156]. A central element in this conversion is the transcription factor C/EBP-homologous protein (CHOP), the upregulation of which is mainly attributed to PERK-ATF4 activation [180]. Main effects of CHOP induction include the downregulation of B-cell lymphoma 2 (Bcl-2) [193,194], the upregulation of Bcl-2 homology 3 (BH3)-only proteins [193,194] and upregulation of growth arrest and DNA damage-inducible 34 (GADD34) protein [195]. The two former proteins are involved in the direct regulation of mitochondria-induced apoptosis, in which decreased Bcl-2 levels and upregulated BH3-only proteins enable an oligomeric pore, the mitochondrial apoptosis-induced channel (MAC), to form in the outer mitochondrial membrane [196]. MAC assembly via hetero-oligomerization of Bcl-2-associated X (BAX) protein and Bcl-2 homologous antagonist killer (BAK) subsequently leads to the release of cytochrome c from the intermembrane space of mitochondria to the cytosol, a prerequisite for the formation of the apoptosome complex [196]. Finally, the apoptosome induces activation of zymogenic cysteine-dependent aspartate-directed proteases (Caspases), which execute cellular apoptosis [196].

Besides this involvement in the intrinsic apoptosis pathway, elevated CHOP levels also impact on ER homeostasis. CHOP-induced GADD34 expression leads to the protein phosphatase 1 (PP1)-mediated dephosphorylation and thereby reactivation of eIF2α [197]. The consequent resuming of global protein synthesis in cells still under the influence of unresolved ER dysfunction has been implicated in reactive oxygen species (ROS) formation and ER stress-mediated apoptosis [193]. Many publications have indicated a role of Ero1, another transcriptional target of CHOP, in this process. Since Ero1 generates stoichiometric amounts of the ROS hydrogen peroxide (H_2O_2) as byproduct of PDI regeneration [112], it was argued that elevated levels of Ero1-derived H_2O_2 cause oxidative stress and cell death [192,198,199]. However, since we have demonstrated that Ero1-derived H_2O_2 is strictly confined to the ER lumen and efficiently detoxified by glutathione peroxidase 8 (GPx8) (see section 2), we favor an alternative model to explain this CHOP/Ero1-mediated, ER stress-induced apoptosis, in which ROS formation is a downstream effect of dysregulated calcium levels [161,180,193,200].

The ER is the main intracellular storage compartment for Ca^{2+} ions, which are actively transferred into the ER lumen by the action of ATP-dependent SERCA pumps [201]. Release of these ions from the ER along their chemical gradient is mainly mediated by the opening of channel proteins of the inositol 1,4,5-trisphosphate (IP3) receptor or the ryanodine receptor (RyR) families within the endoplasmic/sarcoplasmic membrane [201]. The latter have been implicated in the process of calcium-induced calcium release (CICR) [202], whereas members of the former were demonstrated to be enriched in mitochondria-ER contact sites, the so-called mitochondria-associated membranes (MAMs) [203]. Accordingly, IP3Rs, besides other factors, contribute to the physical tethering of these two organelles by formation of a trimeric IP3R-Grp75 (glucose-regulated protein 75)-VDAC1 (voltage-dependent anion selective channel 1) complex [204]. This juxtaposition has been documented to enable specific Ca^{2+} fluxes from the ER to mitochondria, which play an important role under physiological conditions [205]. In ER stress conditions, however, IP3R-activity is potentiated in part as a result of CHOP-mediated upregulation of Ero1 [200,206,207]. The resulting elevated Ca^{2+} fluxes, additionally increased by CICR of RyR [208], are a well appreciated trigger for mitochondrial outer membrane permeabilization (MOMP), which subsequently results in cytochrome c release and apoptosome formation [209]. Furthermore, elevated intramitochondrial Ca^{2+} levels lead to the generation of mitochondria-derived ROS via various pathways [161]. Since ROS can introduce deleterious redox modifications in both, the SERCA pump and the IP3R/RyR calcium channels [210,211], a positive feedback loop can ensue, which most likely contributes to ER stress-induced apoptosis after chronic UPR signaling.

In conclusion, the UPR is a highly dynamic and complex cellular stress response, both under physiological and pathological conditions (see Figure 5). The ability to modulate its outcome not only on the UPR-receptor level but also by specific feedback loops within downstream effectors [156,180] significantly complicates the general conception of this signaling network. Its interrelation with other pathways like intrinsic apoptosis [193], mTOR signaling [212], mitogen-activated protein (MAP) kinases or antioxidant mechanisms (see section 1.7) [167,180] is certainly of great relevance but so far only poorly defined. Further characterization of these interdependencies will most probably constitute a major challenge in future years.

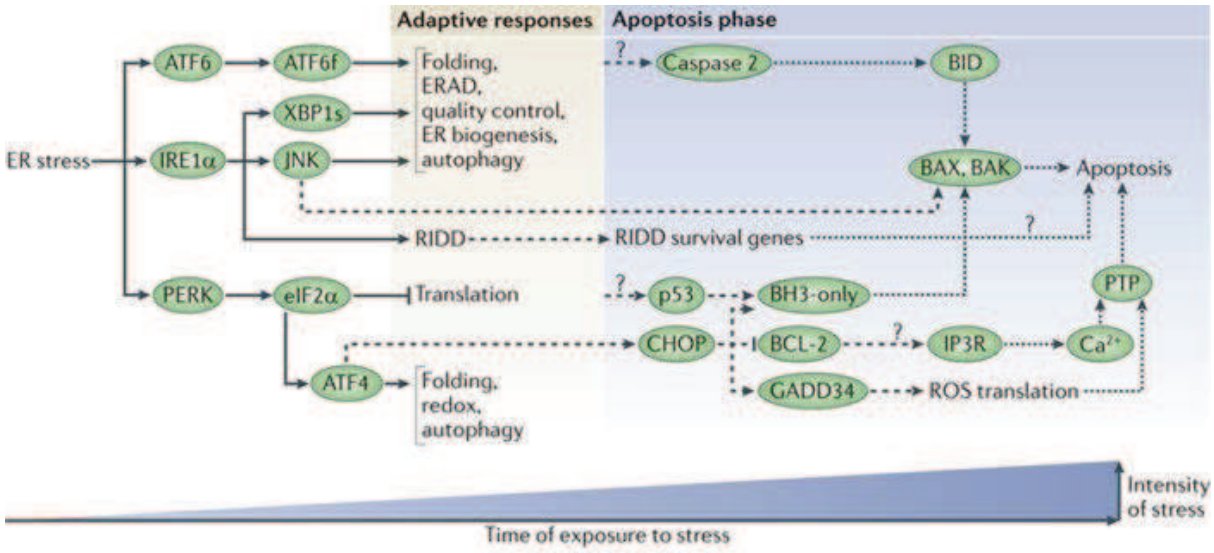

Figure 5: Transition from adaptive to pro-apoptotic UPR signaling. The adaptive response of the unfolded protein response (UPR) is initially characterized by translation attenuation (via phosphorylation of eukaryotic translation initiation factor 2α (eIF2α)) and mRNA decay (via regulated inositol-requiring protein 1 (IRE1)-dependent decay (RIDD)). Subsequent efforts to restore ER homeostasis and maintain cell survival involve the downstream effects of the proteolytically cleaved activating transcription factor 6 (ATF6f), the IRE1α-spliced X box-binding protein 1 (XBP1s) and ATF4. If the combined action of these transcription factors fails to restore ER homeostasis, pro-apoptotic UPR signaling with C/EBP-homologous protein (CHOP) as the central element is initiated. Pro-apoptotic signaling by B cell lymphoma 2 (BCL-2) homology 3 (BH3)-only proteins and Caspase 2-mediated activation of BH3-interacting domain death agonist (BID) converge on BCL-2-associated X protein (BAX) and BCL-2 homologous antagonist/killer (BAK) activation and trigger apoptosis. CHOP-mediated induction of growth arrest and DNA damage-inducible 34 (GADD34) restores protein synthesis and thereby impacts on reactive oxygen species (ROS) formation, which directly or via inositol-1,4,5-trisphosphate receptor (IP3R)-associated calcium release contributes to the opening of the mitochondrial permeability transition pore (PTP) and trigger apoptosis. This figure was reproduced from [156].

1.7. Oxidative Stress and cellular antioxidant mechanisms

ROS generation imposes a potential threat to normal cell physiology. These molecules, due to their naturally high chemical reactivity, have a broad substrate spectrum, which can result in pleiotropic effects like lipid peroxidation, aberrant protein or co-factor modification and DNA damage [213]. They are formed by various intracellular enzymes, like the nicotinamide adenine dinucleotide oxidase (NOX) family, respiratory chain complexes of mitochondria, peroxisomal enzymes and sulfhydryl oxidases in the ER [214,215,216,217,218]. Whereas the detrimental potential of ROS has been studied for decades, recent lines of evidence have additionally suggested important physiological roles in redox signaling for both, ROS-mediated posttranslational modifications like S-glutathionylation, and H_2O_2 as second messengers [215,219,220]. Therefore, ROS formation has to be placed under strict temporal and spatial limitations in order to be utilized for signaling purposes. An intracellular imbalance between

generation and scavenging/detoxification of ROS, the most prevailing being superoxide anions, hydroxyl radicals and H_2O_2 [213], is referred to as oxidative stress [221].

Numerous antioxidant pathways contribute to the alleviation of oxidative stress in mammalian cells and can be classified into enzymatic and non-enzymatic defense mechanisms. Constituents of the latter group are predominantly vitamins like α-tocopherol [222] or ascorbate [223], which, in a cooperative way, can terminate the self-propagating reaction of lipid peroxidation by scavenging lipid peroxyl radicals [224]. Enzymatic defense machinery includes superoxide dismutase (SOD), catalase, thioredoxin, glutaredoxin, peroxiredoxins (Prxs) and glutathione peroxidase (GPxs).

1.7.1. Superoxide dismutase and catalase

In humans, three different isoforms of SOD have been described, which differ in their respective subcellular localization. Whereas SOD1 is present in the cytosol and the mitochondrial intermembrane space, SOD2 can be found in the mitochondrial matrix and SOD3 is secreted from cells [225]. All of them utilize metal co-factors, with which they catalyze the disproportionation reaction of superoxide (O_2^-) to H_2O_2 and O_2. While mutations within SOD1 are linked to familial amyotrophic lateral sclerosis (ALS) [225], no clinical relevance was assigned so far to mutations in SOD2 or SOD3. However, knockout mice lacking either SOD1, 2 or 3 show hepatocellular carcinoma, early neonatal death or increased susceptibility to paraquat treatment, respectively, thereby highlighting the mitochondrial compartment as most fatal producer of superoxide [225]. SODs, together with the previously mentioned α-tocopherol/ascorbate pathway, catalyze the direct detoxification of free radicals, while the following components of the antioxidant defense rather target downstream products of radical reactions like lipid hydroperoxides and H_2O_2. Of note, even though H_2O_2 plays an important role in redox signaling, it can be decomposed to highly reactive hydroxyl radicals via fenton chemistry [226]. Since this reaction is catalyzed by transition metals like iron, which are abundant constituents of cellular co-factors, spatial limitation of H_2O_2 and subsequent detoxification are of critical importance.

Catalase is a tetrameric protein with four prosthetic heme groups and is exclusively expressed in peroxisomes (exceptions being erythrocytes and neutrophils). It catalyzes the disproportionation of excess H_2O_2 produced by peroxisomal oxidases to H_2O and O_2 [227,228]. In erythrocytes, cytosolic catalase, in cooperation with glutathione peroxidases [229] and peroxiredoxins [230], might contribute to the protection of hemoglobin (Hb), the main determinant of the blood O_2–binding capacity, by detoxification of H_2O_2 generated via autoxidation of Hb [231,232].

1.7.2. Thioredoxin and glutaredoxin

Hundreds of different proteins have been associated with the thioredoxin superfamily. Among them are thioredoxin (Trx) itself, glutaredoxins (Grxs), peroxiredoxins, glutathione peroxidases and ER-resident oxidoreductases/PDIs. In analogy to the PDIs, Trx/Grxs are also characterized by the conserved thioredoxin/-like fold [233] and exert their function either with a CxxC (thioredoxin and dithiol Grxs) or a CxxS (monothiol Grxs) active site motif [234]. Accordingly, cytosolic or mitochondrial Trx and dithiol Grxs, when present in a reduced dithiol state, can resolve aberrant disulfide bonds in client proteins. These non-native disulfide linkages can arise e.g. by unspecific protein oxidation via hydroperoxides during oxidative stress conditions [234]. Furthermore, Trx can utilize oxidized peroxiredoxins and glutathione peroxidases as oxidizing substrates and therefore plays an important role in recycling these antioxidant enzymes (see below) [235]. Following dithiol-disulfide exchange reaction, which results in reduced client and oxidized Trx/Grxs, the latter has to be regenerated to complete the catalytic cycle. Whereas Trx is enzymatically recovered by the action of thioredoxin reductase at the expense of NADPH [228], Grxs are mainly reduced by the consecutive reaction with two GSH molecules, which yields GSSG, and the action of glutathione reductase [234]. In contrast to this, aberrant S-glutathionylations of proteins as a consequence of unspecific hydroperoxide oxidation [236] can be reverted by the monothiol mechanism of both types of Grxs [234].

1.7.3. Peroxiredoxins

The human peroxiredoxin (Prx) family is comprised of six different isoforms, all of which are characterized by formation of different types of homooligomers and a common amino acid triad within their active site namely the peroxidatic cysteine (Cys), a threonine/serine (Thr/Ser) and an

arginine (Arg) residue [235,237]. They contribute to redox signaling as well as hydroperoxide detoxification in various cellular compartments and can be separated into 3 different subgroups according to their reaction mechanism: typical 2-Cys Prxs (PrxI-IV), atypical 2-Cys Prxs (PrxV) and 1-Cys Prxs (PrxVI) [226,238]. Upon hydroperoxide/H_2O_2-mediated oxidation of their active site cysteine (C_P) to sulfenic acid, all 2-Cys Prxs form a disulfide bond between C_P and a resolving cysteine residue (C_R) [238,239]. In typical 2-Cys Prxs this C_R is localized in a neighboring Prx molecule within the homooligomeric complex, which generates an intermolecular disulfide linkage. In contrast, atypical 2-Cys Prxs form intramolecular disulfide bonds between C_P and C_R [238,239]. However, the regeneration mechanism of these oxidized Prx species is identical in both groups and involves Trx-mediated reduction of the disulfide bond [237]. PrxVI, which lacks a C_R, has been shown to form mixed disulfides with π glutathione S-transferase (GST) [240,241]. This heterodimer is subsequently resolved by glutathione-mediated regeneration of PrxVI.

1.7.4. Glutathione peroxidases

The human glutathione peroxidase (GPx) family is phylogenetically unrelated to Prxs but shares the ability to reduce and thereby to detoxify hydroperoxide substrates [235]. It is comprised of eight different isoforms, which differ with respect to their subcellular localization, oligomeric state and the architecture of their active sites [242]. While human GPx1-4 and GPx6 rely on selenocysteines (Sec) in order to complete the common active site tetrad of glutamine, tryptophan and asparagine, GPx5, 7 and 8 incorporate cysteines (Cys) instead [243]. The reaction mechanism of GPxs involves peroxidatic selenoate or thiolate active site oxidation via hydroperoxide substrates/H_2O_2 to selenenic or sulfenic acid, respectively, and concomitant reduction of the ROS. Regeneration of Sec-GPxs typically involves the consecutive reaction with two molecules of GSH, which, via formation of a glutathionylated GPx intermediate, ultimately results in the formation of GSSG [228,235]. The GSSG is then reduced to GSH via the NADPH/glutathione reductase pathway. In contrast, Cys-GPxs, upon hydroperoxide/H_2O_2 oxidation of their thiolate active site, typically form an intramolecular disulfide bond with a resolving cysteine residue (C_R) [235]. They thereby resemble the reaction mechanism of atypical peroxiredoxins, which is also reflected by their Trx-mediated regeneration [242].

1.7.5. Regulation of the cellular antioxidant response

A key regulator of cellular redox homeostasis, which critically impacts on the above mentioned antioxidant mechanisms, is the ubiquitously expressed transcription factor nuclear factor erythroid 2-related factor 2 (Nrf2) [244,245,246]. Under homeostatic conditions, Nrf2 is bound in the cytosol by the E3 ubiquitin ligase substrate adaptor Kelch-like ECH-associated protein 1 (Keap1), the association with which constantly subjects Nrf2 to proteasomal degradation [247]. Since human Keap1 possesses 27 cysteine residues, it acts as the redox sensing unit [248]. However, although oxidative insults are well documented triggers for Nrf2 release from Keap1, the exact mechanisms are still under debate [249,250,251]. After dissociation from Keap1, Nrf2 heterodimerizes with the small musculoaponeurotic fibrosarcoma (Maf) protein and translocates to the nucleus where it specifically transactivates antioxidant responsive element (ARE)-possessing target genes [246]. Among others, Nrf2 increases GSH levels by stimulating the expression of the cystine/glutamate transporter SLC7A11, as well as glutamate-cysteine ligase catalytic (GCLC) and modifier (GCLM) subunits, the heterodimer of which catalyzes the rate-limiting step in GSH synthesis [252,253]. Furthermore, Nrf2 positively regulates the expression of a subset of peroxiredoxins and glutathione peroxidases, thioredoxin, thioredoxin reductase and glutathione reductase [252,254,255]. This increase in cellular antioxidants and GSH leads to reduction of aberrant disulfides and thereby to the regeneration of the native thiol state. Furthermore, Nrf2 also enhances biotransformation reactions with the goal to inactivate and excrete harmful xenobiotics by inducing phase I (oxidation, reduction and hydrolysis), phase II (conjugation), as well as phase III (transport) proteins [247].

In conclusion, cellular antioxidant response mechanisms aim to restore redox homeostasis by reverting deleterious posttranslational modifications like S-glutathionylation, aberrant disulfides or sulfoxidation downstream of oxidative insults. Orchestration of this broad and versatile array of antioxidant strategies is achieved by Nrf2, which also impacts on a wide variety of other cellular pathways. However, it is important to note that under homeostatic conditions, many of these defense mechanisms also take part in the modulation of physiological redox signaling cascades like RTK/MAP kinase signaling and thereby impinge on basal programs like cell growth or proliferation [220].

1.8. Aim of this thesis

The fundamental role of the Ero1α-PDI disulfide relay in the process of oxidative folding in the ER of mammalian cells is well established. Great progress has been made regarding the physical interactions in this relay, which enables a preferential flow of electrons [127,133,154]. Along the same line, characterization of feedback-regulated mechanisms, which govern Ero1α activity and concomitant H_2O_2 generation, have contributed to our understanding of the tight balancing of ER redox homeostasis [135,153]. However, it is surprising how well cells tolerate the over-expression of hyperactive Ero1 mutants, which lack these regulatory mechanisms [155]. The recent discovery of ER-resident peroxidases [111,138] provides a theoretical explanation of this mild phenotype, since they could buffer excessive H_2O_2 production by Ero1. However, cell biological evidence supporting the appealing idea of peroxidase-mediated detoxification of Ero1-derived H_2O_2 is still missing. Furthermore, as this "quenching" effect would only control the side product of Ero1 activity, i.e. H_2O_2, what happens to the excess of disulfide bonds being generated by constitutively active Ero1? A possible explanation would be the existence of an additional, hitherto unknown, inhibitory mechanism, which is still intact in hyperactive Ero1 mutants lacking the known regulatory disulfide bonds. Indeed, a crucial step in Ero1 activation has not been unraveled yet. The crystal structure of hyperactive Ero1 did not reveal a pathway or channel, which would provide access of O_2 to the bound FAD cofactor. Thus, since O_2 penetration is essential for regeneration of FAD from $FADH_2$, our mechanistic understanding of Ero1 activity might still be incomplete.

This thesis aimed to shed more light on the fate of Ero1-derived H_2O_2 by dissecting the roles of ER-resident peroxidases of the peroxiredoxin and glutathione peroxidase family. This could potentially clarify the controversially discussed contribution of Ero1-derived H_2O_2 to ER stress-induced apoptosis in human cells, which has been deduced from experiments in the model organisms *Saccharomyces cerevisiae* [256] and *Caenorhabditis elegans* [192] that both lack ER-resident peroxidases. In addition, I wanted to increase our understanding of Ero1 catalysis by elucidating the pathway and regulation of O_2 entry and subsequent H_2O_2 release from the protein-buried FAD. Answers to these questions would provide a molecular-level understanding of ER redox homeostasis in human cells that reaches beyond the previously described regulatory disulfides in Ero1α.

1.9. References

[1] K.A. Dill, J.L. MacCallum, The protein-folding problem, 50 years on, Science 338 (2012) 1042-1046.
[2] T. Gidalevitz, F. Stevens, Y. Argon, Orchestration of secretory protein folding by ER chaperones, Biochimica et biophysica acta doi: 10.1016/j.bbamcr.2013.03.007 (2013).
[3] K. Kojer, J. Riemer, Balancing oxidative protein folding: The influences of reducing pathways on disulfide bond formation, Biochimica et biophysica acta (2014).
[4] J.M. Herrmann, U. Jakob, Special issue: redox regulation of protein folding. Preface, Biochimica et biophysica acta 1783 (2008) 519.
[5] B. Bhandary, A. Marahatta, H.R. Kim, H.J. Chae, An involvement of oxidative stress in endoplasmic reticulum stress and its associated diseases, International journal of molecular sciences 14 (2012) 434-456.
[6] S. High, Protein translocation at the membrane of the endoplasmic reticulum, Progress in biophysics and molecular biology 63 (1995) 233-250.
[7] R. Gilmore, P. Walter, G. Blobel, Protein translocation across the endoplasmic reticulum. II. Isolation and characterization of the signal recognition particle receptor, The Journal of cell biology 95 (1982) 470-477.
[8] R. Gilmore, G. Blobel, P. Walter, Protein translocation across the endoplasmic reticulum. I. Detection in the microsomal membrane of a receptor for the signal recognition particle, The Journal of cell biology 95 (1982) 463-469.
[9] E. Swanton, N.J. Bulleid, Protein folding and translocation across the endoplasmic reticulum membrane, Molecular membrane biology 20 (2003) 99-104.
[10] I. Braakman, N.J. Bulleid, Protein folding and modification in the mammalian endoplasmic reticulum, Annual review of biochemistry 80 (2011) 71-99.
[11] M. Deponte, Glutathione catalysis and the reaction mechanisms of glutathione-dependent enzymes, Biochimica et biophysica acta 1830 (2013) 3217-3266.
[12] C. Hwang, A.J. Sinskey, H.F. Lodish, Oxidized redox state of glutathione in the endoplasmic reticulum, Science 257 (1992) 1496-1502.
[13] D. Montero, C. Tachibana, J. Rahr Winther, C. Appenzeller-Herzog, Intracellular glutathione pools are heterogeneously concentrated, Redox biology 1 (2013) 508-513.
[14] Y. Xiong, J.D. Uys, K.D. Tew, D.M. Townsend, S-glutathionylation: from molecular mechanisms to health outcomes, Antioxidants & redox signaling 15 (2011) 233-270.
[15] Y.M. Go, D.P. Jones, Redox compartmentalization in eukaryotic cells, Biochimica et biophysica acta 1780 (2008) 1273-1290.
[16] S. Piccirella, I. Czegle, B. Lizak, E. Margittai, S. Senesi, E. Papp, M. Csala, R. Fulceri, P. Csermely, J. Mandl, A. Benedetti, G. Banhegyi, Uncoupled redox systems in the lumen of the endoplasmic reticulum. Pyridine nucleotides stay reduced in an oxidative environment, The Journal of biological chemistry 281 (2006) 4671-4677.
[17] C. Appenzeller-Herzog, Glutathione- and non-glutathione-based oxidant control in the endoplasmic reticulum, Journal of cell science 124 (2011) 847-855.
[18] M. Gutscher, A.L. Pauleau, L. Marty, T. Brach, G.H. Wabnitz, Y. Samstag, A.J. Meyer, T.P. Dick, Real-time imaging of the intracellular glutathione redox potential, Nature methods 5 (2008) 553-559.
[19] H. Ostergaard, C. Tachibana, J.R. Winther, Monitoring disulfide bond formation in the eukaryotic cytosol, The Journal of cell biology 166 (2004) 337-345.
[20] J. Birk, M. Meyer, I. Aller, H.G. Hansen, A. Odermatt, T.P. Dick, A.J. Meyer, C. Appenzeller-Herzog, Endoplasmic reticulum: Reduced and oxidized glutathione revisited, Journal of cell science 126 (2013) 1604-1617.
[21] G. Banhegyi, L. Lusini, F. Puskas, R. Rossi, R. Fulceri, L. Braun, V. Mile, P. di Simplicio, J. Mandl, A. Benedetti, Preferential transport of glutathione versus glutathione disulfide in rat liver microsomal vesicles, The Journal of biological chemistry 274 (1999) 12213-12216.
[22] S. Le Gall, A. Neuhof, T. Rapoport, The endoplasmic reticulum membrane is permeable to small molecules, Molecular biology of the cell 15 (2004) 447-455.
[23] A.R. Frand, C.A. Kaiser, The ERO1 gene of yeast is required for oxidation of protein dithiols in the endoplasmic reticulum, Mol Cell 1 (1998) 161-170.
[24] M.G. Pollard, K.J. Travers, J.S. Weissman, Ero1p: a novel and ubiquitous protein with an essential role in oxidative protein folding in the endoplasmic reticulum, Mol Cell 1 (1998) 171-182.
[25] C.S. Sevier, J.W. Cuozzo, A. Vala, F. Aslund, C.A. Kaiser, A flavoprotein oxidase defines a new endoplasmic reticulum pathway for biosynthetic disulphide bond formation, Nature cell biology 3 (2001) 874-882.

[26] J.W. Cuozzo, C.A. Kaiser, Competition between glutathione and protein thiols for disulphide-bond formation, Nature cell biology 1 (1999) 130-135.
[27] S. Chakravarthi, C.E. Jessop, N.J. Bulleid, The role of glutathione in disulphide bond formation and endoplasmic-reticulum-generated oxidative stress, EMBO reports 7 (2006) 271-275.
[28] S. Chakravarthi, N.J. Bulleid, Glutathione is required to regulate the formation of native disulfide bonds within proteins entering the secretory pathway, The Journal of biological chemistry 279 (2004) 39872-39879.
[29] S.N. Molteni, A. Fassio, M.R. Ciriolo, G. Filomeni, E. Pasqualetto, C. Fagioli, R. Sitia, Glutathione limits Ero1-dependent oxidation in the endoplasmic reticulum, The Journal of biological chemistry 279 (2004) 32667-32673.
[30] C.E. Jessop, N.J. Bulleid, Glutathione directly reduces an oxidoreductase in the endoplasmic reticulum of mammalian cells, The Journal of biological chemistry 279 (2004) 55341-55347.
[31] T. Ramming, C. Appenzeller-Herzog, The physiological functions of mammalian endoplasmic oxidoreductin 1: on disulfides and more, Antioxidants & redox signaling 16 (2012) 1109-1118.
[32] C. Appenzeller-Herzog, J. Riemer, E. Zito, K.T. Chin, D. Ron, M. Spiess, L. Ellgaard, Disulphide production by Ero1alpha-PDI relay is rapid and effectively regulated, The EMBO journal 29 (2010) 3318-3329.
[33] A. Jansens, E. van Duijn, I. Braakman, Coordinated nonvectorial folding in a newly synthesized multidomain protein, Science 298 (2002) 2401-2403.
[34] S. Munro, H.R. Pelham, A C-terminal signal prevents secretion of luminal ER proteins, Cell 48 (1987) 899-907.
[35] I. Raykhel, H. Alanen, K. Salo, J. Jurvansuu, V.D. Nguyen, M. Latva-Ranta, L. Ruddock, A molecular specificity code for the three mammalian KDEL receptors, The Journal of cell biology 179 (2007) 1193-1204.
[36] D.W. Wilson, M.J. Lewis, H.R. Pelham, pH-dependent binding of KDEL to its receptor in vitro, The Journal of biological chemistry 268 (1993) 7465-7468.
[37] M.M. Wu, M. Grabe, S. Adams, R.Y. Tsien, H.P. Moore, T.E. Machen, Mechanisms of pH regulation in the regulated secretory pathway, The Journal of biological chemistry 276 (2001) 33027-33035.
[38] T.E. Machen, M.J. Leigh, C. Taylor, T. Kimura, S. Asano, H.P. Moore, pH of TGN and recycling endosomes of H+/K+-ATPase-transfected HEK-293 cells: implications for pH regulation in the secretory pathway, American journal of physiology. Cell physiology 285 (2003) C205-214.
[39] M.J. Lewis, H.R. Pelham, Ligand-induced redistribution of a human KDEL receptor from the Golgi complex to the endoplasmic reticulum, Cell 68 (1992) 353-364.
[40] T. Aoe, A.J. Lee, E. van Donselaar, P.J. Peters, V.W. Hsu, Modulation of intracellular transport by transported proteins: insight from regulation of COPI-mediated transport, Proceedings of the National Academy of Sciences of the United States of America 95 (1998) 1624-1629.
[41] L. Orci, M. Stamnes, M. Ravazzola, M. Amherdt, A. Perrelet, T.H. Sollner, J.E. Rothman, Bidirectional transport by distinct populations of COPI-coated vesicles, Cell 90 (1997) 335-349.
[42] H.R. Pelham, Recycling of proteins between the endoplasmic reticulum and Golgi complex, Current opinion in cell biology 3 (1991) 585-591.
[43] P. Cosson, F. Letourneur, Coatomer interaction with di-lysine endoplasmic reticulum retention motifs, Science 263 (1994) 1629-1631.
[44] P. Sharma, V. Ignatchenko, K. Grace, C. Ursprung, T. Kislinger, A.O. Gramolini, Endoplasmic reticulum protein targeting of phospholamban: a common role for an N-terminal di-arginine motif in ER retention?, PloS one 5 (2010) e11496.
[45] S. Rajagopalan, Y. Xu, M.B. Brenner, Retention of unassembled components of integral membrane proteins by calnexin, Science 263 (1994) 387-390.
[46] L. Ellgaard, A. Helenius, Quality control in the endoplasmic reticulum, Nature reviews. Molecular cell biology 4 (2003) 181-191.
[47] M.J. Bottomley, M.R. Batten, R.A. Lumb, N.J. Bulleid, Quality control in the endoplasmic reticulum: PDI mediates the ER retention of unassembled procollagen C-propeptides, Current biology : CB 11 (2001) 1114-1118.
[48] K. Yamamoto, R. Fujii, Y. Toyofuku, T. Saito, H. Koseki, V.W. Hsu, T. Aoe, The KDEL receptor mediates a retrieval mechanism that contributes to quality control at the endoplasmic reticulum, The EMBO journal 20 (2001) 3082-3091.
[49] J.M. Kowalski, R.N. Parekh, J. Mao, K.D. Wittrup, Protein folding stability can determine the efficiency of escape from endoplasmic reticulum quality control, The Journal of biological chemistry 273 (1998) 19453-19458.

[50] J.M. Kowalski, R.N. Parekh, K.D. Wittrup, Secretion efficiency in Saccharomyces cerevisiae of bovine pancreatic trypsin inhibitor mutants lacking disulfide bonds is correlated with thermodynamic stability, Biochemistry 37 (1998) 1264-1273.
[51] Y. Hagihara, P.S. Kim, Toward development of a screen to identify randomly encoded, foldable sequences, Proceedings of the National Academy of Sciences of the United States of America 99 (2002) 6619-6624.
[52] T. Kjeldsen, S. Ludvigsen, I. Diers, P. Balschmidt, A.R. Sorensen, N.C. Kaarsholm, Engineering-enhanced protein secretory expression in yeast with application to insulin, The Journal of biological chemistry 277 (2002) 18245-18248.
[53] J.L. Goeckeler, J.L. Brodsky, Molecular chaperones and substrate ubiquitination control the efficiency of endoplasmic reticulum-associated degradation, Diabetes, obesity & metabolism 12 Suppl 2 (2010) 32-38.
[54] A.A. McCracken, J.L. Brodsky, Assembly of ER-associated protein degradation in vitro: dependence on cytosol, calnexin, and ATP, The Journal of cell biology 132 (1996) 291-298.
[55] L. Ellgaard, M. Molinari, A. Helenius, Setting the standards: quality control in the secretory pathway, Science 286 (1999) 1882-1888.
[56] C. Hammond, I. Braakman, A. Helenius, Role of N-linked oligosaccharide recognition, glucose trimming, and calnexin in glycoprotein folding and quality control, Proceedings of the National Academy of Sciences of the United States of America 91 (1994) 913-917.
[57] D.N. Hebert, B. Foellmer, A. Helenius, Glucose trimming and reglucosylation determine glycoprotein association with calnexin in the endoplasmic reticulum, Cell 81 (1995) 425-433.
[58] F.E. Ware, A. Vassilakos, P.A. Peterson, M.R. Jackson, M.A. Lehrman, D.B. Williams, The molecular chaperone calnexin binds Glc1Man9GlcNAc2 oligosaccharide as an initial step in recognizing unfolded glycoproteins, The Journal of biological chemistry 270 (1995) 4697-4704.
[59] M. Molinari, A. Helenius, Glycoproteins form mixed disulphides with oxidoreductases during folding in living cells, Nature 402 (1999) 90-93.
[60] J.D. Oliver, H.L. Roderick, D.H. Llewellyn, S. High, ERp57 functions as a subunit of specific complexes formed with the ER lectins calreticulin and calnexin, Molecular biology of the cell 10 (1999) 2573-2582.
[61] J.D. Oliver, F.J. van der Wal, N.J. Bulleid, S. High, Interaction of the thiol-dependent reductase ERp57 with nascent glycoproteins, Science 275 (1997) 86-88.
[62] G.Z. Lederkremer, M.H. Glickman, A window of opportunity: timing protein degradation by trimming of sugars and ubiquitins, Trends in biochemical sciences 30 (2005) 297-303.
[63] K.W. Moremen, M. Molinari, N-linked glycan recognition and processing: the molecular basis of endoplasmic reticulum quality control, Current opinion in structural biology 16 (2006) 592-599.
[64] A.J. Parodi, Protein glucosylation and its role in protein folding, Annual review of biochemistry 69 (2000) 69-93.
[65] S.P. Ferris, V.K. Kodali, R.J. Kaufman, Glycoprotein folding and quality-control mechanisms in protein-folding diseases, Disease models & mechanisms 7 (2014) 331-341.
[66] M. Aebi, R. Bernasconi, S. Clerc, M. Molinari, N-glycan structures: recognition and processing in the ER, Trends in biochemical sciences 35 (2010) 74-82.
[67] R. Ushioda, J. Hoseki, K. Araki, G. Jansen, D.Y. Thomas, K. Nagata, ERdj5 is required as a disulfide reductase for degradation of misfolded proteins in the ER, Science 321 (2008) 569-572.
[68] R. Ushioda, J. Hoseki, K. Nagata, Glycosylation-independent ERAD pathway serves as a backup system under ER stress, Molecular biology of the cell 24 (2013) 3155-3163.
[69] N. Mimura, S. Yuasa, M. Soma, H. Jin, K. Kimura, S. Goto, H. Koseki, T. Aoe, Altered quality control in the endoplasmic reticulum causes cortical dysplasia in knock-in mice expressing a mutant BiP, Molecular and cellular biology 28 (2008) 293-301.
[70] P. Gillece, M. Pilon, K. Romisch, The protein translocation channel mediates glycopeptide export across the endoplasmic reticulum membrane, Proceedings of the National Academy of Sciences of the United States of America 97 (2000) 4609-4614.
[71] E.J. Wiertz, D. Tortorella, M. Bogyo, J. Yu, W. Mothes, T.R. Jones, T.A. Rapoport, H.L. Ploegh, Sec61-mediated transfer of a membrane protein from the endoplasmic reticulum to the proteasome for destruction, Nature 384 (1996) 432-438.
[72] J.C. Christianson, T.A. Shaler, R.E. Tyler, R.R. Kopito, OS-9 and GRP94 deliver mutant alpha1-antitrypsin to the Hrd1-SEL1L ubiquitin ligase complex for ERAD, Nature cell biology 10 (2008) 272-282.
[73] N. Hosokawa, I. Wada, K. Nagasawa, T. Moriyama, K. Okawa, K. Nagata, Human XTP3-B forms an endoplasmic reticulum quality control scaffold with the HRD1-SEL1L ubiquitin ligase complex and BiP, The Journal of biological chemistry 283 (2008) 20914-20924.

[74] S.S. Vembar, J.L. Brodsky, One step at a time: endoplasmic reticulum-associated degradation, Nature reviews. Molecular cell biology 9 (2008) 944-957.
[75] J.W. Yewdell, U. Schubert, J.R. Bennink, At the crossroads of cell biology and immunology: DRiPs and other sources of peptide ligands for MHC class I molecules, Journal of cell science 114 (2001) 845-851.
[76] F.R. Laurindo, L.A. Pescatore, C. Fernandes Dde, Protein disulfide isomerase in redox cell signaling and homeostasis, Free radical biology & medicine 52 (2012) 1954-1969.
[77] J.L. Pan, J.C. Bardwell, The origami of thioredoxin-like folds, Protein science : a publication of the Protein Society 15 (2006) 2217-2227.
[78] G. Kozlov, P. Maattanen, D.Y. Thomas, K. Gehring, A structural overview of the PDI family of proteins, The FEBS journal 277 (2010) 3924-3936.
[79] M. Cortini, R. Sitia, From antibodies to adiponectin: role of ERp44 in sizing and timing protein secretion, Diabetes, obesity & metabolism 12 Suppl 2 (2010) 39-47.
[80] T. Kakihana, K. Araki, S. Vavassori, S. Iemura, M. Cortini, C. Fagioli, T. Natsume, R. Sitia, K. Nagata, Dynamic regulation of Ero1alpha and peroxiredoxin 4 localization in the secretory pathway, The Journal of biological chemistry 288 (2013) 29586-29594.
[81] T. Anelli, M. Alessio, A. Mezghrani, T. Simmen, F. Talamo, A. Bachi, R. Sitia, ERp44, a novel endoplasmic reticulum folding assistant of the thioredoxin family, The EMBO journal 21 (2002) 835-844.
[82] T. Anelli, S. Ceppi, L. Bergamelli, M. Cortini, S. Masciarelli, C. Valetti, R. Sitia, Sequential steps and checkpoints in the early exocytic compartment during secretory IgM biogenesis, The EMBO journal 26 (2007) 4177-4188.
[83] C. Appenzeller-Herzog, L. Ellgaard, The human PDI family: versatility packed into a single fold, Biochim Biophys Acta 1783 (2008) 535-548.
[84] G. Tian, S. Xiang, R. Noiva, W.J. Lennarz, H. Schindelin, The crystal structure of yeast protein disulfide isomerase suggests cooperativity between its active sites, Cell 124 (2006) 61-73.
[85] P. Koivunen, A. Pirneskoski, P. Karvonen, J. Ljung, T. Helaakoski, H. Notbohm, K.I. Kivirikko, The acidic C-terminal domain of protein disulfide isomerase is not critical for the enzyme subunit function or for the chaperone or disulfide isomerase activities of the polypeptide, The EMBO journal 18 (1999) 65-74.
[86] C. Wang, S. Chen, X. Wang, L. Wang, A.K. Wallis, R.B. Freedman, C.C. Wang, Plasticity of human protein disulfide isomerase: evidence for mobility around the X-linker region and its functional significance, The Journal of biological chemistry 285 (2010) 26788-26797.
[87] C. Wang, W. Li, J. Ren, J. Fang, H. Ke, W. Gong, W. Feng, C.C. Wang, Structural insights into the redox-regulated dynamic conformations of human protein disulfide isomerase, Antioxidants & redox signaling 19 (2013) 36-45.
[88] A.Y. Denisov, P. Maattanen, C. Dabrowski, G. Kozlov, D.Y. Thomas, K. Gehring, Solution structure of the bb' domains of human protein disulfide isomerase, The FEBS journal 276 (2009) 1440-1449.
[89] V.D. Nguyen, K. Wallis, M.J. Howard, A.M. Haapalainen, K.E. Salo, M.J. Saaranen, A. Sidhu, R.K. Wierenga, R.B. Freedman, L.W. Ruddock, R.A. Williamson, Alternative conformations of the x region of human protein disulphide-isomerase modulate exposure of the substrate binding b' domain, Journal of molecular biology 383 (2008) 1144-1155.
[90] R.F. Goldberger, C.J. Epstein, C.B. Anfinsen, Acceleration of reactivation of reduced bovine pancreatic ribonuclease by a microsomal system from rat liver, The Journal of biological chemistry 238 (1963) 628-635.
[91] N.J. Bulleid, R.B. Freedman, Defective co-translational formation of disulphide bonds in protein disulphide-isomerase-deficient microsomes, Nature 335 (1988) 649-651.
[92] J.L. Ashworth, V. Kelly, R. Wilson, C.A. Shuttleworth, C.M. Kielty, Fibrillin assembly: dimer formation mediated by amino-terminal sequences, Journal of cell science 112 (Pt 20) (1999) 3549-3558.
[93] R.A. Roth, S.B. Pierce, In vivo cross-linking of protein disulfide isomerase to immunoglobulins, Biochemistry 26 (1987) 4179-4182.
[94] J. Koivu, R. Myllyla, Interchain disulfide bond formation in types I and II procollagen. Evidence for a protein disulfide isomerase catalyzing bond formation, The Journal of biological chemistry 262 (1987) 6159-6164.
[95] J. Koivu, R. Myllyla, T. Helaakoski, T. Pihlajaniemi, K. Tasanen, K.I. Kivirikko, A single polypeptide acts both as the beta subunit of prolyl 4-hydroxylase and as a protein disulfide-isomerase, The Journal of biological chemistry 262 (1987) 6447-6449.
[96] B. Di Jeso, Y.N. Park, L. Ulianich, A.S. Treglia, M.L. Urbanas, S. High, P. Arvan, Mixed-disulfide folding intermediates between thyroglobulin and endoplasmic reticulum resident oxidoreductases ERp57 and protein disulfide isomerase, Molecular and cellular biology 25 (2005) 9793-9805.

[97] M. Baryshev, E. Sargsyan, S. Mkrtchian, ERp29 is an essential endoplasmic reticulum factor regulating secretion of thyroglobulin, Biochemical and biophysical research communications 340 (2006) 617-624.
[98] G. Kuznetsov, L.B. Chen, S.K. Nigam, Multiple molecular chaperones complex with misfolded large oligomeric glycoproteins in the endoplasmic reticulum, The Journal of biological chemistry 272 (1997) 3057-3063.
[99] G. Dong, P.A. Wearsch, D.R. Peaper, P. Cresswell, K.M. Reinisch, Insights into MHC class I peptide loading from the structure of the tapasin-ERp57 thiol oxidoreductase heterodimer, Immunity 30 (2009) 21-32.
[100] C.E. Jessop, S. Chakravarthi, N. Garbi, G.J. Hammerling, S. Lovell, N.J. Bulleid, ERp57 is essential for efficient folding of glycoproteins sharing common structural domains, The EMBO journal 26 (2007) 28-40.
[101] A. Kienast, M. Preuss, M. Winkler, T.P. Dick, Redox regulation of peptide receptivity of major histocompatibility complex class I molecules by ERp57 and tapasin, Nature immunology 8 (2007) 864-872.
[102] B. Park, S. Lee, E. Kim, K. Cho, S.R. Riddell, S. Cho, K. Ahn, Redox regulation facilitates optimal peptide selection by MHC class I during antigen processing, Cell 127 (2006) 369-382.
[103] P. Cresswell, A.L. Ackerman, A. Giodini, D.R. Peaper, P.A. Wearsch, Mechanisms of MHC class I-restricted antigen processing and cross-presentation, Immunological reviews 207 (2005) 145-157.
[104] M. Molinari, C. Galli, V. Piccaluga, M. Pieren, P. Paganetti, Sequential assistance of molecular chaperones and transient formation of covalent complexes during protein degradation from the ER, The Journal of cell biology 158 (2002) 247-257.
[105] Y. Li, P. Camacho, Ca2+-dependent redox modulation of SERCA 2b by ERp57, The Journal of cell biology 164 (2004) 35-46.
[106] T. Higo, M. Hattori, T. Nakamura, T. Natsume, T. Michikawa, K. Mikoshiba, Subtype-specific and ER lumenal environment-dependent regulation of inositol 1,4,5-trisphosphate receptor type 1 by ERp44, Cell 120 (2005) 85-98.
[107] V.K. Kodali, C. Thorpe, Oxidative protein folding and the Quiescin-sulfhydryl oxidase family of flavoproteins, Antioxidants & redox signaling 13 (2010) 1217-1230.
[108] S. Schulman, B. Wang, W. Li, T.A. Rapoport, Vitamin K epoxide reductase prefers ER membrane-anchored thioredoxin-like redox partners, Proc Natl Acad Sci U S A 107 (2010) 15027-15032.
[109] T.J. Tavender, J.J. Springate, N.J. Bulleid, Recycling of peroxiredoxin IV provides a novel pathway for disulphide formation in the endoplasmic reticulum, The EMBO journal 29 (2010) 4185-4197.
[110] E. Zito, E.P. Melo, Y. Yang, A. Wahlander, T.A. Neubert, D. Ron, Oxidative protein folding by an endoplasmic reticulum-localized peroxiredoxin, Molecular cell 40 (2010) 787-797.
[111] V.D. Nguyen, M.J. Saaranen, A.R. Karala, A.K. Lappi, L. Wang, I.B. Raykhel, H.I. Alanen, K.E. Salo, C.C. Wang, L.W. Ruddock, Two endoplasmic reticulum PDI peroxidases increase the efficiency of the use of peroxide during disulfide bond formation, Journal of molecular biology 406 (2011) 503-515.
[112] N.J. Bulleid, L. Ellgaard, Multiple ways to make disulfides, Trends in biochemical sciences 36 (2011) 485-492.
[113] K.L. Hoober, B. Joneja, H.B. White, 3rd, C. Thorpe, A sulfhydryl oxidase from chicken egg white, The Journal of biological chemistry 271 (1996) 30510-30516.
[114] K.L. Hoober, S.L. Sheasley, H.F. Gilbert, C. Thorpe, Sulfhydryl oxidase from egg white. A facile catalyst for disulfide bond formation in proteins and peptides, The Journal of biological chemistry 274 (1999) 22147-22150.
[115] P.C. Rancy, C. Thorpe, Oxidative protein folding in vitro: a study of the cooperation between quiescin-sulfhydryl oxidase and protein disulfide isomerase, Biochemistry 47 (2008) 12047-12056.
[116] S. Chakravarthi, C.E. Jessop, M. Willer, C.J. Stirling, N.J. Bulleid, Intracellular catalysis of disulfide bond formation by the human sulfhydryl oxidase, QSOX1, The Biochemical journal 404 (2007) 403-411.
[117] T. Ilani, A. Alon, I. Grossman, B. Horowitz, E. Kartvelishvily, S.R. Cohen, D. Fass, A Secreted Disulfide Catalyst Controls Extracellular Matrix Composition and Function, Science (2013).
[118] L.A. Rutkevich, D.B. Williams, Vitamin K epoxide reductase contributes to protein disulfide formation and redox homeostasis within the endoplasmic reticulum, Molecular biology of the cell 23 (2012) 2017-2027.
[119] D.Y. Jin, J.K. Tie, D.W. Stafford, The conversion of vitamin K epoxide to vitamin K quinone and vitamin K quinone to vitamin K hydroquinone uses the same active site cysteines, Biochemistry 46 (2007) 7279-7283.
[120] W. Li, S. Schulman, R.J. Dutton, D. Boyd, J. Beckwith, T.A. Rapoport, Structure of a bacterial homologue of vitamin K epoxide reductase, Nature 463 (2010) 507-512.
[121] S. Dias-Gunasekara, J. Gubbens, M. van Lith, C. Dunne, J.A. Williams, R. Kataky, D. Scoones, A. Lapthorn, N.J. Bulleid, A.M. Benham, Tissue-specific expression and dimerization of the endoplasmic reticulum oxidoreductase Ero1beta, J Biol Chem 280 (2005) 33066-33075.

[122] M. Pagani, M. Fabbri, C. Benedetti, A. Fassio, S. Pilati, N.J. Bulleid, A. Cabibbo, R. Sitia, Endoplasmic reticulum oxidoreductin 1-lbeta (ERO1-Lbeta), a human gene induced in the course of the unfolded protein response, J Biol Chem 275 (2000) 23685-23692.
[123] B.P. Tu, S.C. Ho-Schleyer, K.J. Travers, J.S. Weissman, Biochemical basis of oxidative protein folding in the endoplasmic reticulum, Science 290 (2000) 1571-1574.
[124] E. Gross, C.S. Sevier, N. Heldman, E. Vitu, M. Bentzur, C.A. Kaiser, C. Thorpe, D. Fass, Generating disulfides enzymatically: reaction products and electron acceptors of the endoplasmic reticulum thiol oxidase Ero1p, Proceedings of the National Academy of Sciences of the United States of America 103 (2006) 299-304.
[125] G. Bertoli, T. Simmen, T. Anelli, S.N. Molteni, R. Fesce, R. Sitia, Two conserved cysteine triads in human Ero1alpha cooperate for efficient disulfide bond formation in the endoplasmic reticulum, J Biol Chem 279 (2004) 30047-30052.
[126] C.S. Sevier, C.A. Kaiser, Ero1 and redox homeostasis in the endoplasmic reticulum, Biochimica et biophysica acta 1783 (2008) 549-556.
[127] K. Inaba, S. Masui, H. Iida, S. Vavassori, R. Sitia, M. Suzuki, Crystal structures of human Ero1alpha reveal the mechanisms of regulated and targeted oxidation of PDI, EMBO J 29 (2010) 3330-3343.
[128] E.J. Heckler, P.C. Rancy, V.K. Kodali, C. Thorpe, Generating disulfides with the Quiescin-sulfhydryl oxidases, Biochimica et biophysica acta 1783 (2008) 567-577.
[129] T.J. Tavender, N.J. Bulleid, Molecular mechanisms regulating oxidative activity of the Ero1 family in the endoplasmic reticulum, Antioxidants & redox signaling 13 (2010) 1177-1187.
[130] A.M. Benham, A. Cabibbo, A. Fassio, N. Bulleid, R. Sitia, I. Braakman, The CXXCXXC motif determines the folding, structure and stability of human Ero1-Lalpha, EMBO J 19 (2000) 4493-4502.
[131] A. Mezghrani, A. Fassio, A. Benham, T. Simmen, I. Braakman, R. Sitia, Manipulation of oxidative protein folding and PDI redox state in mammalian cells, EMBO J 20 (2001) 6288-6296.
[132] M. Otsu, G. Bertoli, C. Fagioli, E. Guerini-Rocco, S. Nerini-Molteni, E. Ruffato, R. Sitia, Dynamic retention of Ero1alpha and Ero1beta in the endoplasmic reticulum by interactions with PDI and ERp44, Antioxidants & redox signaling 8 (2006) 274-282.
[133] S. Masui, S. Vavassori, C. Fagioli, R. Sitia, K. Inaba, Molecular Bases of Cyclic and Specific Disulfide Interchange between Human ERO1{alpha} Protein and Protein-disulfide Isomerase (PDI), J Biol Chem 286 (2011) 16261-16271.
[134] K. Araki, K. Nagata, Functional in vitro analysis of ERO1 and protein-disulfide isomerase (PDI) pathway, J Biol Chem 286 (2011) 32705-32712.
[135] K.M. Baker, S. Chakravarthi, K.P. Langton, A.M. Sheppard, H. Lu, N.J. Bulleid, Low reduction potential of Ero1alpha regulatory disulphides ensures tight control of substrate oxidation, EMBO J 27 (2008) 2988-2997.
[136] L. Wang, S.J. Li, A. Sidhu, L. Zhu, Y. Liang, R.B. Freedman, C.C. Wang, Reconstitution of human Ero1-Lalpha/protein-disulfide isomerase oxidative folding pathway in vitro. Position-dependent differences in role between the a and a' domains of protein-disulfide isomerase, The Journal of biological chemistry 284 (2009) 199-206.
[137] E. Vitu, S. Kim, C.S. Sevier, O. Lutzky, N. Heldman, M. Bentzur, T. Unger, M. Yona, C.A. Kaiser, D. Fass, Oxidative activity of yeast Ero1p on protein disulfide isomerase and related oxidoreductases of the endoplasmic reticulum, J Biol Chem 285 (2010) 18155-18165.
[138] T.J. Tavender, A.M. Sheppard, N.J. Bulleid, Peroxiredoxin IV is an endoplasmic reticulum-localized enzyme forming oligomeric complexes in human cells, The Biochemical journal 411 (2008) 191-199.
[139] T. Ramming, C. Appenzeller-Herzog, Destroy and exploit: catalyzed removal of hydroperoxides from the endoplasmic reticulum, International journal of cell biology 2013 (2013) 180906.
[140] X. Wang, L. Wang, F. Sun, C.C. Wang, Structural insights into the peroxidase activity and inactivation of human peroxiredoxin 4, The Biochemical journal 441 (2012) 113-118.
[141] Y. Sato, R. Kojima, M. Okumura, M. Hagiwara, S. Masui, K. Maegawa, M. Saiki, T. Horibe, M. Suzuki, K. Inaba, Synergistic cooperation of PDI family members in peroxiredoxin 4-driven oxidative protein folding, Scientific reports 3 (2013) 2456.
[142] Z. Cao, T.J. Tavender, A.W. Roszak, R.J. Cogdell, N.J. Bulleid, Crystal structure of reduced and of oxidized peroxiredoxin IV enzyme reveals a stable oxidized decamer and a non-disulfide-bonded intermediate in the catalytic cycle, The Journal of biological chemistry 286 (2011) 42257-42266.
[143] R.E. Martin, Z. Cao, N.J. Bulleid, Regulating the level of intracellular hydrogen peroxide: the role of peroxiredoxin IV, Biochemical Society transactions 42 (2014) 42-46.

[144] T.J. Tavender, N.J. Bulleid, Peroxiredoxin IV protects cells from oxidative stress by removing H2O2 produced during disulphide formation, Journal of cell science 123 (2010) 2672-2679.
[145] E. Zito, H.G. Hansen, G.S. Yeo, J. Fujii, D. Ron, Endoplasmic reticulum thiol oxidase deficiency leads to ascorbic acid depletion and noncanonical scurvy in mice, Molecular cell 48 (2012) 39-51.
[146] V. Bosello-Travain, M. Conrad, G. Cozza, A. Negro, S. Quartesan, M. Rossetto, A. Roveri, S. Toppo, F. Ursini, M. Zaccarin, M. Maiorino, Protein Disulfide Isomerase and Glutathione are alternative substrates in the one Cys catalytic cycle of Glutathione Peroxidase 7, Biochimica et biophysica acta 1830 (2013) 3846-3857.
[147] L. Wang, L. Zhang, Y. Niu, R. Sitia, C.C. Wang, Glutathione peroxidase 7 utilizes hydrogen peroxide generated by Ero1alpha to promote oxidative protein folding, Antioxidants & redox signaling doi: 10.1089/ars.2013.5236 (2013).
[148] S. Toppo, S. Vanin, V. Bosello, S.C. Tosatto, Evolutionary and structural insights into the multifaceted glutathione peroxidase (Gpx) superfamily, Antioxidants & redox signaling 10 (2008) 1501-1514.
[149] P.C. Wei, Y.H. Hsieh, M.I. Su, X.J. Jiang, P.H. Hsu, W.T. Lo, J.Y. Weng, Y.M. Jeng, J.M. Wang, P.L. Chen, Y.C. Chang, K.F. Lee, M.D. Tsai, J.Y. Shew, W.H. Lee, Loss of the Oxidative Stress Sensor NPGPx Compromises GRP78 Chaperone Activity and Induces Systemic Disease, Molecular cell 48 (2012) 747-759.
[150] C.S. Sevier, H. Qu, N. Heldman, E. Gross, D. Fass, C.A. Kaiser, Modulation of cellular disulfide-bond formation and the ER redox environment by feedback regulation of Ero1, Cell 129 (2007) 333-344.
[151] N. Heldman, O. Vonshak, C.S. Sevier, E. Vitu, T. Mehlman, D. Fass, Steps in reductive activation of the disulfide-generating enzyme Ero1p, Protein Sci 19 (2010) 1863-1876.
[152] H.G. Hansen, C.L. Soltoft, J.D. Schmidt, J. Birk, C. Appenzeller-Herzog, L. Ellgaard, Biochemical evidence that regulation of Ero1beta activity in human cells does not involve the isoform-specific cysteine 262, Bioscience reports (2014).
[153] C. Appenzeller-Herzog, J. Riemer, B. Christensen, E.S. Sorensen, L. Ellgaard, A novel disulphide switch mechanism in Ero1alpha balances ER oxidation in human cells, The EMBO journal 27 (2008) 2977-2987.
[154] K. Araki, S. Iemura, Y. Kamiya, D. Ron, K. Kato, T. Natsume, K. Nagata, Ero1-alpha and PDIs constitute a hierarchical electron transfer network of endoplasmic reticulum oxidoreductases, The Journal of cell biology 202 (2013) 861-874.
[155] H.G. Hansen, J.D. Schmidt, C.L. Soltoft, T. Ramming, H.M. Geertz-Hansen, B. Christensen, E.S. Sorensen, A.S. Juncker, C. Appenzeller-Herzog, L. Ellgaard, Hyperactivity of the ero1alpha oxidase elicits endoplasmic reticulum stress but no broad antioxidant response, The Journal of biological chemistry 287 (2012) 39513-39523.
[156] C. Hetz, The unfolded protein response: controlling cell fate decisions under ER stress and beyond, Nature reviews. Molecular cell biology 13 (2012) 89-102.
[157] J.N. Gass, N.M. Gifford, J.W. Brewer, Activation of an unfolded protein response during differentiation of antibody-secreting B cells, The Journal of biological chemistry 277 (2002) 49047-49054.
[158] N.N. Iwakoshi, A.H. Lee, P. Vallabhajosyula, K.L. Otipoby, K. Rajewsky, L.H. Glimcher, Plasma cell differentiation and the unfolded protein response intersect at the transcription factor XBP-1, Nature immunology 4 (2003) 321-329.
[159] E. van Anken, E.P. Romijn, C. Maggioni, A. Mezghrani, R. Sitia, I. Braakman, A.J. Heck, Sequential waves of functionally related proteins are expressed when B cells prepare for antibody secretion, Immunity 18 (2003) 243-253.
[160] A. Higa, E. Chevet, Redox signaling loops in the unfolded protein response, Cellular signalling 24 (2012) 1548-1555.
[161] J.D. Malhotra, R.J. Kaufman, Endoplasmic reticulum stress and oxidative stress: a vicious cycle or a double-edged sword?, Antioxidants & redox signaling 9 (2007) 2277-2293.
[162] R.J. Kaufman, S.H. Back, B. Song, J. Han, J. Hassler, The unfolded protein response is required to maintain the integrity of the endoplasmic reticulum, prevent oxidative stress and preserve differentiation in beta-cells, Diabetes, obesity & metabolism 12 Suppl 2 (2010) 99-107.
[163] J.B. DuRose, A.B. Tam, M. Niwa, Intrinsic capacities of molecular sensors of the unfolded protein response to sense alternate forms of endoplasmic reticulum stress, Molecular biology of the cell 17 (2006) 3095-3107.
[164] M. Li, P. Baumeister, B. Roy, T. Phan, D. Foti, S. Luo, A.S. Lee, ATF6 as a transcription activator of the endoplasmic reticulum stress element: thapsigargin stress-induced changes and synergistic interactions with NF-Y and YY1, Molecular and cellular biology 20 (2000) 5096-5106.
[165] D. Ron, P. Walter, Signal integration in the endoplasmic reticulum unfolded protein response, Nature reviews. Molecular cell biology 8 (2007) 519-529.

[166] D. Eletto, D. Dersh, T. Gidalevitz, Y. Argon, Protein disulfide isomerase A6 controls the decay of IRE1alpha signaling via disulfide-dependent association, Molecular cell 53 (2014) 562-576.
[167] N.J. Darling, S.J. Cook, The role of MAPK signalling pathways in the response to endoplasmic reticulum stress, Biochimica et biophysica acta (2014).
[168] A. Bertolotti, Y. Zhang, L.M. Hendershot, H.P. Harding, D. Ron, Dynamic interaction of BiP and ER stress transducers in the unfolded-protein response, Nature cell biology 2 (2000) 326-332.
[169] D. Han, A.G. Lerner, L. Vande Walle, J.P. Upton, W. Xu, A. Hagen, B.J. Backes, S.A. Oakes, F.R. Papa, IRE1alpha kinase activation modes control alternate endoribonuclease outputs to determine divergent cell fates, Cell 138 (2009) 562-575.
[170] Y. Kimata, K. Kohno, Endoplasmic reticulum stress-sensing mechanisms in yeast and mammalian cells, Current opinion in cell biology 23 (2011) 135-142.
[171] J. Shen, X. Chen, L. Hendershot, R. Prywes, ER stress regulation of ATF6 localization by dissociation of BiP/GRP78 binding and unmasking of Golgi localization signals, Developmental cell 3 (2002) 99-111.
[172] Y. Sato, S. Nadanaka, T. Okada, K. Okawa, K. Mori, Luminal domain of ATF6 alone is sufficient for sensing endoplasmic reticulum stress and subsequent transport to the Golgi apparatus, Cell structure and function 36 (2011) 35-47.
[173] M. Hong, S. Luo, P. Baumeister, J.M. Huang, R.K. Gogia, M. Li, A.S. Lee, Underglycosylation of ATF6 as a novel sensing mechanism for activation of the unfolded protein response, The Journal of biological chemistry 279 (2004) 11354-11363.
[174] A.H. Lee, N.N. Iwakoshi, L.H. Glimcher, XBP-1 regulates a subset of endoplasmic reticulum resident chaperone genes in the unfolded protein response, Molecular and cellular biology 23 (2003) 7448-7459.
[175] A. Volchuk, D. Ron, The endoplasmic reticulum stress response in the pancreatic beta-cell, Diabetes, obesity & metabolism 12 Suppl 2 (2010) 48-57.
[176] A. Higa, S. Taouji, S. Lhomond, D. Jensen, M.E. Fernandez-Zapico, J.C. Simpson, J.M. Pasquet, R. Schekman, E. Chevet, Endoplasmic Reticulum Stress-Activated Transcription Factor ATF6alpha Requires the Disulfide Isomerase PDIA5 To Modulate Chemoresistance, Molecular and cellular biology 34 (2014) 1839-1849.
[177] S. Nadanaka, T. Okada, H. Yoshida, K. Mori, Role of disulfide bridges formed in the luminal domain of ATF6 in sensing endoplasmic reticulum stress, Molecular and cellular biology 27 (2007) 1027-1043.
[178] G. Jansen, P. Maattanen, A.Y. Denisov, L. Scarffe, B. Schade, H. Balghi, K. Dejgaard, L.Y. Chen, W.J. Muller, K. Gehring, D.Y. Thomas, An interaction map of endoplasmic reticulum chaperones and foldases, Molecular & cellular proteomics : MCP 11 (2012) 710-723.
[179] C.E. Jessop, R.H. Watkins, J.J. Simmons, M. Tasab, N.J. Bulleid, Protein disulphide isomerase family members show distinct substrate specificity: P5 is targeted to BiP client proteins, J Cell Sci 122 (2009) 4287-4295.
[180] D. Eletto, E. Chevet, Y. Argon, C. Appenzeller-Herzog, Redox controls UPR to control redox, Journal of cell science in press (2014).
[181] H.P. Harding, Y. Zhang, A. Bertolotti, H. Zeng, D. Ron, Perk is essential for translational regulation and cell survival during the unfolded protein response, Molecular cell 5 (2000) 897-904.
[182] J. Hollien, J.H. Lin, H. Li, N. Stevens, P. Walter, J.S. Weissman, Regulated Ire1-dependent decay of messenger RNAs in mammalian cells, The Journal of cell biology 186 (2009) 323-331.
[183] M. Calfon, H. Zeng, F. Urano, J.H. Till, S.R. Hubbard, H.P. Harding, S.G. Clark, D. Ron, IRE1 couples endoplasmic reticulum load to secretory capacity by processing the XBP-1 mRNA, Nature 415 (2002) 92-96.
[184] K. Haze, H. Yoshida, H. Yanagi, T. Yura, K. Mori, Mammalian transcription factor ATF6 is synthesized as a transmembrane protein and activated by proteolysis in response to endoplasmic reticulum stress, Molecular biology of the cell 10 (1999) 3787-3799.
[185] H.P. Harding, I. Novoa, Y. Zhang, H. Zeng, R. Wek, M. Schapira, D. Ron, Regulated translation initiation controls stress-induced gene expression in mammalian cells, Molecular cell 6 (2000) 1099-1108.
[186] D. Acosta-Alvear, Y. Zhou, A. Blais, M. Tsikitis, N.H. Lents, C. Arias, C.J. Lennon, Y. Kluger, B.D. Dynlacht, XBP1 controls diverse cell type- and condition-specific transcriptional regulatory networks, Molecular cell 27 (2007) 53-66.
[187] K. Lee, W. Tirasophon, X. Shen, M. Michalak, R. Prywes, T. Okada, H. Yoshida, K. Mori, R.J. Kaufman, IRE1-mediated unconventional mRNA splicing and S2P-mediated ATF6 cleavage merge to regulate XBP1 in signaling the unfolded protein response, Genes & development 16 (2002) 452-466.
[188] M. Schroder, R.J. Kaufman, The mammalian unfolded protein response, Annual review of biochemistry 74 (2005) 739-789.

[189] K. Yamamoto, T. Sato, T. Matsui, M. Sato, T. Okada, H. Yoshida, A. Harada, K. Mori, Transcriptional induction of mammalian ER quality control proteins is mediated by single or combined action of ATF6alpha and XBP1, Developmental cell 13 (2007) 365-376.
[190] K. Mori, Tripartite management of unfolded proteins in the endoplasmic reticulum, Cell 101 (2000) 451-454.
[191] R. Sriburi, H. Bommiasamy, G.L. Buldak, G.R. Robbins, M. Frank, S. Jackowski, J.W. Brewer, Coordinate regulation of phospholipid biosynthesis and secretory pathway gene expression in XBP-1(S)-induced endoplasmic reticulum biogenesis, The Journal of biological chemistry 282 (2007) 7024-7034.
[192] H.P. Harding, Y. Zhang, H. Zeng, I. Novoa, P.D. Lu, M. Calfon, N. Sadri, C. Yun, B. Popko, R. Paules, D.F. Stojdl, J.C. Bell, T. Hettmann, J.M. Leiden, D. Ron, An integrated stress response regulates amino acid metabolism and resistance to oxidative stress, Molecular cell 11 (2003) 619-633.
[193] I. Tabas, D. Ron, Integrating the mechanisms of apoptosis induced by endoplasmic reticulum stress, Nature cell biology 13 (2011) 184-190.
[194] U. Woehlbier, C. Hetz, Modulating stress responses by the UPRosome: a matter of life and death, Trends in biochemical sciences 36 (2011) 329-337.
[195] D.T. Rutkowski, S.M. Arnold, C.N. Miller, J. Wu, J. Li, K.M. Gunnison, K. Mori, A.A. Sadighi Akha, D. Raden, R.J. Kaufman, Adaptation to ER stress is mediated by differential stabilities of pro-survival and pro-apoptotic mRNAs and proteins, PLoS biology 4 (2006) e374.
[196] L.M. Dejean, S. Martinez-Caballero, S. Manon, K.W. Kinnally, Regulation of the mitochondrial apoptosis-induced channel, MAC, by BCL-2 family proteins, Biochimica et biophysica acta 1762 (2006) 191-201.
[197] I. Novoa, H. Zeng, H.P. Harding, D. Ron, Feedback inhibition of the unfolded protein response by GADD34-mediated dephosphorylation of eIF2alpha, The Journal of cell biology 153 (2001) 1011-1022.
[198] J. Han, S.H. Back, J. Hur, Y.H. Lin, R. Gildersleeve, J. Shan, C.L. Yuan, D. Krokowski, S. Wang, M. Hatzoglou, M.S. Kilberg, M.A. Sartor, R.J. Kaufman, ER-stress-induced transcriptional regulation increases protein synthesis leading to cell death, Nature cell biology 15 (2013) 481-490.
[199] S.J. Marciniak, C.Y. Yun, S. Oyadomari, I. Novoa, Y. Zhang, R. Jungreis, K. Nagata, H.P. Harding, D. Ron, CHOP induces death by promoting protein synthesis and oxidation in the stressed endoplasmic reticulum, Genes & development 18 (2004) 3066-3077.
[200] G. Li, M. Mongillo, K.T. Chin, H. Harding, D. Ron, A.R. Marks, I. Tabas, Role of ERO1-alpha-mediated stimulation of inositol 1,4,5-triphosphate receptor activity in endoplasmic reticulum stress-induced apoptosis, The Journal of cell biology 186 (2009) 783-792.
[201] M.J. Berridge, M.D. Bootman, H.L. Roderick, Calcium signalling: dynamics, homeostasis and remodelling, Nature reviews. Molecular cell biology 4 (2003) 517-529.
[202] N.K. Woods, J. Padmanabhan, Neuronal calcium signaling and Alzheimer's disease, Advances in experimental medicine and biology 740 (2012) 1193-1217.
[203] T. Simmen, E.M. Lynes, K. Gesson, G. Thomas, Oxidative protein folding in the endoplasmic reticulum: tight links to the mitochondria-associated membrane (MAM), Biochimica et biophysica acta 1798 (2010) 1465-1473.
[204] G. Szabadkai, K. Bianchi, P. Varnai, D. De Stefani, M.R. Wieckowski, D. Cavagna, A.I. Nagy, T. Balla, R. Rizzuto, Chaperone-mediated coupling of endoplasmic reticulum and mitochondrial Ca2+ channels, The Journal of cell biology 175 (2006) 901-911.
[205] R. Rizzuto, D. De Stefani, A. Raffaello, C. Mammucari, Mitochondria as sensors and regulators of calcium signalling, Nature reviews. Molecular cell biology 13 (2012) 566-578.
[206] T. Anelli, L. Bergamelli, E. Margittai, A. Rimessi, C. Fagioli, A. Malgaroli, P. Pinton, M. Ripamonti, R. Rizzuto, R. Sitia, Ero1alpha regulates Ca(2+) fluxes at the endoplasmic reticulum-mitochondria interface (MAM), Antioxidants & redox signaling 16 (2012) 1077-1087.
[207] S. Kiviluoto, T. Vervliet, H. Ivanova, J.P. Decuypere, H. De Smedt, L. Missiaen, G. Bultynck, J.B. Parys, Regulation of inositol 1,4,5-trisphosphate receptors during endoplasmic reticulum stress, Biochimica et biophysica acta 1833 (2013) 1612-1624.
[208] A.C. Fonseca, E. Ferreiro, C.R. Oliveira, S.M. Cardoso, C.F. Pereira, Activation of the endoplasmic reticulum stress response by the amyloid-beta 1-40 peptide in brain endothelial cells, Biochimica et biophysica acta 1832 (2013) 2191-2203.
[209] J.P. Decuypere, G. Monaco, G. Bultynck, L. Missiaen, H. De Smedt, J.B. Parys, The IP(3) receptor-mitochondria connection in apoptosis and autophagy, Biochimica et biophysica acta 1813 (2011) 1003-1013.
[210] S. Bansaghi, T. Golenar, M. Madesh, G. Csordas, S. RamachandraRao, K. Sharma, D.I. Yule, S.K. Joseph, G. Hajnoczky, Isoform- and species-specific control of inositol 1,4,5-trisphosphate (IP3) receptors by reactive oxygen species, The Journal of biological chemistry 289 (2014) 8170-8181.

[211] A. Raturi, C. Ortiz-Sandoval, T. Simmen, Redox dependence of endoplasmic reticulum (ER) Ca(2)(+) signaling, Histology and histopathology 29 (2014) 543-552.
[212] C. Appenzeller-Herzog, M.N. Hall, Bidirectional crosstalk between endoplasmic reticulum stress and mTOR signaling, Trends in cell biology 22 (2012) 274-282.
[213] E. Cadenas, K.J. Davies, Mitochondrial free radical generation, oxidative stress, and aging, Free radical biology & medicine 29 (2000) 222-230.
[214] D.I. Brown, K.K. Griendling, Nox proteins in signal transduction, Free radical biology & medicine 47 (2009) 1239-1253.
[215] T. Finkel, Signal transduction by reactive oxygen species, The Journal of cell biology 194 (2011) 7-15.
[216] R.B. Hamanaka, N.S. Chandel, Mitochondrial reactive oxygen species regulate cellular signaling and dictate biological outcomes, Trends in biochemical sciences 35 (2010) 505-513.
[217] Y. Shimizu, L.M. Hendershot, Oxidative folding: cellular strategies for dealing with the resultant equimolar production of reactive oxygen species, Antioxidants & redox signaling 11 (2009) 2317-2331.
[218] B.P. Tu, J.S. Weissman, Oxidative protein folding in eukaryotes: mechanisms and consequences, The Journal of cell biology 164 (2004) 341-346.
[219] B.G. Hill, A. Bhatnagar, Protein S-glutathiolation: redox-sensitive regulation of protein function, Journal of molecular and cellular cardiology 52 (2012) 559-567.
[220] S.G. Rhee, Y.S. Bae, S.R. Lee, J. Kwon, Hydrogen peroxide: a key messenger that modulates protein phosphorylation through cysteine oxidation, Science's STKE : signal transduction knowledge environment 2000 (2000) pe1.
[221] H. Sies, Oxidative stress: from basic research to clinical application, The American journal of medicine 91 (1991) 31S-38S.
[222] R. Brigelius-Flohe, M.G. Traber, Vitamin E: function and metabolism, FASEB journal : official publication of the Federation of American Societies for Experimental Biology 13 (1999) 1145-1155.
[223] B. Frei, L. England, B.N. Ames, Ascorbate is an outstanding antioxidant in human blood plasma, Proceedings of the National Academy of Sciences of the United States of America 86 (1989) 6377-6381.
[224] G.R. Buettner, The pecking order of free radicals and antioxidants: lipid peroxidation, alpha-tocopherol, and ascorbate, Archives of biochemistry and biophysics 300 (1993) 535-543.
[225] J.J. Perry, D.S. Shin, E.D. Getzoff, J.A. Tainer, The structural biochemistry of the superoxide dismutases, Biochimica et biophysica acta 1804 (2010) 245-262.
[226] A. Bindoli, M.P. Rigobello, Principles in redox signaling: from chemistry to functional significance, Antioxidants & redox signaling 18 (2013) 1557-1593.
[227] P. Chelikani, I. Fita, P.C. Loewen, Diversity of structures and properties among catalases, Cellular and molecular life sciences : CMLS 61 (2004) 192-208.
[228] C.C. Winterbourn, The biological chemistry of hydrogen peroxide, Methods in enzymology 528 (2013) 3-25.
[229] E. Nagababu, F.J. Chrest, J.M. Rifkind, Hydrogen-peroxide-induced heme degradation in red blood cells: the protective roles of catalase and glutathione peroxidase, Biochimica et biophysica acta 1620 (2003) 211-217.
[230] T.H. Lee, S.U. Kim, S.L. Yu, S.H. Kim, D.S. Park, H.B. Moon, S.H. Dho, K.S. Kwon, H.J. Kwon, Y.H. Han, S. Jeong, S.W. Kang, H.S. Shin, K.K. Lee, S.G. Rhee, D.Y. Yu, Peroxiredoxin II is essential for sustaining life span of erythrocytes in mice, Blood 101 (2003) 5033-5038.
[231] A.I. Alayash, R.P. Patel, R.E. Cashon, Redox reactions of hemoglobin and myoglobin: biological and toxicological implications, Antioxidants & redox signaling 3 (2001) 313-327.
[232] E. Nagababu, J.M. Rifkind, Determination of s-nitrosothiols in biological fluids by chemiluminescence, Methods in molecular biology 704 (2011) 27-37.
[233] H.J. Atkinson, P.C. Babbitt, An atlas of the thioredoxin fold class reveals the complexity of function-enabling adaptations, PLoS computational biology 5 (2009) e1000541.
[234] C.H. Lillig, C. Berndt, Glutaredoxins in thiol/disulfide exchange, Antioxidants & redox signaling 18 (2013) 1654-1665.
[235] L. Flohe, S. Toppo, G. Cozza, F. Ursini, A comparison of thiol peroxidase mechanisms, Antioxidants & redox signaling 15 (2011) 763-780.
[236] I. Dalle-Donne, R. Rossi, G. Colombo, D. Giustarini, A. Milzani, Protein S-glutathionylation: a regulatory device from bacteria to humans, Trends in biochemical sciences 34 (2009) 85-96.
[237] S.G. Rhee, H.A. Woo, Multiple functions of peroxiredoxins: peroxidases, sensors and regulators of the intracellular messenger H(2)O(2), and protein chaperones, Antioxidants & redox signaling 15 (2011) 781-794.
[238] Z.A. Wood, E. Schroder, J. Robin Harris, L.B. Poole, Structure, mechanism and regulation of peroxiredoxins, Trends in biochemical sciences 28 (2003) 32-40.

[239] L.B. Poole, The catalytic mechanism of peroxiredoxins, Sub-cellular biochemistry 44 (2007) 61-81.
[240] A.B. Fisher, Peroxiredoxin 6: a bifunctional enzyme with glutathione peroxidase and phospholipase A(2) activities, Antioxidants & redox signaling 15 (2011) 831-844.
[241] L.A. Ralat, Y. Manevich, A.B. Fisher, R.F. Colman, Direct evidence for the formation of a complex between 1-cysteine peroxiredoxin and glutathione S-transferase pi with activity changes in both enzymes, Biochemistry 45 (2006) 360-372.
[242] R. Brigelius-Flohe, M. Maiorino, Glutathione peroxidases, Biochimica et biophysica acta 1830 (2013) 3289-3303.
[243] S.C. Tosatto, V. Bosello, F. Fogolari, P. Mauri, A. Roveri, S. Toppo, L. Flohe, F. Ursini, M. Maiorino, The catalytic site of glutathione peroxidases, Antioxidants & redox signaling 10 (2008) 1515-1526.
[244] T. Ishii, K. Itoh, S. Takahashi, H. Sato, T. Yanagawa, Y. Katoh, S. Bannai, M. Yamamoto, Transcription factor Nrf2 coordinately regulates a group of oxidative stress-inducible genes in macrophages, The Journal of biological chemistry 275 (2000) 16023-16029.
[245] K. Itoh, T. Chiba, S. Takahashi, T. Ishii, K. Igarashi, Y. Katoh, T. Oyake, N. Hayashi, K. Satoh, I. Hatayama, M. Yamamoto, Y. Nabeshima, An Nrf2/small Maf heterodimer mediates the induction of phase II detoxifying enzyme genes through antioxidant response elements, Biochemical and biophysical research communications 236 (1997) 313-322.
[246] K. Itoh, K.I. Tong, M. Yamamoto, Molecular mechanism activating Nrf2-Keap1 pathway in regulation of adaptive response to electrophiles, Free radical biology & medicine 36 (2004) 1208-1213.
[247] J.D. Hayes, A.T. Dinkova-Kostova, The Nrf2 regulatory network provides an interface between redox and intermediary metabolism, Trends in biochemical sciences 39 (2014) 199-218.
[248] J.D. Hayes, M. McMahon, NRF2 and KEAP1 mutations: permanent activation of an adaptive response in cancer, Trends in biochemical sciences 34 (2009) 176-188.
[249] R.N. Karapetian, A.G. Evstafieva, I.S. Abaeva, N.V. Chichkova, G.S. Filonov, Y.P. Rubtsov, E.A. Sukhacheva, S.V. Melnikov, U. Schneider, E.E. Wanker, A.B. Vartapetian, Nuclear oncoprotein prothymosin alpha is a partner of Keap1: implications for expression of oxidative stress-protecting genes, Molecular and cellular biology 25 (2005) 1089-1099.
[250] W. Li, S.W. Yu, A.N. Kong, Nrf2 possesses a redox-sensitive nuclear exporting signal in the Neh5 transactivation domain, The Journal of biological chemistry 281 (2006) 27251-27263.
[251] M. McMahon, N. Thomas, K. Itoh, M. Yamamoto, J.D. Hayes, Dimerization of substrate adaptors can facilitate cullin-mediated ubiquitylation of proteins by a "tethering" mechanism: a two-site interaction model for the Nrf2-Keap1 complex, The Journal of biological chemistry 281 (2006) 24756-24768.
[252] B.N. Chorley, M.R. Campbell, X. Wang, M. Karaca, D. Sambandan, F. Bangura, P. Xue, J. Pi, S.R. Kleeberger, D.A. Bell, Identification of novel NRF2-regulated genes by ChIP-Seq: influence on retinoid X receptor alpha, Nucleic acids research 40 (2012) 7416-7429.
[253] A.K. MacLeod, M. McMahon, S.M. Plummer, L.G. Higgins, T.M. Penning, K. Igarashi, J.D. Hayes, Characterization of the cancer chemopreventive NRF2-dependent gene battery in human keratinocytes: demonstration that the KEAP1-NRF2 pathway, and not the BACH1-NRF2 pathway, controls cytoprotection against electrophiles as well as redox-cycling compounds, Carcinogenesis 30 (2009) 1571-1580.
[254] A.S. Agyeman, R. Chaerkady, P.G. Shaw, N.E. Davidson, K. Visvanathan, A. Pandey, T.W. Kensler, Transcriptomic and proteomic profiling of KEAP1 disrupted and sulforaphane-treated human breast epithelial cells reveals common expression profiles, Breast cancer research and treatment 132 (2012) 175-187.
[255] D. Malhotra, E. Portales-Casamar, A. Singh, S. Srivastava, D. Arenillas, C. Happel, C. Shyr, N. Wakabayashi, T.W. Kensler, W.W. Wasserman, S. Biswal, Global mapping of binding sites for Nrf2 identifies novel targets in cell survival response through ChIP-Seq profiling and network analysis, Nucleic acids research 38 (2010) 5718-5734.
[256] C.M. Haynes, E.A. Titus, A.A. Cooper, Degradation of misfolded proteins prevents ER-derived oxidative stress and cell death, Molecular cell 15 (2004) 767-776.

2. Project I: GPx8 peroxidase prevents leakage of H_2O_2 from the endoplasmic reticulum

Free Radical Biology and Medicine 70 (2014) 106–116

Contents lists available at ScienceDirect

Free Radical Biology and Medicine

journal homepage: www.elsevier.com/locate/freeradbiomed

Original Contribution

GPx8 peroxidase prevents leakage of H_2O_2 from the endoplasmic reticulum

Thomas Ramming [a], Henning G. Hansen [b,1], Kazuhiro Nagata [c], Lars Ellgaard [b], Christian Appenzeller-Herzog [a,*]

[a] Division of Molecular and Systems Toxicology, Department of Pharmaceutical Sciences, University of Basel, 4056 Basel, Switzerland
[b] Department of Biology, University of Copenhagen, 2200 Copenhagen N, Denmark
[c] Faculty of Life Sciences, Kyoto Sangyo University, Kyoto 603-8555, Japan

ARTICLE INFO

Article history:
Received 25 September 2013
Received in revised form
6 January 2014
Accepted 13 January 2014
Available online 22 February 2014

Keywords:
Apoptosis
Endoplasmic reticulum stress
Hydrogen peroxide
Peroxidases
Redox homeostasis
Free radicals

ABSTRACT

Unbalanced endoplasmic reticulum (ER) homeostasis (ER stress) leads to increased generation of reactive oxygen species (ROS). Disulfide-bond formation in the ER by Ero1 family oxidases produces hydrogen peroxide (H_2O_2) and thereby constitutes one potential source of ER-stress-induced ROS. However, we demonstrate that Ero1α-derived H_2O_2 is rapidly cleared by glutathione peroxidase (GPx) 8. In 293 cells, GPx8 and reduced/activated forms of Ero1α co-reside in the rough ER subdomain. Loss of GPx8 causes ER stress, leakage of Ero1α-derived H_2O_2 to the cytosol, and cell death. In contrast, peroxiredoxin (Prx) IV, another H_2O_2-detoxifying rough ER enzyme, does not protect from Ero1α-mediated toxicity, as is currently proposed. Only when Ero1α-catalyzed H_2O_2 production is artificially maximized can PrxIV participate in its reduction. We conclude that the peroxidase activity of the described Ero1α–GPx8 complex prevents diffusion of Ero1α-derived H_2O_2 within and out of the rough ER. Along with the induction of *GPX8* in ER-stressed cells, these findings question a ubiquitous role of Ero1α as a producer of cytoplasmic ROS under ER stress.

Roughly one-third of the human proteome resides in exocytic endomembrane compartments or travels via exocytic compartments to the cell surface. These proteins are synthesized at and translocated into the endoplasmic reticulum (ER), the largest and most extended compartment of the secretory pathway. The ER lumen provides a unique environment for protein folding that mimics the extracellular space [1]. For instance, reduction–oxidation (redox) conditions are more oxidizing in the ER (and in the extracellular space) than in the cytosol [2,3], thereby favoring the formation of disulfide bonds in proteins. This process, known as oxidative protein folding, is catalyzed by a number of distinct pathways [4,5], the most conserved of which is driven by endoplasmic oxidoreductin 1 (Ero1) oxidases [6]. In human cells, the housekeeping isoform Ero1α introduces disulfide bonds into the disulfide-shuttling enzyme protein disulfide isomerase (PDI) [7,8]. This reaction involves the generation of one molecule of hydrogen peroxide (H_2O_2) for every disulfide formed [9]. Of note, Ero1 activity is essential only in lower eukaryotes, but not, e.g., in flies or mice [6].

Protein misfolding in the ER triggers a cell program called the ER stress response or unfolded protein response (UPR) [10], which in the majority of cases is accompanied by an increase in intracellular reactive oxygen species (ROS) and oxidative damage [11–16]. Importantly, ROS also act upstream of ER stress [15,17–19]. ER stress and ROS therefore constitute a self-perpetuating vicious cycle, which contributes to cell degeneration in the context of ER-stress-centered disorders [20]. The fact that potentially massive amounts of the ROS H_2O_2 are being produced during Ero1α-mediated oxidative protein folding has attracted ample attention [21–23]. Thus, one model for the generation of ER-stress-induced ROS holds that stress-mediated formation of aberrant disulfides results in repeated protein reduction and reoxidation cycles, leading to increased H_2O_2 generation by Ero1 [24–26]. Ero1-derived H_2O_2 is then proposed to pass the ER membrane and spill into the cytoplasm.

In addition to H_2O_2-generating machinery, the ER in mammalian cells harbors three H_2O_2-reducing peroxidases, peroxiredoxin IV (PrxIV), glutathione peroxidase 7 (GPx7), and the transmembrane

Abbreviations: BCNU, carmustine; DRM, detergent-resistant membrane; DTT, dithiothreitol; ER, endoplasmic reticulum; Ero1, endoplasmic oxidoreductin 1; GFP, green fluorescent protein; GSSG, glutathione disulfide; GPx, glutathione peroxidase; MAM, mitochondria-associated membrane; NEM, *N*-ethylmaleimide; Prx, peroxiredoxin; PMSF, phenylmethylsulfonyl fluoride; PNS, postnuclear supernatant; PDI, protein disulfide isomerase; ROS, reactive oxygen species; redox, reduction–oxidation; GS_{tot}, total glutathione; TCA, trichloroacetic acid

* Corresponding author. Fax: +41 61 267 1515.
E-mail address: Christian.Appenzeller@unibas.ch (C. Appenzeller-Herzog).
[1] Present address: Novo Nordisk Foundation Center for Biosustainability, Technical University of Denmark, 2970 Hørsholm, Denmark.

http://dx.doi.org/10.1016/j.freeradbiomed.2014.01.018
0891-5849

2.1. Abstract

Imbalanced endoplasmic reticulum (ER) homeostasis (ER stress) leads to increased generation of reactive oxygen species (ROS). Disulfide-bond formation in the ER by Ero1 family oxidases produces hydrogen peroxide (H_2O_2) and thereby constitutes one potential source of ER-stress-induced ROS. However, we demonstrate that Ero1α-derived H_2O_2 is rapidly cleared by glutathione peroxidase (GPx) 8. In 293 cells, GPx8 and reduced/activated forms of Ero1α co-reside in the rough ER subdomain. Loss of GPx8 causes ER stress, leakage of Ero1α-derived H_2O_2 to the cytosol, and cell death. In contrast, peroxiredoxin (Prx) IV, another H_2O_2-detoxifying rough ER enzyme, does not protect from Ero1α-mediated toxicity, as is currently proposed. Solely when Ero1α-catalyzed H_2O_2 production is artificially maximized, PrxIV can participate in its reduction. We conclude that the peroxidase activity of the described Ero1α–GPx8 complex prevents diffusion of Ero1α-derived H_2O_2 within and out of the rough ER. Along with the induction of *GPX8* in ER stressed cells, these findings question a ubiquitous role of Ero1α as a producer of cytoplasmic ROS under ER stress.

2.2. Introduction

Roughly one third of the human proteome resides in exocytic endomembrane compartments or travels via exocytic compartments to the cell surface. These proteins are synthesized at and translocated into the endoplasmic reticulum (ER), the largest and most extended compartment of the secretory pathway. The ER lumen provides a unique environment for protein folding that mimics the extracellular space [1]. For instance, reduction-oxidation (redox) conditions are more oxidizing in the ER (and in the extracellular space) than in the cytosol [2,3], thereby favoring the formation of disulfide bonds in proteins. This process known as oxidative protein folding is catalyzed by a number of distinct pathways [4,5], the most conserved of which is driven by endoplasmic oxidoreductin 1 (Ero1) oxidases [6]. In human cells, the housekeeping isoform Ero1α introduces disulfide bonds into the disulfide shuttling enzyme protein disulfide isomerase (PDI) [7,8]. This reaction involves the generation of one molecule of hydrogen peroxide (H_2O_2) for every disulfide formed [9]. Of note, Ero1 activity is essential only in lower eukaryotes, but not e.g. in flies or mice [6].

Protein misfolding in the ER triggers a cell program called the ER stress response or unfolded protein response (UPR) [10], which in the majority of cases is accompanied by an increase in intracellular reactive oxygen species (ROS) and oxidative damage [11,12,13,14,15,16]. Importantly, ROS also act upstream of ER stress [15,17,18,19]. ER stress and ROS therefore constitute a self-perpetuating vicious cycle, which contributes to cell degeneration in the context of ER-stress-centered disorders [20]. The fact that potentially massive amounts of the ROS H_2O_2 are being produced during Ero1α-mediated oxidative protein folding has attracted ample attention [21,22,23]. Thus, one model for the generation of ER-stress-induced ROS holds that stress-mediated formation of aberrant disulfides results in repeated protein reduction and reoxidation cycles, leading to increased H_2O_2 generation by Ero1 [24,25,26]. Ero1-derived H_2O_2 is then proposed to pass the ER membrane and spill into the cytoplasm.

In addition to H_2O_2-generating machinery, the ER in mammalian cells harbors three H_2O_2-reducing peroxidases, peroxiredoxin IV (PrxIV), glutathione peroxidase 7 (GPx7), and the transmembrane protein GPx8 [27,28,29]. PrxIV is a 2-cysteine peroxiredoxin that can couple the reduction of H_2O_2 to the oxidation of PDI family members [30,31,32], but is not induced in response to ER stress [29]. Accordingly, PrxIV can supplement the ER with disulfide bonds and contribute to oxidative protein folding [5,32]. In mice, loss of PrxIV causes a mild phenotype with defects in spermatogenesis [33]. Conversely, GPx7 knockout mice display signs of widespread oxidative injury, develop cancer, and die prematurely [34]. In the same vein, endogenous GPx7 protects oesophageal cells from acid-mediated oxidative stress [35] and fibroblasts from pharmacologically induced ER stress [34]. *In vitro*, GPx7 can react with phospholipid hydroperoxides or H_2O_2 [36] as well as with the reducing substrates PDI family members [27,37,38], glutathione [37], or Grp78 [34]. Little is known about the role of GPx8 in ER physiology, except that, as for GPx7, ectopically expressed GPx8 can bind to Ero1α in cells [27].

In this study, we show that Ero1α-derived H_2O_2 cannot diffuse from ER to cytosol owing to the peroxidase activity of GPx8, which is induced on ER stress. This mechanism is independent of PrxIV and essential to protect cells from Ero1α-mediated hyperoxidation and death. GPx8-centered control of Ero1α-derived H_2O_2 necessitates a reevaluation of the source of ER-stress-induced ROS.

2.3. Results

2.3.1. GPx8 but not PrxIV protects cells against Ero1α-mediated stress

To address the fate specifically of Ero1α-derived H_2O_2 and a possible involvement of ER-resident peroxidases, we used cells with inducible expression of hyperactive Ero1α-C104A/C131A (Ero1α-ACTIVE) [18,47] and peroxidase-specific siRNA. A 120 h transfection protocol was developed, which in case of PrxIV [5] but not GPx8 was necessary for efficient depletion (Fig 6A and S1A+B), whereas endogenous GPx7 was undetectable (Fig. S1C+D). Silencing of PrxIV or GPx8 compromised cell proliferation (Fig. 6B and S1E), underscoring the importance of H_2O_2 turnover in the ER. However, only knockdown of GPx8 elicited ER stress as judged by moderate transcriptional activation of UPR target genes (Fig. 6C, bars 3 and 5), which was exacerbated by induction of Ero1α-ACTIVE (Fig. 6C, bars 6). Similarly, antioxidant response markers, which were marginally induced by Ero1α-ACTIVE alone (Fig. 6D, bars 2) [18], responded additively to GPx8 knockdown and Ero1α-ACTIVE (Fig. 6D, bars 5 and 6). Although PrxIV knockdown partially triggered the antioxidant response, this induction was not intensified by Ero1α-ACTIVE (Fig. 6D, bars 3 and 4). GPx8+PrxIV double knockdown did not enhance the effects of GPx8 single knockdown in the majority of readouts (Fig. 6B+C+D, bars 7 and 8; and see below). Thus, GPx8, but not PrxIV is linked to Ero1 and ER homeostasis. Consistent with a detoxifying role during compromised ER homeostasis, GPx8 transcript was upregulated under ER stress, which again was not the case for PrxIV (Fig. 6E) [29].

Silencing of GPx8 increased expression of PrxIV (Fig. 6A+F). As PrxIV levels were unresponsive to chemical ER stressors but did increase upon knockdown of the negative antioxidant response regulator Keap1 (Fig. S1F), we concluded that PrxIV responded to GPx8 siRNA-induced antioxidant response (Fig. 6D) rather than the UPR.

Of note, GPx8 knockdown and concomitant overexpression of hyperactive Ero1α elicited a weak UPR only, as activation of PERK/eIF2α signaling, which confers protection against oxidative stress [25], and of the proapoptotic JNK pathway was not detected (Fig. S1G). Consistently, the magnitude of UPR target gene induction by GPx8 knockdown (Fig. 6C) was low compared with

the induction by chemical inducers of ER stress (data not shown). Cleavage of caspase 3 (a hallmark of apoptosis) predominantly occurred in PrxIV-silenced cells (Fig. S1G).

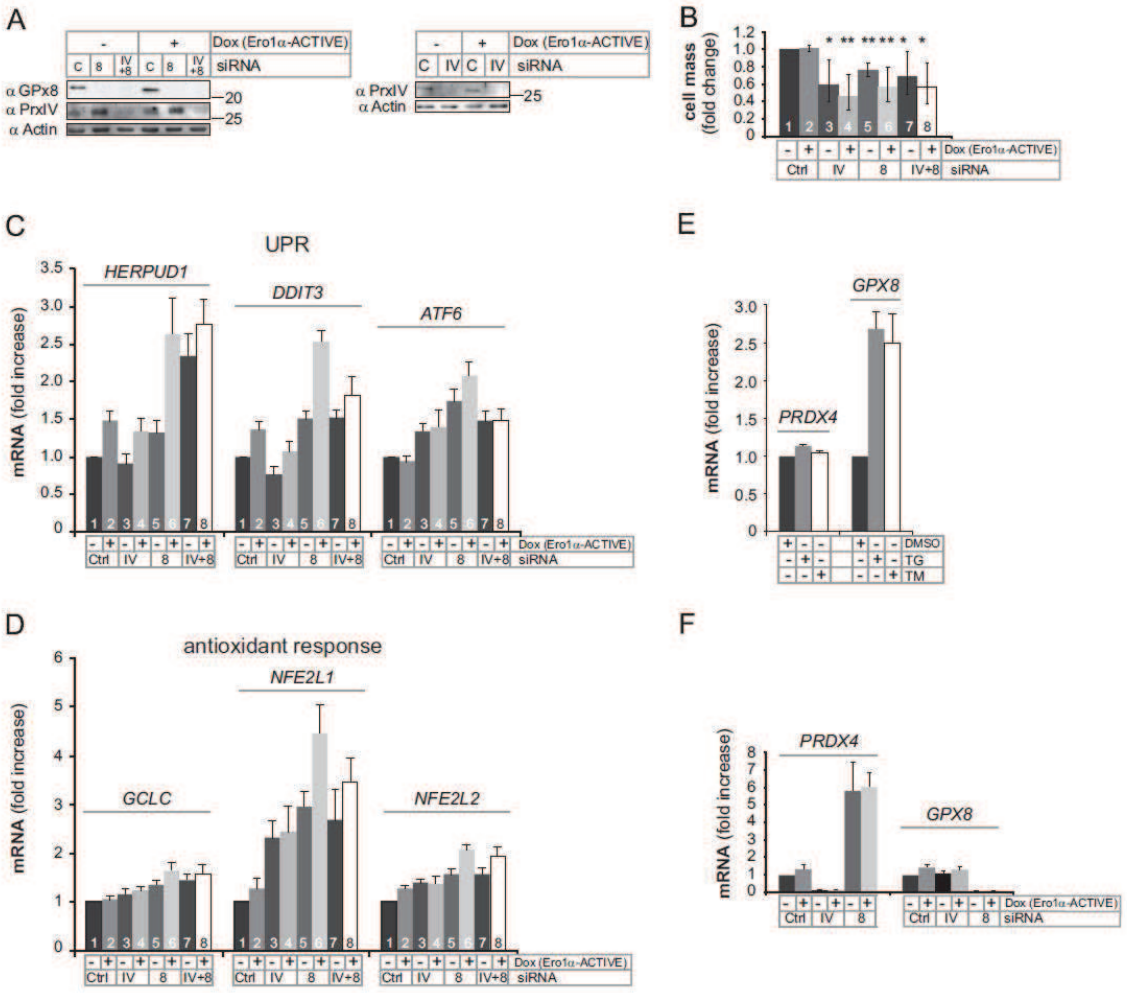

Figure 6: GPx8, but not PrxIV is functionally linked to Ero1α to prevent ER stress. (A) Ero1α-C104A/C131A cells were treated with control (C), PrxIV-targeting (IV), GPx8-targeting (8), or a mixture of IV and 8 (IV+8) siRNA for 120 h (see Materials and methods). Where indicated, expression of Ero1α-ACTIVE was induced by doxycycline (Dox) during the last 24 h of knockdown. Western blot analysis was carried out using the indicated primary antibodies. Note that PrxIV protein levels are increased in GPx8-silenced cells. **(B)** Cell mass of Ero1α-C104A/C131A cells was determined after treatment with siRNAs and/or Dox as in panel (A) by sulforhodamine B staining. Changes relative to control siRNA-treated cells are plotted along with 95% confidence intervals (n = 3; mean ± SEM). * $p < 0.05$; ** $p < 0.01$ **(C and D)** Ero1α-C104A/C131A cells were treated with siRNAs and Dox as in panel (A) and subjected to quantitative real-time RT-PCR using primers specific for the ER stress (UPR) markers *HERPUD1* (encoding Herp), *DDIT3* (encoding CHOP), and *ATF6* or the antioxidant response markers *GCLC* (encoding Glutamate–cysteine ligase), *NFE2L1* (encoding Nrf1), and *NFE2L2* (encoding Nrf2). Values are expressed as fold increase relative to control (Ctrl) siRNA-treated cells (n = 5; mean ± SEM). **(E)** Ero1α-C104A/C131A cells were exposed for 8 h to vehicle (0.33% DMSO), 5 µM thapsigargin (TG), or 2.5 µg/ml tunicamycin (TM) to induce ER stress and analyzed by quantitative real-time RT-PCR (qPCR) using primers specific for *PRDX4* and *GPX8* (n = 3; mean ± SEM). **(F)** mRNA levels relative to control of *PRDX4* and *GPX8* were determined upon knockdown of either gene for 120 h in Ero1α-C104A/C131A cells treated with or without Dox during the last 24 h of knockdown (n = 5; mean ± SEM).

2.3.2. GPx8 reduces Ero1α-derived H_2O_2 in the ER

To explore how GPx8 knockdown induced ER stress markers, we assayed ER redox homeostasis, which – when perturbed – triggers ER stress [10]. We surmised that increased ER oxidation in response to hyperactive Ero1α [18] could be amplified in the absence of GPx8 due to uncontrolled generation of Ero1α-derived H_2O_2. Indeed, hyperoxidation of the ER protein ERp57 upon expression of Ero1α-ACTIVE was more prominent in GPx8-silenced compared with control cells (Fig. 7A). By contrast, knocking down PrxIV had no effect (Fig. 7B). As the redox state of ERp57 may not faithfully reflect ER H_2O_2 levels, we also used the fluorescent HyPer probe, which directly reacts with H_2O_2 [48]. Consistent with published data [43], ER-targeted HyPer ($HyPer_{ER}$; Fig. S2A) was more oxidized – as indicated by a higher fluorescence excitation ratio (Fig. S2B) – upon Ero1α-ACTIVE expression (Fig. 7C, bars 1 and 5). This increase in $HyPer_{ER}$ oxidation was amplified by GPx8- but not by PrxIV-targeting siRNA (Fig. 7C, bars 6 and 7). In fact, PrxIV knockdown lowered the fluorescence excitation ratio of $HyPer_{ER}$ (Fig. 7C, bars 2 and 6). A $HyPer_{ER}$ C199S control mutant, which is insensitive to oxidation but retains pH-sensitivity [49], was not affected by GPx8 knockdown but similarly sensitive to PrxIV knockdown (Fig. S2C), raising the possibility that the sensitivity of $HyPer_{ER}$ to PrxIV depletion may be partially redox-independent. Taken together, consistent with the observed induction of UPR and antioxidant response genes (Fig. 6C+D), GPx8 knockdown aggravates Ero1α-ACTIVE-mediated ER hyperoxidation. Interestingly, in contrast to Ero1α-ACTIVE, the oxidizing effect of hyperactive Ero1β-C100A/C130A [2] was not enhanced by GPx8 knockdown (Fig. 7D, bars 4 and 6), suggesting that functional coupling of Ero1 and GPx8 is restricted to the Ero1α paralog.

We considered the possibility that $HyPer_{ER}$ oxidation upon GPx8 knockdown could be partially explained by increased PrxIV levels (Fig. 6A+F), since knockdown of PrxIV causes ER hypooxidation [32]. However, overexpression of PrxIV-FLAG failed to hyperoxidize the probe (Fig. S2D+E). Moreover, overexpression of GPx8-HA showed inverse effects on $HyPer_{ER}$ oxidation compared with GPx8 knockdown (Fig. S2D+E), but did not lower PrxIV expression (Fig. S2F).

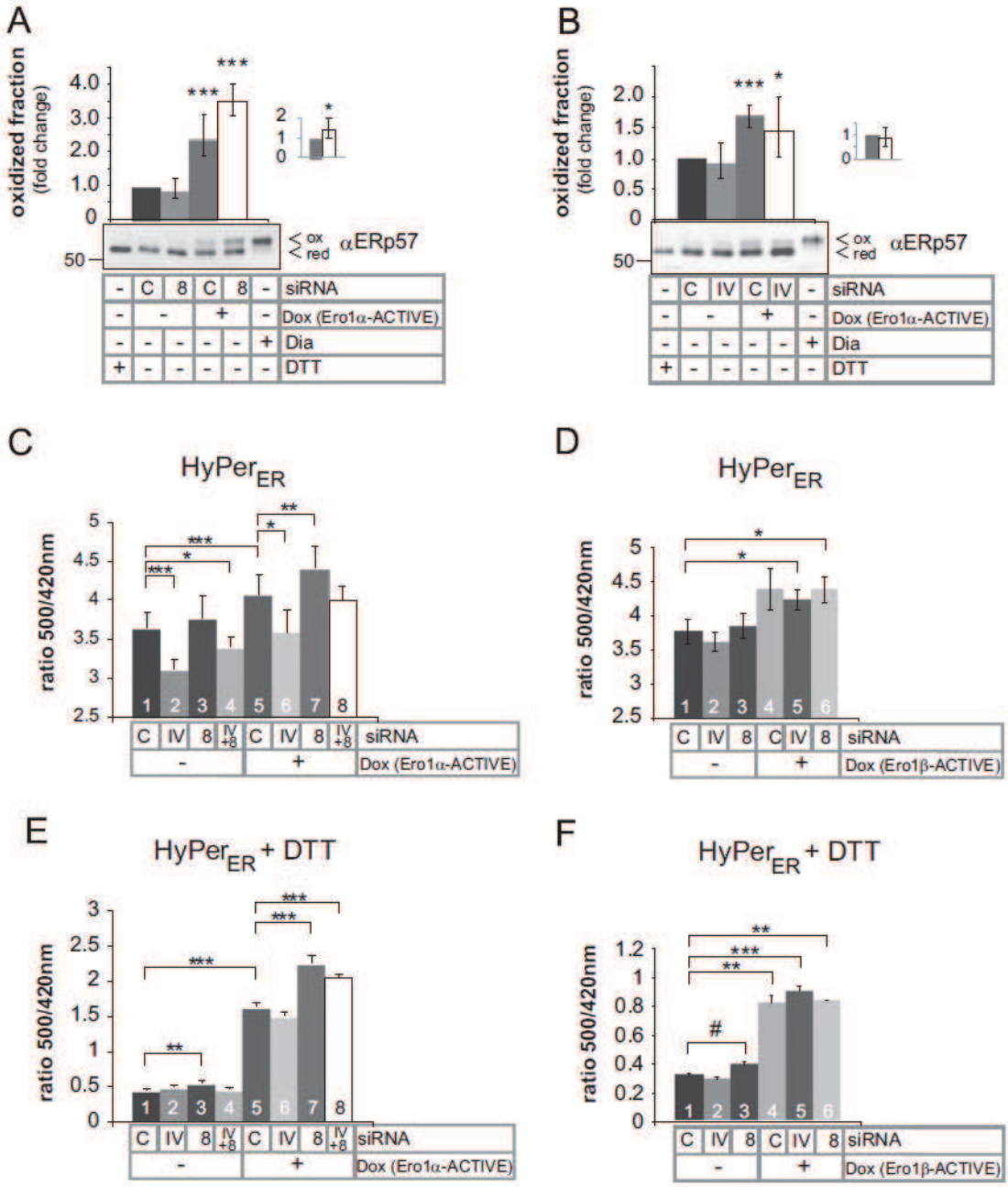

Figure 7: GPx8, but not PrxIV clears Ero1α-derived H_2O_2 from the ER. (A) Ero1α-C104A/C131A cells were treated for 48 h with siRNAs (Fig. S1B) and, where indicated, doxycycline (Dox, 24 h), followed by differential alkylation and Western blot analysis of ERp57. This assay monitors the dithiol–disulfide state of the **a´** domain active site in ERp57 (FIG. S6 in [40]). The mobilities of **a´** domain reduced (red) and oxidized (ox) ERp57, as verified by control samples from DTT- or diamide-treated (Dia) cells, are indicated. The diagram shows the oxidized fraction (as determined by densitometry) expressed as change relative to control (C) siRNA-treated cells without Dox (or with Dox in inset) ± 95% confidence intervals (n = 3). **(B)** Experiment as in panel (A) but using PrxIV knockdown or control siRNA-treated cells (120 h; n = 3). **(C)** SiRNA(120 h)/Dox(24 h)-treated Ero1α-C104A/C131A:$HyPer_{ER}$ cells were subjected to fluorescence excitation spectrum analysis (for spectra see Fig. S2B). Plotted are the ratios of the 500 and 420 nm peak amplitudes (n ≥ 4; mean ± SEM). **(D)** Analogous experiment to panel (C) using Ero1β-C100A/C130A:$HyPer_{ER}$ cells (n = 3; mean ± SEM). **(E)** Ero1α-C104A/C131A:$HyPer_{ER}$ cells were treated and analyzed as in panel (C) 5 minutes after the addition of 0.5 mM DTT (n ≥ 4; mean ± SEM). **(F)** Analogous experiment to panel (E) using Ero1β-C100A/C130A:$HyPer_{ER}$ cells (n = 3; mean ± SEM). # $p < 0.08$; * $p < 0.05$; ** $p < 0.01$; *** $p < 0.001$

As under steady-state conditions, $HyPer_{ER}$ can be oxidized in a H_2O_2-independent manner via PDIs [50,51], we also conducted $HyPer_{ER}$ measurements in presence of the reductant dithiothreitol (DTT). This treatment strongly activates disulfide- and H_2O_2-generation by Ero1α while maintaining PDIs in a reduced state [41,52]. Accordingly, any increased oxidation of $HyPer_{ER}$ in DTT-flooded cells is likely to predominantly reflect a rise in [H_2O_2] or of H_2O_2-derived radicals formed by Fenton chemistry [53]. The effects of Ero1α-ACTIVE, Ero1β-C100A/C130A, and GPx8 knockdown observed at steady state (Fig. 7C+D) were reproduced under these conditions (Fig. 7E, bars 5 and 7; Fig. 7F, bars 4 and 6). Furthermore, silencing of GPx8 increased $HyPer_{ER}$ oxidation also in uninduced cells (Fig. 7E+F, bar 3), indicating a functional interaction between endogenous proteins. Again, this effect was not observed upon silencing of PrxIV (Fig. 7F, bar 2). Taken together, GPx8, but not PrxIV, protects the cell from ER stress by clearing Ero1α-derived H_2O_2 from the ER lumen.

2.3.3. Non-physiologically elevated Ero1α activity and GPx8 knockdown allow leakage of H_2O_2 from ER to cytosol

There is evidence that the ER membrane is permeable to H_2O_2 [24,54], and it has been suggested that Ero1-derived H_2O_2 can affect overall cellular redox homeostasis [23,25,26]. We therefore assayed cytosolic H_2O_2 using $HyPer_{cyto}$ [48] (Fig. S3A). Upon DTT-mediated activation of Ero1α, both GPx8 silencing and Ero1α-ACTIVE expression induced cytosolic hyperoxidation (Fig. 8A, bars 3 and 5, and S3B). As for $HyPer_{ER}$ (see above), the two treatments additively raised the oxidation of $HyPer_{cyto}$ (Fig. 8A inset, bar 7). The sensitivity of $HyPer_{cyto}$ to GPx8 siRNA depended on the presence of Cys^{199} and therefore reflected a redox-dependent sensor response (Fig. S3C). Conversely, the fluorescence excitation ratio of $HyPer_{cyto}$ was lowered upon PrxIV knockdown (Fig. 8A, bars 2 and 6), which was at least in part a redox-independent effect (Fig. S3C). In absence of DTT, Ero1α-ACTIVE expression caused no detectable oxidation of $HyPer_{cyto}$, whereas the sensor was more oxidized in GPx8-silenced than control cells by a mechanism that remains to be elucidated (Fig. 8B). Accordingly, Ero1α-derived H_2O_2 leaks through the ER membrane to oxidize the cytosol only in response to DTT-mediated Ero1α hyperactivity and GPx8 knockdown.

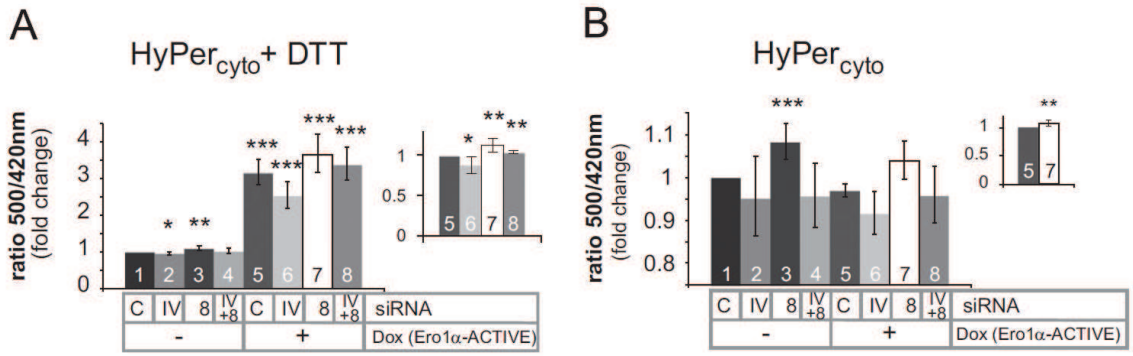

Figure 8: Elevated Ero1α activity and GPx8 knockdown allow leakage of H_2O_2 from ER to cytosol. (A) SiRNA(120 h)/Dox(24 h)-treated Ero1α-C104A/C131A:HyPer$_{cyto}$ cells were subjected to fluorescence excitation spectrum analysis 5 minutes after addition of 0.5 mM DTT (for spectra see Fig. S3B). Plotted are the changes in ratios of 500 and 420 nm peak amplitudes relative to C siRNA-transfected cells without Dox (or with Dox in inset) along with 95% confidence intervals ($n \geq 4$). **(B)** Ero1α-C104A/C131A:HyPer$_{cyto}$ cells were treated and analyzed as in panel (A) without addition of DTT ($n \geq 4$). * $p < 0.05$; ** $p < 0.01$; *** $p < 0.001$

2.3.4. GPx8- and PrxIV-catalyzed H_2O_2 reduction alleviates Ero1α-dependent cellular hyperoxidation upon DTT treatment

We next revisited the previously reported, transient peak of cellular glutathione disulfide (GSSG) upon overexpression of wild-type Ero1α (Ero1α-WT) and DTT washout (Fig. 4C in [41]). Based on our findings with HyPer$_{cyto}$ (Fig. 8A), we reasoned that under such non-physiological conditions, runaway H_2O_2 might diffuse from ER to cytosol where the activities of glutathione peroxidases and glutathione reductase could catalyze GSSG increase and decrease, respectively. As such, this setup would be suitable to study the impact of ER peroxidases in presence of transiently high [H_2O_2]. In support of GSSG formation in the cytosol, a cytosolic glutathione sensor (Grx1-roGFP2 [55]) was oxidized in response to Ero1α overexpression and DTT washout (Fig. 9A), and cellular GSSG accumulation and hyperoxidation of Grx1-roGFP2 was amplified in cells treated with the glutathione reductase inhibitor carmustine (BCNU) (Fig. 9B+C). Mechanistically, although GSSG has been published not to pass the ER membrane *in vitro* [56], we presently cannot exclude that GSSG rather than H_2O_2 is transported from ER to cytosol in our cell-based assay. Despite this uncertainty, we concluded that DTT-mediated activation of overexpressed Ero1α causes a short-lived rise in cytosolic GSSG upon washout of DTT.

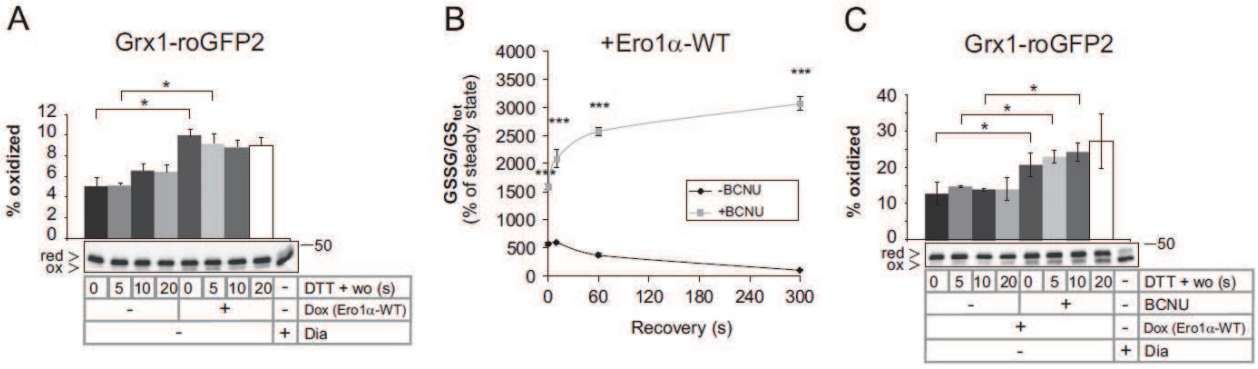

Figure 9: Cytosolic GSSG peaks upon DTT washout in Ero1α-overexpressing cells. (A) Ero1α cells were transfected with Grx1-roGFP2 in presence or absence of doxycycline (Dox) and subjected to DTT washout. At indicated time points after DTT removal, recovery was stopped by NEM, and the samples analyzed by αGFP immunoprecipitation and Western blot under non-reducing conditions. Diamide (Dia)-treated cells were used to mark the mobility of oxidized (ox) Grx1-roGFP2. Oxidized fractions were quantified by densitometry (n = 3; mean ± SEM). **(B)** Dox-induced Ero1α cells were pretreated or not with 1 mM BCNU for 45 min before DTT washout and quantification of intracellular GSSG and GS_{tot} levels. The fraction of GSSG is plotted as percentage of the value at steady state (mean ± SEM; two independent experiments each performed in triplet). **(C)** Grx1-roGFP2-transfected and Dox-induced Ero1α cells were treated with or without BCNU as in panel (B) and processed as in panel (A). * $p < 0.05$; *** $p < 0.001$

Consistent with an involvement of H_2O_2, Ero1α-overexpression-dependent accumulation of GSSG after DTT washout was more prominent when GPx8 levels were lowered by doxycycline-inducible shRNA (Fig. 10A and S4A). Of note, GSSG formation was also increased in PrxIV-silenced cells compared to control (Fig. 10B and S4B). This indicated that under conditions of artificially maximized production of H_2O_2 by Ero1α, also PrxIV participates in detoxification. In further support of this, stable overexpression of both GPx8-HA and PrxIV-FLAG inhibited Ero1α-dependent GSSG accumulation after DTT washout (Fig. 10C+D and S4C). In case of GPx8-HA, this inhibition depended on its active site cysteine (Fig. 10E). This was less obvious for PrxIV (Fig. 10F), which is likely explained by formation of PrxIV wild-type–mutant heterodecamers [29]. Finally, alleviation of glutathione oxidation after DTT washout was also observed upon ectopic overexpression of GPx7-HA (Fig. S4D). The PrxIV results contrasted with the lack of quenching impact of this peroxidase on Ero1α-derived H_2O_2 observed in HyPer experiments, even in presence of DTT (Fig. 7E and 8A). This may be due to more powerful cellular hyperoxidation following the washout of DTT and – likely – redox-independent effects of PrxIV siRNA on the HyPer sensor (Fig. S2C and S3C).

Collectively, the experiments demonstrated that PrxIV contributes to the reduction of Ero1α-derived H_2O_2 only upon non-physiological activation of Ero1α by DTT, which is consistent with

the data, but not the conclusions of a previous study [52]. Our findings therefore suggest an Ero1-independent H_2O_2 source for PrxIV under normal physiology and reveal compartmentalization of H_2O_2-reducing pathways in the ER.

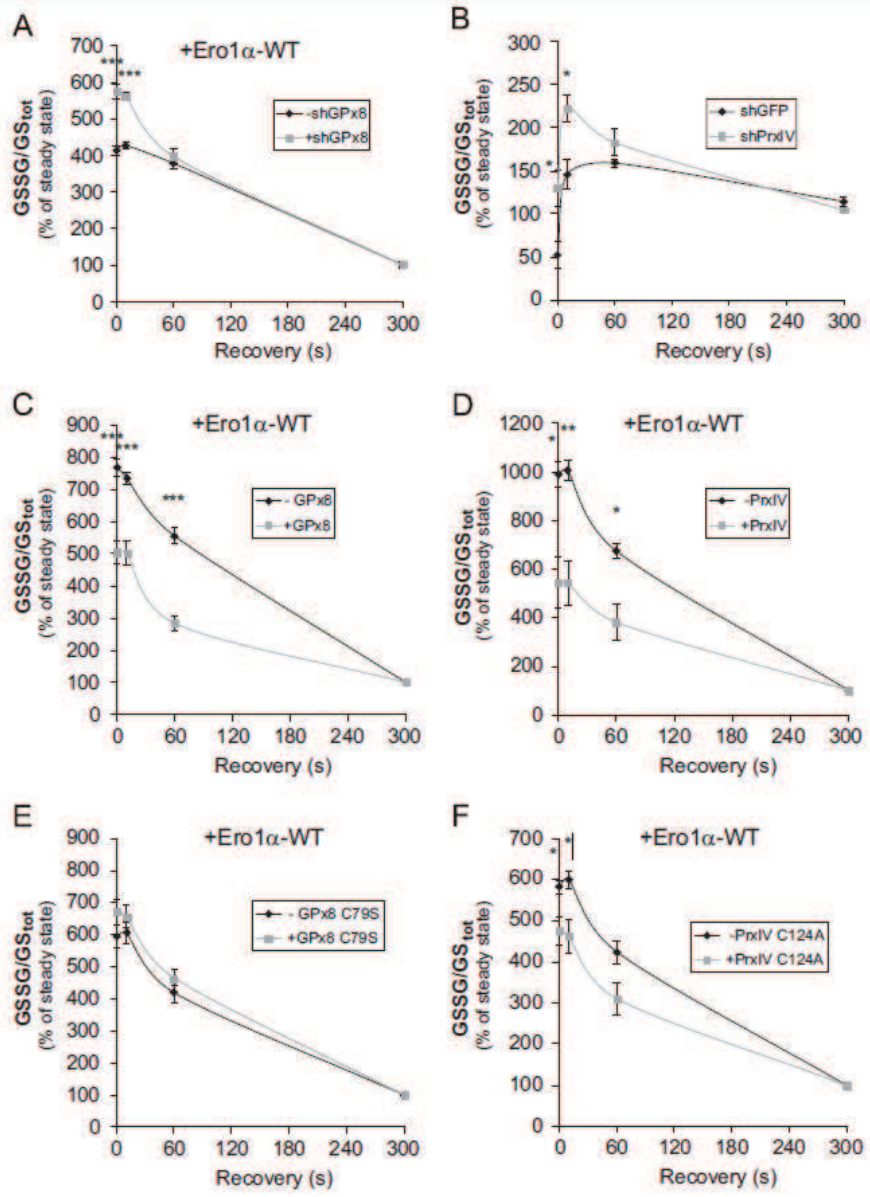

Figure 10: ER-resident peroxidases antagonize the accumulation of GSSG in the cytosol. (A) GSSG:GS_{tot} recovery after DTT was studied as in Fig. 9B in shGPx8:Ero1α cells, which had been induced or not for 72 h with doxycycline (Dox) (mean ± SEM; two independent experiments each performed in triplet). These cells are Dox-inducible for the expression of GPx8-targeting shRNA and, in addition, constitutively overexpress Ero1α-WT. **(B)** GSSG:GS_{tot} recovery assay in HT1080 cells stably transfected with GFP- or PrxIV-targeting shRNA [29] (mean ± SEM; one of three independent experiments performed in triplet; other experiments are shown in Fig. S4B). **(C-F)** GSSG:GS_{tot} recovery upon DTT washout in Ero1α cells was compared to the recovery in Ero1α:GPx8-HA (C), Ero1α:PrxIV-FLAG (D), Ero1α:GPx8-HA-C79S (E), or Ero1α:PrxIV-FLAG-C124A (F) cells (mean ± SEM; at least two independent experiments each performed in triplet). It should be noted that due to the complexity of this assay absolute numbers can only be compared within the same experiment as verified by the consistency of technical replicates. * $p < 0.05$; ** $p < 0.01$; *** $p < 0.001$

2.3.5. GPx8, PrxIV and Ero1α reside in the rough ER

The preference of GPx8 over PrxIV to react with Ero1α-derived H_2O_2 could be due to residence in different ER subcompartments [57]. We tested whether GPx8 was enriched in mitochondria-associated ER membranes (MAM), as has been reported for Ero1α [58,59]. However, using a biochemical fractionation protocol optimized for the separation of rough ER membranes (rER) and MAM [44,58] we found that GPx8 as well as PrxIV co-fractionated with rER markers (Fig. 11A). Remarkably, endogenous Ero1α was not enriched in MAM fractions either (Fig. 11B). It is possible that the latter finding is due to lower Ero1α levels in FlpIn TRex 293 cells compared to cell types where Ero1α is predominantly MAM-localized [58,59]. On non-reducing gels, at least three redox species of endogenous Ero1α are separable, whereas their relative abundance varies significantly between experiments (Fig. S2 in [40]). Similarly, the distribution of Ero1α redox species in non-MAM fractions showed variation (Fig. 11B and S5). When detected, reduced and semi-reduced forms of Ero1α, which likely constitute the activated fraction of the oxidase [8], were co-enriched with GPx8 in the rER or ran at the top of the gradient (Fig. 11B and S5). Finally, we examined whether GPx8 localizes to detergent-resistant membranes (DRMs), which is a common feature for MAM-resident transmembrane proteins [60]. As shown in Fig. 11C and in agreement with GPx8 residing in the rER, the peroxidase was not enriched in DRMs. Unfortunately, available antibodies did not permit accurate immunofluorescence analyses of GPx8. These data suggested that Ero1α-catalyzed oxidative protein folding and H_2O_2 formation does not predominantly take place in MAM and that the functional separation of ER peroxidases is mediated by a mechanism other than ER subcompartmentalization (see Discussion).

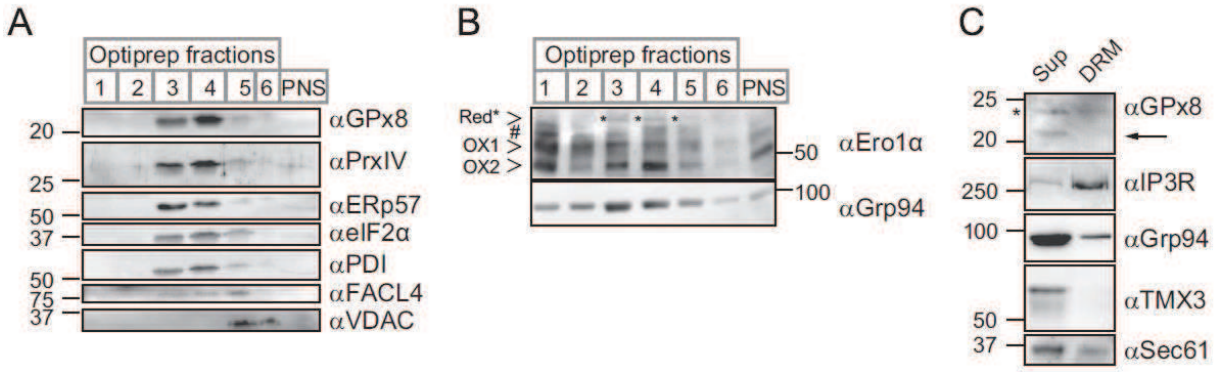

Figure 11: GPx8 and active Ero1α are enriched in the rER. (A) Homogenates of Ero1α-C104A/C131A cells were fractionated on an Optiprep gradient, and equal amounts of total protein analyzed by Western blot using the indicated antibodies. ERp57, eIF2α, and PDI are rER markers, FACL4 a MAM marker, and VDAC a mitochondrial marker. Note that the concentration of Optiprep negatively affects the smoothness of the gel. **(B)** Fractions from an Optiprep gradient equivalent to the one shown panel (A) were treated with N-ethylmaleimide as described in Materials and Methods, and the glycoproteins precipitated with concanavalin A-sepharose. This concentration step was necessary, because endogenous Ero1α was consistently hard to detect in total lysates of FlpIn TRex 293 cells. Precipitates were subjected to non-reducing SDS-PAGE and αEro1α Western blot. As a positive control for the precipitation of glycoproteins, Grp94 was detected on the same blot. The identity of the subcellular compartment enriched in fraction 1, where a significant fraction of endogenous Ero1α resides, is currently unclear. The mobilities of known redox forms of Ero1α (Red*, OX1, OX2) [40] are indicated. #, unknown "semi-reduced" redox forms of Ero1α. Note that in agreement with previous data [40], the detection of the Red* and the # forms was variable (see experimental replica in Fig. S5). **(C)** Post-nuclear supernatant of Ero1α-C104A/C131A cells was solubilized with Triton X-114, DRM-associated proteins (DRM) separated from detergent-soluble supernatants (Sup), and the fractions analyzed by Western blot using antibodies against GPx8, IP3R-I/II/III (a DRM marker), TMX3 and Sec61α (ER transmembrane proteins), and Grp94 (a soluble, ER-luminal protein). PNS, post-nuclear supernatant; asterisk, unspecific band detected by αGPx8.

2.4. Discussion

Excessive generation of cytotoxic H_2O_2 during Ero1-driven oxidative protein folding could promote apoptosis during ER stress [21,22,23,25,26]. This simple model for the generation of ER-stress-induced ROS is supported by the proapoptotic activity of Ero1α, which is upregulated by the UPR [12,61,62]. Inconsistently however, acute and homogeneous overexpression of Ero1α neither affects cell proliferation nor redox maintenance [40]. This was ascribed to the presence of inactivating, feedback-regulated disulfide bonds in Ero1α [31], but overexpression of a hyperactive Ero1α mutant lacking those disulfide bonds (Ero1α-ACTIVE) – while detectably hyperoxidizing the ER – also fails to promote cell death [18,47] (Fig. 6B).

Using inducible expression of Ero1α-ACTIVE, which resulted in overproduction of Ero1α-derived H_2O_2, we identified GPx8 as a molecular gatekeeper that confers protection against this challenge (Fig. 12): Knockdown of GPx8 enhanced the efficacy of Ero1α-ACTIVE to overoxidize the ER, to cause ER stress, and to decrease cell viability. Additionally, we

demonstrated for the first time in mammalian cells that Ero1α-derived H_2O_2 can, in principle, leak from ER to cytosol. It is important to emphasize that the rationale of applying non-physiological induction of Ero1α-ACTIVE was not to represent normal cell physiology, but to specifically raise the concentration of Ero1α-derived H_2O_2 to detectable levels. Indeed, leakage into the cytosol of ER-derived H_2O_2 was evident only upon non-physiological short-term activation of Ero1α with DTT either in combination with GPx8 knockdown or Ero1α overexpression. Thus, a multilayer control system consisting of negative feedback regulation [40] and low expression [41] of Ero1α along with GPx8 activity (this study) and the endogenous antioxidant glutathione [18] ensures that cellular redox homeostasis in non-manipulated 293 cells is not destabilized by Ero1α activity. How far these conclusions are relevant for other mammalian cell types with different gene expression profiles (e.g. of *GPX7*) is yet unclear. Still, our findings suggest that earlier work on Ero1-dependent oxidative stress in *S. cerevisiae* [26] and *C. elegans* [25], which have no ER-resident peroxidases [6], may not reflect the physiology of human cells. Alternative sources for ER-stress-induced ROS and mechanisms for Ero1α-facilitated apoptosis have been discussed elsewhere [8,24].

Despite the tight shielding of the cytoplasm against Ero1α-derived H_2O_2, knockdown of GPx8 in otherwise non-manipulated cells also led to phenotypic changes. These changes included elevation of UPR and antioxidant response markers, slowed proliferation, and increased oxidation of the cytosol. While this presumably underscores the physiological importance of efficient clearing of Ero1α-derived H_2O_2, the mechanism underlying cell toxicity in absence of GPx8 remains to be worked out.

Our study reveals a previously unappreciated functional compartmentalization of electron transport pathways in the rER where two peroxide-scavenging enzymes – GPx8 and PrxIV – target distinct pools of H_2O_2 (Fig. 12). Whereas GPx8 reacts with Ero1α-derived H_2O_2 (see above), we could not confirm the proposed role of PrxIV in detoxifying these ROS [32,52]. Contrary to GPx8, depletion of PrxIV did not add up with Ero1α-ACTIVE to precipitate ER hyperoxidation and expression of UPR and antioxidant response target genes. The functional separation of PrxIV and GPx8 with respect to Ero1α-derived H_2O_2 was only overcome using an artificial setup combining overexpression of Ero1α and application of DTT, which entails massive generation of H_2O_2 in the ER (Fig. 12). These data explain the misleading identification

of a functional interplay between Ero1α and PrxIV, which was based on experiments with DTT-activated Ero1α [52]. It is important to note though that peroxidase activity of PrxIV towards H_2O_2 of unknown origin is important, since its depletion triggered the antioxidant response (Fig. 6D) and affected cell proliferation at least in part through activation of caspase 3 (Fig. 6B and S1G). The existence of an Ero1-independent H_2O_2 source for PrxIV has also been concluded from experiments in mice [63].

We excluded that the functional compartmentalization of GPx8 and PrxIV in 293 cells is achieved through recruitment of GPx8 to MAM where – in certain cell types – Ero1α predominantly resides [58,59]. Our cell fractionation experiments rather indicated that Ero1α and GPx8 operate in the rER where disulfide bonds need to be introduced into incoming substrate proteins. Since PrxIV is also concentrated in the rER, the observed preference of GPx8 over PrxIV to handle Ero1α-derived H_2O_2 is likely explained by formation of specific protein complexes such as the Ero1α–GPx8 complex previously observed by a split YFP-complementation approach [27]. Indeed, the fact that PrxIV, which can react with H_2O_2 at a high turnover rate [64], does normally not gain access to Ero1α-derived H_2O_2 strongly suggests that H_2O_2 cannot diffuse away from the Ero1α–GPx8 complex and is reduced on the spot.

In addition to its function as a H_2O_2 scavenger, PrxIV constitutes an important Ero1-independent generator of new disulfide bonds [5,28,63,65]. Recently published *in vitro* reconstitution experiments indicated that both PrxIV-driven substrate oxidation and the Ero1–PDI disulfide relay are required for reliable and efficient oxidative protein folding [30]. Our data, which dissociate the function of PrxIV from Ero1α-derived H_2O_2 in the ER of live cells, are in agreement with this view.

Whereas oxidized PrxIV contributes to oxidative protein folding by transferring its disulfide onto PDI family members [5,30,32,65], the reducing substrate(s) of GPx8 is/are currently unclear [28]. Although GPx7 and GPx8 can act as PDI-oxidizing peroxidases *in vitro* [27,37,38], reducing substrates other than PDI including glutathione have been suggested [28,34,37]. Here, we observed that knockdown of GPx8 increased ER hyperoxidation by Ero1α-ACTIVE (Fig. 7), demonstrating that unchecked Ero1α-derived H_2O_2 twists the ER redox balance more potently than the final product of the GPx8 pathway. We propose that this product is mainly oxidized PDI,

which is the central element in the negative feedback regulation of Ero1α [40]. Accordingly, disulfide bonds fed into PDI-mediated oxidative protein folding *via* GPx8 will directly prevent the generation of new disulfides (and of new H_2O_2) by Ero1α thereby maintaining redox homeostasis. Conversely, in absence of GPx8, H_2O_2 can indiscriminately oxidize protein thiols to sulfenic acid (a precursor of disulfide-bond formation) so that the specific funneling of disulfides into PDI-mediated negative feedback regulation is hampered.

In conclusion, while we demonstrated that Ero1α-derived H_2O_2 can in principle leak into the cytosol, the ER harbors dedicated machinery to prevent such leakage. Since GPx8, the core component of this machinery, is induced on ER stress, Ero1α activity cannot be the source of ER-stress-induced cytoplasmic ROS.

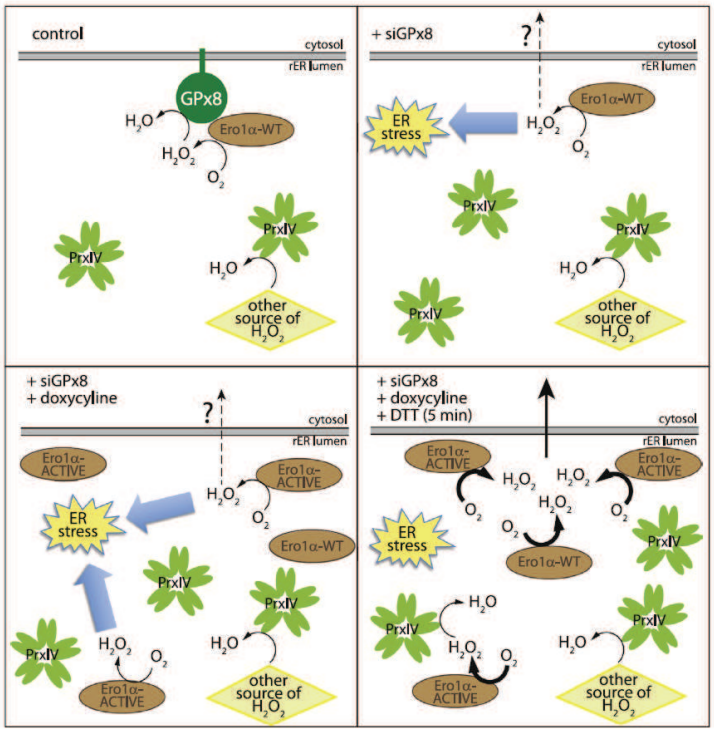

Figure 12: Processing of H_2O_2 in the ER of human cells. *Upper left panel:* Under control conditions, Ero1α operates at low turnover rate in the lumen of the rough ER (rER) to sustain steady-state disulfide-bond formation. H_2O_2, produced as a side product of this activity, is converted to H_2O by GPx8, which directly binds to Ero1α [27]. In parallel, PrxIV reacts with H_2O_2 from a source other than Ero1α, as evidenced by the induction of antioxidant response target genes upon knockdown of PrxIV (Fig. 6D). The identity of this alternative source of H_2O_2 is currently not known [32,63]. *Upper right panel:* Knockdown of GPx8 (siGPx8) leads to a moderate increase in [H_2O_2] in the ER lumen, which is below the detection limit of $HyPer_{ER}$ but causes discernible ER stress. Whether – upon siGPx8 treatment alone – H_2O_2 leaks into the cytosol or quantitatively reacts with local thiol groups e.g. in PDI or glutathione (not shown) is not known (as indicated by the question mark). GPx8 knockdown cells exhibit increased levels of PrxIV. *Lower left panel:* Doxycycline-mediated overexpression of Ero1α-ACTIVE on top of GPx8 knockdown elicits a more pronounced increase in [H_2O_2] and ER stress. However, H_2O_2 may still be confined to the ER lumen (as indicated by the question mark). *Lower right panel:* Short-term activation of Ero1α by DTT in combination with GPx8 knockdown and/or overexpression of Ero1α-ACTIVE leads to substantial accumulation of H_2O_2 in the ER and to detectable leakage of H_2O_2 through the ER membrane. Only under these conditions, also PrxIV can react with Ero1α-derived H_2O_2.

Acknowledgements

We are grateful to Alex Odermatt for generous support. We also thank Mike Hall and Ineke Braakman for comments on the manuscript, Julia Birk for help with statistical analysis, Thomas Simmen, Emily Lynes, and Charles Betz for help with subcellular fractionation and for sharing unpublished data, Denise Kratschmar and Adam Lister for help with qPCR, Lori Rutkevich for help with PrxIV knockdown, and Lloyd Ruddock, Miklos Geiszt, Tobias Dick, Christopher Nicchita, Ineke Braakman, Sang Yoon Kim, Mike Hall, Hans-Peter Hauri, and Ari Helenius for sharing reagents. This work was supported by the Freiwillige Akademische Gesellschaft and the University of Basel. TR is a fellow of the Boehringer Ingelheim Fonds, HGH is a recipient of an EliteForsk Travel Stipend from the Danish Ministry of Science, Innovation and Higher Education, LE obtained funding from the Danish Council for Independent Research (Natural Sciences) and the Lundbeck Foundation, and CAH is a recipient of an Ambizione grant by the Swiss National Science Foundation.

2.5. Materials and Methods

2.5.1. RNA Isolation and qPCR analysis

Total RNA was isolated using TRI Reagent (Sigma) and reverse transcribed with Superscript III (Invitrogen) using poly-dT primers. The resulting cDNA was subjected to qPCR analysis on a Corbett Research Rotor-Gene 6000 (V 1.7) using SYBR FAST qPCR Master Mix (KAPA Biosystems) and the following primer pairs (all 5'-3'): *Prdx4* Fw CGAAGATTTCCAAGCCAGCGCCC, *Prdx4* Rev CGAGGGGTATTAATCCAGGCCAAATGGG, *GPx8* Fw CTACGGAGTAACTTTCCCCATCTTCCACAAG, *GPx8* Rev CTGCTATGTCAGGCCTGATGACTTCAATGG, *GPx7* Fw GCAAACTGGTGTCGCTGGAGAAGTACC, *GPx7* Rev GAAGTCTGGGCCAGGTACTTGAAGG, *KEAP1* Fw GGACAAACCGCCTTAATTCA, *KEAP1* Rev CATAGCCTCCAAGGACGTAG, *NQO1* Fw ATTTGAATTCGGGCGTCTGCTG , *NQO1* Rev GGGATCCACGGGGACATGAATG, *GCLC* Fw TCTCTAATAAAGAGATGAGCAACATGC, *GCLC* Rev TTGACGATAGATAAAGAGATCTACGAA, *NFE2L1* Fw GTGCGAGAAAGCGAAACG, *NFE2L1* Rev CCCCAGATCAATATCCTGTCG, *NFE2L2* Fw GCAGTCATCAAAGTACAAAGCAT, *NFE2L2* Rev CATCCAGTCAGAAACCAGTGG, *DDIT3* Fw AAGGCACTGAGCGTATCATGT, *DDIT3* Rev TGAAGATACACTTCCTTCTTGAACA, *ATF6* Fw GTCCCAGATATTAATCACGGA, *ATF6* Rev TATCATACGTTGCTGTCTCCTT, *HERPUD1* Fw GAGCAGATTCCTCATGGTCAT, *HERPUD1* Rev GGCCTCGGTCTAAATGGAAA, *GAPDH* Fw TCCTTGGAGGCCATGTGGGCCAT, *GAPDH* Rev TGATGACATCAAGAAGGTGGTGAA, *PPIA* Fw CATCTGCACTGCCAAGACTGA, *PPIA* Rev TGCAATCCAGCTAGGCATG, *HPRT1* Fw GGCTCCGTTATGGCGACCCG, *HPRT1* Rev CGAGCAAGACGTTCAGTCCTGTCC; Genes used as internal standards were *GAPDH* and *HPRT1* (geometric mean calculated using the Bestkeeper Software [39]) or (for experiments in Fig. S1A+F and S2F) *PPIA*.

2.5.2. RNA interference

SiRNA transfections were conducted with Lipofectamine RNAiMAX (Invitrogen) using the following siRNAs: negative control siRNA 1022076 (10-60nM; Qiagen), siPRDX4 HSS173720 (40nM; Invitrogen), siGPX8 HSS166723 (10nM; Invitrogen) and siKEAP1 D-012456-04 (10nM; Thermo Scientific). For combined depletion of GPx8 and PrdxIV HSS166723 (20nM) and HSS173720 (40nM) were mixed.

Ero1α-C104A/C131A cells were seeded in 6-well plates and transfected with siRNAs the following day (day 0). 48 h post-transfection the cells were trypsinized and reseeded onto 6-well plates (day 2), followed by a second round of transfection (day 3) and subsequent analysis (day 5). In the case of siRNA-mediated depletion of Keap1, a single transfection was performed and the cells analyzed 72 h post-transfection.

2.5.3. Alkylation assay of ERp57

The protocol for alkylation of originally oxidized cysteines with 4-acetamido-4′-maleimidylstilbene-2,2′-disulfonic acid (Life Technologies) has previously been published [40].

2.5.4. DTT washout assays

The cellular GSSG:total glutathione (GS_{tot}) ratio after DTT washout was measured using a DTNB/glutathione reductase recycling assay as previously described [41]. Where indicated, BCNU (Sigma) was used at a concentration of 1 mM.

In order to visualize the redox state of Grx1-roGFP2 after DTT washout, transiently transfected cells were grown on UV-sterilized coverslips and treated as previously published [41]. Subsequently the cells were analyzed by αGFP immunoprecipitation/Western blot as described previously [2]. To generate a mobility marker for the oxidized from of Grx1-roGFP2, transfected cells were treated for 5 min with 5 mM diamide (Sigma).

2.5.5. Sulphorhodamin B assay

Ero1α-C104A/C131A cells were seeded in 6-well plates and transfected with siRNA the following day. 48 h post-transfection the cells were trypsinized and reseeded onto 96-well plates (three wells per condition). On the following day, cells were either harvested or subjected to a second round of transfection with the respective siRNA(s) for either 24 h or 48 h. Ero1α-

C104A/C131A expression was induced for the last 24 h of knockdown. The medium was removed and the proteins precipitated by addition of 10% trichloroacetic acid (TCA). Staining with 0.4% Sulphorhodamin B (Sigma) was performed as described elsewhere [42] and OD_{565} measured in a UV max microplate reader (Molecular Devices).

2.5.6. Fluorescence excitation spectrum analysis

Cells stably transfected with $HyPer_{ER}$ or $HyPer_{cyto}$ were subjected to fluorescence excitation spectrum analysis as described elsewhere [43]. If present, 0.5 mM DTT was added 5 min before analysis. To validate the sensor response, cells treated with either 100 μM H_2O_2 or 10 mM DTT for 5 min were routinely co-analyzed in separate wells.

2.5.7. Indirect immunofluorescence staining

Ero1α-C104A/C131A:$HyPer_{ER}$ or Ero1α-C104A/C131A:$HyPer_{cyto}$ cells were grown for 48 h on glass coverslips, fixed with 4% paraformaldehyde for 20 min at room temperature, quenched with 50 mM NH_4Cl and either directly mounted in Mowiol 4-88 (Hoechst) (Ero1α-C104A/C131A:$HyPer_{cyto}$) or permeabilized with 0.1% Triton X-100 (Ero1α-C104A/C131A:$HyPer_{ER}$). In the case of the latter, cells were blocked with 1% bovine serum albumin in PBS and incubated in the same buffer with αPDI for 1 h followed by Hilyte 555-conjugated goat-anti-mouse (AnaSpec). Stained cells were analyzed on an Olympus Fluoview 1000 laser scanning confocal microscope.

2.5.8. Subcellular fractionation

Ero1α-C104A/C131A cells were homogenized by 15 passages through a ball-bearing homogenizer (clearance 18μm) in 0.25 M sucrose, 10 mM HEPES pH 7.4, 1 mM EDTA, 1 mM EGTA, 0.2 mM phenylmethylsulphonylfluoride (PMSF). The homogenate was centrifuged twice for 10 min at 1000*g* to remove unbroken cells and nuclei. Postnuclear supernatant (PNS) was layered on top of a discontinuous OPTIPREP gradient using 20%, 16.25%, 12.5%, 8.75% and 5% OPTIPREP (Progen Biotechnik). The samples were centrifuged at 39,000 rpm for 3h at 4°C in a TLS-55 rotor (Beckman). Six equal fractions were collected from the top of the gradient and precipitated with either 10% TCA or 80% acetone. Free cysteines in the TCA pellets were modified with N-ethylmaleimide (NEM) as previously described [41] and subjected to

precipitation with Concanavalin A sepharose (GE healthcare) prior to non-reducing SDS-PAGE and Western blot. Equal amounts of protein from acetone-precipitated fractions were subjected to reducing SDS-PAGE and Western blot.

DRMs were isolated essentially as published [44]. Briefly, PNS of Ero1α-C104A/C131A cells was centrifuged for 10 min at 10,400*g* to obtain a heavy membrane pellet, which was homogenized on ice in 200 µl 10 mM Tris, pH 7.4, 150 mM NaCl, 5 mM EDTA, 0.2 mM PMSF by sonication. The suspension was lyzed by addition of Triton X-114 (0.5% final concentration) and incubation for 30 min on ice, followed by the pelleting of DRMs for 1 h at 100,000*g* in a TLA-55 rotor (Beckman). Equal volumes of solubilized pellet and supernatant were analyzed by Western blot.

2.5.9. Statistics

Data sets were analyzed for statistical significance using student's T-test (two-tailed distribution; heteroscedastic). When batch-specific differences in absolute values rendered a direct comparison of averages impossible, logarithmically transformed values were fitted to a linear model using a batch-specific offset. 95% confidence intervals and P values were calculated using linear regression in Microsoft Excel. For GSSG:GS_{tot} recovery curves after DTT washout in Ero1α cells, consistent with previously published data [41], the 300 s recovery time point was set to 100% of steady state for joint presentation of individual washout experiments.

2.5.10. Cell culture, recombinant DNA and transfections

The culturing of HEK293 and FlipIn TRex293 cells for doxycycline (1µg/ml, Sigma)-inducible expression of Ero1 variants has been described [40]. The following FlipIn TRex293 cell lines have been published previously: Ero1α [40], Ero1α-C104A/C131A [18], and Ero1β-C100A/C130A [2]. HT1080 shPrdx4 and HT1080 shGFP cells [29] were a kind gift of Neil Bulleid (University of Glasgow, UK).

ShGPx8:Ero1α cells were created as follows: In a first step, two complementary oligos encoding a GPx8-targeting short hairpin (Fw: GATCCCCGGACTGTCCCAGTCAACATGATTCAAGAGATCATGTTGACTGGGACAGTC CTTTTTGGAAA; Rev: AGCTTTTCCAAAAAGGACTGTCCCAGTCAACATGATCTCTTGAATCATGTTGACTGG

GACAGTCCGGG) were annealed and ligated into HindIII/BamHI-digested pSuperior.neo+GFP. The resulting shRNA plasmid was transfected into FlipIn TRex 293 cells (Invitrogen), and stable shGPx8 clones selected with 1 mg/ml G418 (Sigma). In a second step, Ero1α-myc6his [40] was subcloned into the pcDNA3.1+.puro vector using XhoI and BamHI, which was stably transfected into shGPx8 cells using 1 μg/ml puromycin (Sigma) for clonal selection.

Ero1α-C104A/C131A:HyPer and Ero1β-C100A/C130A:HyPer cells were created by transfecting Ero1α-C104A/C131A or Ero1β-C100A/C130A cells with the respective HyPer [45] (kindly provided by Miklos Geiszt, Semmelweis University, Hungary) followed by clonal selection with 1 mg/ml G418. Ero1α-C104A/C131A:SypHer cells were equally created but using HyPer plasmids carrying the C121S mutation, which was inserted by site-directed mutagenesis (QuikChange, Stratagene) according to manufacturer's guidelines.

GPx7-HA and GPx8-HA sequences on pRK7 vector (kindly provided by Lloyd Ruddock, University of Oulu, Finland) were excised and cloned into pcDNA3 using HindIII and BamHI. The latter plasmid was used for site-directed mutagenesis to introduce the C79S mutation. PrxIV-FLAG and PrxIV C124A-FLAG were amplified by PCR and cloned into pcDNA3.1+ using EcoRI and BamHI. These plasmids encoding for wild-type or mutant GPx7, GPx8, and PrxIV were transfected into Ero1α cells and clonal selection was conducted with 1 mg/ml G418.

All transfections of plasmids were carried out with Metafectene Pro (Biontex) according to manufacturer's guidelines.

2.5.11. Antibodies

The following antibodies were used: 9E10 (αmyc, Covance), αHA (a kind gift of Hans-Peter Hauri, University of Basel, Switzerland), M5 (αFLAG, Sigma), αERp57 (a kind gift of Ari Helenius, ETH Zürich, Switzerland), αGFP (a kind gift of Jan Riemer, University of Kaiserslautern, Germany), αGPx8 (a kind gift of Lloyd Ruddock, University of Oulu, Finland), αGPx7 (ProteinTech; GeneTex), αPrxIV (Abfrontier), αeIF2α, αP-eIF2α, αJNK1, αP-JNK1, αCasp3, αPERK, αVDAC (all Cell Signaling Technology), αEro1α (a kind gift of Ineke Braakman, University of Utrecht, Netherlands), αGrp94 (DU-120, a kind gift of Christopher Nicchitta, Duke University Medical Center, USA), αIP3R-I/II/III , αFACL4, αActin (I-19) (all Santa Cruz), αTMX3 [46], αSec61α (a kind gift of Richard Zimmermann, Saarland University, Germany).

2.6. Supplemental Information

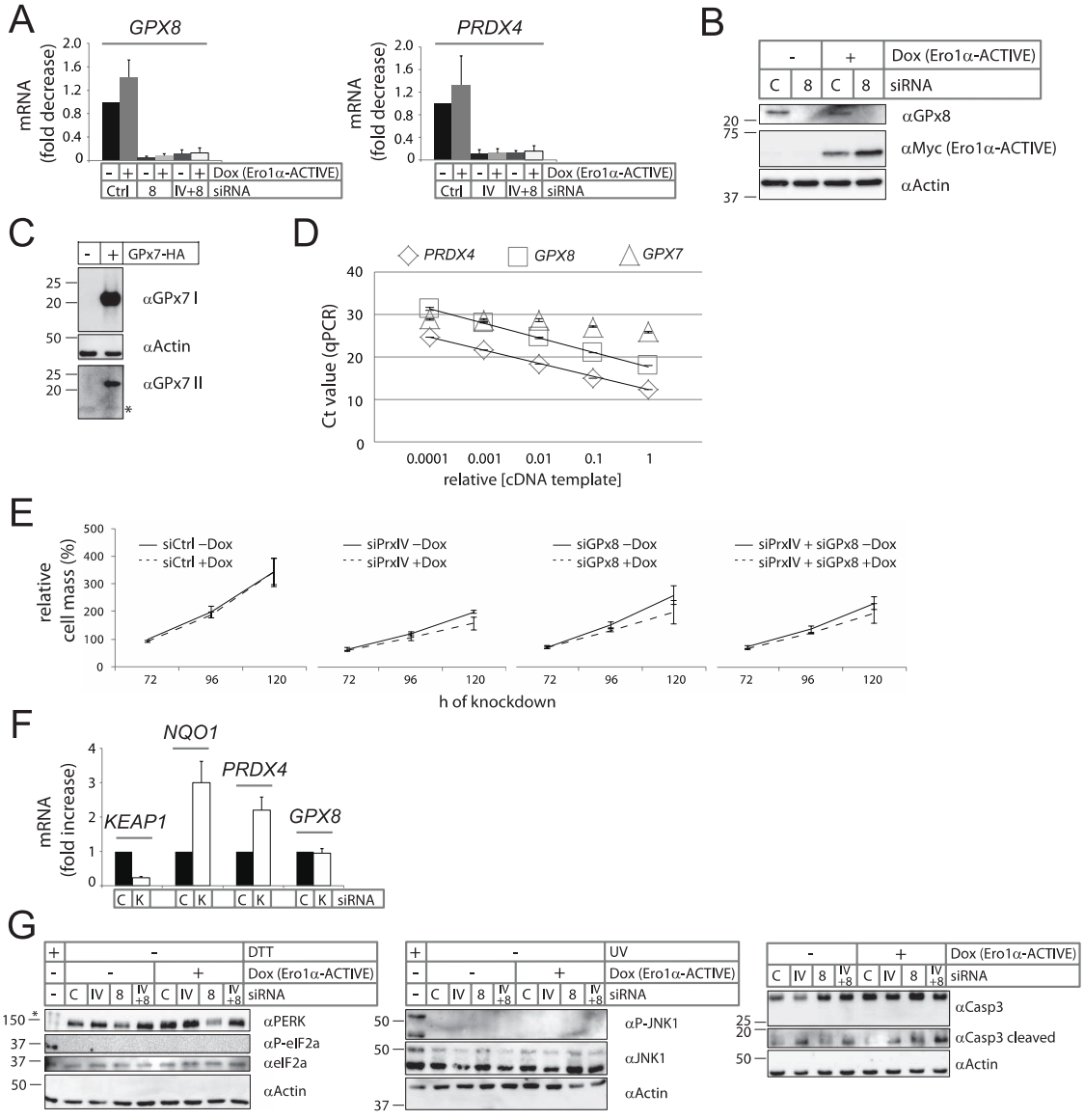

Figure S1: Characterization of peroxidase knockdown cells.

(A) For single and double knockdown, Ero1α-C104A/C131A cells were treated with the indicated siRNAs for 120 h and, where indicated, with doxycycline (Dox) during the last 24 h of knockdown and changes in mRNA levels of *GPX8* and *PRDX4* determined by qPCR ($n \geq 4$; mean ± SEM).

(B) Ero1α-C104A/C131A cells were transfected with GPx8-targeting or control siRNA for 48 h and, where indicated, with Dox for 24 h and analyzed by Western blot using the indicated antibodies.

(C) 293 cells were transfected or not with GPx7-HA and analyzed by Western blot using two different antibodies against GPx7 (denoted αGPx7 I and II) or with αActin. The asterisk marks an unspecific band used as a loading control.

(D) Expression of *PRDX4*, *GPX7*, and *GPX8* in Ero1α-C104A/C131A cells was analyzed by qPCR using serial 10x dilutions of the reverse transcribed cDNA template. Plotted are the measured cycle threshold (Ct) values, which are supposed to be

proportional to the log-transformed [cDNA]. Note that the *PRDX4* and *GPX8* data points connect to a linear slope, indicating mRNA quantification to be accurate and specific. Conversely, no linear fit applies for *GPX7* data points, pointing to unspecific DNA amplification. Indeed, unspecific products were apparent on agarose gels, although a single specific product was amplified from GPx7-HA-overexpressing cells (data not shown). The lower Ct values for *PRDX4* compared to *GPX8* demonstrate higher gene expression of the former.

(E) Cell mass was quantified using sulforhodamine B staining of Ero1α-C104A/C131A cells transfected with control siRNA (siCtrl), or siRNAs targeting PrxIV (siPrxIV), GPx8 (siGPx8), or both for the indicated time periods. Dashed lines denote treatment with Dox during the last 24 h of knockdown. Values were normalized to 72 h knockdown without Dox (n = 3; mean ± SEM).

(F) Ero1α-C104A/C131A cells were transfected with control (C) or *KEAP1*-targeting (K) siRNA 72 h before qPCR analysis of expression of the indicated genes (n = 3; mean ± SEM). *NQO1* is a *bona fide* AR target gene, which is upregulated in response to *KEAP1* siRNA.

(G) Ero1α-C104A/C131A cells were treated with siRNAs and Dox as in Fig. 6A and subjected to Western blot analysis using the indicated antibodies. Positive control treatments of cells were 2 mM DTT for 1 h (for PERK/eIF2α signaling, left panel) or UV irradiation for 0.5 h followed by 0.5 h recovery (for JNK signaling, middle panel). For the detection of cleaved caspase-3 (Casp3), longer exposures of the same blot as for full-length Casp3 were used. One of at least two independent experiments is shown. Asterisk, phosphorylated (activated) form of PERK.

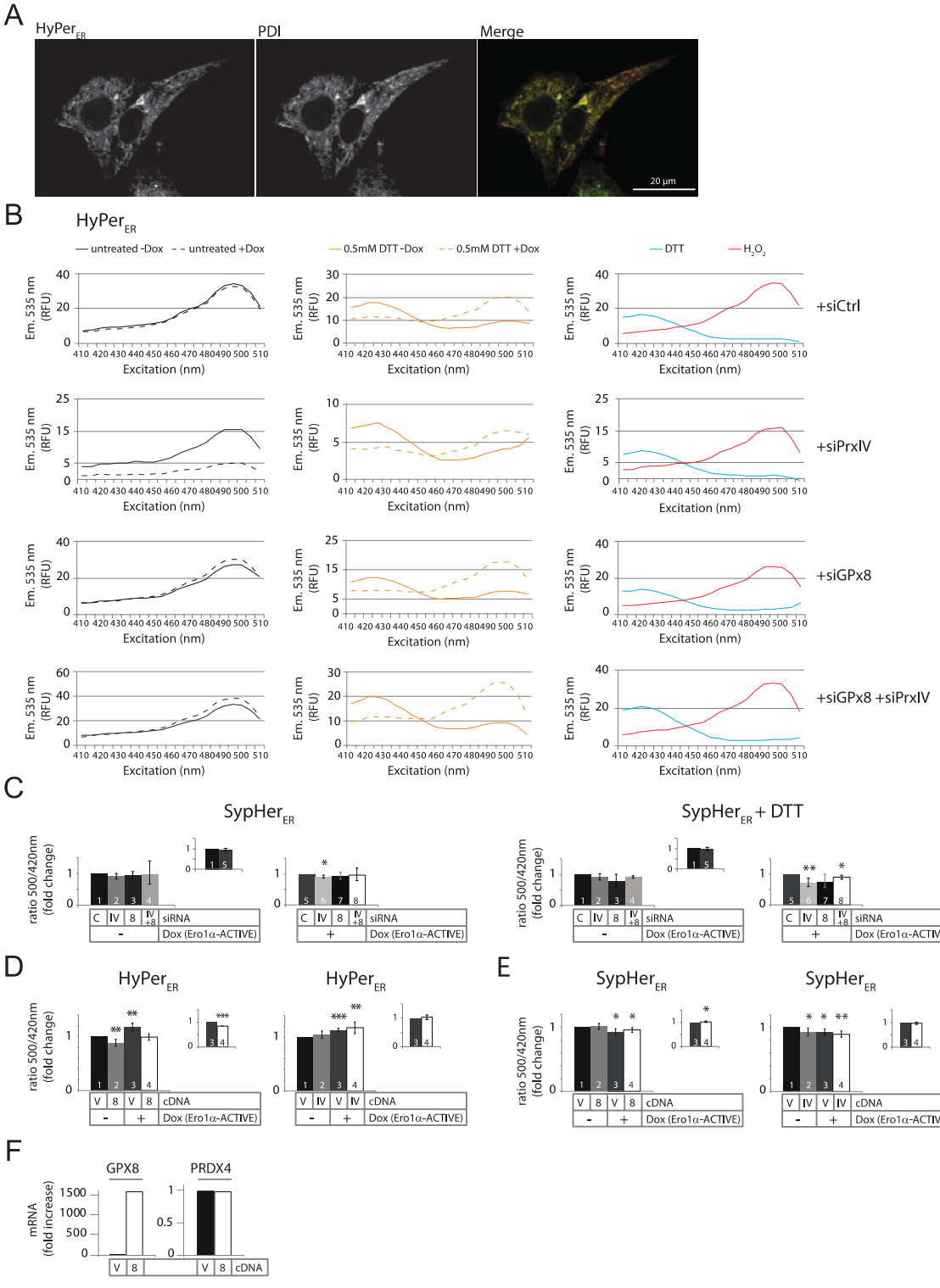
A
HyPer ER
PDI
Merge
20 µm
B
HyPer ER
untreated -Dox
untreated +Dox
0.5mM DTT -Dox
0.5mM DTT +Dox
DTT
H2O2
Em. 535 nm (RFU)
Excitation (nm)
+siCtrl
+siPrxIV
+siGPx8
+siGPx8 +siPrxIV
C
SypHer ER
SypHer ER + DTT
ratio 500/420nm (fold change)
siRNA
Dox (Ero1α-ACTIVE)
D
HyPer ER
HyPer ER
cDNA
Dox (Ero1α-ACTIVE)
E
SypHer ER
SypHer ER
F
GPX8
PRDX4
mRNA (fold increase)
cDNA

Figure S2: $HyPer_{ER}$ control experiments.

(A) Ero1α-C104A/C131A:$HyPer_{ER}$ cells were fixed, stained using αPDI, and analyzed by confocal fluorescence microscopy.

(B) Example $HyPer_{ER}$ spectra from experiments presented in Fig. 7C (left graphs) or Fig. 7E (middle graphs). Dashed lines represent fluorescence data from cells treated with doxycycline (Dox). Graphs on the right depict reference spectra recorded from cells treated for 5 min with 100 μM H_2O_2 (red) or 10 mM DTT, which were routinely obtained in every experiment but were not used for quantification because of reproducible ratio manipulations by peroxidase knockdowns. For unknown reasons, Ero1α-C104A/C131A:$HyPer_{ER}$ cells were proliferation-inhibited upon knockdown of PrxIV in combination with Dox, explaining the lower amplitudes of the respective curves. Em., emission; RFU, relative fluorescence units.

(C) SiRNA(120 h)/Dox(24 h)-treated Ero1α-C104A/C131A:$SypHer_{ER}$ cells (stably expressing $HyPer_{ER}$-C199S) were subjected to fluorescence excitation spectrum analysis in absence (left) or presence (right) of 0.5 mM DTT. Plotted are the changes in ratios of 500 and 420 nm peak amplitudes relative to control (C) siRNA-transfected cells along with 95% confidence intervals (n = 3). The inset shows the relative change in C-transfected cells upon Dox treatment.

(D) 48 h post transfection with empty vector (V), GPx8-HA (8), or PrxIV-FLAG (IV) in presence or absence of Dox, Ero1α-C104A/C131A:$HyPer_{ER}$ cells were subjected to fluorescence excitation spectrum analysis. Changes in the 500/420 nm ratio relative to V-transfected cells without Dox (or with Dox in insets) are plotted along with 95% confidence intervals ($n \geq 3$).

(E) Experiment as described in panel D but using Ero1α-C104A/C131A:$SypHer_{ER}$ cells.

(F) Ero1α-C104A/C131A:$HyPer_{ER}$ cells were transfected with empty vector (V) or GPx8-HA cDNA (8) and analyzed by qPCR using primers against *GPX8* or *PRDX4*.

* $p < 0.05$; ** $p < 0.01$; *** $p < 0.001$

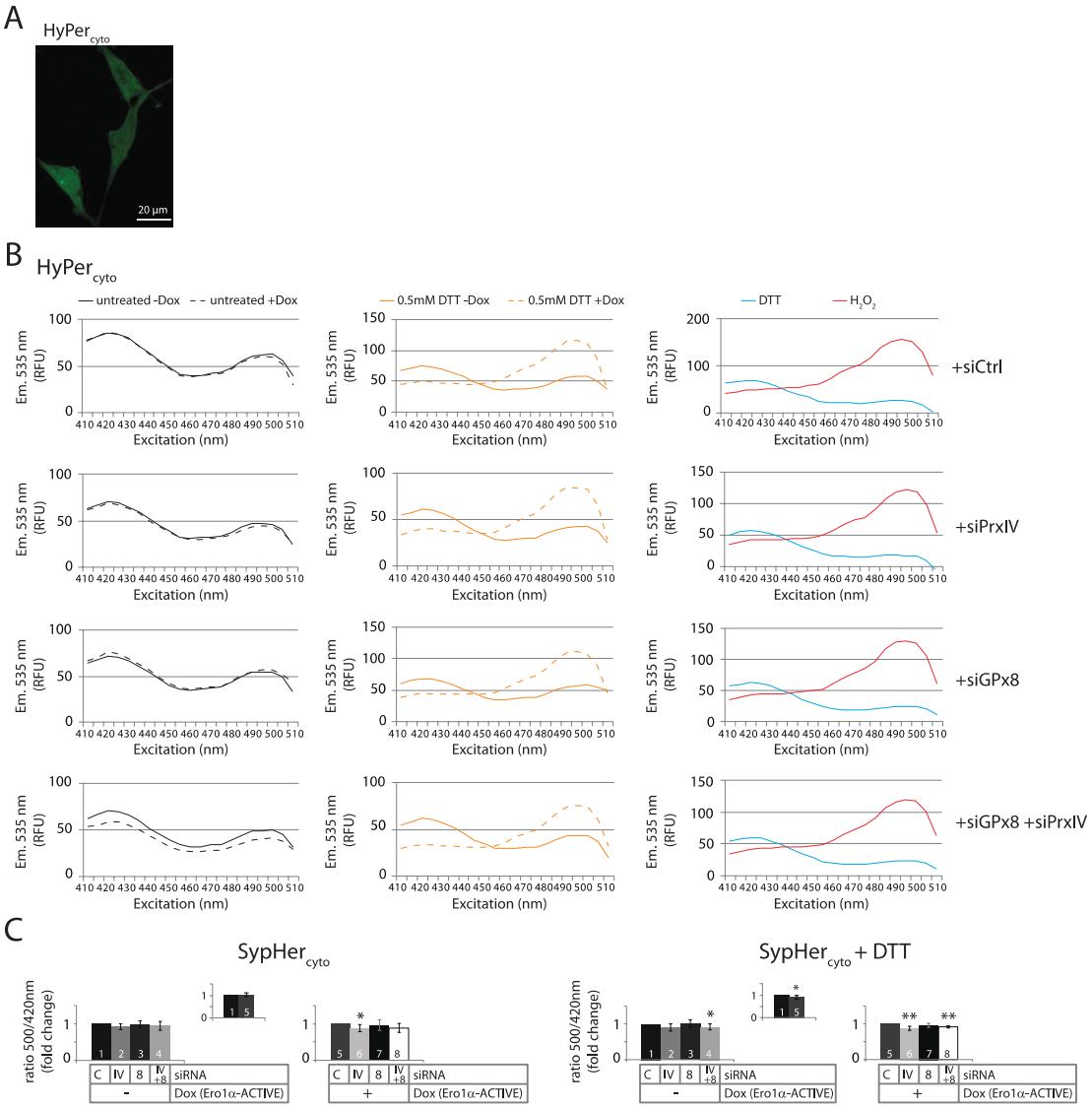

Figure S3: HyPer$_{cyto}$ control experiments.

(**A**) Ero1α-C104A/C131A:HyPer$_{cyto}$ cells were fixed and subjected to confocal microscopy.

(B) Example HyPer$_{cyto}$ spectra from experiments presented in Fig. 8B (left graphs) or Fig. 8A (middle graphs).

(**C**) Same experiment as Fig. S2 panel (C) using Ero1α-C104A/C131A:SypHer$_{cyto}$ cells (stably expressing HyPer$_{cyto}$-C199S).

* $p < 0.05$; ** $p < 0.01$; *** $p < 0.001$

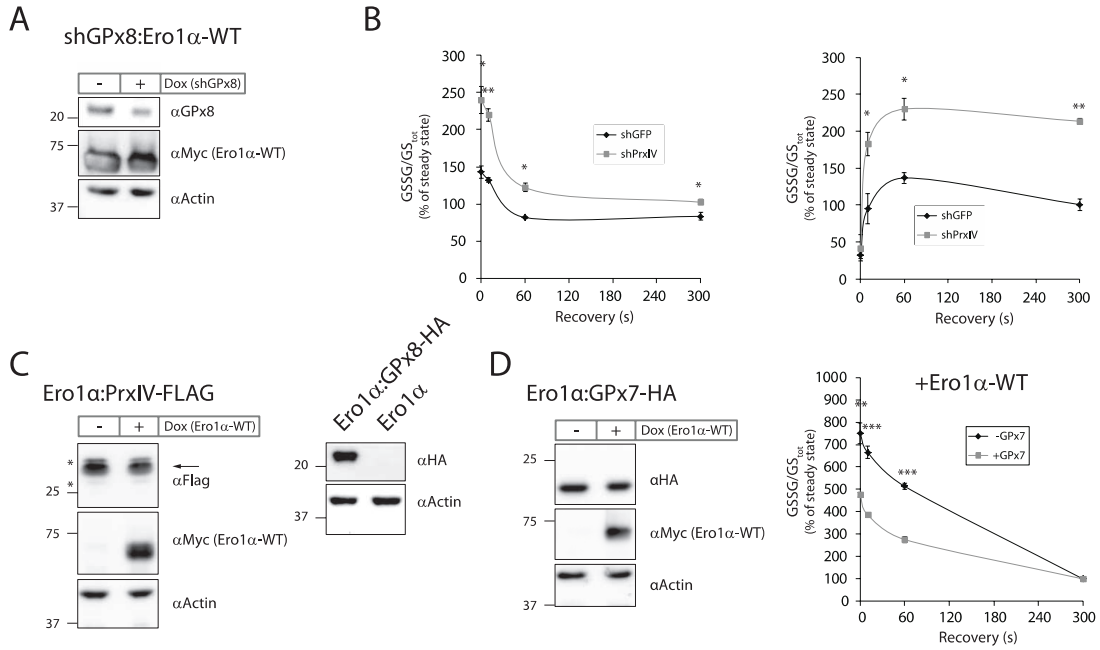

Figure S4: Supplementary and control experiments relating to DTT washout.

(A) Lysates from shGPx8:Ero1α-WT cells treated or not for 72 h with doxycycline (Dox) were analyzed by Western blotting using the indicated antibodies. These cells are Dox-inducible for the expression of GPx8-targeting shRNA and, in addition, constitutively overexpress Ero1α-WT.

(B) Experimental replica of Fig. 10B. For unknown reasons, the time window of shPrxIV-dependent overshoot of the GSSG:GS_{tot} ratio varied significantly, which made joint presentation of the three independent experiments impossible.

(C) Lysates from Ero1α:PrxIV-FLAG or Ero1α:GPx8-HA cells treated or not for 24 h with Dox (where indicated) were analyzed by Western blotting using the indicated antibodies.

(D) GSSG:GS_{tot} recovery upon DTT washout in Ero1α cells was compared to the recovery in Ero1α:GPx7-HA cells (mean ± SEM; two independent experiments each performed in triplet). Lysates from the same cells treated or not for 24 h with Dox were analyzed by Western blotting using the indicated antibodies.

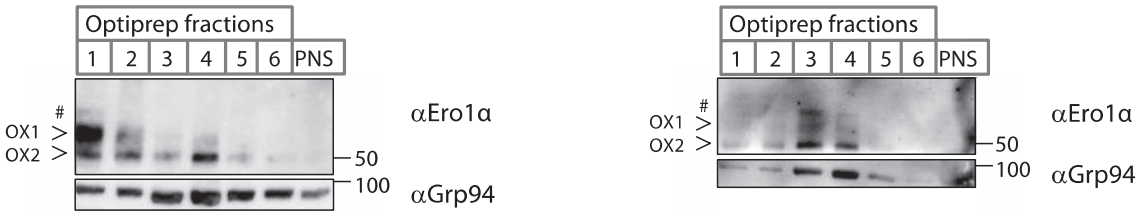

Figure S5: Experimental replica of Fig. 11B

Concanavalin A-precipitated Ero1α and Grp94 was analyzed as in Fig. 11B. These experiments document that the reduced and semi-reduced forms of endogenous Ero1α were not consistently detected in every experiment, as has been observed previously [40]. OX1, OX2, oxidized redox forms of Ero1α; #, unknown semi-reduced redox form of Ero1α.

2.7.References

[1] T. Gidalevitz, F. Stevens, Y. Argon, Orchestration of secretory protein folding by ER chaperones, Biochimica et biophysica acta 1833 (2013) 2410-2424.
[2] J. Birk, M. Meyer, I. Aller, H.G. Hansen, A. Odermatt, T.P. Dick, A.J. Meyer, C. Appenzeller-Herzog, Endoplasmic reticulum: Reduced and oxidized glutathione revisited, Journal of cell science 126 (2013) 1604-1617.
[3] D. Montero, C. Tachibana, J. Rahr Winther, C. Appenzeller-Herzog, Intracellular glutathione pools are heterogeneously concentrated, Redox biology 1 (2013) 508-513.
[4] N.J. Bulleid, L. Ellgaard, Multiple ways to make disulfides, Trends in biochemical sciences 36 (2011) 485-492.
[5] L.A. Rutkevich, D.B. Williams, Vitamin K epoxide reductase contributes to protein disulfide formation and redox homeostasis within the endoplasmic reticulum, Molecular biology of the cell 23 (2012) 2017-2027.
[6] K. Araki, K. Inaba, Structure, mechanism, and evolution of Ero1 family enzymes, Antioxidants & redox signaling 16 (2012) 790-799.
[7] K. Araki, S. Iemura, Y. Kamiya, D. Ron, K. Kato, T. Natsume, K. Nagata, Ero1-alpha and PDIs constitute a hierarchical electron transfer network of endoplasmic reticulum oxidoreductases, The Journal of cell biology 202 (2013) 861-874.
[8] T. Ramming, C. Appenzeller-Herzog, The physiological functions of mammalian endoplasmic oxidoreductin 1: on disulfides and more, Antioxidants & redox signaling 16 (2012) 1109-1118.
[9] L. Wang, S.J. Li, A. Sidhu, L. Zhu, Y. Liang, R.B. Freedman, C.C. Wang, Reconstitution of human Ero1-Lalpha/protein-disulfide isomerase oxidative folding pathway in vitro. Position-dependent differences in role between the a and a' domains of protein-disulfide isomerase, The Journal of biological chemistry 284 (2009) 199-206.
[10] C. Hetz, The unfolded protein response: controlling cell fate decisions under ER stress and beyond, Nature reviews. Molecular cell biology 13 (2012) 89-102.
[11] S.H. Back, D. Scheuner, J. Han, B. Song, M. Ribick, J. Wang, R.D. Gildersleeve, S. Pennathur, R.J. Kaufman, Translation attenuation through eIF2alpha phosphorylation prevents oxidative stress and maintains the differentiated state in beta cells, Cell metabolism 10 (2009) 13-26.
[12] J. Han, S.H. Back, J. Hur, Y.H. Lin, R. Gildersleeve, J. Shan, C.L. Yuan, D. Krokowski, S. Wang, M. Hatzoglou, M.S. Kilberg, M.A. Sartor, R.J. Kaufman, ER-stress-induced transcriptional regulation increases protein synthesis leading to cell death, Nature cell biology 15 (2013) 481-490.
[13] G. Li, C. Scull, L. Ozcan, I. Tabas, NADPH oxidase links endoplasmic reticulum stress, oxidative stress, and PKR activation to induce apoptosis, The Journal of cell biology 191 (2010) 1113-1125.
[14] J.D. Malhotra, H. Miao, K. Zhang, A. Wolfson, S. Pennathur, S.W. Pipe, R.J. Kaufman, Antioxidants reduce endoplasmic reticulum stress and improve protein secretion, Proceedings of the National Academy of Sciences of the United States of America 105 (2008) 18525-18530.
[15] C.X. Santos, L.Y. Tanaka, J. Wosniak, F.R. Laurindo, Mechanisms and implications of reactive oxygen species generation during the unfolded protein response: roles of endoplasmic reticulum oxidoreductases, mitochondrial electron transport, and NADPH oxidase, Antioxidants & redox signaling 11 (2009) 2409-2427.
[16] Q. Yuan, W. Tang, X. Zhang, J.A. Hinson, C. Liu, K. Osei, J. Wang, Proinsulin atypical maturation and disposal induces extensive defects in mouse Ins2+/Akita beta-cells, PloS one 7 (2012) e35098.
[17] E. Buytaert, G. Callewaert, N. Hendrickx, L. Scorrano, D. Hartmann, L. Missiaen, J.R. Vandenheede, I. Heirman, J. Grooten, P. Agostinis, Role of endoplasmic reticulum depletion and multidomain proapoptotic BAX and BAK proteins in shaping cell death after hypericin-mediated photodynamic therapy, FASEB journal : official publication of the Federation of American Societies for Experimental Biology 20 (2006) 756-758.
[18] H.G. Hansen, J.D. Schmidt, C.L. Soltoft, T. Ramming, H.M. Geertz-Hansen, B. Christensen, E.S. Sorensen, A.S. Juncker, C. Appenzeller-Herzog, L. Ellgaard, Hyperactivity of the ero1alpha oxidase elicits endoplasmic reticulum stress but no broad antioxidant response, The Journal of biological chemistry 287 (2012) 39513-39523.
[19] I. Moserova, J. Kralova, Role of ER stress response in photodynamic therapy: ROS generated in different subcellular compartments trigger diverse cell death pathways, PloS one 7 (2012) e32972.
[20] J.D. Malhotra, R.J. Kaufman, Endoplasmic reticulum stress and oxidative stress: a vicious cycle or a double-edged sword?, Antioxidants & redox signaling 9 (2007) 2277-2293.
[21] B. Bhandary, A. Marahatta, H.R. Kim, H.J. Chae, An involvement of oxidative stress in endoplasmic reticulum stress and its associated diseases, International journal of molecular sciences 14 (2012) 434-456.

[22] Y. Shimizu, L.M. Hendershot, Oxidative folding: cellular strategies for dealing with the resultant equimolar production of reactive oxygen species, Antioxidants & redox signaling 11 (2009) 2317-2331.
[23] B.P. Tu, J.S. Weissman, Oxidative protein folding in eukaryotes: mechanisms and consequences, The Journal of cell biology 164 (2004) 341-346.
[24] C. Appenzeller-Herzog, Glutathione- and non-glutathione-based oxidant control in the endoplasmic reticulum, Journal of cell science 124 (2011) 847-855.
[25] H.P. Harding, Y. Zhang, H. Zeng, I. Novoa, P.D. Lu, M. Calfon, N. Sadri, C. Yun, B. Popko, R. Paules, D.F. Stojdl, J.C. Bell, T. Hettmann, J.M. Leiden, D. Ron, An integrated stress response regulates amino acid metabolism and resistance to oxidative stress, Molecular cell 11 (2003) 619-633.
[26] C.M. Haynes, E.A. Titus, A.A. Cooper, Degradation of misfolded proteins prevents ER-derived oxidative stress and cell death, Molecular cell 15 (2004) 767-776.
[27] V.D. Nguyen, M.J. Saaranen, A.R. Karala, A.K. Lappi, L. Wang, I.B. Raykhel, H.I. Alanen, K.E. Salo, C.C. Wang, L.W. Ruddock, Two endoplasmic reticulum PDI peroxidases increase the efficiency of the use of peroxide during disulfide bond formation, Journal of molecular biology 406 (2011) 503-515.
[28] T. Ramming, C. Appenzeller-Herzog, Destroy and Exploit: Catalyzed Removal of Hydroperoxides from the Endoplasmic Reticulum, International journal of cell biology 180906 (2013).
[29] T.J. Tavender, A.M. Sheppard, N.J. Bulleid, Peroxiredoxin IV is an endoplasmic reticulum-localized enzyme forming oligomeric complexes in human cells, The Biochemical journal 411 (2008) 191-199.
[30] Y. Sato, R. Kojima, M. Okumura, M. Hagiwara, S. Masui, K. Maegawa, M. Saiki, T. Horibe, M. Suzuki, K. Inaba, Synergistic cooperation of PDI family members in peroxiredoxin 4-driven oxidative protein folding, Scientific reports 3 (2013) 2456.
[31] T.J. Tavender, N.J. Bulleid, Molecular mechanisms regulating oxidative activity of the Ero1 family in the endoplasmic reticulum, Antioxidants & redox signaling 13 (2010) 1177-1187.
[32] E. Zito, E.P. Melo, Y. Yang, A. Wahlander, T.A. Neubert, D. Ron, Oxidative protein folding by an endoplasmic reticulum-localized peroxiredoxin, Molecular cell 40 (2010) 787-797.
[33] Y. Iuchi, F. Okada, S. Tsunoda, N. Kibe, N. Shirasawa, M. Ikawa, M. Okabe, Y. Ikeda, J. Fujii, Peroxiredoxin 4 knockout results in elevated spermatogenic cell death via oxidative stress, The Biochemical journal 419 (2009) 149-158.
[34] P.C. Wei, Y.H. Hsieh, M.I. Su, X.J. Jiang, P.H. Hsu, W.T. Lo, J.Y. Weng, Y.M. Jeng, J.M. Wang, P.L. Chen, Y.C. Chang, K.F. Lee, M.D. Tsai, J.Y. Shew, W.H. Lee, Loss of the Oxidative Stress Sensor NPGPx Compromises GRP78 Chaperone Activity and Induces Systemic Disease, Molecular cell 48 (2012) 747-759.
[35] D. Peng, A. Belkhiri, T. Hu, R. Chaturvedi, M. Asim, K.T. Wilson, A. Zaika, W. El-Rifai, Glutathione peroxidase 7 protects against oxidative DNA damage in oesophageal cells, Gut 61 (2012) 1250-1260.
[36] R. Brigelius-Flohe, M. Maiorino, Glutathione peroxidases, Biochimica et biophysica acta 1830 (2013) 3289-3303.
[37] V. Bosello-Travain, M. Conrad, G. Cozza, A. Negro, S. Quartesan, M. Rossetto, A. Roveri, S. Toppo, F. Ursini, M. Zaccarin, M. Maiorino, Protein Disulfide Isomerase and Glutathione are alternative substrates in the one Cys catalytic cycle of Glutathione Peroxidase 7, Biochimica et biophysica acta 1830 (2013) 3846-3857.
[38] L. Wang, L. Zhang, Y. Niu, R. Sitia, C.C. Wang, Glutathione peroxidase 7 utilizes hydrogen peroxide generated by Ero1alpha to promote oxidative protein folding, Antioxidants & redox signaling doi: 10.1089/ars.2013.5236 (2013).
[39] M.W. Pfaffl, A. Tichopad, C. Prgomet, T.P. Neuvians, Determination of stable housekeeping genes, differentially regulated target genes and sample integrity: BestKeeper--Excel-based tool using pair-wise correlations, Biotechnology letters 26 (2004) 509-515.
[40] C. Appenzeller-Herzog, J. Riemer, B. Christensen, E.S. Sorensen, L. Ellgaard, A novel disulphide switch mechanism in Ero1alpha balances ER oxidation in human cells, The EMBO journal 27 (2008) 2977-2987.
[41] C. Appenzeller-Herzog, J. Riemer, E. Zito, K.T. Chin, D. Ron, M. Spiess, L. Ellgaard, Disulphide production by Ero1alpha-PDI relay is rapid and effectively regulated, The EMBO journal 29 (2010) 3318-3329.
[42] V. Vichai, K. Kirtikara, Sulforhodamine B colorimetric assay for cytotoxicity screening, Nature protocols 1 (2006) 1112-1116.
[43] J. Wright, J. Birk, L. Haataja, M. Liu, T. Ramming, M.A. Weiss, C. Appenzeller-Herzog, P. Arvan, Endoplasmic Reticulum Oxidoreductin-1alpha (Ero1alpha) Improves Folding and Secretion of Mutant Proinsulin and Limits Mutant Proinsulin-Induced ER Stress, The Journal of biological chemistry doi: 10.1074/jbc.M113.510065 (2013).
[44] E.M. Lynes, T. Simmen, Urban planning of the endoplasmic reticulum (ER): how diverse mechanisms segregate the many functions of the ER, Biochimica et biophysica acta 1813 (2011) 1893-1905.

[45] B. Enyedi, P. Varnai, M. Geiszt, Redox state of the endoplasmic reticulum is controlled by Ero1L-alpha and intraluminal calcium, Antioxidants & redox signaling 13 (2010) 721-729.
[46] J. Haugstetter, M.A. Maurer, T. Blicher, M. Pagac, G. Wider, L. Ellgaard, Structure-function analysis of the endoplasmic reticulum oxidoreductase TMX3 reveals interdomain stabilization of the N-terminal redox-active domain, The Journal of biological chemistry 282 (2007) 33859-33867.
[47] J. Wright, J. Birk, L. Haataja, M. Liu, T. Ramming, M.A. Weiss, C. Appenzeller-Herzog, P. Arvan, Endoplasmic Reticulum Oxidoreductin-1alpha (Ero1alpha) Improves Folding and Secretion of Mutant Proinsulin and Limits Mutant Proinsulin-Induced ER Stress, The Journal of biological chemistry 288 (2013) 31010-31018.
[48] V.V. Belousov, A.F. Fradkov, K.A. Lukyanov, D.B. Staroverov, K.S. Shakhbazov, A.V. Terskikh, S. Lukyanov, Genetically encoded fluorescent indicator for intracellular hydrogen peroxide, Nature methods 3 (2006) 281-286.
[49] D. Poburko, J. Santo-Domingo, N. Demaurex, Dynamic regulation of the mitochondrial proton gradient during cytosolic calcium elevations, The Journal of biological chemistry 286 (2011) 11672-11684.
[50] T. Kakihana, K. Nagata, R. Sitia, Peroxides and peroxidases in the endoplasmic reticulum: integrating redox homeostasis and oxidative folding, Antioxidants & redox signaling 16 (2012) 763-771.
[51] I. Mehmeti, S. Lortz, S. Lenzen, The H2O2-sensitive HyPer protein targeted to the endoplasmic reticulum as a mirror of the oxidizing thiol-disulfide milieu, Free radical biology & medicine 53 (2012) 1451-1458.
[52] T.J. Tavender, N.J. Bulleid, Peroxiredoxin IV protects cells from oxidative stress by removing H2O2 produced during disulphide formation, Journal of cell science 123 (2010) 2672-2679.
[53] J.M. Gutteridge, Biological origin of free radicals, and mechanisms of antioxidant protection, Chemico-biological interactions 91 (1994) 133-140.
[54] M. Bertolotti, S. Bestetti, J.M. Garcia-Manteiga, I. Medrano-Fernandez, A. Dal Mas, M.L. Malosio, R. Sitia, Tyrosine kinase signal modulation: a matter of H2O2 membrane permeability?, Antioxidants & redox signaling 19 (2013) 1447-1451.
[55] M. Gutscher, A.L. Pauleau, L. Marty, T. Brach, G.H. Wabnitz, Y. Samstag, A.J. Meyer, T.P. Dick, Real-time imaging of the intracellular glutathione redox potential, Nature methods 5 (2008) 553-559.
[56] G. Banhegyi, L. Lusini, F. Puskas, R. Rossi, R. Fulceri, L. Braun, V. Mile, P. di Simplicio, J. Mandl, A. Benedetti, Preferential transport of glutathione versus glutathione disulfide in rat liver microsomal vesicles, The Journal of biological chemistry 274 (1999) 12213-12216.
[57] J. Leitman, E. Ron, N. Ogen-Shtern, G.Z. Lederkremer, Compartmentalization of endoplasmic reticulum quality control and ER-associated degradation factors, DNA and cell biology 32 (2013) 2-7.
[58] S.Y. Gilady, M. Bui, E.M. Lynes, M.D. Benson, R. Watts, J.E. Vance, T. Simmen, Ero1alpha requires oxidizing and normoxic conditions to localize to the mitochondria-associated membrane (MAM), Cell stress & chaperones 15 (2010) 619-629.
[59] T. Anelli, L. Bergamelli, E. Margittai, A. Rimessi, C. Fagioli, A. Malgaroli, P. Pinton, M. Ripamonti, R. Rizzuto, R. Sitia, Ero1alpha regulates Ca(2+) fluxes at the endoplasmic reticulum-mitochondria interface (MAM), Antioxidants & redox signaling 16 (2012) 1077-1087.
[60] T. Hayashi, M. Fujimoto, Detergent-resistant microdomains determine the localization of sigma-1 receptors to the endoplasmic reticulum-mitochondria junction, Molecular pharmacology 77 (2010) 517-528.
[61] G. Li, M. Mongillo, K.T. Chin, H. Harding, D. Ron, A.R. Marks, I. Tabas, Role of ERO1-alpha-mediated stimulation of inositol 1,4,5-triphosphate receptor activity in endoplasmic reticulum stress-induced apoptosis, The Journal of cell biology 186 (2009) 783-792.
[62] S.J. Marciniak, C.Y. Yun, S. Oyadomari, I. Novoa, Y. Zhang, R. Jungreis, K. Nagata, H.P. Harding, D. Ron, CHOP induces death by promoting protein synthesis and oxidation in the stressed endoplasmic reticulum, Genes & development 18 (2004) 3066-3077.
[63] E. Zito, H.G. Hansen, G.S. Yeo, J. Fujii, D. Ron, Endoplasmic reticulum thiol oxidase deficiency leads to ascorbic acid depletion and noncanonical scurvy in mice, Molecular cell 48 (2012) 39-51.
[64] X. Wang, L. Wang, F. Sun, C.C. Wang, Structural insights into the peroxidase activity and inactivation of human peroxiredoxin 4, The Biochemical journal 441 (2012) 113-118.
[65] T.J. Tavender, J.J. Springate, N.J. Bulleid, Recycling of peroxiredoxin IV provides a novel pathway for disulphide formation in the endoplasmic reticulum, The EMBO journal 29 (2010) 4185-4197.

3. Project II: A sealable oxygen/hydrogen peroxide diffusion path in human Ero1

A sealable oxygen/hydrogen peroxide diffusion path in human Ero1

Thomas Ramming[1], Masaki Okumura[2], Shingo Kanemura[2], Sefer Baday[3], Julia Birk[1], Suzette Moes[3], Paul Jenö[3], Simon Bernèche[3], Kenji Inaba[2] and Christian Appenzeller-Herzog[1]*

[1] Division of Molecular & Systems Toxicology, Department of Pharmaceutical Sciences, University of Basel, 4056 Basel, Switzerland

[2] Institute of Multidisciplinary Research for Advanced Materials, Tohoku University

Katahira 2-1-1, Sendai 980-8577, Japan

[3] Biozentrum, University of Basel, 4056 Basel, Switzerland

*Contact

Christian.Appenzeller@unibas.ch

Running title: Regulated O_2 access in Ero1α

3.1.Summary

Oxidative folding in the endoplasmic reticulum (ER) involves disulfide formation in protein disulfide isomerase (PDI) by ER oxidoreductin 1 (Ero1), which consumes oxygen (O_2) and releases hydrogen peroxide (H_2O_2). Strikingly, however, none of the available Ero1 structures discloses a path for entry and exit of these reactants. We report that mutation of Cys^{208}/Cys^{241} previously thought to form a static disulfide aggravates ER oxidation and cell toxicity by hyperactive Ero1α. The disulfide clamps two helices, which seal the flavin cofactor where O_2 is reduced to H_2O_2. Through its carboxyterminal active site, PDI unlocks this seal by forming a Cys^{208}/Cys^{241}-dependent mixed-disulfide complex with Ero1α. The H_2O_2-detoxifying glutathione peroxidase 8 binds to the Cys^{208}/Cys^{241} loop region at the site of H_2O_2 exit. We describe the first actively regulated O_2/H_2O_2 diffusion path, provide molecular-level understanding of Ero1α regulation and H_2O_2 control, and establish the deleterious consequences of constitutive Ero1 activity.

3.2.Introduction

Oxidative protein folding is defined as the assisted process of tertiary structure acquisition of a polypeptide chain, which requires the formation of covalent disulfide crosslinks between specific cysteine side chains. The enzymatic machinery for oxidative protein folding has been extensively described in three subcellular locations: the periplasmic space in gram-negative bacteria [4], as well as the mitochondrial intermembrane space [5] and the endoplasmic reticulum (ER) [6] in eukaryotic cells. In all three compartments, the electrons derived from disulfide-bond formation are transported along specialized biochemical cascades to finally target molecular oxygen (O_2) [7]. In the ER, this final step can be catalyzed by the flavoproteins of the endoplasmic oxidoreductin 1 (Ero1) family (Ero1α and Ero1β in mammals), which are the best-conserved disulfide-producing enzymes of the ER [8,9]. The catalytic cycle of Ero1 produces stoichiometric amounts of hydrogen peroxide (H_2O_2) [10,11]. Newly generated disulfides are transferred from a flavin adenine dinucleotide (FAD)-associated active site via a “shuttle disulfide” cysteine pair in Ero1 to protein disulfide isomerase (PDI) and from there on to substrate proteins [8,9].

Mechanistically, all of these disulfide transfer reactions occur via interchain mixed-disulfide intermediates.

The synthesis of disulfide bonds in the ER, the compartment where secretory and membrane proteins are formed and folded, is essential. Not only reducing but also oxidizing disturbances, which compromise native disulfide-bond formation in the ER, result in locally hampered protein homeostasis – a state referred to as ER stress [12]. Exaggerated Ero1 activity is also a source of limited ER hyper-oxidation and stress [13,14], which is aggravated in the absence of the H_2O_2-detoxifying ER peroxidase GPx8 [15]. Accordingly, the catalytic rate of Ero1 enzymes requires tight negative feedback regulation in order to prevent Ero1-dependent toxicity [16].

In their inactive state, the "shuttle disulfide" cysteines (Cys^{94} and Cys^{99} in Ero1α or Cys^{90} and Cys^{95} in Ero1β) are engaged in intramolecular regulatory disulfides (Cys^{94}–Cys^{131} and Cys^{99}–Cys^{104} in Ero1α or Cys^{90}–Cys^{130} and Cys^{95}–Cys^{100} in Ero1β) [13,14,17,18,19]. However, although the inhibitory mechanism of these regulatory disulfide bonds in mammalian Ero1 is understood, it is surprising how well cells tolerate the over-expression of hyperactive Ero1 mutants lacking those disulfide bonds [13,14,20]. Furthermore, controversy exists as to the questions how O_2 reaches the active center in Ero1 and how H_2O_2 can be released again [8,9].

Here, we report the existence of an additional regulated disulfide bond in mammalian Ero1, which is located at the distal side of the molecule relative to cofactor and "shuttle disulfide" and was previously considered to serve a structural role. When this disulfide is unlocked by reduced PDI, conformational rearrangements open a diffusion pathway, through which O_2 can penetrate and reach the cofactor. Ero1 devoid of all regulatory disulfides is constitutively active and produces cytotoxic levels of H_2O_2. We also show that GPx8 binding specifically occurs at the distal, H_2O_2-releasing end of Ero1α.

3.3. Results

3.3.1. Yet another regulatory switch in Ero1α

Previous data showed that the catalytic turnover of a hyperactive Ero1α mutant lacking all known regulatory disulfide bonds (Ero1α-C104A/C131A, in the following dubbed Ero1α-AA) was still enhanced by treatment of cells with the disulfide reductant dithiothreitol (DTT) [15]. Furthermore, DTT-mediated activation of Ero1α and Ero1β lowered the gel mobility of the Ero1–PDI mixed-disulfide complex [21]. This suggested the presence of at least one residual disulfide conferring negative regulation of Ero1α-AA, which we sought to identify. Concentrating on the housekeeping isoform Ero1α, we first showed that the conversion of the slower-migrating Ero1α–PDI complex (Ero1α–PDI^{slow}) to the faster-migrating complex (Ero1α–PDI^{fast}) was independent of the Cys^{94}–Cys^{131} and Cys^{99}–Cys^{104} regulatory disulfides (Fig. 13A). The shutdown of Ero1α-AA was illustrated by assaying Ero1α activity following DTT washout [15,21] where the Ero1α-dependent peak of cellular $GSSG:GS_{tot}$ declined in parallel with the shift in gel mobility of Ero1α–PDI (Fig. 13B+C and S6A-C).

We next tested the hypothesis that the long-range Cys^{85}–Cys^{391} disulfide, which is homologous to one of the regulatory disulfides in yeast Ero1 [22], was resolved upon full activation of the oxidase [9]. For this purpose, we immunoprecipitated Ero1α-AA from cells activated with DTT followed by treatment with N-ethylmaleimide (NEM) to disable post-lysis thiol-disulfide rearrangements (Fig. S6D). Ero1α–PDI^{slow} was then subjected to reduction and alkylation with iodoacetamide, tryptic digest and mass spectrometry (Fig. S6E). The peptides harboring Cys^{85} or Cys^{391} were exclusively detected as iodoacetamide-modified species (Table S1), suggesting a structural Cys^{85}–Cys^{391} disulfide. Moreover, we found Ero1α-AA+C85A/C391A not to display any signs of increased hyperactivity relative to Ero1α-AA in cells subjected to DTT washout, but instead to be incorporated into non-native oligomeric mixed-disulfide complexes (Fig. 13D+E). These observations were consistent with the literature [23,24] and suggested that the conversion of Ero1α–PDI^{slow} to Ero1α–PDI^{fast} did not involve formation of Cys^{85}–Cys^{391}.

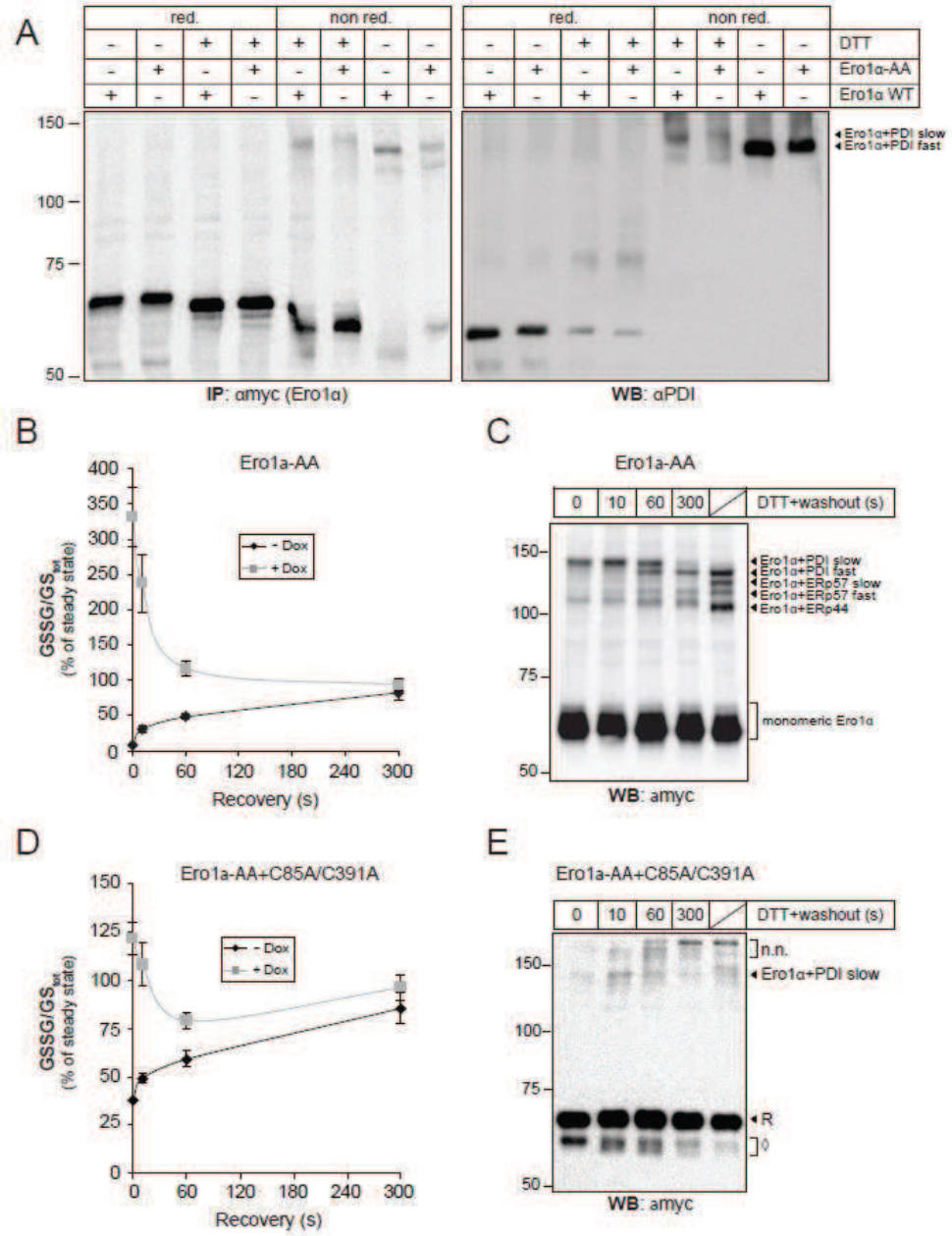

Figure 13: Ero1α–PDI^{slow} to Ero1α–PDI^{fast} transition does not involve closure of the Cys^{94}–Cys^{131}, Cys^{99}–Cys^{104}, or Cys^{85}–Cys^{391} disulfides. (**A**) Doxycycline-induced Ero1α WT and Ero1α-AA cells were metabolically labeled with ^{35}S-methionine, treated with TCA, and subjected to αmyc immunoprecipitation (IP) followed by reducing (red.) or non-reducing (non red.) SDS-PAGE and western blot (WB) analysis using αPDI. Where indicated, cells were treated with 1 mM DTT ahead of TCA lysis. A phosphoimager scan (IP: αmyc (Ero1α)) and an immunoblot (WB: αPDI) of the same membrane are shown. The gel mobilities of dimeric Ero1α–PDI complexes are indicated. (**B**) Intracellular levels of GSSG and GS_{tot} were recorded from DTT-treated Ero1α-AA cells, which were cultured for 24 h with or without doxycycline (Dox), after washout of the reductant for 0, 10, 60, or 300 s. The $GSSG/GS_{tot}$ ratio is expressed as percentage of the steady-state value that was independently measured. (**C**) Acid-precipitated pellets from doxycycline-induced cells from the experiment described in (B) were treated with NEM and subjected to precipitation with concanavalin A-sepharose followed by non-reducing SDS-PAGE and WB using αmyc. The labeled identities of mixed-disulfide complexes involving Ero1α were determined by separate immunoblots using antibodies against the respective PDI family member (Fig. S6A-C). (**D** and **E**) Experiment performed as in (C) and (D) using Ero1α-AA+C85A/C391A cells. R, monomeric Ero1α with the mobility of reduced Ero1α; Diamond, probably non-native Ero1α redox forms of unknown identity; n. n., non-native mixed-disulfide complexes involving Ero1α. see also Fig. S6, Table S1

3.3.2. The Cys^{208}/Cys^{241} pair does not form a static disulfide

Ero1α–PDI^{slow} trapped after DTT treatment during full catalytic Ero1α activity involves Cys^{94} in Ero1α and represents the disulfide transfer complex between Ero1α and PDI [21]. Therefore, Ero1α–PDI^{fast}, which arose concomitantly with Ero1α-AA inactivation and was prominent at steady state (Fig. 13C), reflected the formation of either an inhibitory intramolecular disulfide in Ero1α-AA or an Ero1α–PDI complex that was molecularly distinct from Ero1α–PDI^{slow}. In support of the latter explanation, Ero1α–PDI^{fast} still formed in the absence of Cys^{94} (Fig. 14A).

We envisioned an involvement of the Cys^{208}/Cys^{241} pair, which forms a disulfide in inactive Ero1α and in the available crystal structures [17,19]. Cell lines inducible for the expression of Ero1α-C104A/C131A/C208S/C241S (in the following dubbed Ero1α-AASS) were therefore generated (Fig. S7). Indeed, Ero1α-AASS displayed a qualitatively different Ero1α–PDI mixed-disulfide pattern following DTT washout, the most obvious difference to the Ero1α-AA pattern being the lack of Ero1α–PDI mobility transition over time (Fig. 14B and S7B-D). Co-transfected wild-type PDI was detected in a Ero1α–PDI^{fast} complex with Ero1α-AA+C94S at steady state, but not with Ero1α-AASS+C94S (Fig. 14C). Furthermore, the Ero1α–PDI^{fast} complex between endogenous PDI and Ero1α-AA disappeared upon mutation of either Cys^{208} or Cys^{241} (Fig. 14D). PDI trapping mutants where C-terminal active-site cysteines were mutated to serine were used to further characterize the interchain disulfide between Cys^{208} or Cys^{241} and PDI. The trapping mutation in the **a´** domain active site (CXXS-2) promoted the formation of the same complex as detected with wild-type PDI and also moderately stabilized a complex of unclear identity with Ero1α-AASS+C94S (Fig. 14C). In contrast, the **a** domain trapping mutant (CXXS-1) formed a distinct Ero1α–PDI complex irrespective of the presence of Cys^{208}/Cys^{241} (Fig. 14C). Similar albeit less prominently detectable complexes were found using ERp57 trapping mutants (Fig. 14E), which was consistent with the observation of a Cys^{208}/Cys^{241}-dependent slow-migrating complex between Ero1α-AA and endogenous ERp57 (Fig. 13C and 14B). These data revealed nucleophilic attack by the **a´** domain active site in PDI family members on Cys^{208}–Cys^{241} in Ero1α.

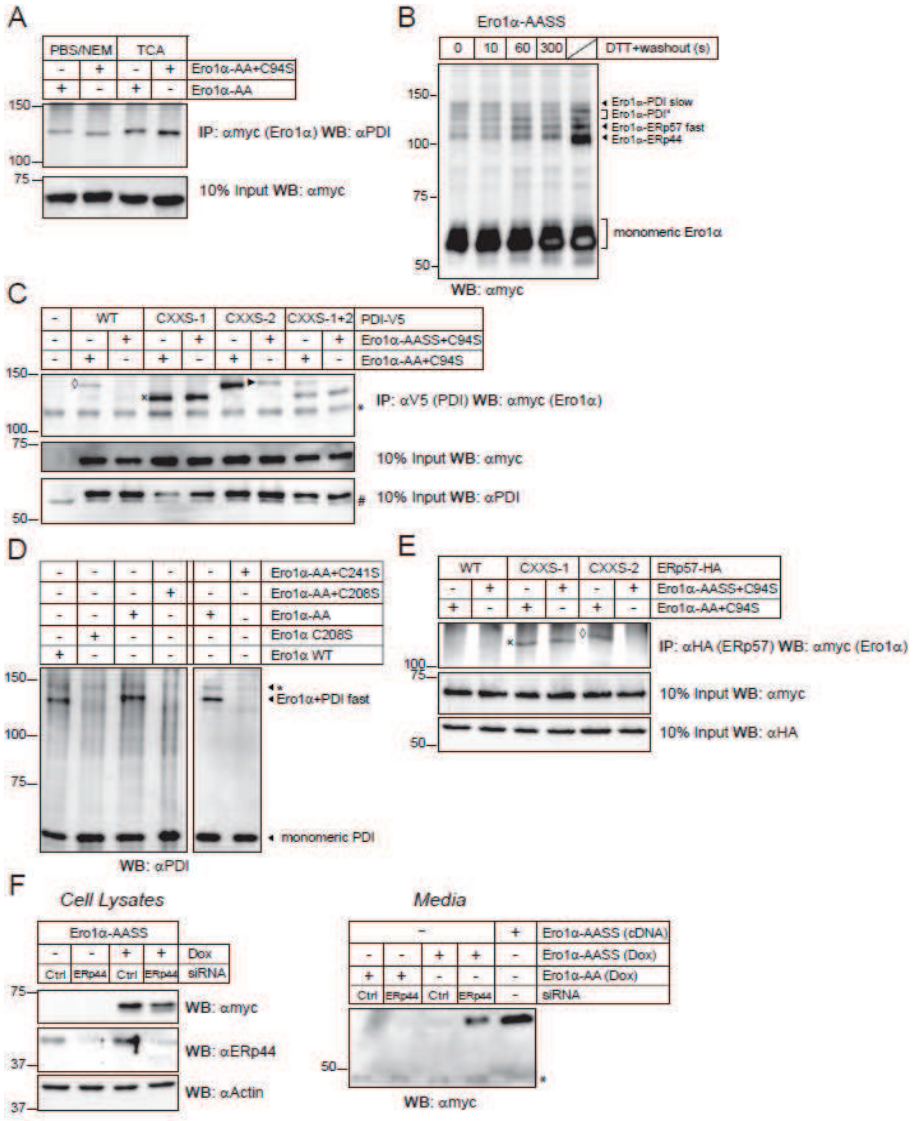

Figure 14: In Ero1α–PDI^{fast}, PDI links to the distal end of Ero1α in a Cys^{208}/Cys^{241}-dependent way. (**A**) Ero1α-AA or Ero1α-AA+C94S cells were induced with doxycycline for 24 h and free sulfhydryl groups blocked by treatment with PBS/NEM or TCA before cell lysis. 10% of the cell lysates were subjected to reducing SDS-PAGE (lower panel) and western blot (WB) using αmyc, and the rest to αmyc immunoprecipitation (IP) using covalently coupled immunobeads and non-reducing SDS-PAGE (upper panel). Ero1α-PDI mixed disulfide complexes were revealed by WB using αPDI. The minor downward shift in response to C94S could potentially reflect the stabilization of a Cys^{99}–Cys^{394} disulfide in analogy to yeast Ero1 [1]. (**B**) Experiment performed as in Fig. 13C using Ero1α-AASS cells. The labeled identities of mixed-disulfide complexes involving Ero1α were determined by separate immunoblots using antibodies against the respective PDI family member (Fig. S7B-D). (**C**) HeLa cells were co-transfected with wild-type (WT) or mutant V5-tagged PDI and the indicated Ero1α mutants followed by IP using covalently coupled αV5. Immunoprecipitates and 10% of total cell lysates (input) were resolved by non-reducing or reducing SDS-PAGE, respectively, and the indicated proteins or protein complexes visualized by WB. Asterisk, background band; #, endogenous PDI; diamond, Ero1α–PDI^{fast}; X, Ero1α–PDI complex presumably analogous to Ero1α–ERp44 (see Discussion); arrowhead, Ero1α–PDI complex of unknown identity. (**D**) Lysates from HeLa cells that were transiently transfected with the indicated Ero1α mutants and treated with PBS/NEM were resolved by non-reducing SDS-PAGE followed by αPDI WB. Asterisk, unidentified mixed-disulfide complex involving PDI. (**E**) Experiment as in (C) using HA-tagged ERp57 and αHA. Ero1α–ERp57 complexes are labeled in analogy to (C). (**F**) Ero1α-AASS cells were transfected with control (Ctrl) or ERp44-targeting siRNA and subsequently induced or not for 24 h with doxycycline (Dox). Cells and media were collected, and the latter incubated with concanavalin A-sepharose to precipitate/concentrate secreted glycoproteins. Cell lysates and secreted glycoproteins were analyzed by SDS-PAGE and WB using the indicated antibodies. Note that in ERp44-silenced cells, intracellular Ero1α-AASS decreases due to secretion. As a positive control for Ero1α-AASS secretion, the mutant protein was overexpressed by transient cDNA transfection. Asterisk, background band. see also Fig. S7

As the intracellular retention of Ero1α relies on the formation of mixed disulfides with PDI and ERp44 [25], we also tested the impact of Cys^{208}/Cys^{241} on Ero1α secretion. Of potential relevance, we noted that the Ero1α-AASS–ERp44 complex formed more prominently at steady state than the Ero1α-AA–ERp44 complex (Fig. 13C and 14B). Consistent with our expectations, a fraction of Ero1α-AASS was secreted from ERp44 knockdown but not from control cells, while Ero1α-AA was not secreted at all in this setup (Fig. 14F). Thus, Cys^{208}/Cys^{241}-dependent complex formation with PDI contributes to ER localization of Ero1α.

3.3.3. Ero1α-AASS is constitutively active

Based on the above results, we speculated that rearrangement of the Cys^{208}–Cys^{241} disulfide was an essential step in the activation of Ero1α, which prompted us to characterize Ero1α-AASS-expressing cells. Already after 24 h expression of Ero1α-AASS but not of Ero1α-AA, cell proliferation and viability were significantly affected, which was aggravated by glutathione depletion (Fig. 15A+B). Interestingly, this was not correlated with higher expression of ER-stress-regulated target genes in Ero1α-AASS- compared to Ero1α-AA-expressing cells (Fig. S8A). We particularly noted that the ATF6-target genes *HSPA5* and *HERPUD1* [26] were less induced in response to Ero1α-AASS, which could potentially be due to the stabilization of disulfide-linked, inactive ATF6 oligomers [12]. Ero1α-AASS-dependent ER redox changes were also hinted by the findings that viability and proliferation of Ero1α-AASS-expressing cells were significantly rescued by the antioxidant N-acetylcysteine (Fig. S8B+C).

Indeed, ERp57 was more oxidized following Ero1α-AASS compared to Ero1α-AA expression (Fig. 15C). A similar difference was observed using analogous mutants of Ero1β (Fig. S8D), underlining a previous report on the conservation of regulatory disulfides between human Ero1 isoforms [14]. Ero1α-AASS did not specifically affect ERp57 oxidation, since also the ER-targeted glutathione-specific Grx1-roGFP1-iE_{ER} sensor [2] and the H_2O_2-responsive $HyPer_{ER}$ sensor [27] were more oxidized upon Ero1α-AASS compared to Ero1α-AA expression (Fig. 15D+E). Thus, profound hyperoxidation of the ER was the likely cause of the Ero1α-AASS-

induced decrease in cell health. In contrast, cells expressing Ero1α-C208S/C241S displayed only a trend towards ER hyperoxidation and no drop in cell viability/proliferation (FIG. S8E-G).

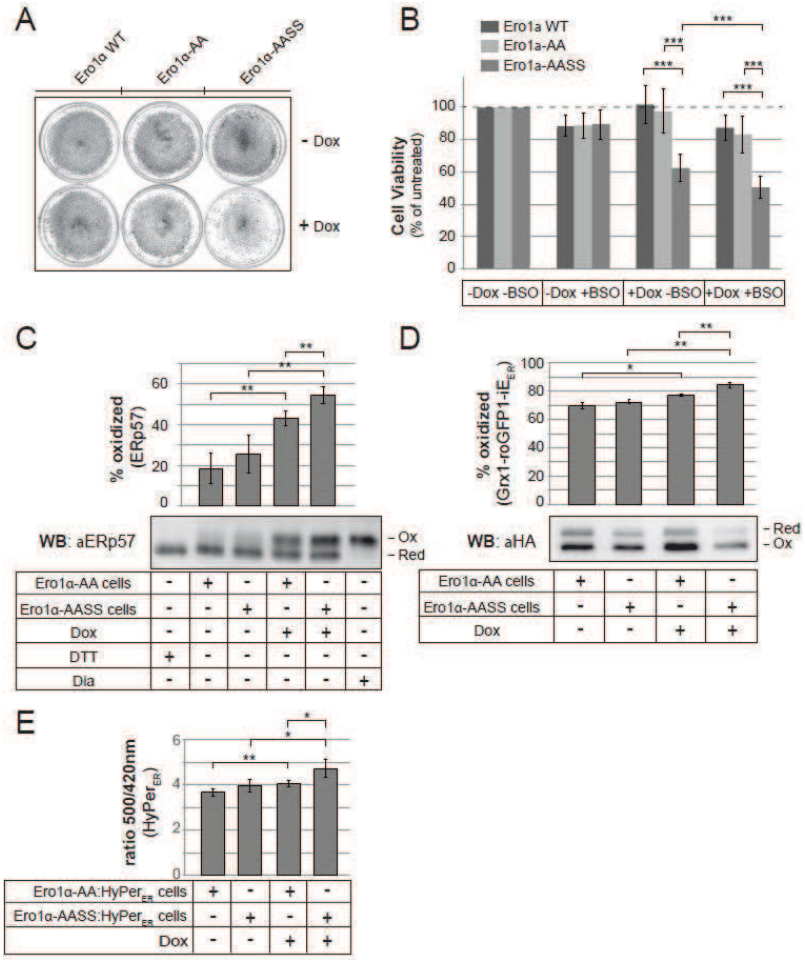

Figure 15: Ero1α-AASS increases ER oxidation and decreases cell viability. (**A**) The indicated cell lines were induced or not for 24 h with doxycycline (Dox) and stained with crystal violet. (**B**) Cell viability was determined by the WST-1 assay upon induction of Ero1α variants for 24 h and/or depletion of glutathione by 1 mM L-Buthionine-sulfoximine (BSO) for 16 h (n = 5; mean ± SD). (**C**) Cells were treated or not with Dox for 24 h followed by differential alkylation and western blot (WB) analysis of ERp57. The mobilities of oxidized (Ox) and reduced (Red) ERp57, as verified by control lysates from DTT- or diamide (Dia)-treated cells, are indicated. The diagram shows the oxidized fraction in percent (n = 4; mean ± SD). (**D**) Cells were transfected with Grx1-roGFP1-iE$_{ER}$, induced or not with Dox (24 h), treated with PBS/NEM, and subjected to αGFP immunoprecipitation followed by non-reducing SDS-PAGE and αHA WB [2]. The mobilities of oxidized (Ox) and reduced (Red) Grx1-roGFP1-iE$_{ER}$ are indicated (n = 3; mean ± SD). (**E**) Indicated cell lines treated or not with Dox for 24 h were subjected to HyPer$_{ER}$ fluorescence excitation spectrum analysis. Plotted are the ratios of the 500 and 420 nm peak amplitudes (n = 4; mean ± SD). *$p < 0.05$; **$p < 0.01$; ***$p < 0.001$. see also Fig S8

Increased catalytic efficiency of Ero1α-AASS was also observed *in vitro*. Addition of Ero1α-AASS to a solution containing saturating O_2 and reduced PDI led to faster and higher transient accumulation of H_2O_2 compared to the Ero1α-2x-catalyzed reaction (Fig. 16A). We also

analyzed the kinetics of PDI oxidation by malPEG2k modification followed by SDS-PAGE. During Ero1α-AA-catalyzed oxidation, reduced PDI completely disappeared at the expense of partially or fully oxidized forms within 3 min of reaction (Fig. 16B). Ero1α-AASS, however, consumed reduced PDI more rapidly within 1.5 min (Fig. 16B), which was in agreement with the faster generation of H_2O_2.

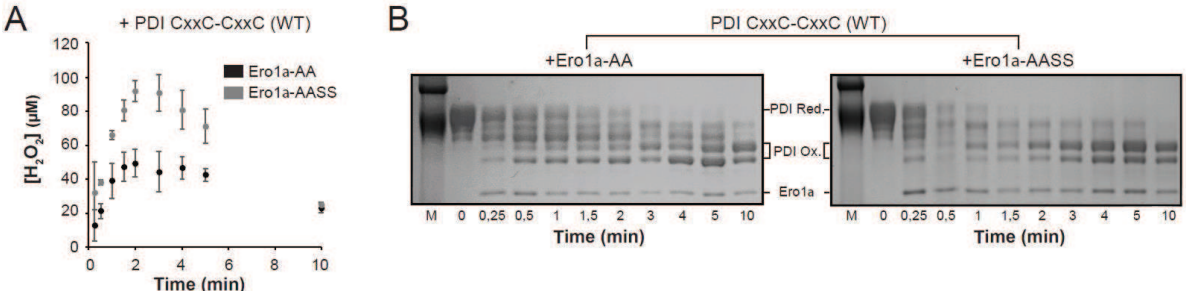

Figure 16: Improved catalytic efficiency of Ero1α-AASS in oxidation of PDI. (**A**) Quantitative analyses of Ero1α-generated H_2O_2. Profiles indicate the time course of oxidation of PDI catalyzed by Ero1α-AA or Ero1α-AASS. Experiments were performed at 30°C using 4 µM Ero1α, 100 µM reduced PDI and a saturated level of O_2. At indicated time points, the reaction mixture was subjected to Pierce Quantitative Peroxide Assay (n = 3; mean ± SD). (**B**) Time course of PDI oxidation. Protein concentrations and assay conditions were the same as in (A). At indicated time points, the reaction mixture was quenched with TCA, washed with acetone and alkylated with malPEG2k prior to non-reducing SDS-PAGE.

3.3.4. Ero1α-AASS is catalytically hampered

Despite its increased catalytic efficiency, Ero1α-AASS was catalytically less active than Ero1α-AA when assayed under hyper-activating (i.e. reducing) conditions. Thus, when GSH was added to the reaction mixture to constantly regenerate reduced PDI for repeated oxidase cycles, the catalytic turnover rate of purified Ero1α-AASS was lower than that of Ero1α-AA (Fig. 17A+B). Likewise, Ero1-dependent H_2O_2 generation in the ER of DTT-bathed cells and cellular GSSG accumulation upon DTT washout [15] was less prominent in Ero1α-AASS- or Ero1α-C208S/C241S- compared to Ero1α-AA-expressing cells (Fig. 17C+D). It should be noted that DTT washout with Ero1α-AASS-expressing cells was technically challenging due to their loose adherence in response to compromised cell viability (Fig. 15A+B). We therefore repeated the experiments using an Ero1α-AASS clone with lower inducible expression (Fig. S7A) and improved adherence (unpublished observation) and obtained comparable GSSG:GS_{tot} curves (Fig. S9). Collectively, these results suggested that the constitutive absence of the Cys^{208}–Cys^{241}

disulfide from Ero1α could affect optimal catalysis of PDI oxidation possibly by allowing non-native protein–protein interactions or conformational freedom.

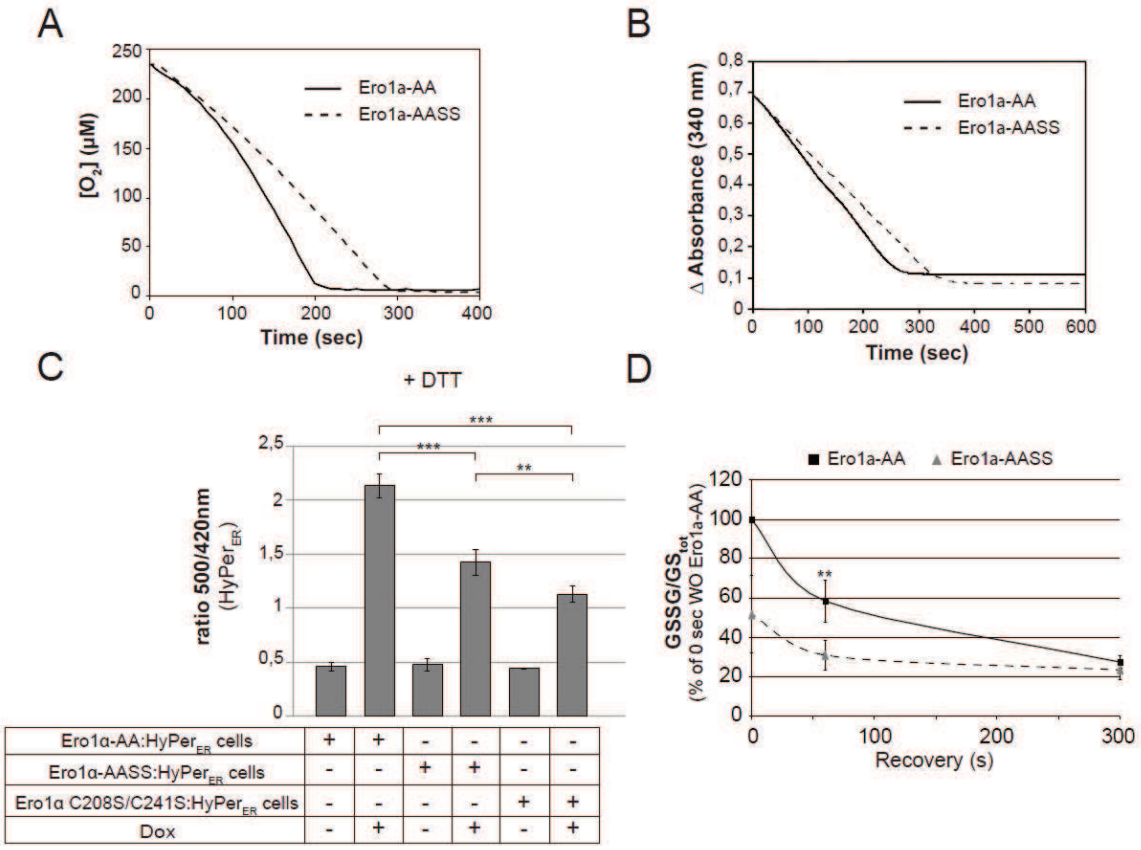

Figure 17: Ero1α-AASS displays suboptimal oxidase activity under reducing conditions. (**A**) O_2 consumption was monitored over time in a mixture of 2 µM Ero1α-AA or Ero1α-AASS, 10 µM PDI, and 10 mM reduced glutathione. (**B**) Consumption of NADPH coupled to Ero1α catalysis (see Materials and Methods; 2 µM Ero1α mutant, 10 µM PDI) was detected by following the absorbance at 340 nm. (**C**) Indicated cell lines were treated and analyzed as in Fig. 15E 5 min after the addition of 0.5 mM DTT (n ≥ 3; mean ± SD). (**D**) $GSSG/GS_{tot}$ recovery curves upon DTT washout were compared between Ero1α-AA- and Ero1α-AASS-expressing cells. Values are expressed as percentage of 0 s washout (WO) in Ero1α-AA cells (mean ± SD; two independent experiments each performed at least in doublet). $^{**}p < 0.01$; $^{***}p < 0.001$. see also Fig. S9

3.3.5. GPx8 interacts with the mouth of the putative O_2/H_2O_2 channel

The discharge of Ero1α-derived H_2O_2 into the ER lumen is prevented specifically by the peroxidase GPx8 [15], which is likely mediated by the physical interaction of GPx8 (or the closely related GPx7) with Ero1α [28]. We therefore examined the possibility that GPx7 or GPx8 bound to the Cys^{208}/Cys^{241} region in Ero1α. Bimolecular fluorescence complementation (BiFC)

analyses in the ER of living cells demonstrated significantly weaker interaction of GPx7 or GPx8 with Ero1α-AASS than with Ero1α-AA (Fig. 18A and S10A). This result suggested that unlike Ero1α-AA, the constitutively active Ero1α-AASS was impaired in associating with its endogenous H_2O_2 scavenger GPx8 [15]. Consistent with this interpretation, ERp57 and $HyPer_{ER}$ redox assays did not show increased ER oxidation in Ero1α-AASS-expressing cells upon knockdown of GPx8 (Fig. 18B+C), as was reported in Ero1α-AA-expressing cells [15]. Surprisingly though, the stability of GPx8 was affected by expression of Ero1α-AASS (Fig. 18D). While the precise trigger and mechanism of GPx8 degradation is currently unknown, we propose that increased generation of free H_2O_2 by Ero1α-ASS (Fig. 15E and 16A) may elicit enhanced turnover of the peroxidase.

The data so far supported the notion that GPx8 interacted with the distal end of Ero1α where H_2O_2 is presumably expelled. Using BiFC, we characterized the GPx8–Ero1α interaction in more detail. First, as Cys^{208} and Cys^{241} in Ero1α were required for the binding of GPx8, we tested whether or not the active-site Cys^{79} in GPx8 was required, too. As Fig. S10B shows, this was not the case, indicating the interaction not to be founded on thiol-disulfide exchange. Next, we followed up on our previous finding that GPx8 knockdown led to Ero1α-derived but not to Ero1β-derived H_2O_2 accumulation [15], which suggested a stronger interaction of GPx8 with Ero1α than with Ero1β. The 32 amino acid loop between Cys^{208} and Cys^{241} (Cys^{207} and Cys^{240} in Ero1β) is highly conserved between the two isoforms except for a divergent nonapeptide sequence (Fig. S10C). As hypothesized, replacement of the nonapeptide sequence in wild-type Ero1α with the Ero1β sequence decreased the BiFC signal, whereas deletion of the nonapeptide somewhat unexpectedly enhanced it (Fig. 18E). Thus, the nonapeptides in Ero1α and Ero1β negatively control GPx8 binding to varying extents. Taken together, the results demonstated that GPx8 (and GPx7) specifically associated with the loop region between Cys^{208} and Cys^{241}, which we consider as the site of H_2O_2 exit.

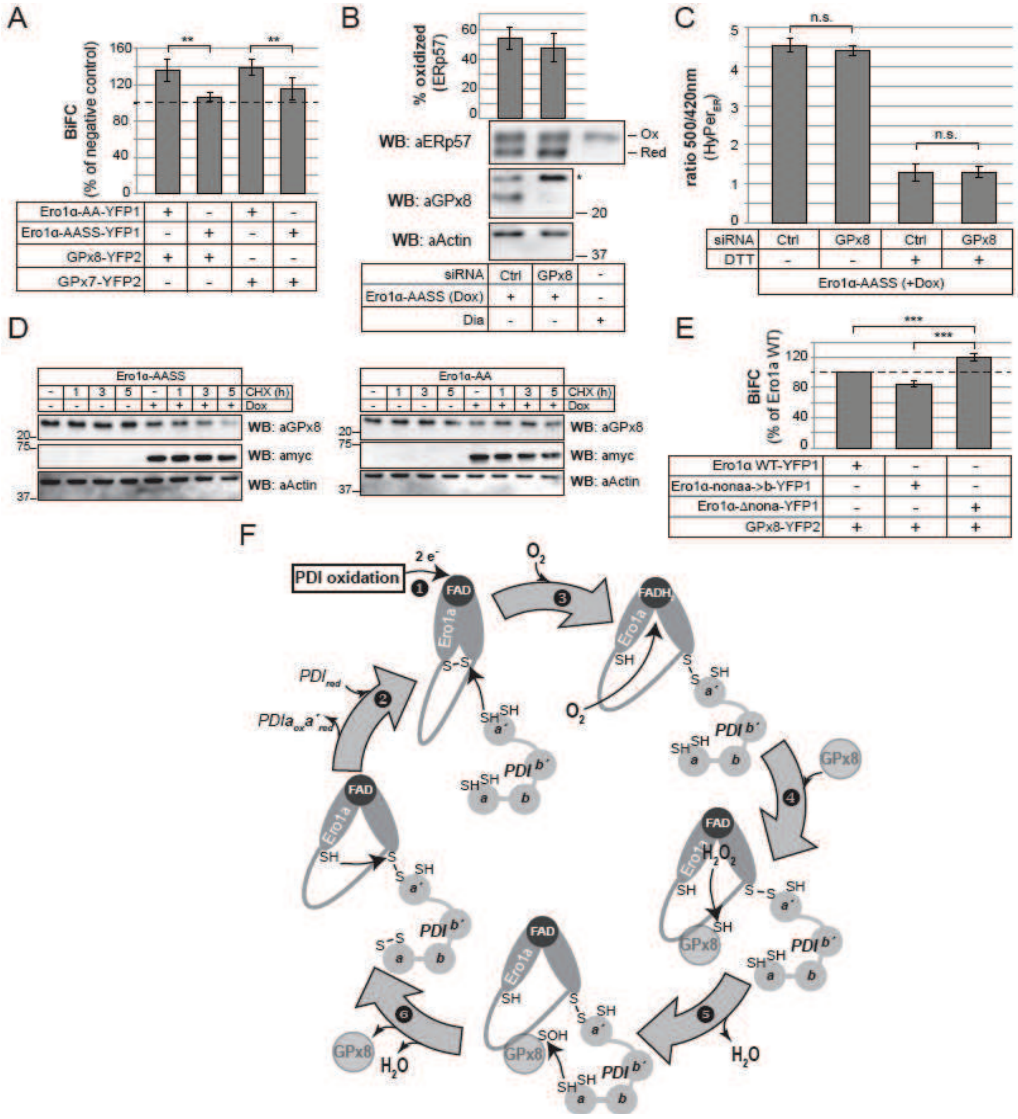

Figure 18: GPx7 and GPx8 interact with the distal end of Ero1α. (**A**) 18 h after transfection with the indicated constructs, HeLa cells were trypsinized and analyzed by flow cytometry for BiFC fluorescence. As negative control, P5-YFP1 was co-transfected with GPx7-YFP2 or GPx8-YFP2, respectively. Values are expressed as percentage of negative control (dashed line). (**B**) Ero1α-AASS cells were treated for 48 h with the indicated siRNAs and for 24 h with doxycycline (Dox), followed by redox analysis of ERp57 as in Fig. 15C (upper blot and chart) and control western blot (WB) using αGPx8 and αactin (lower blots) (n = 9; mean ± SD). Asterisk, background band. (**C**) $HyPer_{ER}$ measurements in Ero1α-AASS-expressing cells 48 h after transfection with control (Ctrl) or GPx8-targeting siRNA in presence or absence of 0.5 mM DTT (n = 4; mean ± SD). (**D**) Ero1α-AASS and Ero1α-AA cells were induced or not for 24 h with Dox and then treated for indicated times with 100 µg/ml cycloheximide (CHX), followed by WB analyses as indicated. Note that GPx8 is destabilized in response to Ero1α-AASS. (**E**) BiFC analysis as in (A) using the indicated constructs. Values are expressed as percentage of fluorescence by Ero1α WT-YFP1 and GPx8-YFP2 (dashed line). (**F**) Mechanism of regulated O_2 access and H_2O_2 detoxification in Ero1α. (1) Oxidation of PDI**a´** at the proximal end of Ero1α leads to the reduction of FAD to $FADH_2$. (2) Via its C-terminal active site, reduced PDI (PDI_{red}) attacks the Cys^{208}–Cys^{241} disulfide (either at Cys^{208} or Cys^{241}), which leads to the formation of a long-lived interchain disulfide and the opening of a diffusion pathway towards $FADH_2$ in Ero1α. (3) O_2 diffuses to and reacts with $FADH_2$ to H_2O_2 and FAD. (4) GPx8 is recruited to the peptide loop connecting Cys^{208} and Cys^{241} and reacts with H_2O_2 to produce H_2O and a sulfenylated active-site cysteine (SOH). (5) As worked out for GPx7 [3], the active site in GPx8 is reductively restored by the N-terminal active site in PDI, which occurs either directly by nucleophilic attack at SOH or indirectly *via* an intramolecular disulfide-bond in GPx8 (not depicted) and produces H_2O. (6) Upon dissociation of reduced GPx8, the Ero1α–PDI interchain disulfide is resolved, leading to release of PDI oxidized in its N-terminal domain ($PDIa_{ox}a'_{red}$) and restoration of Cys^{208}–Cys^{241}. For simplicity, the deprotonations of thiol groups prior to nucleophilic attack are not depicted. n.s., not significant; $^{**}p < 0.01$; $^{***}p < 0.001$. see also Fig. S10

3.4. Discussion

The chemical basis for O_2 reactivity of flavoenzymes is an actively investigated area in enzymology and cofactor biochemistry. In particular, how O_2 can diffuse into the active sites of oxidases and monooxygenases has attracted ample interest [29]. Some of these flavoenzymes have well-defined channels predicted to funnel the gas to the FAD cofactor in a constitutive manner [30,31,32]. For many others including Ero1 the molecular basis for O_2 reactivity is a puzzling enigma [8,9]. Here, by scrutinizing the molecular basis of reductive activation of human Ero1 we discovered, to our knowledge, the first disulfide-sealable and, therefore, actively regulated pathway for O_2 diffusion into a flavoenzyme active site. In addition, our results strongly suggest that the same path guides the exit of the reaction product H_2O_2, because the peroxidase in charge of cleaning up Ero1α-derived H_2O_2, GPx8 [15], binds to this very region of the enzyme.

Cofactor unlocking for O_2 penetration requires rearrangement of the Cys^{208}–Cys^{241} disulfide. From a homeostatic point of view, it is intuitive that this reaction is driven by the reduced **a´** domain active site in PDI, which is also the *bona fide* substrate of the Ero1 "shuttle disulfide" [11,18,21,33]. Thus, Ero1α itself controls the gating of its O_2 consumption and activity *via* the redox state of its major substrate PDI**a´**. This negative feedback mechanism provides an elegant additional mode of PDI-dependent regulation of human Ero1 [17,34].

While Ero1–PDI mixed-disulfide complexes were formerly thought to depend on the "shuttle disulfide" [23,35], our data indicate that the major complex formed at steady state in human cells ("Ero1α–PDI^{fast}") involves the distal end of Ero1 instead. As mixed-disulfide intermediates of thiol–disulfide exchange reactions are short-lived, the abundance of this complex is remarkable. In fact, it is comparable to the one of the Ero1α–ERp44 complex (Fig. 13C), which, due to the CXXS active-site sequence in ERp44, is not a thiol–disulfide exchange intermediate but a trapped species. We therefore propose Ero1α–PDI^{fast} to be stabilized by non-covalent interactions reminiscent of the disulfide-linked dimer formed by tapasin and ERp57 in the MHC class I peptide-loading complex [36]. These considerations imply that there is no net oxidation of PDI**a´** taking place at the Ero1α distal end, but rather an equilibrium being formed between PDI-bound, open state and Cys^{208}–Cys^{241} disulfide-bound, closed state. Consistently, despite the presence of a

CXXC active-site motif, PDI**a**´ apparently cannot interact with Ero1α mutants where either Cys^{208} or Cys^{241} is absent (Fig. 14D). Unfortunately, our proposal that the dithiol configuration of Cys^{208}/Cys^{241} does not occur in the catalytic cycle of Ero1α could not be tested by mass spectrometry, since the corresponding peptides were consistently undetectable (Table S1 and unpublished observations). In contrast to Ero1α–PDI^{fast}, the Ero1α–ERp44 complex is not diminished but rather enhanced upon mutation of Cys^{208}/Cys^{241}, suggesting a vicinal disulfide such as Cys^{35}–Cys^{48} or Cys^{37}–Cys^{46} as a target of ERp44 [19]. It is likely that the "ERp44-like" CXXS-1 mutants of PDI and ERp57 attack the same disulfide (Fig. 14C+E).

Based on the facts that (i) Ero1α–GPx8 association depends on Cys^{208}/Cys^{241} (Fig. 18A) but not on Cys^{79} in GPx8 (Fig. S10B) and that (ii) our efforts to detect this association with isothermal titration calorimetry or size-exclusion chromatography using purified proteins all failed (unpublished observations), the data suggest that Ero1α–PDI^{fast} serves as a platform for GPx8 binding to the Cys^{208}/Cys^{241} region in Ero1α (Fig. 18E). This proposition makes functional sense, because GPx8 would be recruited to the H_2O_2 exit site in the open configuration. We propose the following sequence of events (Fig. 18F): By its reduced active site in the C-terminal **a**´ domain, PDI attacks the Cys^{208}–Cys^{241} disulfide and thereby opens a diffusion pathway towards reduced FAD ($FADH_2$). In the resulting Ero1α–PDI^{fast} complex, $FADH_2$ reduces penetrated O_2 to H_2O_2. Concomitantly, GPx8 (or GPx7) is recruited to the site of H_2O_2 exit where it is oxidized by H_2O_2 to form a sulfenylated active site cysteine. Oxidized GPx8 then reacts with the N-terminal **a** domain active site in PDI to form a disulfide in PDI [3]. Finally, GPx8 and PDI dissociate from Ero1α following the reformation of Cys^{208}–Cys^{241}, thereby restoring the original state.

The model in Fig. 18F only covers the mechanism of $FADH_2$ oxidation. The catalytic cycle of Ero1α is completed by subsequent FAD reduction, which is accomplished by PDI**a**´-derived electrons *via* the "shuttle disulfide", an inner active-site cysteine pair, and a charge transfer complex (see also Introduction) [8,9]. Although not formally proven, two observations indicate that these two phases of the catalytic cycle are temporally separated. First, the Cys^{94}-dependent disulfide-transfer complex between the "shuttle disulfide" and PDI (Ero1α–PDI^{slow} in Fig. 14C) [21] predominantly exists without a second PDI molecule attached to the distal end of Ero1α. This indicates that the O_2 diffusion path is closed during PDI oxidation/FAD reduction. Second, Ero1α-AASS, which features a constitutively open O_2 diffusion path and, presumably, a flexible

Cys^{208}/Cys^{241} region, is catalytically hampered (Fig. 17A-D). Thus, we speculate that Ero1α operates through a yin-yang mechanism where the active conformations of the O_2-reducing end and the PDI-oxidizing end alternate.

The catalytic cycle of yeast Ero1 can also be fuelled by addition of FAD instead of O_2 as an oxidant [10,37]. Thus, although the removal of the Cys^{208}–Cys^{241} disulfide permanently unblocks an access path for O_2 to FAD, the exchange of FAD molecules within the core of Ero1α upon Cys^{208}–Cys^{241} reduction cannot be excluded. However, purified Ero1α-AASS was found to firmly associate with FAD (our unpublished observations), indicating O_2 and H_2O_2 and not FAD to be the diffusible entities. This interpretation is consistent with a recent study, demonstrating the inability of Ero1α to use FAD as alternate electron acceptor [34].

This work demonstrates that Ero1α-AASS represents the first variant of human Ero1 that is truly constitutively active. Accordingly, although this mutant is catalytically crippled for the reasons discussed above, it has strong effects on ER redox homeostasis and cell viability (Fig. 15). We therefore posit that expression of Ero1α-AASS (or of Ero1β-AASS) constitutes the currently best tool to study the impact of ER hyper-oxidation on physiological processes such as protein folding, ER-associated degradation, Ca^{2+} signaling, unfolded protein response activation, membrane trafficking, lipid droplet formation, or autophagy. It will also be interesting to investigate the subroutine of cell death that is triggered by Ero1α-AASS. Given the predominant ER localization of the reactive oxygen species-generating photosensitizer hypericin, it is quite possible that Ero1α-AASS has mechanistically similar cytotoxic effects as hypericin-based photodynamic cancer therapy [38].

On the basis of three regulatory disulfides (Cys^{94}–Cys^{131}, Cys^{99}–Cys^{104}, Cys^{208}–Cys^{241}) in Ero1α, which are present in the majority of Ero1α molecules to mediate their shutdown [17], the question arises as to why the cell would maintain such a repertoire of inactive oxidase molecules in the ER. One possible answer relates to the known oxidase-independent functions of Ero1α, namely the regulation of ER Ca^{2+} signaling and of the secretion of disulfide-linked oligomers [9]. In addition, it is likely that the hyperoxic setup of tissue culture does not reflect the *in vivo* situation where O_2 supply is more limited. Indeed, regulatory disulfides in Ero1α are opened

upon O_2 withdrawal [39], and *ERO1L* is transcriptionally upregulated in response to hypoxia [40,41], e.g. in solid tumors where its levels positively correlate with tumor aggressiveness [42].

In summary, we provide a molecular-level understanding of ER redox homeostasis in human cells that reaches beyond the previously described regulatory disulfides in Ero1α. This involves both the control of O_2 consumption by a novel mechanism of regulated "FAD sealing" and the local conversion of the reaction product H_2O_2 into a disulfide bond and water, which is catalyzed within the Ero1α–PDI–GPx8 oxidase–peroxidase complex defined herein.

3.5. Materials and Methods

3.5.1. RNA isolation and qPCR analysis

Total RNA isolation, qPCR analysis, and target gene-specific primer sequences have been described [43].

3.5.2. RNA interference

SiRNA transfections were conducted as previously published [43]. For depletion of ERp44 (10 nM for 72 h) the following siRNA was used (only coding strand): GUAGUGUUUGCCAGAGUUGTT (Microsynth).

3.5.3. Redox state analysis of ERp57 and Grx1-roGFP1-iE$_{ER}$

The protocol for alkylation of originally oxidized cysteines with 4-acetamido-4'-maleimidylstilbene-2,2'-disulfonic acid (Life Technologies) has been described [17]. Redox western blot of the Grx1-roGFP1-iE$_{ER}$ sensor has been published [2].

3.5.4. Fluorescence excitation spectrum analysis

Cells stably transfected with HyPer$_{ER}$ were subjected to fluorescence excitation spectrum analysis as described before [2].

3.5.5. Metabolic labeling

Metabolic labeling with ^{35}S-methionine (Perkin Elmer) followed by western blot has been described [21].

3.5.6. WST-1 assay

This assay was essentially performed as published elsewhere [13]. However, 50,000 cells were seeded per well in a 24-well plate and treated the following day, where indicated, with 1 µg/ml doxycycline and/or 1 mM L-Buthionine-sulfoximine (BSO; Sigma) for 24 h.

3.5.7. Dithiothreitol (DTT) washout assays

The cellular GSSG:total glutathione (GS_{tot}) ratio after DTT washout was measured using a 5,5'-dithiobis(2-nitrobenzoic acid)/glutathione reductase recycling assay as previously described [21].

3.5.8. Bi-molecular fluorescence complementation (BiFC)

A total of $5*10^5$ HeLa cells were seeded per well into a 6-well plate and co-transfected the following day with YFP1 and YFP2 constructs (2 µg each) using Turbofect (Thermo Scientifc). To minimize non-specific BiFC complex formation cells were trypsinized 18 h post-transfection [44] and washed twice with phosphate buffered saline (PBS). Routinely, one half of each sample was subjected to αGFP western blot analysis using normalized amounts of total protein. These control analyses (data not shown) were essential to exclude unequal expression of different YFP fusion proteins. The other half of the cells was gently re-suspended in PBS containing 1% fetal calve serum, subjected to fluorescence analysis using a Becton Dickinson FACSCanto II, and data processed with Flowing Software 2 (version 2.5.1).

3.5.9. Crystal violet staining

$2,5*10^5$ cells were grown in 60 mm dishes for 24 h before treatment with or without 1 µg/ml doxycycline for 24 h. The cells were fixed with 4% paraformaldehyde for 5 minutes prior to staining for 30 minutes with 0,05% crystal violet (dissolved in distilled water and filtered (0,45 µm filter); Sigma). After washing twice with tap water, the dishes were dried and photographed.

3.5.10. Indirect immunofluorescence staining

Staining procedure and image acquisition were published before [2], with the only exception here being the use of conjugated secondary goat-anti-mouse antibody Hilyte 647 (AnaSpec).

3.5.11. Antibodies

The following antibodies were used: 9E10 (αmyc, a kind gift from Hans-Peter Hauri, University of Basel, Switzerland); 12CA5 (αHA, a kind gift from Hans-Peter Hauri, University of Basel, Switzerland); αERp57 (a kind gift from Ari Helenius ETH Zürich, Switzerland); αGFP (a kind gift from Jan Riemer, University of Kaiserslautern, Germany); αGPx8 (a kind gift from Lloyd

Ruddock, University of Oulu, Finland); I-19 (αactin, Santa Cruz Biotechnology); RL90 (αPDI, Abcam); 36C9 (αERp44, a kind gift from Roberto Sitia, Vita-Salute San Raffaele, Italy).

3.5.12. Statistics

Data sets were analyzed for statistical significance using Student's *t* test (two-tailed distribution; heteroscedastic).

3.5.13. In situ acid trapping, immunoprecipitation, and concavanalin A precipitation

Preparation of thiol-disulfide quenched protein samples was done as before [21]. Where indicated antibodies for immunoprecipitation were chemically cross-linked to protein A sepharose using dimethyl pimelimidate (Sigma) or Anti V5 agarose affinity gel (Sigma) was used.

3.5.14. Sample preparation and mass spectrometry analysis

Twenty 10 cm dishes of doxycycline-induced (24 h) Ero1α-AA cells were grown to 90% confluency. Following treatment with 1 mM DTT the cells were subjected to in situ acid trapping and αmyc-IP (see above). After SDS-PAGE, proteins were stained with Simply Blue (Life Technologies) followed by de-staining with water. The protein band was excised, reduced with 10 mM DTT for 2 h at 37^{o}C and alkylated with 50 mM iodoacetamide for 15 min at room temperature in the dark. Subsequently, the gel piece was digested with 125 ng trypsin (Sequencing Grade, Promega) for 18 h at 37^{o}C. The peptides in the supernatant were collected and the gel piece was extracted with 0.1% acetic acid/50% acetonitrile. The extract was pooled with the tryptic peptides, dried in a speed vac and redissolved in 0.1% acetic acid. 10 µl were used for mass spectrometric analysis.

The trypic peptides were analyzed by capillary liquid chromatography tandem MS (LC/MS/MS) using a homemade separating column (0.075mm x 15cm) packed with Reprosil C18 reverse-phase material (2.4 µm particle size, Dr. Maisch, Ammerbuch-Entringen, Germany). The column was connected on line to an Orbitrap FT hybrid instrument (Thermo Scientific). The solvents used for peptide separation were 0.1% acetic acid in water/0.005% TFA (solvent A) and 0.1% acetic acid/0.005% TFA and 80% acetonitrile in water (solvent B). 2 µl of peptide digest were injected with a Proxeon nLC capillary pump (Thermo Scientific) set to 0.3 µl/min. A linear gradient from 0 to 40% solvent B in solvent A in 95 min was delivered with the nano pump at a

flow rate of 300 nl/min. After 95 min, the percentage of solvent B was increased to 75% in ten minutes. The eluting peptides were ionized at 2.5 kV. The mass spectrometer was operated in data-dependent mode. The precursor scan was done in the Orbitrap set to 60,000 resolution, while the fragment ions were mass analyzed in the LTQ instrument. A top ten method was run so that the ten most intense precursors were selected for fragmentation. The MS/MS spectra were then searched against a databank consisting of Ero1α-AA-myc6HIS and PDI using the Sequest HT software (Thermo Scientific) with 20 ppm precursor ion tolerance, while the fragment ions were set to 0.5 Da tolerance. The following modifications were used during the search: carbamidomethyl-cysteine, NEM-cysteine, and oxidized methionine as variable modifications. The peptide search matches were set to 'high confidence'.

3.5.15. Recombinant DNA

The following expression vectors have been previously published: HA-ERp57 [45] and HA-ERp57 CxxS-1 and CxxS-2 [17], CRTss+EYFP1+mature Ero1α, CRTss+EYFP2+mature GPx7, CRTss+EYFP2+luminal domain GPx8, CRTss+EYFP1+P5 [28] (kind gifts from Lloyd Ruddock, University of Oulu, Finland).

For generation of the PDI-V5 CxxS1, PDI-V5 CxxS2 and PDI-V5 CxxS1+2 we used pcDNA3.1/PDI-V5 (a gift from Neil Bulleid, University of Glasgow, UK) as a template for QuikChange mutagenesis (Stratagene) using the following primers (only coding strand sequences): CxxS1: 5'-GGTGTGGCCACAGCAAGGCTCTGGC-3'; CxxS2: 5'-CATGGTGTGGTCACTCCAAACAGTTGGCTCC-3'; the combined mutant construct PDI-V5 CxxS1+2 was produced by two rounds of mutagenesis.

For generation of the Ero1α-AA+C94S, Ero1α-AA+C208S, and Ero1α-AA+C241S we used pcDNA5/FRT/TO/Ero1α-C104A/C131A [13] as a template for QuikChange mutagenesis (Stratagene) using the following primers: C94S: 5′-GAATGACATCAGCCAGTCTGGAAGAAGGGACTG-3′, C208S: 5'-GGAATGTCATCTACGAAGAAAACTCTTTTAAGCCACAGAC-3', C241S: 5'-GGCTAGAAGGTCTCTCTGTAGAAAAAAGAGCATTCTAC-3', the combined mutant construct Ero1α-AASS was produced by two rounds of mutagenesis.

For generation of Ero1α-C208S and Ero1α-C208S/C241S we used pcDNA5/FRT/TO/Ero1α [17] as template for Quikchange mutagenesis (Stratagene) and the same primers as above.

For generation of the Ero1β-AASS mutant we used pcDNA5/FRT/TO/Ero1β–C100A/C130A [2] as template for QuikChange mutagenesis (Stratagene) using the following primers: C207S: 5'-GCATCTATGAAGAGAACTCTTTCAAGCCTCGATCTGTTTATC-3', C240S: 5'-GCTAGAAGGTTTGTCTCTGGAGAAAAGAGTCTTCTATAAGC-3'.

For generation of BiFC Ero1a point mutant constructs we performed the same QuikChanges and C104A and C131A QuikChanges [13,17] using pcDNA3.1/CRTss+EYFP1+mature Ero1α as template. For the nonapeptide mutations, we first mutated the NdeI restriction site within the CMV promoter of the template pcDNA3.1/CRTss+EYFP1+mature Ero1α using the following primers: 5'-GCAGTACATCAAGTGTATCATTTGCCAAGTACGCC-3'. The resulting construct could then be digested with NdeI and BamHI to excise the mature Ero1α coding sequence, which was replaced by either mature Ero1α–nonaα–>β or mature Ero1α–Δnona. These two sequences were generated by sequence overlap extension PCR using the following primers: mature Ero1α–nonaα–>β: NdeI-fragment: 5'-CCGTCATCTTCTCCTCGGGATGGAGCCAAAGGATTTAAAGGTC-3'/5'-AGAGAGCATATGGAGGAGCAGCCC-3' (restriction site underlined); BamHI-fragment: 5'-CCATCCCGAGGAGAAGATGACGGAGAAACTTTTTACAGTTGGCTAGAAGGTC-3'/5'-CTCTCTGGATCCTCAATGAATATTCTGTAACAAGTTCCTGAAG-3';
mature Ero1α–Δnona: NdeI-fragment: 5'-GCCAACTGTAAAAAGTAGCCAAAGGATTTAAAGGTC-3'/5'-AGAGAGCATATGGAGGAGCAGCCC-3'; BamHI-fragment: 5'-CCTTTGGCTACTTTTTACAGTTGGCTAGAAGGTC-3'/5'-CTCTCTGGATCCTCAATGAATATTCTGTAACAAGTTCCTGAAG-3'; the two corresponding fragments were annealed and amplified with the following primer pair: 5'-AGAGAGCATATGGAGGAGCAGCCC-3'/5'-CTCTCTGGATCCTCAATGAATATTCTGTAACAAGTTCCTGAAG-3'; Finally the products were ligated via NdeI/BamHI into the BiFC vector backbone.

For generation of CRTss+EYFP2+luminal domain GPx8-C79S we used CRTss+EYFP2+luminal domain GPx8 as template for QuikChange mutagenesis (Stratagene) using the following primers: 5'-CGTGGCCAGTGACTCCCAACTCACAGACAG-3'.

3.5.16. Cell culture and transient transfections

The culturing of HeLa cells [2] and FlipIn TRex293 cells for doxycycline (1 μg/ml, Sigma)-inducible expression of Ero1 variants [17] has been described. The following FlipIn TRex293 cell lines have been published previously: Ero1α [17], Ero1α-AA [13], Ero1α-AA:$HyPer_{ER}$ [43], Ero1α-AA+C85A/C391A [13] Ero1β-C100A/C130A [2]. Corresponding cell lines with inducible expression of Ero1α-AA+C94S, Ero1α–C208S/C241S, Ero1α–AASS, and Ero1β–AASS were generated equally. Ero1α–C208S/C241S:$HyPer_{ER}$ and Ero1α-AASS:$HyPer_{ER}$ cell lines were created as before [43] (with the $HyPer_{ER}$ vector kindly provided by Miklos Geiszt, Semmelweis University, Hungary).

Transient transfections of HeLa cells were carried out using Turbofect (Thermo Scientific). Transient transfections of FlipIn TRex293 cells were carried out using Metafectene Pro (Biontex).

3.5.17. Analysis of H_2O_2 generation

Reduced PDI (final concentration of 100 μM) was incubated with 4 μM of either Ero1α-AA or Ero1α-AASS in buffer (50mM Tris pH7.5, 300 mM NaCl) saturated with O_2. The concentration of Ero1α-generated H_2O_2 was analyzed by Pierce Quantitative Peroxide Assay Kit (Thermo). At several time points, 10 μl of the reaction mixture was mixed with 100 μL of Pierce Quantitative Peroxide Assay reagents solution. After incubation for 20 min at room temperature in the dark, the absorbance at 560 nm was measured using spectrophotometer Hitachi-U3310.

3.5.18. Oxygen and NADPH consumption assay, MalPEG2k modification

Oxygen consumption was measured as previously described [46]. NADPH consumption assay and MalPEG2k modification of PDI have been described before [47].

3.6.Supplemental Information

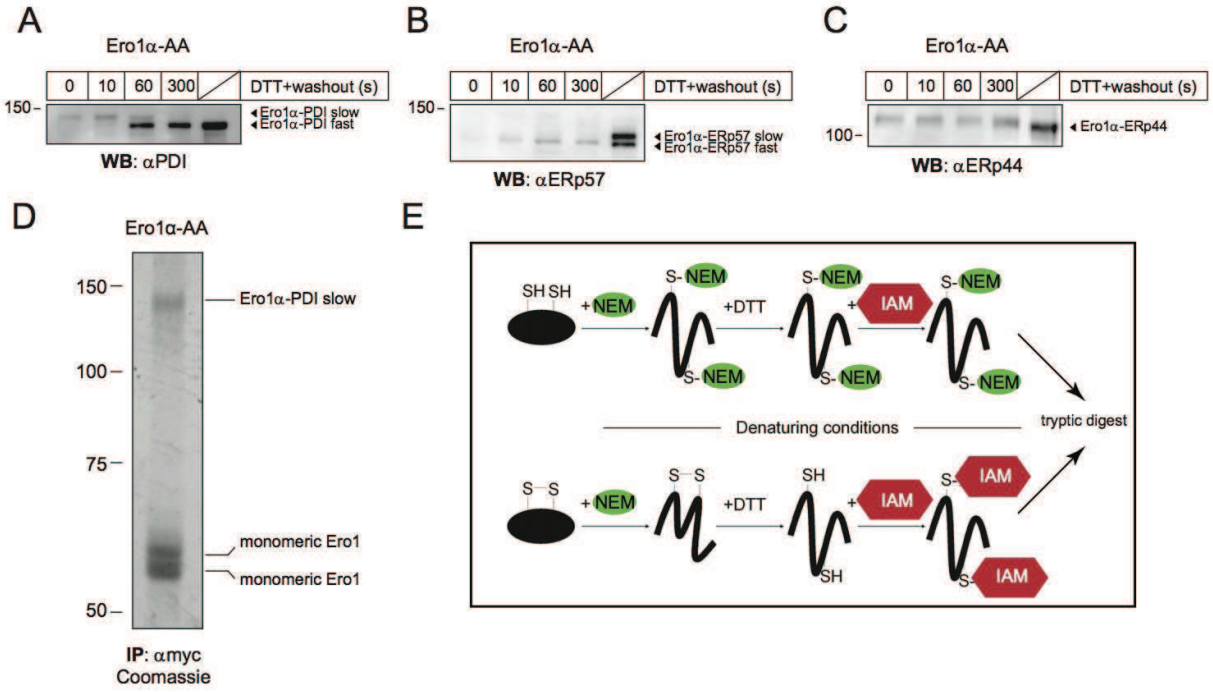

Figure S6: Characterization of Ero1α–PDI^{slow}.

(**A-C**) Replicate samples of the experiment presented in Fig1B+C were immunoblotted using the indicated antibodies to identify the mixed-disulfide partners of myc-tagged Ero1α-AA (as labeled in Fig. 13C). The lower antigenicity of Ero1α–PDI^{slow} to αPDI (A) compared to Ero1α–PDI^{fast} was observed before [21].

(**D**) Large-scale immunoprecipitation of Ero1α-AA from cells treated with 1 mM DTT followed by 10% TCA and 15 mM NEM (as described in Experimental Procedures) using αmyc covalently crosslinked to protein A-sepharose. The immunoprecipitate was separated by 7.5% non-reducing SDS-PAGE and stained with Coomassie blue. Subsequently, Ero1α–PDI^{slow} was excised and subjected to mass spectrometry.

(**E**) Cartoon depicting the processing of reduced and disulfide-bound cysteines in Ero1α-AA. Upon treatment with NEM and immunopreciptation, Ero1α-AA was denatured for SDS-PAGE, reduction by DTT, re-alkylation with iodoacetamide (IAM), and tryptic digest ahead of mass spectrometry analysis. Accordingly, originally reduced cysteines were NEM-modified and originally disulfide-bound cysteines carried the mass of IAM.

Sequence	Amino acids	Cysteines	Modifications	XCorr[a]	Charge	MH+ [Da][b]	ΔM [ppm][c]	m/z [Da][d]	# Missed Cleavages
Human ERO1-like protein α C104A/C131A-myc6HIS:									
LLESDYFR	68-75			2.95	2	1042.52776	7.04	521.76752	0
VNLKRPcPFWNDISQcGR	79-96	C85; C94	C7(Carbamidomethyl); C16(Carbamidomethyl)	3.28	3	2247.11332	9.89	749.70929	2
RPcPFWNDISQcGR	83-96	C85; C94	C3(Carbamidomethyl); C12(Carbamidomethyl)	4.89	3	1792.81253	6.60	598.27570	1
RDcAVKPAQSDEVPDGIK	97-114	C99	C3(Carbamidomethyl)	4.54	3	1984.99179	8.07	662.33545	2
DcAVKPAQSDEVPDGIK	98-114	C99	C2(N-ethylmaleimide)	3.91	3	1896.91404	6.94	632.97620	1
DcAVKPAQSDEVPDGIK	98-114	C99	C2(Carbamidomethyl)	4.03	3	1828.88944	8.08	610.30133	1
YSEEANNLIEEAEQAER	120-136			4.82	2	1994.90752	6.85	997.95740	0
LGAVDESLSEETQK	137-150			4.28	2	1505.74272	6.44	753.37500	0
YTGYKGPDAVK	188-198			3.18	2	1285.63017	6.98	643.31873	1
YLLQETWLEK	266-275			2.48	2	1322.71013	8.32	661.85870	0
YLLQETWLEKK	266-276			2.58	2	1450.80498	7.50	725.90613	1
FDGILTEGEGPR	288-299			3.26	2	1290.64141	6.88	645.82434	0
PDFQLFTGNK	325-334			2.96	2	1166.59258	7.27	583.79993	0
mLLLEILHEIK	342-352		M1(Oxidation)	2.16	2	1367.80840	8.51	684.40784	0
IMDcVGcFK	388-396	C391;C394	C4(Carbamidomethyl); C7(Carbamidomethyl)	2.90	2	1129.49101	6.26	565.24915	0
ImDcVGcFK	388-396	C391;C394	M2(Oxidation); C4(Carbamidomethyl); C7(Carbamidomethyl)	3.35	2	1145.48711	7.20	573.24719	0
LQTQGLGTALK	403-413			2.74	2	1129.66472	6.30	565.33600	0
LIANmPESGPSYEFHLTR	420-437		M5(Oxidation)	3.49	3	2078.01853	8.32	693.34436	0
QEIVSLFNAFGR	438-449			2.98	2	1380.73699	7.17	690.87213	0
ISTSVKELENFR	450-461			2.87	2	1422.77056	8.28	711.88892	1
NLLQNIHGTK	462-471			2.63	2	1137.64543	6.95	569.32635	0
LISEEDLNSAVDHHHHHH	478-495			2.66	3	2126.99485	9.26	709.66980	0
Human protein disulfide isomerase (PDI):									
SNFAEALAAHK	32-42			3.00	2	1158.59844	7.06	579.50286	0
LKAEGSEIR	70-78			2.83	3	1002.56650	8.59	334.86035	1
LAKVDATEESDLAQQYGVR	79-97			4.08	3	2093.06760	7.92	698.36072	1
VDATEESDLAQQYGVR	82-97			4.36	3	1780.84934	8.12	594.28796	0
YQLDKDGVVLFK	196-207			3.18	3	1424.78876	7.24	475.60110	1
YQLDKDGVVLFKK	196-208			3.28	4	1552.88772	9.21	388.97739	2
NNFEGEVTK	214-222			2.07	2	1037.49675	6.64	519.25201	0
HNQLPLVIEFTEQTAPK	231-247			3.78	3	1965.05875	7.46	655.69110	0
THILFLFLPK	255-263			2.66	3	1081.68518	7.69	361.23325	0
SVSDYDGKLSNFK	264-276			2.55	2	1459.71831	8.16	730.36279	1
GKILFIFIDSDHTDNQR	284-300			2.60	3	2019.04557	7.96	673.68671	1
ILFIFIDSDHTDNQR	286-300			2.53	2	1833.93010	9.29	917.46869	0
LITLEEEMTK	317-326			2.72	2	1206.63677	6.70	603.82202	0
LITLEEEmTK	317-326		M8(Oxidation)	2.77	2	1222.63152	6.48	611.81940	0
YKPESEELTAER	327-338			3.61	3	1451.71350	8.39	484.57602	1
PESEELTAER	329-338			2.61	2	1160.55266	8.30	580.77997	0
ITEFCHR	339-345	343	C5(Carbamidomethyl)	2.03	2	962.45806	7.02	481.73267	0
NFEDVAFDEK	376-385			2.62	2	1213.54521	6.59	607.27625	0
NFEDVAFDEKK	376-386			3.49	2	1341.64214	7.41	671.32471	1
LGETYKDHENIVIAK	410-424			3.24	3	1729.92423	7.07	577.31293	1
MDSTANEVEAVK	425-436			2.94	2	1293.61101	9.14	647.30914	0
mDSTANEVEAVK	425-436		M1(Oxidation)	3.00	2	1309.60344	7.14	655.30536	0
MDSTANEVEAVKHSFPTLK	425-444			3.05	4	2203.11855	5.49	551.53510	1

[a] Calculated cross-correlation score for all candidate peptides queried from the database (sequest searches only)

[b] Protonated monoisotopic mass of the peptides in Daltons

[c] Difference between the theoretical mass of the peptide and the experimental mass of the precursor ion

[d] Mass-to-charge ratio of the precursor ion in Dalton;

Table S1: Identified peptides in Ero1α–PDI^{slow}.

Ero1α-AA (Human ERO1-like protein α C104A/C131A-myc6HIS) and PDI peptides that were identified by liquid chromatography tandem mass spectrometry (LC/MS/MS) were sorted according to their position. Cysteine residues were annotated as either iodoacetamide (Carbamidomethyl)- or N-ethylmaleimide-modified. Note that the peptides harboring Cys^{85} and Cys^{391} (rows highlighted in grey) were exclusively found in the carbamidomethyl-modified form, indicating their participation in a disulfide bond.

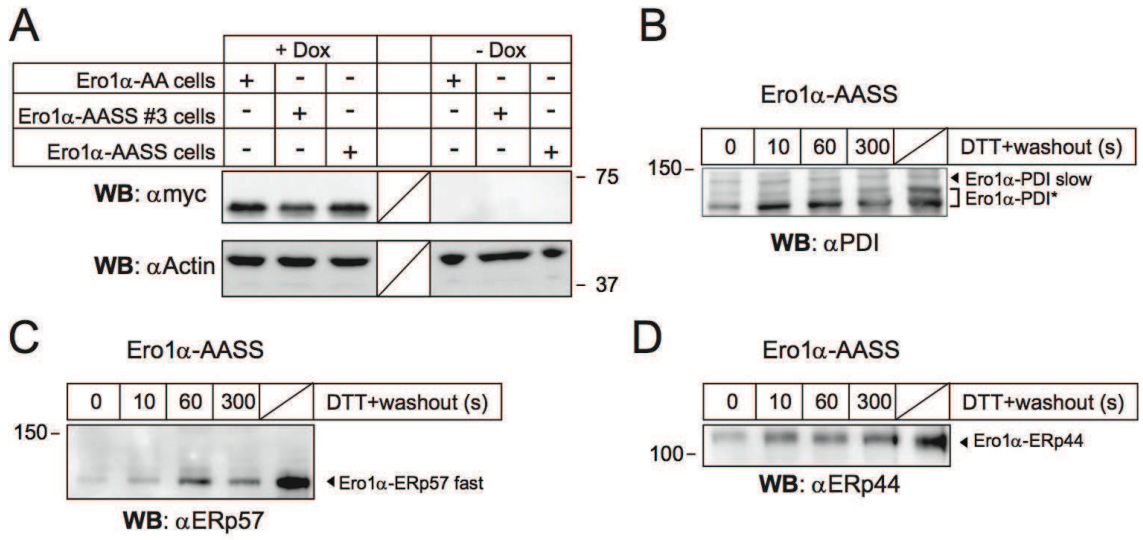

Figure S7: Mixed disulfide complexes involving Ero1α-AASS: Absence of Ero1α–PDI^{fast} and Ero1α–ERp57^{slow}.

(**A**) Doxycycline (Dox)-inducible expression of Ero1α-AASS in two FlpIn TRex 293 cell clones was compared to Ero1α-AA cells using western blot (WB) and indicated antibodies. Note that clone #3 shows lower expression relative to the other two clones (primarily used in this study).

(**B**-**D**) Replicate samples of the experiment presented in Fig. 14B were immunoblotted using the indicated antibodies to identify the mixed-disulfide partners of myc-tagged Ero1α-AASS (as labeled in Fig. 14B).

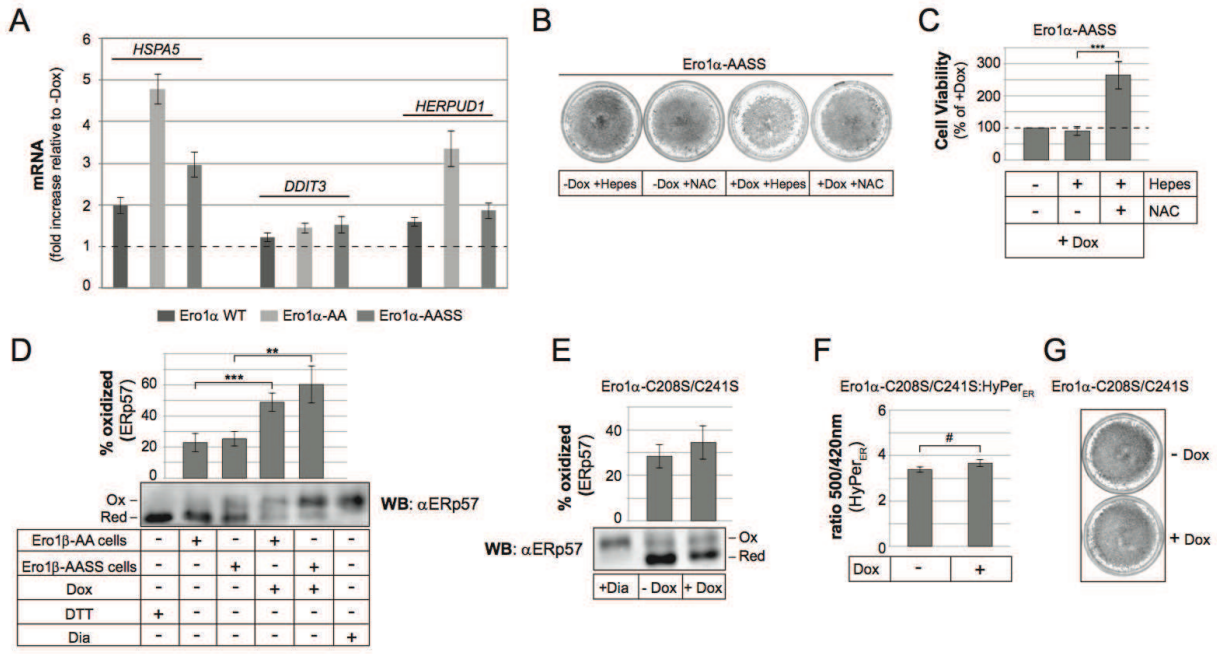

Figure S8: Physiological consequences of C208S/C241S mutant: Supplemental experiments.

(**A**) Ero1α WT, Ero1α-AA, and Ero1α-AASS cells were induced or not for 24 h with doxycycline (Dox) and subjected to quantitative real-time RT-PCR using primers specific for *HSPA5* (encoding BiP/GRP78), *DDIT3* (encoding CHOP/GADD153), or *HERPUD1* (encoding Herp). Plotted are fold increases of mRNA levels relative to the uninduced control sample (-Dox, dashed line) ($n \geq 4$; mean ± SEM).

(**B**) Crystal violet staining of Ero1α-AASS cells treated, where indicated, with 5 mM N-acetyl cysteine (NAC) in 2 mM HEPES pH 7 (or with buffer alone) with or without Dox for 24 h.

(**C**) Viability of Ero1α-AASS cells was determined by the WST-1 assay following indicated treatments (n = 5; mean ± SD).

(**D** and **E**) Experiments analogous to Fig. 15C using Ero1β-AA and Ero1β-AASS cells (n = 4; mean ± SD) (D) or Ero1α-C208S/C241S cells (n = 4; mean ± SD) (E).

(**F**) Experiment analogous to Fig. 15E using Ero1α-C208S/C241S:HyPer$_{ER}$ cells (n = 3; mean ± SD).

(**G**) Experiment analogous to Fig. 15A using Ero1α-C208S/C241S cells.

#$p < 0.07$; **$p < 0.01$; ***$p < 0.001$.

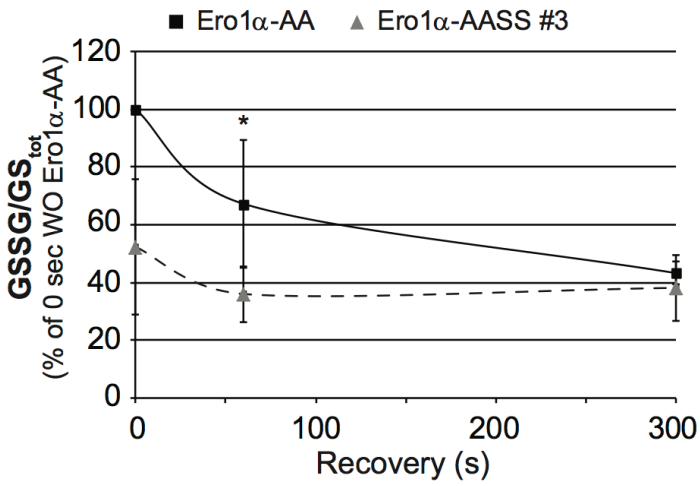

Figure S9: Results in Fig. 17D are likely not an artifact of compromised cell viability.

Experiment performed as in Fig. 17D using Ero1α-AASS clone #3 cells (mean ± SD; two independent experiments each performed at least in doublet).

*$p < 0.05$

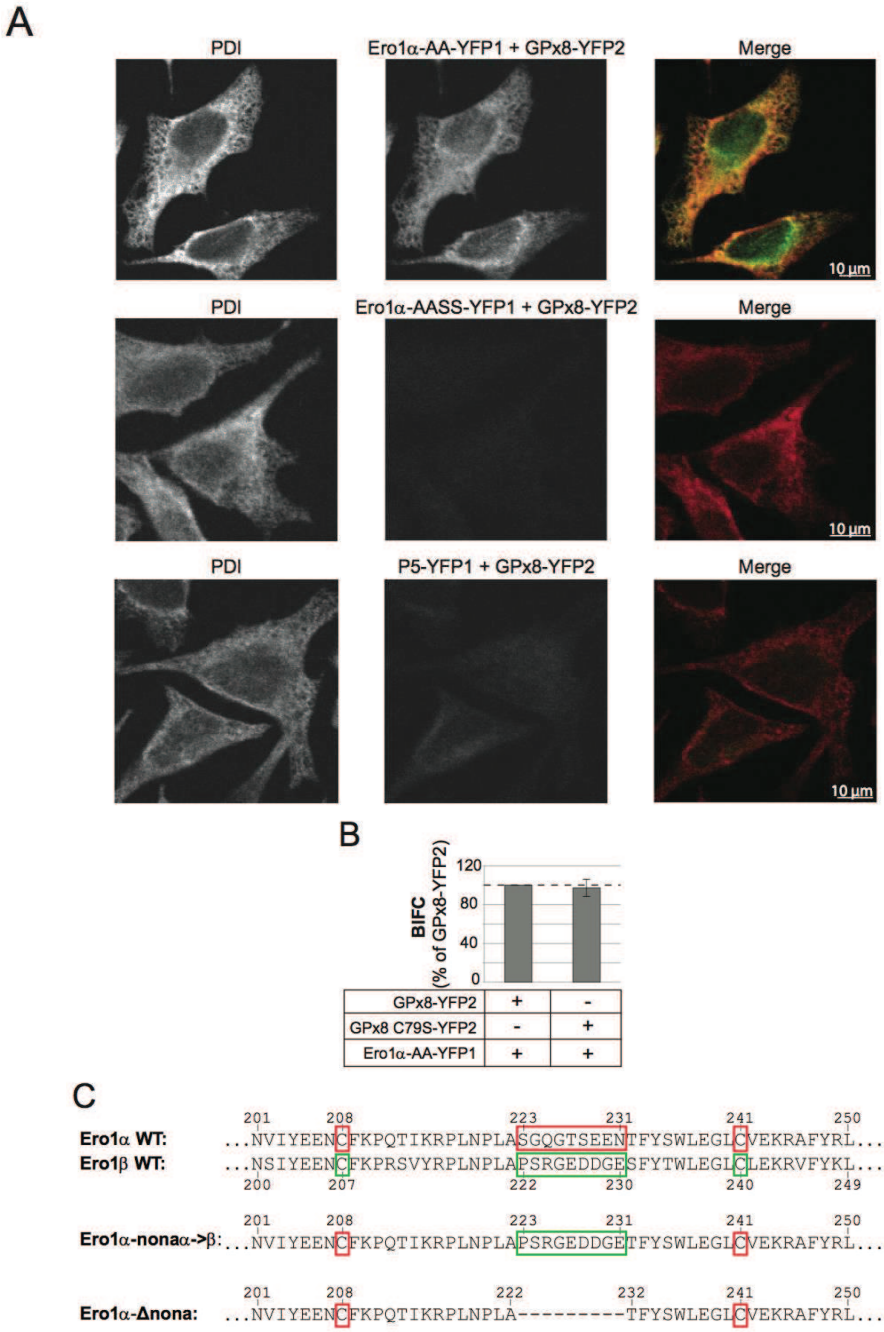

Figure S10: Supplementary experiments relating to BiFC.

(**A**) HeLa cells were co-transfected with the indicated YFP half site fusion proteins for BiFC and fixed 48 h post-transfection. For co-localization, endogenous PDI was stained with indirect immunofluorescence. PDI staining (red) and BiFC fluorescence (green) were recorded by confocal microscopy. Scale bars (10 µm) are indicated.

(**B**) BiFC assay using the indicated combinations of YFP half site constructs. BiFC fluorescence is expressed as percentage of the signal by Ero1α-AA-YFP1 and GPx8-YFP2 (dashed line).

(**C**) The amino acid sequences of the loop regions connecting Cys^{208} and Cys^{241} in Ero1α or Cys^{207} and Cys^{240} in Ero1β are shown, along with the engineered loop regions of the Ero1α-nonaα–>β and Ero1α-Δnona mutants.

3.7.References

[1] C.S. Sevier, C.A. Kaiser, Disulfide transfer between two conserved cysteine pairs imparts selectivity to protein oxidation by Ero1, Molecular biology of the cell 17 (2006) 2256-2266.
[2] J. Birk, M. Meyer, I. Aller, H.G. Hansen, A. Odermatt, T.P. Dick, A.J. Meyer, C. Appenzeller-Herzog, Endoplasmic reticulum: Reduced and oxidized glutathione revisited, Journal of cell science 126 (2013) 1604-1617.
[3] L. Wang, L. Zhang, Y. Niu, R. Sitia, C.C. Wang, Glutathione peroxidase 7 utilizes hydrogen peroxide generated by Ero1alpha to promote oxidative protein folding, Antioxidants & redox signaling 20 (2014) 545-556.
[4] K. Denoncin, J.F. Collet, Disulfide bond formation in the bacterial periplasm: major achievements and challenges ahead, Antioxidants & redox signaling 19 (2013) 63-71.
[5] M. Fischer, J. Riemer, The Mitochondrial Disulfide Relay System: Roles in Oxidative Protein Folding and Beyond, International journal of cell biology 2013 (2013) 742923.
[6] O.B. Oka, N.J. Bulleid, Forming disulfides in the endoplasmic reticulum, Biochimica et biophysica acta 1833 (2013) 2425-2429.
[7] Y. Sato, K. Inaba, Disulfide bond formation network in the three biological kingdoms, bacteria, fungi and mammals, The FEBS journal 279 (2012) 2262-2271.
[8] K. Araki, K. Inaba, Structure, mechanism, and evolution of Ero1 family enzymes, Antioxidants & redox signaling 16 (2012) 790-799.
[9] T. Ramming, C. Appenzeller-Herzog, The physiological functions of mammalian endoplasmic oxidoreductin 1: on disulfides and more, Antioxidants & redox signaling 16 (2012) 1109-1118.
[10] E. Gross, C.S. Sevier, N. Heldman, E. Vitu, M. Bentzur, C.A. Kaiser, C. Thorpe, D. Fass, Generating disulfides enzymatically: reaction products and electron acceptors of the endoplasmic reticulum thiol oxidase Ero1p, Proceedings of the National Academy of Sciences of the United States of America 103 (2006) 299-304.
[11] L. Wang, S.J. Li, A. Sidhu, L. Zhu, Y. Liang, R.B. Freedman, C.C. Wang, Reconstitution of human Ero1-Lalpha/protein-disulfide isomerase oxidative folding pathway in vitro. Position-dependent differences in role between the a and a' domains of protein-disulfide isomerase, The Journal of biological chemistry 284 (2009) 199-206.
[12] D. Eletto, E. Chevet, Y. Argon, C. Appenzeller-Herzog, Redox controls UPR to control redox, Journal of cell science in press (2014).
[13] H.G. Hansen, J.D. Schmidt, C.L. Soltoft, T. Ramming, H.M. Geertz-Hansen, B. Christensen, E.S. Sorensen, A.S. Juncker, C. Appenzeller-Herzog, L. Ellgaard, Hyperactivity of the ero1alpha oxidase elicits endoplasmic reticulum stress but no broad antioxidant response, The Journal of biological chemistry 287 (2012) 39513-39523.
[14] H.G. Hansen, C.L. Soltoft, J.D. Schmidt, J. Birk, C. Appenzeller-Herzog, L. Ellgaard, Biochemical evidence that regulation of Ero1beta activity in human cells does not involve the isoform-specific cysteine 262, Bioscience reports (2014).
[15] T. Ramming, H.G. Hansen, K. Nagata, L. Ellgaard, C. Appenzeller-Herzog, GPx8 peroxidase prevents leakage of HO from the endoplasmic reticulum, Free radical biology & medicine 70C (2014) 106-116.
[16] T.J. Tavender, N.J. Bulleid, Molecular mechanisms regulating oxidative activity of the Ero1 family in the endoplasmic reticulum, Antioxidants & redox signaling 13 (2010) 1177-1187.
[17] C. Appenzeller-Herzog, J. Riemer, B. Christensen, E.S. Sorensen, L. Ellgaard, A novel disulphide switch mechanism in Ero1alpha balances ER oxidation in human cells, The EMBO journal 27 (2008) 2977-2987.
[18] K.M. Baker, S. Chakravarthi, K.P. Langton, A.M. Sheppard, H. Lu, N.J. Bulleid, Low reduction potential of Ero1alpha regulatory disulphides ensures tight control of substrate oxidation, The EMBO journal 27 (2008) 2988-2997.
[19] K. Inaba, S. Masui, H. Iida, S. Vavassori, R. Sitia, M. Suzuki, Crystal structures of human Ero1alpha reveal the mechanisms of regulated and targeted oxidation of PDI, The EMBO journal 29 (2010) 3330-3343.
[20] J. Wright, J. Birk, L. Haataja, M. Liu, T. Ramming, M.A. Weiss, C. Appenzeller-Herzog, P. Arvan, Endoplasmic reticulum oxidoreductin-1alpha (Ero1alpha) improves folding and secretion of mutant proinsulin and limits mutant proinsulin-induced endoplasmic reticulum stress, The Journal of biological chemistry 288 (2013) 31010-31018.
[21] C. Appenzeller-Herzog, J. Riemer, E. Zito, K.T. Chin, D. Ron, M. Spiess, L. Ellgaard, Disulphide production by Ero1alpha-PDI relay is rapid and effectively regulated, The EMBO journal 29 (2010) 3318-3329.
[22] C.S. Sevier, H. Qu, N. Heldman, E. Gross, D. Fass, C.A. Kaiser, Modulation of cellular disulfide-bond formation and the ER redox environment by feedback regulation of Ero1, Cell 129 (2007) 333-344.

[23] G. Bertoli, T. Simmen, T. Anelli, S.N. Molteni, R. Fesce, R. Sitia, Two conserved cysteine triads in human Ero1alpha cooperate for efficient disulfide bond formation in the endoplasmic reticulum, The Journal of biological chemistry 279 (2004) 30047-30052.
[24] K. Araki, K. Nagata, Functional in vitro analysis of the ERO1 protein and protein-disulfide isomerase pathway, The Journal of biological chemistry 286 (2011) 32705-32712.
[25] T. Kakihana, K. Araki, S. Vavassori, S. Iemura, M. Cortini, C. Fagioli, T. Natsume, R. Sitia, K. Nagata, Dynamic regulation of Ero1alpha and peroxiredoxin 4 localization in the secretory pathway, The Journal of biological chemistry 288 (2013) 29586-29594.
[26] M.D. Shoulders, L.M. Ryno, J.C. Genereux, J.J. Moresco, P.G. Tu, C. Wu, J.R. Yates, 3rd, A.I. Su, J.W. Kelly, R.L. Wiseman, Stress-independent activation of XBP1s and/or ATF6 reveals three functionally diverse ER proteostasis environments, Cell reports 3 (2013) 1279-1292.
[27] B. Enyedi, P. Varnai, M. Geiszt, Redox state of the endoplasmic reticulum is controlled by Ero1L-alpha and intraluminal calcium, Antioxidants & redox signaling 13 (2010) 721-729.
[28] V.D. Nguyen, M.J. Saaranen, A.R. Karala, A.K. Lappi, L. Wang, I.B. Raykhel, H.I. Alanen, K.E. Salo, C.C. Wang, L.W. Ruddock, Two endoplasmic reticulum PDI peroxidases increase the efficiency of the use of peroxide during disulfide bond formation, Journal of molecular biology 406 (2011) 503-515.
[29] P. Chaiyen, M.W. Fraaije, A. Mattevi, The enigmatic reaction of flavins with oxygen, Trends in biochemical sciences 37 (2012) 373-380.
[30] R. Baron, C. Riley, P. Chenprakhon, K. Thotsaporn, R.T. Winter, A. Alfieri, F. Forneris, W.J. van Berkel, P. Chaiyen, M.W. Fraaije, A. Mattevi, J.A. McCammon, Multiple pathways guide oxygen diffusion into flavoenzyme active sites, Proceedings of the National Academy of Sciences of the United States of America 106 (2009) 10603-10608.
[31] A. Alon, E.J. Heckler, C. Thorpe, D. Fass, QSOX contains a pseudo-dimer of functional and degenerate sulfhydryl oxidase domains, FEBS letters 584 (2010) 1521-1525.
[32] D. Fass, The Erv family of sulfhydryl oxidases, Biochimica et biophysica acta 1783 (2008) 557-566.
[33] S. Masui, S. Vavassori, C. Fagioli, R. Sitia, K. Inaba, Molecular bases of cyclic and specific disulfide interchange between human ERO1alpha protein and protein-disulfide isomerase (PDI), The Journal of biological chemistry 286 (2011) 16261-16271.
[34] C. Shepherd, O.B. Oka, N.J. Bulleid, Inactivation of Mammalian Ero1alpha is catalysed by Specific Protein Disulfide Isomerases, The Biochemical journal in press (2014).
[35] A.R. Frand, C.A. Kaiser, Two pairs of conserved cysteines are required for the oxidative activity of Ero1p in protein disulfide bond formation in the endoplasmic reticulum, Molecular biology of the cell 11 (2000) 2833-2843.
[36] D.R. Peaper, P.A. Wearsch, P. Cresswell, Tapasin and ERp57 form a stable disulfide-linked dimer within the MHC class I peptide-loading complex, The EMBO journal 24 (2005) 3613-3623.
[37] B.P. Tu, J.S. Weissman, The FAD- and O(2)-dependent reaction cycle of Ero1-mediated oxidative protein folding in the endoplasmic reticulum, Molecular cell 10 (2002) 983-994.
[38] A.D. Garg, P. Agostinis, ER stress, autophagy and immunogenic cell death in photodynamic therapy-induced anti-cancer immune responses, Photochemical & photobiological sciences : Official journal of the European Photochemistry Association and the European Society for Photobiology 13 (2014) 474-487.
[39] K.T. Chin, G. Kang, J. Qu, L.B. Gardner, W.A. Coetzee, E. Zito, G.I. Fishman, D. Ron, The sarcoplasmic reticulum luminal thiol oxidase ERO1 regulates cardiomyocyte excitation-coupled calcium release and response to hemodynamic load, FASEB journal : official publication of the Federation of American Societies for Experimental Biology 25 (2011) 2583-2591.
[40] D. May, A. Itin, O. Gal, H. Kalinski, E. Feinstein, E. Keshet, Ero1-L alpha plays a key role in a HIF-1-mediated pathway to improve disulfide bond formation and VEGF secretion under hypoxia: implication for cancer, Oncogene 24 (2005) 1011-1020.
[41] B. Gess, K.H. Hofbauer, R.H. Wenger, C. Lohaus, H.E. Meyer, A. Kurtz, The cellular oxygen tension regulates expression of the endoplasmic oxidoreductase ERO1-Lalpha, European journal of biochemistry / FEBS 270 (2003) 2228-2235.
[42] G. Kutomi, Y. Tamura, T. Tanaka, T. Kajiwara, K. Kukita, T. Ohmura, H. Shima, T. Takamaru, F. Satomi, Y. Suzuki, T. Torigoe, N. Sato, K. Hirata, Human endoplasmic reticulum oxidoreductin 1-alpha is a novel predictor for poor prognosis of breast cancer, Cancer science 104 (2013) 1091-1096.
[43] T. Ramming, H.G. Hansen, K. Nagata, L. Ellgaard, C. Appenzeller-Herzog, GPx8 peroxidase prevents leakage of H2O2 from the endoplasmic reticulum, Free radical biology & medicine 70 (2014) 106-116.
[44] T.K. Kerppola, Bimolecular fluorescence complementation (BiFC) analysis of protein interactions in live cells, Cold Spring Harbor protocols 2013 (2013) 727-731.

[45] M. Otsu, G. Bertoli, C. Fagioli, E. Guerini-Rocco, S. Nerini-Molteni, E. Ruffato, R. Sitia, Dynamic retention of Ero1alpha and Ero1beta in the endoplasmic reticulum by interactions with PDI and ERp44, Antioxidants & redox signaling 8 (2006) 274-282.
[46] K. Inaba, S. Masui, H. Iida, S. Vavassori, R. Sitia, M. Suzuki, Crystal structures of human Ero1alpha reveal the mechanisms of regulated and targeted oxidation of PDI, EMBO J 29 (2010) 3330-3343.
[47] Y. Sato, R. Kojima, M. Okumura, M. Hagiwara, S. Masui, K. Maegawa, M. Saiki, T. Horibe, M. Suzuki, K. Inaba, Synergistic cooperation of PDI family members in peroxiredoxin 4-driven oxidative protein folding, Scientific reports 3 (2013) 2456.

4. Project III: Elucidation of the PDI interactome

4.1. Introduction

The most conserved disulfide relay responsible for oxidative folding in the ER of mammalian cells is comprised of the disulfide-generating oxidase Ero1α and the disulfide-transferring proteins of the PDI family [1]. Among the total of over 20 PDIs in human cells [2], ample evidence exists suggesting a preferential role of PDI, the archetypal member of this protein family, as electron donor for Ero1α [3,4,5,6,7]. Therefore, PDI is thought to be a central element in the transfer of disulfide bonds from Ero1α onto a broad range of client proteins. However, knowledge on specific *in situ* substrates for PDI-mediated oxidation is limited (see section 1.3). An intermediate step in this dithiol disulfide exchange reaction is the formation of a short-lived mixed disulfide complex between the N-terminal active site cysteine in the oxidoreductase and a cysteine in the folding client. Thus, the potential trapping and isolation of a mixed-disulfide complex between PDI and another protein strongly indicates the participation of the former in the folding pathway of the latter. These complexes can be trapped by quenching the dithiol disulfide exchange reaction either using acids or alkylating agents like NEM or iodoacetamide (IAM).

PDIs serve another function besides this role as disulfide introducing enzymes. They can detect erroneously introduced non-native disulfides, which they are able to reduce or isomerize, if their active site cysteines are in the dithiol state [8,9]. Since these reactions also proceed via the formation of transient mixed disulfide complexes, one way to discriminate between PDIs-mediated oxidation and reduction is the mutation of the C-terminal active site cysteine in the oxidoreductases. A comprehensive analysis employing this method was carried out using V5 epitope-tagged CxxA-trapping mutants of different PDIs, in order to elucidate PDIs-specific substrates for reduction/isomerization [10]. However, whereas for other PDI family members various reduction substrates could be documented, the results for PDI itself in this study were rather disappointing, since only Ero1α and PrxIV, two known disulfide donors, but no client proteins were detected [10]. This result, together with the preferential oxidation of PDI by Ero1α, point into the direction, that PDI predominantly acts as disulfide donor.

Therefore, I employed a different approach in order to elucidate the PDI interactome, which was based on an *in situ* acidification/*in vitro* alkylation protocol recently developed in our lab (appenzeller-herzog et al embo 2010) and proven to quench dithiol-disulfide exchange reactions more efficiently than the previously used *in situ* alkylation (data not shown). In an untargeted-screening effort, mixed-disulfide complexes between PDI and cognate substrates were immunoprecipitated and subsequently subjected to mass spectrometry (MS) analysis.

4.2. Results

In a first set of analytical-scale experiments, I transiently transfected HEK293 cells with a recombinant variant of PDI, which contains a V5 epitope immediately upstream of the C-terminal ER-retrieval signal KDEL (PDI-V5) [10]. Transfected cells were radiolabeled with ^{35}S-methionine and subjected to the *in situ* acidification/*in vitro* alkylation protocol to trap mixed disulfide intermediates. As negative control for subsequent immunoprecipitation (IP) I used mock transfected cells and cells pretreated with the reductant DTT, which breaks existing intermolecular disulfide bonds. As Fig. 19 shows, immunoisolation of PDI-V5 was both efficient and specific, highlighted by the lack of signal in the mock transfected lanes. Whereas reducing SDS-PAGE mainly resulted in the detection of monomeric PDI-V5, four prominent complexes with a molecular weight between 100 and 150 kilo Dalton (kDa) were visible upon resolving the immunoprecipitate under non-reducing conditions. Formation of the lower three complexes was largely abolished upon pretreatment with DTT, whereas the slowest running complex at ~150 kDa partially persisted. The latter is in agreement with previously published data and most likely represents a DTT-resistant mixed disulfide complex of PDI and a glycoprotein of unknown identity, since this complex can be precipitated by concanavalin A (ConA) sepharose, too (Fig 6B in [4]). Having established the isolation of mixed-disulfide complexes using the novel trapping protocol and anti-V5 IP, I continued with the development of a suitable method for release of the PDI-bound interactors.

To specifically elute disulfide-bound PDI interactors, I treated one half of an anti-V5 immunoprecipitate with DTT. Following a short incubation period, I separated the supernatant (elution fraction) and the beads by centrifugation and subjected both together with the non-DTT treated sample to non-reducing SDS-PAGE (Fig. 20). Even though the signal of the previously

appreciated mixed disulfide complexes was lower than in Fig. 19 (probably due to decreased transfection/IP efficiency), the overall pattern was largely reproduced. Additionally, efficient DTT-mediated reductive release of the PDI-bound interactors was observed, and the interaction of covalently coupled V5 antibody with PDI-V5 was mainly unaffected.

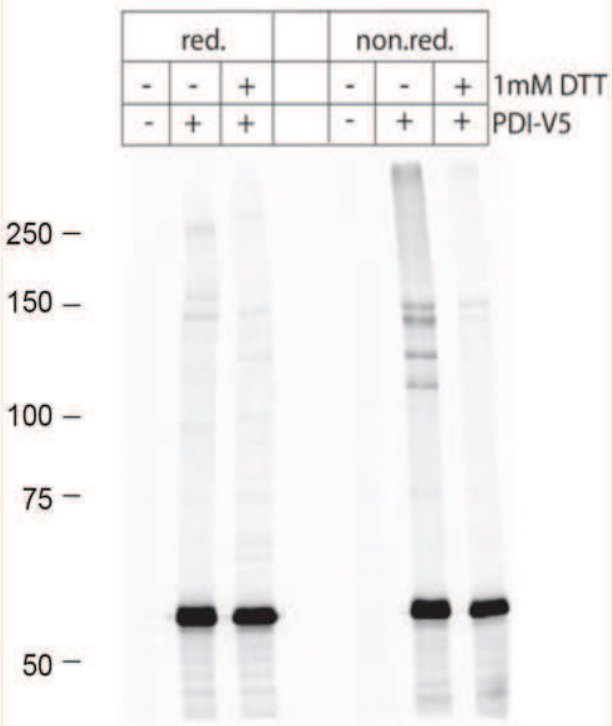

Figure 19: Anti-V5 IP of ^{35}S-radiolabeled cells with or without DTT pretreatment in either mock or PDI-V5 transfected HEK 293 cells.

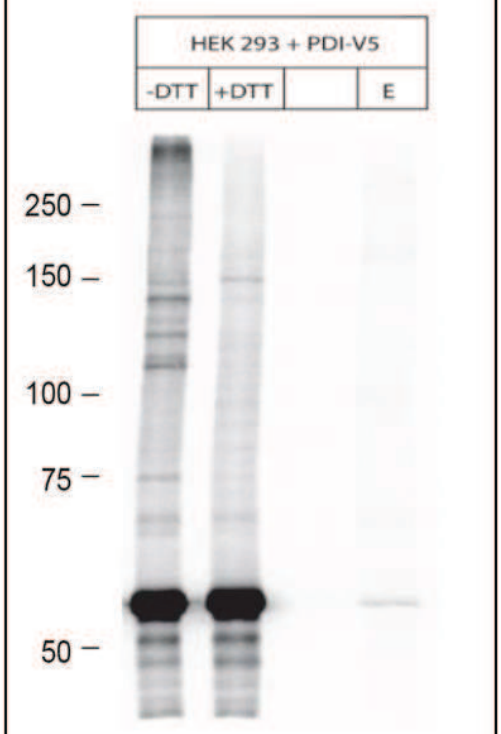

Figure 20: Reductive release of PDI-V5-bound proteins via addition of DTT following anti-V5 IP; E, elution fraction.

Having established this workflow, I omitted the ^{35}S-methionine radiolabeling and increased the scale of the experiment from analytic to preparative quantity. Following acid/NEM-quenched immunoisolation from transiently transfected HEK293 cells, the eluate after reductive release was subjected to proteomic analysis, which was performed in collaboration with the laboratory of Dr. Paul Jenö at the Biozentrum of the University of Basel. PDI interactors were identified by searching against the human SwissProt database using the Mascot search engine. Thereby, I obtained a list of potential candidates, which was filtered with regard to subcellular localization (ER) and the presence of cysteine residues or known intramolecular disulfide bonds. Furthermore

I subclassified the potential interaction partners of PDI-V5 into either "client" (C), i.e. proteins that are processed in the ER, but destined for further transport through the secretory pathway, or ER-resident (R), i.e. proteins that – like PDI – belong to the protein folding machinery or embody an unrelated enzymatic activity of the ER (Table 1).

Protein	Client (C)/Resident (R)
Ero1α	R
PrxIV	R
ERp72	R
ERp57	R
ERp46	R
P5	R
Laminin γ 1	C
Integrin β 1	C
Fibrillin 2	C
Saposin precursor	C
Follistatin-related protein 1	C
Kunitz-type protease inhibitor	C

Table 1: Filtered hits from the LC/MSMS analysis of the elution fraction obtained after anti-V5 IP of acid/NEM-quenched HEK 293 cells transfected with PDI-V5

The known PDI-interacting proteins Ero1α and PrxIV, were the top hits on this list and served as proof-of-principle. Thus, I concluded that the obtained results likely reflected specific interactions with PDI. Furthermore, I could validate the interaction between ERp57, ERp72 and PrxIV by western blot analysis (data not shown), further strengthening the significance of the analysis. Unfortunately, however, my effort to identify the glycoprotein covalently interacting with PDI in a DTT-resistant manner (see above), the protein band of which was excised from a Coomassie-stained non-reducing SDS gel, was not successful.

4.3. Discussion

The outlined untargeted proteomic approach enabled me to shed some light on the hitherto poorly characterized *in situ* interactome of human PDI. Knowledge on specific substrates for PDI-mediated oxidative folding was so far scarce and confined to MHC class I molecules [11] and thyroglobulin [12]. I could potentially expand this list of "clients" by the following proteins:

- Laminin γ1: component of heterotrimeric, cross-shaped and disulfide linked extracellular laminin glycoproteins [13]
- Integrin β1: also called CD29, forms disulfide-linked hetero-dimers with α integrins, involved in cell adhesion/migration and pathogen invasion [14]
- Fibrillin 2: involved in formation and maintenance of extracellular microfibrils [15], mutations are associated with congenital contractural arachnodactyly [16]
- Saposin precursor: proteolytically cleaved in five different sphingolipid activator proteins, involved in (glycol)sphingolipid degradation [17]
- Follistatin-related protein 1: member of the secreted protein acidic rich in cysteines (SPARC) family; involved in various developmental processes [18] and implicated in IL-1β secretion modulation by NLRP3 inflammasome [19]
- Kunitz-type protease inhibitor: transmembrane serine proteinase inhibitor, which impacts (among others) pericellular proteolysis of kallikrein, plasmin, hepatocyte growth factor activator [20]

In order to validate these candidates we have initiated a collaboration with Prof. Ineke Braakman at the University of Utrecht, since her laboratory is expert in monitoring oxidative protein folding using well-established *in vitro* transcription/translation assays. The anticipated results will most certainly provide novel insights regarding the folding kinetics of selected client proteins and further characterize their dependency on PDI-mediated maturation.

The most prominent hits identified in this study were proteins of the PDI family, namely ERp46, ERp57, ERp72 and P5. Therefore, the idea of a PDI-specific subclass of substrates might actually not reflect the *in vivo* situation. Since PDI is the preferential target for Ero1α-mediated oxidation [3,4,5,6,7] a major function, besides direct client oxidation might be the specific delivery of Ero1-derived disulfides to other PDI family members. These PDIs in turn could then engage with

their respective substrates and promoting folding by transferring oxidative equivalents. Accordingly, a unidirectional network of electron transport pathways from diverse folding clients to the different PDIs could eventually converge on the PDI-Ero1α disulfide relay. In this sense, PDI would act as a redox sensor for other oxidoreductases [5] and, if needed, initiate *de novo* disulfide production by reduction of the non-catalytic regulatory disulfide bonds in Ero1. It is important to note that oxidation of PDI family members is not strictly dependent on PDI, since ERp46 and ERp57, albeit to a lesser extent than PDI, can be oxidized by Ero1 directly [5]. Even though the PDI-mediated route is thought to be more efficient, disulfide transfer from PDI to other PDI family members is limited by the respective redox equilibrium constants [5]. Therefore, this mechanism might confer an additional regulatory layer in ER redox homeostasis, which protects against ER hyperoxidation and enables reduction/isomerization reactions executed by PDIs.

In conclusion, the described approach to identify new substrates for PDI-mediated oxidation seems to have been successful, even though validation of the observed client hits from the MS analysis will require further attention. Beyond that, the generated results possibly open an exciting new field of oxidative folding-centered research, which will aim on deciphering the cooperation of different PDI family members in client maturation. Mutual exchange of oxidizing/reducing equivalents likely coupled with complementary actions between PDIs will render future dissection of this multifactorial folding system a challenging task.

4.4. Materials and Methods

4.4.1. Cell culture, Transfection, recombinant DNA

HEK293 cells were cultivated in minimum essential medium eagle (MEM) alpha modification (Sigma), which was supplemented with 10% fetal calf serum (FCS), 100 U/ml penicillin, 100 µg/ml streptomycin at 37°C in 5% CO_2. Transient transfections were carried out for 24 h with Metafectene Pro (Biontex) according to the manufacturer's guidelines. pcDNA3.1/PDI-V5 was a kind gift of Neil Bulleid, University of Glasgow, UK.

4.4.2. Radiolabeling, *in situ* acidification/*in vitro* alkylation, anti-V5 IP

Transfected cells were starved for 15 min in Dulbecco's Modified Eagle's Medium (DMEM) without methionine and cysteine (Sigma). Subsequently, the cells were labeled with 50 µCi/ml ^{35}S-protein labeling mix (Perkin Elmer) for 2 h. Where indicated cells were pretreated with 1 mM dithiothreitol (DTT) prior to *in situ* acidification with 10% trichloroacetic acid (TCA). Precipitated cells were incubated for 15 min on ice, pelleted for 10 min and resuspended by sonication in a buffer containing 58mM Tris ph7, 1,5% SDS, 7,3% glycerol, 0,1% bromocresol purple, 27% dimethyl sulphoxide, 15 mM N-ethylmaleimide (NEM) and 200 µM phenylmethanessulfonylfluoride (PMSF). Following incubation at room temperature (RT) for 1h, 10 sample volumes of cold 30 mM Tris/HCl pH 8.1, 100 mM NaCl, 5 mM EDTA and 1,5% TX-100 were added, incubated on ice for 30 min, centrifuged for 1 h and the supernatant subjected to anti-V5 IP using Anti V5 agarose affinity gel (Sigma). After overnight incubation at 4°C on an end over end shaker, IPs were washed four times with 30 mM Tris/HCl pH 8.1, 100 mM NaCl, 5 mM EDTA, 1,5% TX-100 and 0,2% SDS and once with the same buffer without detergents. Where indicated reductive release of disulfide-bound interactors was carried out using 50 µl of a buffer containing 100 mM Tris/HCl pH 8, 150 mM NaCl and 10 mM DTT. Samples to be subjected to non-reducing SDS-PAGE were solubilized at 95°C for 5 min in a suitable volume of 58 mM Tris/HCl pH 6.8, 5% glycerol, 1,67% SDS, 0,002% bromophenol blue.

4.4.3. SDS-PAGE, gel dyring and phosphoimaging

Following separation of the samples by 7,5% SDS-PAGE, run at 30 milliamperes for ~1 h, gels were fixed with 45% methanol/10% acetic acid for 15 min, washed twice with dH_2O and dried

under vacuum on Whatman paper at ~80°C for 1 h. Dried gels were placed into a phosphoimaging cassette (GE Healthcare) and labeled proteins visualized by scanning on a Typhoon 7000 (GE Healthcare).

4.4.4. Mass spectrometry (MS) analysis

Anti-V5 IPs were obtained as outlined above using three confluent 10 cm cell culture dishes of transiently transfected HEK293 cells. The elution fraction after reductive release of disulfide-based PDI-interactors was transferred into a separate Eppendorf tube (see below), while the beads were subjected to non-reducing SDS-PAGE. The gel was stained with Simply Blue (Life Technologies) followed by de-staining with water. The protein band was excised, reduced with 10 mM DTT for 2 h at 37^{o}C and alkylated with 50 mM iodoacetamide for 15 min at room temperature in the dark. Subsequently, the gel piece was digested with 125 ng trypsin (Sequencing Grade, Promega) for 18 h at 37^{o}C. The resulting peptides in the supernatant were collected and the gel piece was extracted with 0.1% acetic acid/50% acetonitrile. The extract was pooled with the tryptic peptides, dried in a SpeedVac and redissolved in 0.1% acetic acid. 10 µl were used for mass spectrometric analysis. In contrast, 15 µl of the elution fraction was reduced with 10 mM DTT for 1 h at 37°C and alkylated with 50 mM IA for 15 min at RT in the dark. Proteins were treated with 0,25 µg endoproteinase LysC (Wako Chemicals) for 2h at 37°C and further digested with 0,5 µg trypsin overnight. Digestion was stopped with 1% trifluoro acetic acid (TFA) and peptides desalted on a MicroSpin cartridge (The Nest Group) according to manufacturer's recommendations. The peptides were dried in a SpeedVac and dissolved in 50 µl 0,1% acetic acid in water/0,005% TFA. 2 µl were used for mass spectrometric analysis (for details see section 3.5). The obtained MS/MS spectra were searched against the human SwissProt database using the Mascot search engine.

4.5.References

[1] K. Araki, K. Inaba, Structure, mechanism, and evolution of Ero1 family enzymes, Antioxidants & redox signaling 16 (2012) 790-799.
[2] F.R. Laurindo, L.A. Pescatore, C. Fernandes Dde, Protein disulfide isomerase in redox cell signaling and homeostasis, Free radical biology & medicine 52 (2012) 1954-1969.
[3] C. Appenzeller-Herzog, J. Riemer, B. Christensen, E.S. Sorensen, L. Ellgaard, A novel disulphide switch mechanism in Ero1alpha balances ER oxidation in human cells, The EMBO journal 27 (2008) 2977-2987.
[4] C. Appenzeller-Herzog, J. Riemer, E. Zito, K.T. Chin, D. Ron, M. Spiess, L. Ellgaard, Disulphide production by Ero1alpha-PDI relay is rapid and effectively regulated, The EMBO journal 29 (2010) 3318-3329.
[5] K. Araki, S. Iemura, Y. Kamiya, D. Ron, K. Kato, T. Natsume, K. Nagata, Ero1-alpha and PDIs constitute a hierarchical electron transfer network of endoplasmic reticulum oxidoreductases, The Journal of cell biology 202 (2013) 861-874.
[6] K. Inaba, S. Masui, H. Iida, S. Vavassori, R. Sitia, M. Suzuki, Crystal structures of human Ero1alpha reveal the mechanisms of regulated and targeted oxidation of PDI, EMBO J 29 (2010) 3330-3343.
[7] S. Masui, S. Vavassori, C. Fagioli, R. Sitia, K. Inaba, Molecular Bases of Cyclic and Specific Disulfide Interchange between Human ERO1{alpha} Protein and Protein-disulfide Isomerase (PDI), J Biol Chem 286 (2011) 16261-16271.
[8] S. Chakravarthi, C.E. Jessop, N.J. Bulleid, The role of glutathione in disulphide bond formation and endoplasmic-reticulum-generated oxidative stress, EMBO reports 7 (2006) 271-275.
[9] C.E. Jessop, N.J. Bulleid, Glutathione directly reduces an oxidoreductase in the endoplasmic reticulum of mammalian cells, The Journal of biological chemistry 279 (2004) 55341-55347.
[10] C.E. Jessop, R.H. Watkins, J.J. Simmons, M. Tasab, N.J. Bulleid, Protein disulphide isomerase family members show distinct substrate specificity: P5 is targeted to BiP client proteins, J Cell Sci 122 (2009) 4287-4295.
[11] B. Park, S. Lee, E. Kim, K. Cho, S.R. Riddell, S. Cho, K. Ahn, Redox regulation facilitates optimal peptide selection by MHC class I during antigen processing, Cell 127 (2006) 369-382.
[12] B. Di Jeso, Y.N. Park, L. Ulianich, A.S. Treglia, M.L. Urbanas, S. High, P. Arvan, Mixed-disulfide folding intermediates between thyroglobulin and endoplasmic reticulum resident oxidoreductases ERp57 and protein disulfide isomerase, Molecular and cellular biology 25 (2005) 9793-9805.
[13] M. Aumailley, The laminin family, Cell adhesion & migration 7 (2013) 48-55.
[14] S.E. Winograd-Katz, R. Fassler, B. Geiger, K.R. Legate, The integrin adhesome: from genes and proteins to human disease, Nature reviews. Molecular cell biology 15 (2014) 273-288.
[15] H. Zhang, S.D. Apfelroth, W. Hu, E.C. Davis, C. Sanguineti, J. Bonadio, R.P. Mecham, F. Ramirez, Structure and expression of fibrillin-2, a novel microfibrillar component preferentially located in elastic matrices, The Journal of cell biology 124 (1994) 855-863.
[16] M.R. Davis, K.M. Summers, Structure and function of the mammalian fibrillin gene family: implications for human connective tissue diseases, Molecular genetics and metabolism 107 (2012) 635-647.
[17] H. Schulze, K. Sandhoff, Sphingolipids and lysosomal pathologies, Biochimica et biophysica acta 1841 (2014) 799-810.
[18] M. Sylva, A.F. Moorman, M.J. van den Hoff, Follistatin-like 1 in vertebrate development, Birth defects research. Part C, Embryo today : reviews 99 (2013) 61-69.
[19] Y. Chaly, Y. Fu, A. Marinov, B. Hostager, W. Yan, B. Campfield, J.A. Kellum, D. Bushnell, Y. Wang, J. Vockley, R. Hirsch, Follistatin-like protein 1 enhances NLRP3 inflammasome-mediated IL-1beta secretion from monocytes and macrophages, European journal of immunology 44 (2014) 1467-1479.
[20] H. Kataoka, S. Miyata, S. Uchinokura, H. Itoh, Roles of hepatocyte growth factor (HGF) activator and HGF activator inhibitor in the pericellular activation of HGF/scatter factor, Cancer metastasis reviews 22 (2003) 223-236.

5. Project IV: Reducing substrates of GPx7

5.1. Introduction

GPx7 is an ER-resident member of the glutathione peroxidase family. Whereas the peroxidase function of GPx7 has been validated by various groups, glutathione specificity for subsequent reduction, as the family name implies, is largely absent [1,2,3]. In contrast members of the PDI family have been implicated in the process of GPx7 regeneration, which provides a link between ER H_2O_2 detoxification and oxidative folding [2,3]. Along this line, a recent knockout study has further underlined the physiological importance of GPx7, since transgenic mice devoid of GPx7 suffered from multiple organ dysfunctions, malignant neoplasms and shortened lifespan [4]. GPx7 was proposed to play a crucial role as oxidative stress sensor, which catalyzes peroxide-driven disulfide transfer onto the reducing substrate BiP, thereby stimulating the activity of the latter [4]. Similarly, Peng *et al.* could link a decrease of GPx7 expression, as a consequence of promoter hypermethylation, to the neoplastic transformation of premalignant Barrett's oesophagus to oesophageal adenocarcinoma (OAC) [5]. The implicated tumor suppressor activity for GPx7 was validated in both *in vitro* and *in vivo* OAC models by reconstitution of GPx7 expression [6]. Furthermore, GPx7 has also been linked to the processing of small RNAs. In this context, GPx7 expression was found to be induced upon nontargeting siRNA transfection and thiol-disulfide transfer to the nuclear exoribonuclease XRN2, albeit topologically prohibited, was reported [7].

In conclusion, GPx7 seems to be involved in a variety of different (patho)physiological processes, which is likely mediated by the oxidation of specific reducing substrates. Therefore, I sought to trap potential reducing substrates of GPx7 using an unbiased proteomic approach. With the help of the previously described *in situ* acidification/*in vitro* alkylation protocol combined with anti-GPx7 immunoprecipitation (IP) I isolated mixed-disulfide complexes, which will be subjected to mass spectrometry analysis.

5.2. Results

In a first set of analytical-scale experiments, I transiently transfected FlipIn TRex cells inducible for the expression of Ero1α with recombinant variants of GPx7 or GPx8, which contain an influenza hemagglutinin (HA) epitope tag immediately upstream of the C-terminal ER-retrieval signal REDL (GPx7-HA) or KEDL (GPx8-HA), respectively. GPx7-HA-transfected cells were radiolabeled with ^{35}S-methionine and either treated with DTT or not. Following washout of the reductant, cells were subjected to an *in situ* acidification/*in vitro* alkylation protocol to trap mixed disulfide intermediates prior to anti-HA immunoprecipitation. Upon resolving the samples by non-reducing SDS-PAGE, multiple mixed-disulfide complexes could be isolated with GPx7-HA, which disappeared under reducing conditions (Fig. 21). Furthermore, I could observe that DTT washout resulted in more prominent formation of mixed-disulfide complexes compared to control conditions. This at first glance unexpected effect is most likely ascribed to DTT-mediated activation of Ero1 and concomitant H_2O_2 production [8,9]. Thus, GPx7 peroxidase activity was stimulated with this treatment and the abundance of oxidized GPx7 increased, which subsequently resulted in more prominent formation of mixed-disulfide complexes. In contrast, doxycycline-mediated induction of Ero1α expression prior to DTT washout did not increase the abundance of mixed-disulfide complexes (data not shown). Based on these results, subsequent pulldowns were performed without addition of doxycycline but including DTT-mediated activation.

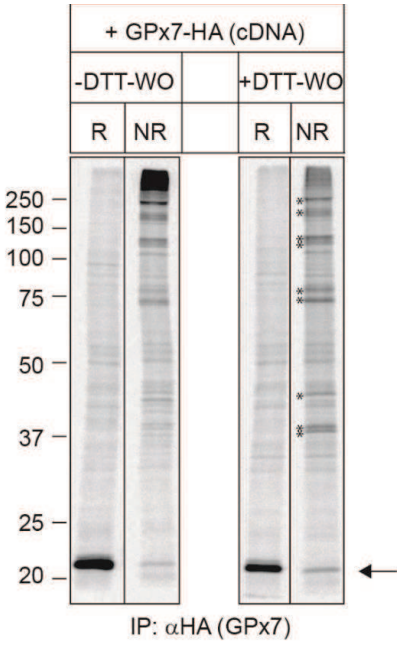

Figure 21: Isolation of mixed-disulfide complexes after DTT washout is more efficient. Anti-HA IP of ^{35}S-radiolabeled cells after either DTT washout or not from GPx7-HA transfected FlipIn TRex cells. Monomeric GPxs-HA are indicated with arrows, mixed-disulfide complexes involving GPx7 with asterisks. R, reducing and NR, non-reducing SDS-PAGE

In order to address the specificity of the trapping and isolation procedure for potential reducing substrates I repeated the pulldown together with GPx8-HA-transfected cells and also included the respective active site cysteine mutants (GPx7-C57S-HA and GPx8-C79S-HA), which lack peroxidase activity. As Fig. 22 shows, the pattern of mixed-disulfide complexes isolated with GPx7-HA was reproduced and dependency on Cys^{57} for all complexes except for one (running between 37 and 50 kDa) was noted. In contrast, GPx8-HA pulldowns displayed only a few weakly detectable, Cys^{79}-dependent complexes, which were not further analyzed.

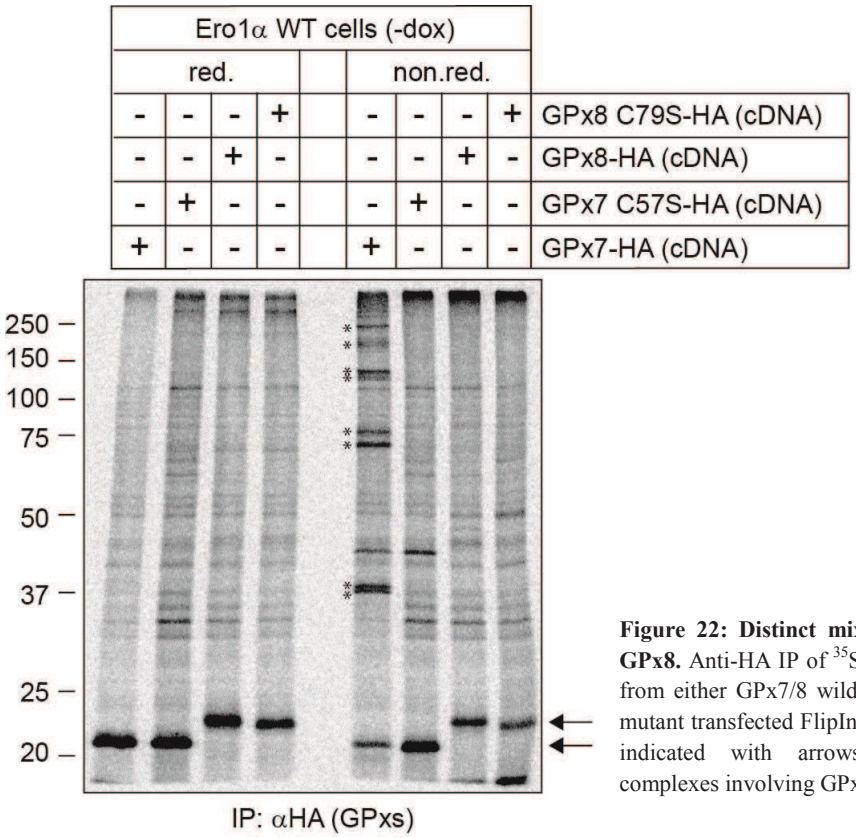

Figure 22: Distinct mixed-disulfide patterns of GPx7 and GPx8. Anti-HA IP of ^{35}S-radiolabeled cells after DTT washout from either GPx7/8 wildtype or respective active site cysteine mutant transfected FlipIn TRex cells. Monomeric GPxs-HA are indicated with arrows, Cys^{57}-dependent mixed-disulfide complexes involving GPx7 with asterisks.

Having established this workflow, I omitted the ^{35}S-methionine radiolabeling and increased the scale of the experiment from analytic to preparative quantity using a FlipIn TRex cell line stably expressing GPx7-HA. To this end, twenty confluent 10 cm tissue culture dishes were subjected to DTT washout, *in situ* acidification/*in vitro* alkylation and subsequent anti-HA IP. The resulting precipitate was resolved by non-reducing SDS-PAGE, the gel stained with Coomassie blue and a total of eleven visible protein bands was excised (Fig. 23). In the near future, mass spectrometry

analysis of these samples will be conducted in collaboration with the laboratory of Dr. Paul Jenö at the Biozentrum of the University of Basel. The anticipated results are expected to contain known interaction partners as proof-of-principle and, in addition, novel potential reducing substrates that will broaden our knowledge of the cellular functions of GPx7.

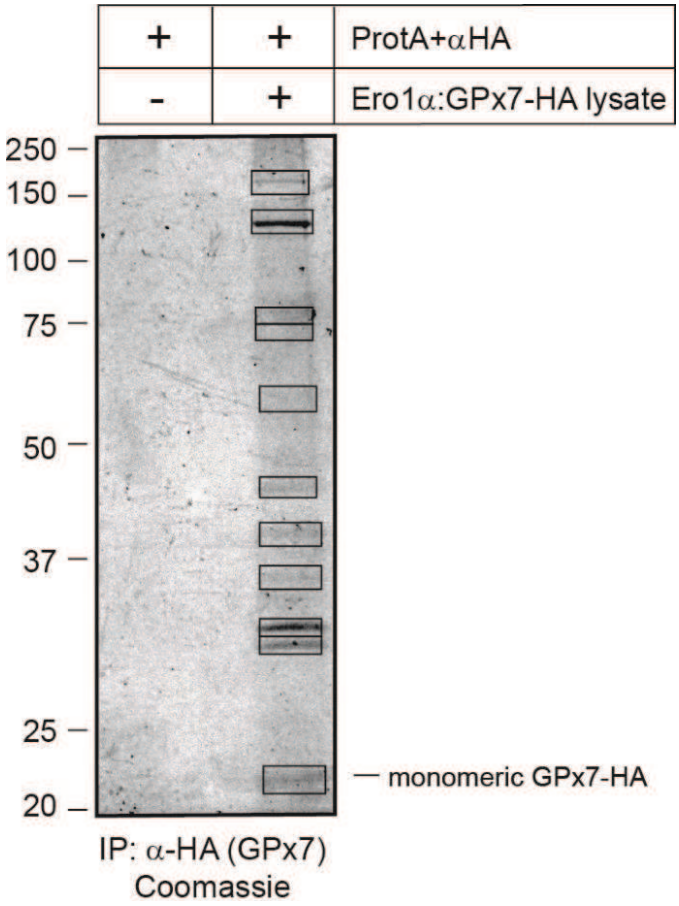

Figure 23: Coomassie-stained gel of an αGPx7-HA IP. Preparative isolation of GPx7-HA bound mixed-disulfide complexes after DTT washout in FlipIn TRex cells stably transfected with GPx7-HA. αHA antibodies covalently coupled to ProtA sepharose were used as negative control. Excised bands, which will be subjected to mass spectrometry analysis, are highlighted with black boxes.

5.3. Materials and Methods

5.3.1. Cell culture, Transfection, recombinant DNA

Cultivation of FlipIn-TRex293 cells inducible for Ero1α expression [10] and the stable GPx7 cell line (Ero1α:GPx7) [11] was previously described. Transient transfections were conducted for 24 h with Metafectene Pro (Biontex) according to the manufacturer's guidelines. The following expression vectors have been published before: pcDNA3/GPx7-HA, pcDNA3/GPx8-HA and pcDNA3/GPx8-C79S-HA [11]. For generation of pcDNA3/GPx7-C57S-HA I used pcDNA3/GPx7 as template for QuikChange mutagenesis (Stratagene) using the following primer (only coding strand sequence): 5'- GGCCAGCGAGTCCGGCTTCACAGACC -3'

5.3.2. Radiolabeling, *in situ* acidification/*in vitro* alkylation, anti-HA IP

Radiolabeling and *in situ* acidification/*in vitro* alkylation was performed as described in section 4.4.2. Anti-HA IP was conducted by chemically crosslinking 12CA5 antibodies (αHA, a kind gift of Hans-Peter Hauri, University of Basel, Switzerland) to protein A sepharose with dimethyl pimelimidate (Sigma).

After overnight incubation at 4°C on an end over end shaker, IPs were washed four times with 30 mM Tris/HCl pH 8.1, 100 mM NaCl, 5 mM EDTA, 1,5% TX-100 and 0,2% SDS and once with the same buffer without detergents. Prior to reducing/non-reducing SDS-PAGE samples were solubilized at 95°C for 5 min in a suitable volume of 58 mM Tris/HCl pH 6.8, 5% glycerol, 1,67% SDS, 0,002% bromophenol blue with or without β-mercaptoethanol, respectively.

5.3.3. SDS-PAGE, staining, gel dyring and phosphoimaging

Following separation of the samples by 11% SDS-PAGE, run at 30 milliamperes for ~1 h, gels were fixed with 45% methanol/10% acetic acid for 15 min, washed twice with dH_2O and dried on Whatman paper under vacuum at ~80°C for 1 h. Dried gels were placed into a phosphoimaging cassette (GE Healthcare) and labeled proteins visualized by scanning on a Typhoon 7000 (GE Healthcare). In the case of sample preparation for MS analysis, non-reducing SDS-PAGE was followed by staining with Simply Blue (Life Technologies), de-staining with water and subsequent excision of protein bands.

5.4. References

[1] V. Bosello-Travain, M. Conrad, G. Cozza, A. Negro, S. Quartesan, M. Rossetto, A. Roveri, S. Toppo, F. Ursini, M. Zaccarin, M. Maiorino, Protein Disulfide Isomerase and Glutathione are alternative substrates in the one Cys catalytic cycle of Glutathione Peroxidase 7, Biochimica et biophysica acta 1830 (2013) 3846-3857.

[2] V.D. Nguyen, M.J. Saaranen, A.R. Karala, A.K. Lappi, L. Wang, I.B. Raykhel, H.I. Alanen, K.E. Salo, C.C. Wang, L.W. Ruddock, Two endoplasmic reticulum PDI peroxidases increase the efficiency of the use of peroxide during disulfide bond formation, Journal of molecular biology 406 (2011) 503-515.

[3] L. Wang, L. Zhang, Y. Niu, R. Sitia, C.C. Wang, Glutathione peroxidase 7 utilizes hydrogen peroxide generated by Ero1alpha to promote oxidative protein folding, Antioxidants & redox signaling doi: 10.1089/ars.2013.5236 (2013).

[4] P.C. Wei, Y.H. Hsieh, M.I. Su, X.J. Jiang, P.H. Hsu, W.T. Lo, J.Y. Weng, Y.M. Jeng, J.M. Wang, P.L. Chen, Y.C. Chang, K.F. Lee, M.D. Tsai, J.Y. Shew, W.H. Lee, Loss of the Oxidative Stress Sensor NPGPx Compromises GRP78 Chaperone Activity and Induces Systemic Disease, Molecular cell 48 (2012) 747-759.

[5] D. Peng, A. Belkhiri, T. Hu, R. Chaturvedi, M. Asim, K.T. Wilson, A. Zaika, W. El-Rifai, Glutathione peroxidase 7 protects against oxidative DNA damage in oesophageal cells, Gut 61 (2012) 1250-1260.

[6] D. Peng, T. Hu, M. Soutto, A. Belkhiri, A. Zaika, W. El-Rifai, Glutathione peroxidase 7 has potential tumour suppressor functions that are silenced by location-specific methylation in oesophageal adenocarcinoma, Gut 63 (2014) 540-551.

[7] P.C. Wei, W.T. Lo, M.I. Su, J.Y. Shew, W.H. Lee, Non-targeting siRNA induces NPGPx expression to cooperate with exoribonuclease XRN2 for releasing the stress, Nucleic acids research 40 (2012) 323-332.

[8] C. Appenzeller-Herzog, J. Riemer, E. Zito, K.T. Chin, D. Ron, M. Spiess, L. Ellgaard, Disulphide production by Ero1alpha-PDI relay is rapid and effectively regulated, The EMBO journal 29 (2010) 3318-3329.

[9] T.J. Tavender, N.J. Bulleid, Peroxiredoxin IV protects cells from oxidative stress by removing H2O2 produced during disulphide formation, Journal of cell science 123 (2010) 2672-2679.

[10] C. Appenzeller-Herzog, J. Riemer, B. Christensen, E.S. Sorensen, L. Ellgaard, A novel disulphide switch mechanism in Ero1alpha balances ER oxidation in human cells, The EMBO journal 27 (2008) 2977-2987.

[11] T. Ramming, H.G. Hansen, K. Nagata, L. Ellgaard, C. Appenzeller-Herzog, GPx8 peroxidase prevents leakage of H2O2 from the endoplasmic reticulum, Free radical biology & medicine 70 (2014) 106-116.

6. Discussion I: The physiological functions of mammalian endoplasmic oxidoreductin 1 (Ero1): on disulfides and more

ANTIOXIDANTS & REDOX SIGNALING
Volume 16, Number 10, 2012

DOI: 10.1089/ars.2011.4475

FORUM REVIEW ARTICLE

The Physiological Functions of Mammalian Endoplasmic Oxidoreductin 1 (Ero1): On Disulfides and More

Thomas Ramming and Christian Appenzeller-Herzog

Abstract

Significance: The oxidative process of disulfide-bond formation is essential for the folding of most secretory and membrane proteins in the endoplasmic reticulum (ER). It is driven by electron relay pathways that transfer two electrons derived from the fusion of two adjacent cysteinyl side chains onto various types of chemical oxidants. The conserved, ER-resident endoplasmic oxidoreductin 1 (Ero1) sulfhydryl oxidases that reduce molecular oxygen to generate an active-site disulfide represent one of these pathways. In mammals, two family members exist, Ero1α and Ero1β. ***Recent Advances:*** The two mammalian Ero1 enzymes differ in transcriptional and post-translational regulation, tissue distribution, and catalytic turnover. A specific protein–protein interaction between either isoform and protein disulfide isomerase (PDI) facilitates the propagation of disulfides from Ero1 *via* PDI to nascent polypeptides, and inbuilt oxidative shutdown mechanisms in Ero1α and Ero1β prevent excessive oxidation of PDI. ***Critical Issues:*** Besides disulfide-bond generation, Ero1α also regulates calcium release from the ER and the secretion of disulfide-linked oligomers through its reversible association with the chaperone ERp44. This review explores the functional repertoire and possible redundancy of mammalian Ero1 enzymes. ***Future Directions:*** Systematic analyses of different knockout mouse models will be the most promising strategy to shed new light on unique and tissue-specific roles of Ero1α and Ero1β. Moreover, in-depth characterization of the known physical interactions of Ero1 with peroxidases and PDI family members will help broaden our functional and mechanistic understanding of Ero1 enzymes. *Antioxid. Redox Signal.* 00, 000–000.

Introduction: Primary Lessons from Yeast

A COMMON CHARACTERISTIC of a vast majority of secretory and membrane proteins is their need to form disulfide bonds. These covalent linkages, generated between two cysteine side chains by dehydrogenation (oxidation), can either be located within a single polypeptide chain (intramolecular disulfide) or connect two proteins to form dimeric/oligomeric complexes (intermolecular disulfide). Disulfide bonds often play a pivotal role in promoting proper folding of native polypeptide chains entering the endoplasmic reticulum (ER) and in stabilizing the structure of folded proteins destined for the secretory system. An elaborate enzymatic machinery that is responsible for oxidative protein folding, that is, the introduction of disulfide bonds into folding substrates, is present in the ER of all eukaryotic organisms. During this process, disulfide bonds move from one pair of cysteines to another (Fig. 1). These thiol-disulfide exchange reactions are orchestrated by a specialized family of disulfide carrier enzymes, the protein disulfide isomerases (PDIs) (5). Importantly though, the ER is also capable of generating disulfide bonds *de novo*. While several pathways that can convert diverse types of oxidants into disulfides exist in parallel (13), this review—along with a review by Araki and Inaba that elaborately works out the structural and evolutionary point of view (8)—will discuss endoplasmic oxidoreductin 1 (Ero1) enzymes, which use molecular oxygen (O_2) as electron acceptor (and are therefore termed "oxidases").

ERO1 has first been described in baker's yeast as an essential gene (20, 44). Its product Ero1p is an ER-resident glycoprotein and a critical determinant for the oxidizing capacity of the yeast cell (20, 44). It possesses two redox-active di-cysteine active sites. The "inner active site" is oxidized by a proximally bound flavin adenine dinucleotide (FAD) cofactor (25, 50), which itself receives oxidizing equivalents by reducing O_2 to hydrogen peroxide (H_2O_2) (26). The resulting disulfide bond is then transferred from the core of the protein to the "outer active site" (47), which is located in a flexible peptide loop (25). *Via* its outer active site—also termed the "shuttle disulfide"—Ero1p can directly and specifically oxidize one of the two active-site cysteine pairs in PDI, the archetypal member of the PDI family (21, 22, 50). This disulfide relay from Ero1p to PDI enables oxidized PDI to subsequently introduce disulfide bonds into folding substrates (Fig. 2) (21, 50).

Division of Molecular and Systems Toxicology, Department of Pharmaceutical Sciences, University of Basel, Basel, Switzerland.

6.1. Abstract

Significance The oxidative process of disulfide-bond formation is essential for the folding of most secretory and membrane proteins in the endoplasmic reticulum (ER). It is driven by electron relay pathways that transfer two electrons derived from the fusion of two adjacent cysteinyl side chains onto various types of chemical oxidants. The conserved, ER-resident endoplasmic oxidoreductin 1 (Ero1) sulfhydryl oxidases that reduce molecular oxygen to generate an active-site disulfide represent one of these pathways. In mammals, two family members exist, Ero1α and Ero1β.

Recent Advances The two mammalian Ero1 enzymes differ in transcriptional and post-translational regulation, tissue distribution, and catalytic turnover. A specific protein-protein interaction between either isoform and protein disulfide isomerase (PDI) facilitates the propagation of disulfides from Ero1 *via* PDI to nascent polypeptides, and inbuilt oxidative shutdown mechanisms in Ero1α and Ero1β prevent excessive oxidation of PDI.

Critical Issues Besides disulfide-bond generation, Ero1α also regulates calcium release from the ER and the secretion of disulfide-linked oligomers through its reversible association with the chaperone ERp44. This review explores the functional repertoire and possible redundancy of mammalian Ero1 enzymes.

Future Directions Systematic analyses of different knockout mouse models will be the most promising strategy to shed new light on unique and tissue-specific roles of Ero1α and Ero1β. Moreover, in-depth characterization of the known physical interactions of Ero1 with peroxidases and PDI family members will help broaden our functional and mechanistic understanding of Ero1 enzymes.

6.2. Introduction: Primary lessons from yeast

A common characteristic of a vast majority of secretory and membrane proteins is their need to form disulfide bonds. These covalent linkages, generated between two cysteine side chains by dehydrogenation (oxidation), can either be located within a single polypeptide chain (intramolecular disulfide) or connect two proteins to form dimeric/oligomeric complexes

(intermolecular disulfide). Disulfide bonds often play a pivotal role in promoting proper folding of native polypeptide chains entering the endoplasmic reticulum (ER) and in stabilizing the structure of folded proteins destined for the secretory system. An elaborate, enzymatic machinery that is responsible for oxidative protein folding, i.e. the introduction of disulfide bonds into folding substrates, is present in the ER of all eukaryotic organisms. During this process, disulfide bonds move from one pair of cysteines to another (Fig. 24). These thiol-disulfide exchange reactions are orchestrated by a specialized family of disulfide carrier enzymes, the protein disulfide isomerases (PDIs) [1]. Importantly though, the ER is also capable of generating disulfide bonds *de novo*. While several pathways that can convert diverse types of oxidants into disulfides exist in parallel [2], this review – along with a review by Araki and Inaba that elaborately works out the structural and evolutionary point of view [3] – will discuss endoplasmic oxidoreductin 1 (Ero1) enzymes, which use molecular oxygen (O_2) as electron acceptor (and are therefore termed "oxidases").

ERO1 has first been described in baker's yeast as an essential gene [4,5]. Its product Ero1p is an ER-resident glycoprotein and a critical determinant for the oxidizing capacity of the yeast cell [4,5]. It possesses two redox-active di-cysteine active sites. The "inner active site" is oxidized by a proximally bound flavin adenine dinucleotide (FAD) cofactor [6,7], which itself receives oxidizing equivalents by reducing O_2 to hydrogen peroxide (H_2O_2) [8]. The resulting disulfide bond is then transferred from the core of the protein to the "outer active site" [9], which is located in a flexible peptide loop [6]. *Via* its outer active site – also termed the "shuttle disulfide" – Ero1p can directly and specifically oxidize one of the two active-site cysteine pairs in PDI, the archetypal member of the PDI family [7,10,11]. This disulfide relay from Ero1p to PDI enables oxidized PDI to subsequently introduce disulfide bonds into folding substrates [7,10] (Fig. 25).

Since the resolution of mismatched substrate disulfides by reduced PDIs is a fundamental component of oxidative protein folding, an unregulated (hyper-)oxidation of PDI by Ero1p would be undesirable. Thus, a redox-sensitive shutdown mechanism represented by non-catalytic, intramolecular disulfide bonds effectively impairs Ero1p activity [12,13]. As the oxidation state of these cysteine pairs is controlled by the ER redox poise, a regulatory feedback loop ensues in which Ero1p is solely active when new disulfides are required [12]. Taken together, many of the conserved features of Ero1 sulfhydryl oxidases including their fold, mechanism of action,

physiological relevance, substrate specificity, and the principle of their tunable activation status have been unraveled in experiments with the yeast enzyme.

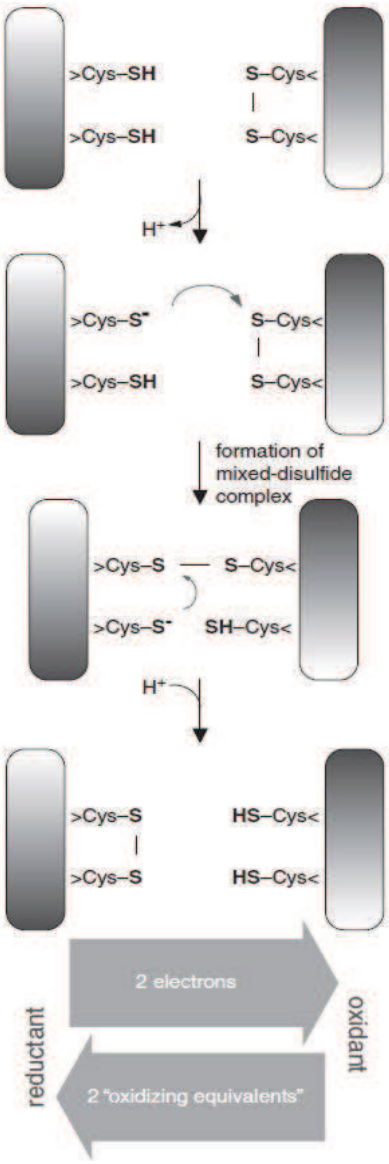

Figure 24: The thiol-disulfide exchange reaction. Cartoon depicting the mechanism of thiol-disulfide exchange between a reduced (SH) and a disulfide-linked (S-S) cysteine pair (e.g. residing on two separate proteins). Upon deprotonation of one of the cysteinyl thiol groups, the resulting thiolate anion nucleophilically attacks one of the disulfide-bound sulphur atoms, leading to the formation of a mixed-disulfide complex. Deprotonation of and nucleophilic attack by the second thiol group then prompts the formerly reduced pair of cysteines to form a disulfide bond. In the course of this redox reaction, two electrons are transferred from the reductant to the oxidant in exchange of two "oxidizing equivalents".

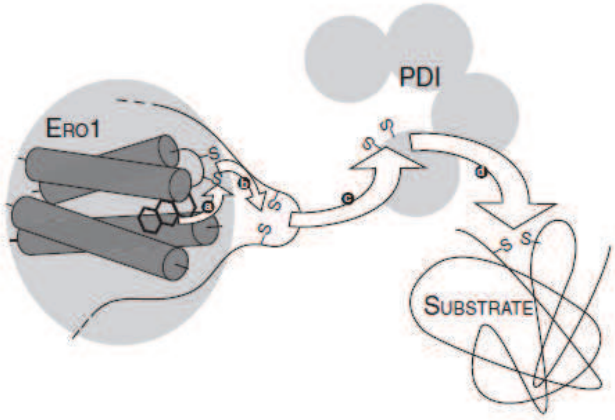

Figure 25: Disulfide relay from Ero1 *via* PDI to substrate proteins. A disulfide bond is generated by the transfer of two oxidizing equivalents from the FAD cofactor (shown as three black rings embedded between the four Ero1 core α-helices, drawn as dark grey cylinders) to the inner-active-site cysteine pair in Ero1 (step a). Following the intramolecular thiol-disulfide exchange reaction (see Fig. 24) between inner and outer active site of Ero1 (step b), the disulfide bond is transferred from the outer active site (located within a flexible loop region in Ero1, depicted by a sinuous black curve) to one of the two di-cysteine active sites in PDI (step c). As a consequence, PDI is capable of introducing disulfide bonds into native polypeptides (dubbed "substrate") through thiol-disulfide exchange (step d). Arrows denote the flow of two oxidizing equivalents; cysteine pairs are depicted only by their sulfur atoms (S); the four thioredoxin-like domains in PDI are represented by grey circles.

6.3. What yeast has failed to teach us

Orthologs of Ero1p exist in all eukaryotes. Mammalian genomes harbor two Ero1-like genes, *ERO1L* and *ERO1LB*, which encode Ero1α and Ero1β, respectively [14,15], and will be the subject of this review. Interestingly, the study of Ero1α and Ero1β has not only unveiled many parallels to the yeast enzyme, but also a number of important differences. Most prominently among these, the mammalian Ero1 genes appear to be non-essential, as evidenced by the viability of mice carrying mutated copies of both *ERO1L* and *ERO1LB* [16]. The mutated genes feature an intronic "gene trapping" insertion containing a strong viral splice acceptor. As a consequence, the vast majority of mRNAs derived from the *ERO1L/ERO1LB* loci will give rise to non-functional, truncated protein.

Lipopolysaccharide-activated spleen cells (LPS blasts) isolated from the mutant mice were nearly indistinguishable from their wild type counterparts with regard to the efficiency of oxidative folding of immunoglobulin M (IgM) [16,17]. With one known exception (the oxidative folding of proinsulin in the β-cells of the pancreas, discussed further below), it is therefore reasonable to assume that the overall pace of disulfide-bond formation is not severely compromised in *ERO1L/ERO1LB* mutant mice and does not phenocopy the fatal situation in Ero1p-deficient yeast cells.

These observations can be explained by alternative mechanisms for *de novo* disulfide-bond generation in the mammalian ER [2] and/or by incomplete gene trapping, which would allow the low-level synthesis of operational Ero1 molecules. Indeed, residual amounts of Ero1β were detected on mRNA level in cardiomyocytes [18] as well as on protein level in pancreatic tissue and LPS blasts from Ero1 double mutant mice [16]. In all cell types studied so far, only a minor portion of Ero1α and, presumably, Ero1β is maintained in an active form [18,19,20] (see also below). Consequently, when shifted to increased activity through redox regulation, the residual levels of Ero1β in *ERO1L/ERO1LB* compound mutant mice might actually suffice to support disulfide-bond formation. Along the same lines, yeast cells can proliferate in the presence of very low amounts of Ero1p. Sufficient levels of Ero1p to allow for growth of an ero1-null strain can be provided by a plasmid encoding *ERO1* under the control of a galactose-inducible promoter even when cells are grown in glucose (where the promoter is largely repressed) (Carolyn S. Sevier, personal communication). It is therefore important to consider that the designation of

ERO1L/ERO1LB mutant mice as "knockout animals" can provoke an underestimation of the functional significance of Ero1 enzymes in mammals. Interestingly, the high proliferation rate of immortalized mouse embryonic fibroblasts is profoundly affected by the *ERO1L/ERO1LB* compound mutation (Ester Zito, David Ron and C. A.-H., unpublished observations), suggesting that under *in vitro* conditions, normal levels of Ero1 enzymes are required for optimal cell growth. On the other hand, flies homozygous for a nonsense allele of their single *ERO1L* gene develop almost normally [21], which strongly suggests the existence of *ERO1L*-independent pathways for disulfide-bond formation.

In addition, while both Ero1p and Ero1α (and, most likely, Ero1β) are soluble ER proteins, which are peripherally membrane-associated [4,14,15], only Ero1p possesses a C-terminal membrane-targeting domain [22]. Further differences between Ero1p and the mammalian Ero1 enzymes include a distinct set of regulatory disulfide bonds for the shutdown of oxidase activity as well as different mechanisms of substrate recognition and oxidation. These issues will be covered in subsequent sections.

6.4. Ero1 enzymes are feedback-regulated sulfhydryl oxidases

Of note, not all of the cysteines within the primary sequence of Ero1 are positionally conserved from yeast to mammals. While the inner and outer active-site cysteines (Cys^{394}-Cys^{397} and Cys^{94}-Cys^{99} in human Ero1α) as well as the long-range disulfide connecting the two active-site peptides (Cys^{85}-Cys^{391} in Ero1α) are preserved, intramolecular disulfide bonds homologous to the regulatory Cys^{143}-Cys^{166} and Cys^{150}-Cys^{295} in Ero1p are absent from both Ero1α and Ero1β (Fig. 26). Amino acid substitution and mass spectrometry analysis revealed that Ero1α in its most oxidized redox state forms a disulfide bond between Cys^{94} and Cys^{131} [19,23]. As Cys^{94} is a constituent of the outer active site, Cys^{94}-Cys^{131} has to be resolved in order to allow disulfide shuttling to PDI. Interestingly, also Cys^{99} very likely forms a "non-active-site" disulfide with Cys^{104} in the shut-off state of Ero1α [23]. Like Cys^{131}, Cys^{104} has no equivalent in Ero1p.

The identification of these new types of regulatory disulfide, which are likely to be present in Ero1β, too [24], has implications for the redox-driven mechanisms of enzyme (in)activation. Thus, in an oxidizing ER environment when reduced substrates for Ero1α are scarce, newly

produced disulfide bonds arising from the inner active site will be "stored" as Cys^{94}-Cys^{131} and Cys^{99}-Cys^{104}. Molecularly, a likely scenario would be the nucleophilic attack of the shuttle disulfide by Cys^{131} (giving rise to Cys^{94}-Cys^{131}) followed by the transfer of a second disulfide from the inner active site *via* the transient formation of Cys^{99}-Cys^{394} (in analogy to Ero1p; [9]), which is then resolved through nucleophilic attack by Cys^{104}. As to the reactivation under reducing conditions, the situation is less straightforward. Two electrons are required to break either of the two regulatory disulfide bonds, before the shuttle disulfide can be reformed through nucleophilic attack. The finding that the concentration of reduced PDI in the ER influences the extent of Cys^{94}-Cys^{131} formation suggests PDI as the reductant [19]. However, PDI has proven to be an ineffective activator of Ero1α in a reconstituted reaction [23,25,26,27]. In keeping with the predominantly inactive state of Ero1α in the ER [18,19,20], this relative resistance of Ero1α towards PDI-mediated reduction could be a critical determinant of ER redox control rather than a manifestation of its poor catalytic proficiency. Indeed, when the thiol load of the ER is maximized by treatment with a strong reducing agent, the Ero1α-dependent re-formation of disulfides is exceptionally fast upon washout of the reductant [28]. These findings are consistent with the concept that Ero1α is an environment-dependent sulfhydryl oxidase, the activity of which is governed by the redox state of its own substrate(s).

In contrast to the aforementioned disulfide bonds, the long-range disulfide, which is conserved in all Ero1 orthologs, does not involve any active-site cysteines (Fig. 26). Two alternative views exist on the role of this disulfide during catalysis. Based on the finding that purified Ero1α C85A-C104A-C131A-C391A – although well-folded – is less active in an oxidase assay than Ero1α C104A-C131A [26], one opinion holds that Cys^{85}-Cys^{391} must be intact for efficient substrate oxidation. The second view, which we tend to favor, suggests a rearrangement of this disulfide during enzyme activation. Thus, an as yet unidentified cysteinyl thiolate anion might attack e.g. Cys^{85} and thereby free Cys^{391} to create a new short-range disulfide in Ero1α that facilitates the communication between inner and outer active site. It can also be speculated that the presumed isomerisation reaction is not readily triggered through intramolecular attack, but instead catalyzed by a thiol-disulfide isomerase such as ERp44 or another PDI that could initially resolve the long-range disulfide (for discussion of mixed-disulfide interactions of Ero1, see below). In potential support of this second view, activated Ero1α [23] and Ero1β [24] virtually co-migrate with the fully reduced forms on non-reducing gels. In addition, presumably catalytic

mixed-disulfide complexes between Ero1α or Ero1β and PDI trapped in living cells following treatment with a reductant display markedly decreased gel mobility – indicative of long-range disulfide resolution – as compared to the complexes trapped at steady state [28]. Intriguingly, the crystal structure of a hyperactive Ero1α C104A-C131A mutant, which still harbors Cys^{85}-Cys^{391}, does not reveal any obvious pathway for O_2 to reach the protein-embedded FAD moiety [29]. We speculate that structural flexibility upon disruption of Cys^{85}-Cys^{391} will be instrumental for the emergence of such an aqueous O_2 channel. A detailed study on the reductive activation of Ero1p has also indicated that a subfraction of the long-range disulfide is resolved prior to the catalysis of substrate oxidation [13].

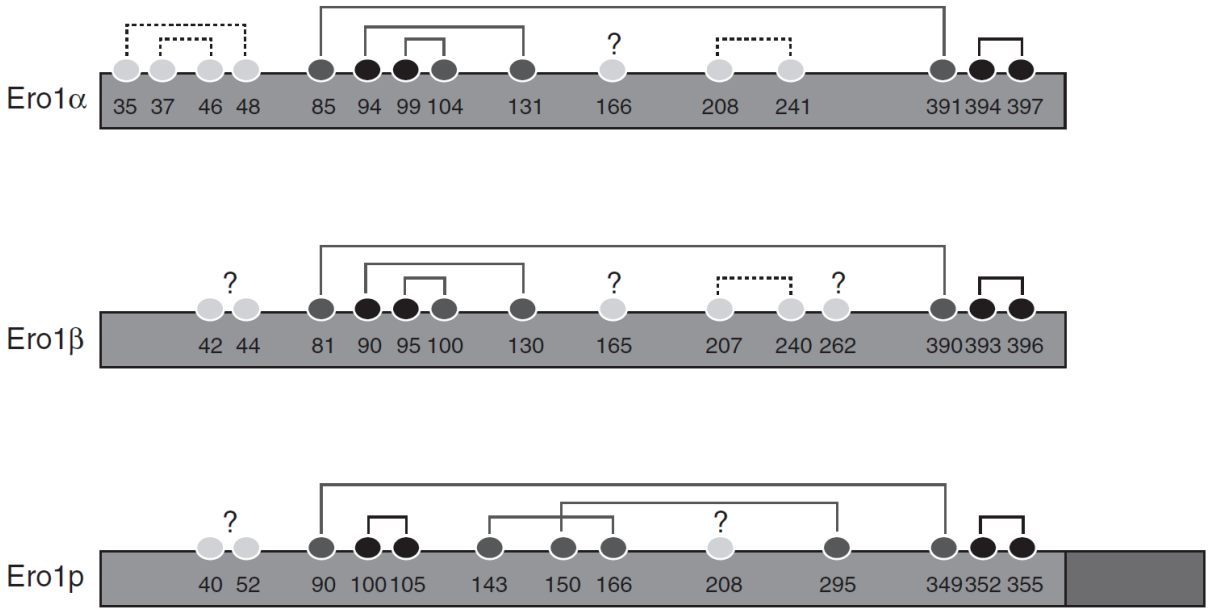

Figure 26: Cysteine connectivity of oxidatively silenced Ero1 enzymes. Ero1α, Ero1β, and Ero1p polypeptides are depicted by grey bars. Numbered dots represent the positions of cysteine residues within the respective Ero1 sequences, and brackets connecting two dots show intramolecular disulfide bonds. Ero1α, Ero1β, and Ero1p possess two di-cysteine active sites (black dots), the C-terminal inner active sites ($Cys^{394+397}$, $Cys^{393+396}$, $Cys^{352+355}$) and the N-terminal outer active sites (Cys^{94+99}, Cys^{90+95}, $Cys^{100+105}$). Regulatory disulfides, which negatively control oxidase activity, are pictured by dark grey brackets. Not all of the regulatory cysteines (dark grey) are positionally conserved between Ero1p and Ero1α/β, and disulfide linkages between regulatory and outer-active-site cysteines only exist in the mammalian enzymes. Note that the functional colouring of the long-ranging disulfide (Cys^{85}-Cys^{391}, Cys^{81}-Cys^{390}, Cys^{90}-Cys^{349}) as well as the cysteine connectivity of Ero1β is speculative at present (see main text for details). Cysteines of structural or unknown function (light grey) are connected with dotted brackets in case of disulfide-bond connection. Question marks denote that no conclusive redox state has been demonstrated, yet. Ero1p possesses an additional C-terminal domain that is responsible for its tethering to the membrane (dark grey box). For more detailed information regarding redox-state-dependent changes in the cysteine connectivity refer to the main text.

6.5. Mechanisms of selection of specific sulfhydryl substrates

Among the total of approximately twenty PDI-like proteins in humans [1], PDI itself has been shown to be the major substrate for Ero1-mediated oxidation. Numerous cues in favor of this view exist including data from both cell culture and *in vitro* assays [19,24,28,29]. Ero1α recognizes PDI by a lock-and-key principle irrespective of whether or not the redox-active cysteines are present in PDI [29,30]. Thus, initial binding prior to the formation of a catalytic mixed disulfide occurs through non-covalent interactions. It has been conclusively demonstrated that these interactions are of hydrophobic nature [29]. They involve a protruding β-hairpin in Ero1α, which contains a critical tryptophan residue at its very tip (Trp^{272}), and a hydrophobic cleft in the substrate-binding domain of PDI [31]. Even though experimental data were exclusively generated with Ero1α, both the hairpin structure and the crucial tryptophan are present in Ero1β as well (Fig. 27). Accordingly, the principle of substrate recognition is probably conserved among the mammalian isoforms. In addition, as hinted by *in silico* complex modeling [31], this mode of interaction presumably facilitates the specific thiol-disulfide exchange between the C-terminal active-site domain of PDI and the shuttle disulfide in Ero1α [23,25,26,27,28]. In contrast, Ero1p harbors no tryptophan-containing β-hairpin [6] and preferentially oxidizes the N-terminal active-site domain of yeast PDI [32].

As opposed to the *bona fide* substrate PDI, its homolog ERp44 can efficiently bind to Ero1α even in the absence of the β-hairpin [31]. Furthermore, equal amounts of ERp44–Ero1α mixed disulfides are detected with all single-cysteine mutants of Ero1α [33], indicating that ERp44 can attack at least one disulfide other than the shuttle disulfide with its active-site cysteine. Besides these, also other PDI-family members – although inferior substrates for oxidation [24,29] – form mixed disulfides with Ero1α and Ero1β within cells under steady-state conditions [28,34,35]. As pointed out for PDI [28], these complexes most likely involve an oxidized (non-catalytic) form of Ero1α. In addition, they are not strictly dependent on the presence of an intact shuttle disulfide [28,33] so that they might be formed in analogy to the ERp44–Ero1α interaction. The physiological roles of these covalent complexes are currently unclear.

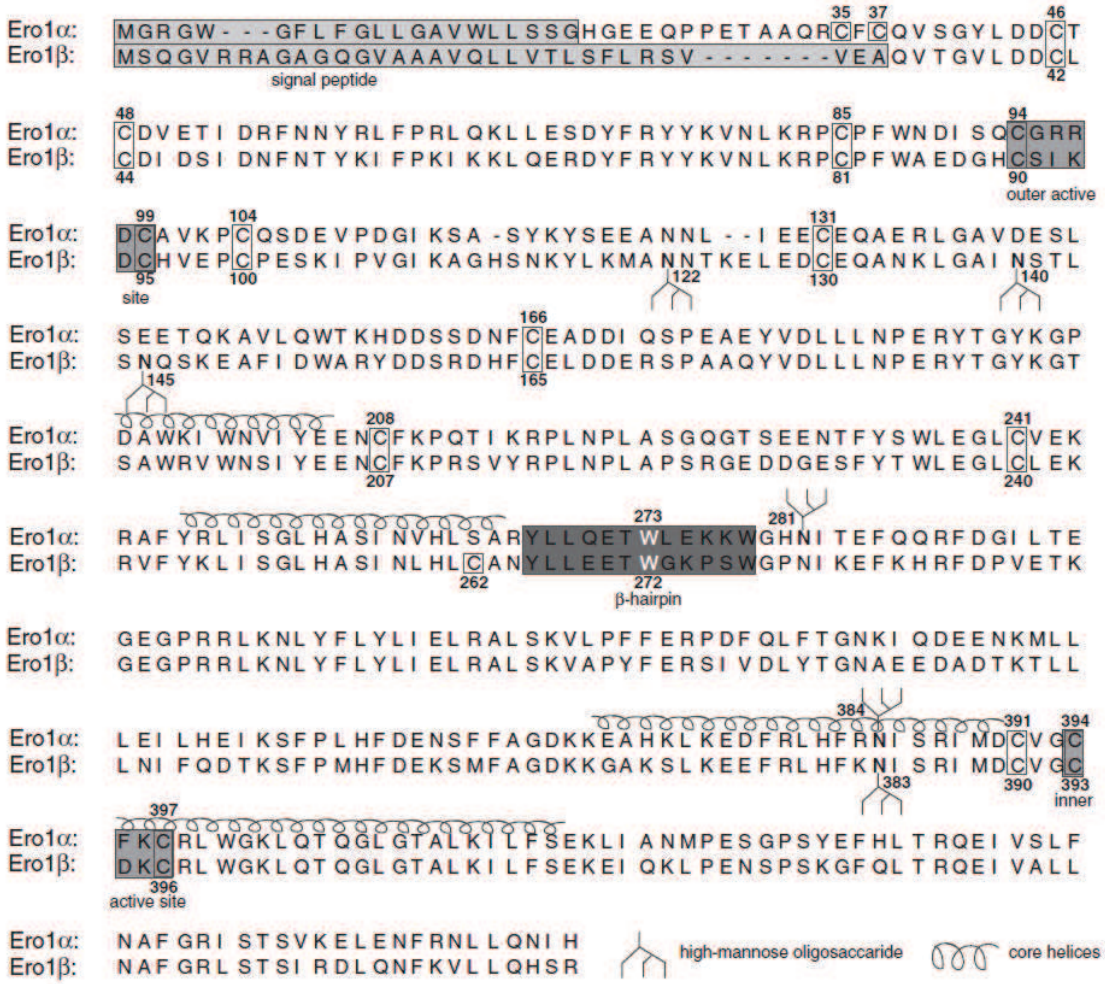

Figure 27: Annotated sequence alignment of human Ero1α and Ero1β. The aligned amino acid sequences are shown in single letter code. Both proteins possess an N-terminal ER-targeting signal peptide (light grey boxes; predicted by the SignalP 3.0 program available at http://www.cbs.dtu.dk/services/SignalP), an inner and outer di-cysteine active site (grey boxes), four core α–helices (marked by coiled hairlines above the sequence) as well as a tryptophan (white)-containing β-hairpin (dark grey box) that is crucial for the interaction with PDI. Cysteine residues are highlighted by black-framed boxes, and asparagine residues within N-glycosylation consensus sites by bold letters and the attachment of a schematised high-mannose oligosaccharide. Numbers next to cysteines, N-glycosylation sites, and the PDI-binding tryptophan show the respective position in the amino acid sequence.

6.6. Ero1α and Ero1β: Functional substitutes or brothers in arms?

While the above sections have highlighted many shared catalytic characteristics between Ero1α and Ero1β, the two homologs have also diverged in a number of features. For instance, the transcriptional regulation of *ERO1L* and *ERO1LB* is different, which undoubtedly contributes to the distinct expression profiles in human tissues [14] (Fig. 28). The high Ero1β levels in insulin-producing β-cells of the pancreas are maintained by the key pancreatic transcription factor PDX1

[36]. The importance of Ero1β in these cells is highlighted by the finding that the oxidative maturation of proinsulin is delayed in pancreatic islets from *ERO1LB* mutant mice, which manifests in a diabetic phenotype [16]. Intriguingly, this phenotype is neither complemented by a compensatory increase in Ero1α levels nor exacerbated by additional mutation of *ERO1L*, which argues against redundancy of Ero1 isoforms in the endocrine pancreas of mice [16]. *ERO1LB* is also a target of the ER-stress-responsive transcription factor ATF6α [37] that is preferentially activated under reducing ER conditions [38].

ERO1L, on the other hand, is a transcriptional target of HIF1α that is upregulated in response to hypoxia or hypoglycemia [39,40]. Indeed, Ero1α is instrumental in counteracting ER hypo-oxidation brought about by hypoxic treatment of cells [18]. In addition, the expression of *ERO1L* is enhanced during adipogenesis, which depends on the nuclear hormone receptor peroxisome proliferator-activated receptor gamma (PPARγ) [41]. Finally, Ero1α is induced during a late stage of ER stress signaling through the binding of C/EBP homologous protein (CHOP; also known as Gadd153) to its promoter [42] (see below).

Ectopic expression of Ero1β – in contrast to Ero1α that has no discernible effect – moderately increases the oxidation of ER oxidoreductases and glutathione [19]. This is likely owing to the relative lability of the regulatory disulfide bonds in Ero1β, since mutation of Cys^{100} and Cys^{130} in Ero1β does not activate the purified enzyme to the same extent as the equivalent mutations in Ero1α [24]. Furthermore, wild-type Ero1β shows higher rates of oxygen consumption during *in vitro* substrate oxidation compared to Ero1α [24]. At the same time, however, the initial slope of glutathione re-oxidation after complete chemical reduction is less pronounced in Ero1β- than in Ero1α-over-expressing cells [28]. Thus, the catalytic turnover rates of Ero1α and Ero1β differ in a context-dependent manner.

Can these disparities be explained at the molecular level? The two intercalating amino acids between the inner active-site cysteines in Ero1α and Ero1β are different (Fig. 27). When mutated to the Ero1β active-site sequence, the catalytic turnover number of Ero1α increases [24]. Moreover, Ero1β harbors an additional cysteine at position 262 (Fig. 27), which has been proposed to form a unique type of regulatory disulfide together with Cys^{100} [24]. However, as predictable by homology to Ero1α, Cys^{262} is located at the end of one of the four core α-helices

and immediately upstream of the PDI-interacting β-hairpin loop (Fig. 27). We therefore consider it unlikely that this region adopts a fundamentally different conformation in Ero1β. In a structural homology model, the side chain of Cys^{262} is located ~30 Å away from Cys^{100} and buried in the structure (data not shown). Finally, Ero1β harbors three unique N-glycosylation sites in the peptide surrounding Cys^{130} (Fig. 27). In the model, the glycosylated asparagines are solvent exposed and positioned between the PDI-binding site and the shuttle disulfide (data not shown), raising the possibility that substrate recruitment might be modulated by the presence of bulky oligosaccharides. Overall, Ero1β – basally expressed at low levels (Fig. 28). and an early target of the ER stress response [37] – represents an effective stress oxidase that can counteract ER hypo-oxidation. Ero1α, on the other hand, likely fulfills a tightly regulated housekeeping function with regard to disulfide generation. Whether and to what extent the two isoforms functionally and/or physically interact in tissues where they are co-expressed remains to be examined.

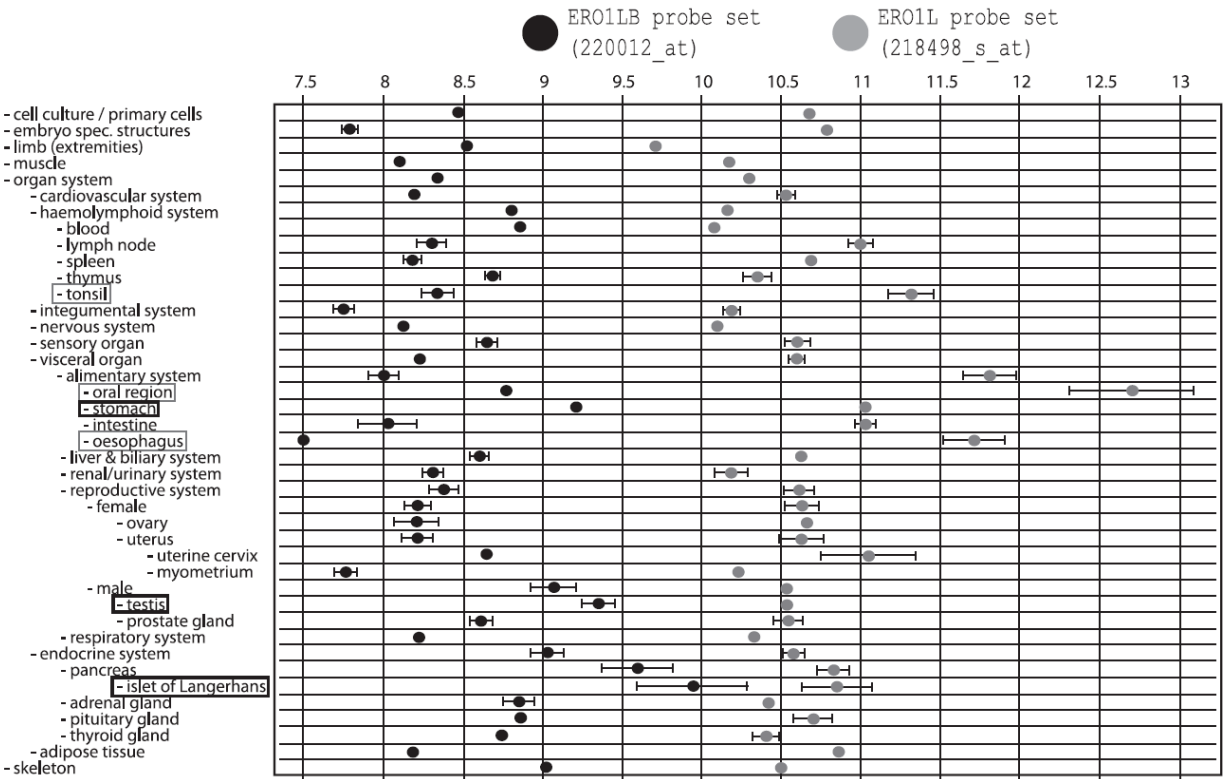

Figure 28: Tissue-specific mRNA levels of human *ERO1L* and *ERO1LB*. Expression levels of *ERO1L* and *ERO1LB* mRNAs (encoding Ero1α and Ero1β, respectively) in a range of human tissues shown as signal intensity on Affymetrix Human Genome U133A array (probe sets: 218498_s_at for *ERO1L* and 220012_at for *ERO1LB*). The figure was generated with all available datasets using the Genevestigator software (https://www.genevestigator.com/gv). The signal intensity on the abscissa is expressed on an arbitrary, logarithmic scale. The abundance of *ERO1L* mRNA is overall higher than that of *ERO1LB*. *ERO1LB* expression peaks in stomach, testis, and the pancreatic islets of Langerhans (highlighted with dark grey boxes). In contrast, elevated levels of *ERO1L* mRNA can be detected especially in tonsils, oral region, and oesophagus (highlighted with light grey boxes).

6.7. Ero1α is critical for ER-stress induced apoptosis

Besides the regulated production of disulfides, Ero1α has additional roles. A major fraction of Ero1α molecules localizes to so-called mitochondria-associated membranes (MAMs), a subdomain of the ER that is tethered to mitochondria [43,44]. When activated by exogenous reductants or under hypoxic conditions, Ero1α relocates to the bulk of the ER [43], suggesting that its function at the MAM might be independent of its activity as an oxidase. The excitable calcium channels of the inositol 1,4,5-trisphosphate receptor (IP_3R) family are also enriched in MAMs, and IP_3R-facilitated calcium shuttling to cytosol and mitochondria is a critical branch of apoptotic cell death signaling during severe ER stress [45]. One of the switches that positively regulate such calcium flow is Ero1α [46], which is induced by the ER stress-dependent, apoptogenic transcription factor CHOP [42]. Since the channeling activity of IP_3R subtype 1 is impeded by reversible binding of ERp44 [47], elevated levels of Ero1α – a preferred ligand of ERp44 [31,48] – likely activate IP_3R1 during ER stress by sequestering ERp44 (in analogy to the mechanism described in the next section). Conversely and similar to the knockdown of IP_3R1, silencing of Ero1α in macrophages inhibits ER-stress-induced apoptosis by lowering ER calcium release [46]. Recently, knockdown of Ero1α in HeLa cells has been demonstrated to predominantly hamper the accumulation of calcium in mitochondria upon stimulation of IP3Rs (and only marginally in the cytosol), which is in agreement with the enrichment of Ero1α in MAMs [44].

An alternative, although less plausible possibility is that Ero1α does not enhance IP_3R1 activity by lowering the availability of ERp44 but by hyper-oxidizing the ER. The association with ERp44 depends on two reduced cysteinyl thiols in IP_3R1 [47], the oxidation of which upon ER stress could consequently lead to channel derepression. In potential support of this, antioxidant treatment mimicked the inhibitory effect of Ero1α knockdown on ER calcium release [46]. However, as the CHOP–Ero1α–IP_3R1 signaling pathway induces NADPH oxidase 2-derived reactive oxygen species (ROS), which in turn further amplify CHOP [49], the application of antioxidants did not necessarily exert its effect by counteracting Ero1α activity. Moreover, given the tight regulatory mechanisms that prevent excessive disulfide and H_2O_2 synthesis by Ero1α (see above), its increased expression does not *per se* hyper-oxidize the ER [19,28]. The probably

minor contribution of Ero1-derived ROS to ER-stress-induced cell death has recently been evaluated in detail elsewhere [50].

6.8. Role of Ero1α in ERp44-mediated ER retention/retrieval

Apart from their involvement in calcium signaling, Ero1α and ERp44 orchestrate the secretion of diverse disulfide-linked dimers and higher order oligomers by the reversible formation of mixed-disulfide ERp44–protein adducts (Fig. 29). ERp44 binds to substrates *via* its non-classical CXXS active-site motif [48], which lacks a resolving cysteine and therefore renders these intermolecular disulfide adducts longer-lived than typical catalytic complexes. Moreover, despite its C-terminal ER retrieval signal ERp44 is atypically enriched in the ER-Golgi intermediate compartment (ERGIC)/cis-Golgi [51,52], which favors a model in which ERp44 retrieves substrates from ERGIC/cis-Golgi to ER.

What is the role of Ero1α in the intracellular retention of secretory proteins? Increased expression of Ero1α displaces ERp44 from most of its endogenous substrates [48], indicating it to be a preferred mixed-disulfide ligand of ERp44. Accordingly, the secretion of ERp44 retention substrates such as IgM [48], the adipose-derived hormone adiponectin [51], or sulfatase modifying factor 1 (SUMF1; also known as formylglycine-generating enzyme) [52,53] is enhanced upon over-expression of Ero1α (Fig. 29). In the case of adipocytes, endogenous induction of Ero1α by PPARγ agonists is physiologically relevant during differentiation and stimulation [41,51]. Although speculative, vascular endothelial growth factor (VEGF) might also add to the list of ERp44 substrates, as its secretion, which is prominent in hypoxic tumors, is positively regulated by Ero1α [39] (Fig. 29).

All secretory ERp44 substrates identified so far (and VEGF) undergo cysteine-dependent dimerization/oligomerization in order to be secreted. The cysteines engaged in this process have – in case of retention – previously been linked to ERp44 (Fig. 29), which is consistent with the concept that ERp44 traps incompletely assembled subunits. Although this concept is commonly referred to as “thiol-mediated retention”, it is still unclear how these trapping interactions are formed. As ERp44 comprises a single-cysteine active site, the oxidizing equivalents to join two thiol groups would either have to be contributed by the binding partner (e.g. through an

intramolecular disulfide or glutathionylation) or by ERp44 itself. The latter possibility could involve a disulfide-linked homodimer or a heterodimer composed of Ero1α and ERp44. However, as detailed above, abundant Ero1α–ERp44 complexes rather inhibit than promote ”thiol-mediated retention”.

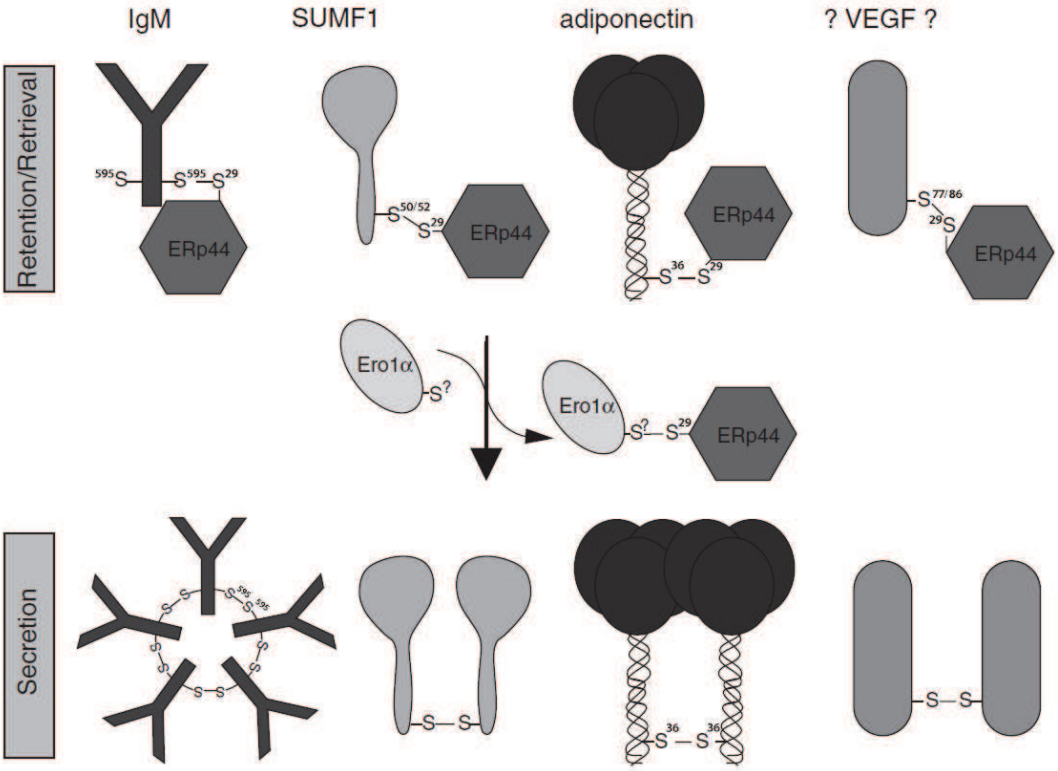

Figure 29: Interplay between Ero1α and ERp44 governs the secretion of various disulfide-linked dimers/oligomers. ERp44 mediates ER retention or retrieval from ERGIC/cis-Golgi of various immature monomers destined for dimerization/oligomerization and secretion. In this process, substrate binding by ERp44 is stabilized by formation of an interchain disulfide bond involving Cys^{29} in ERp44. Upon exogenous overexpression or endogenous induction, Ero1α can – most likely by a competitive mechanism – displace these substrates from ERp44, thus promoting their maturation into disulfide-linked protein complexes and subsequent secretion. In addition to the known ERp44 substrates immunoglobulin M (IgM), sulfatase modifying factor 1 (SUMF1), and adiponectin, vascular endothelial growth factor (VEGF) displays similar properties, rendering it a potential ERp44 substrate (as indicated by the question marks). While the cysteine residues responsible for ERp44-association and oligomerization have been identified in the substrate proteins, it is still unclear, whether a specific cysteine in Ero1α is involved or Ero1α acts as a multivalent mixed-disulfide partner of ERp44 (question mark). The graphical depiction of the structure of the mature IgM pentamer (that contains two heavy and two light chains per monomer) is simplified, and the existence of alternative oligomers (involving a J-chain) is neglected. The N-terminal domains of the adiponectin trimer form a collagen-like triple helix that can dimerize (or multimerize, not show) through Cys^{36}-mediated interchain disulfide-bond formation. Regarding SUMF1, it is important to point out that the drawn mechanism of Ero1α-induced secretion only applies to over-expressed protein (endogenous SUMF1 is an ER-resident enzyme). Cysteine residues are represented only by their sulfur atoms, S; numbers, where indicated, show the position of the cysteine in the human amino acid sequence.

6.9. Conclusions and perspectives

Ero1 enzymes are an integral part in our understanding of redox maintenance in the ER. The two mammalian isoforms, which differ from the yeast enzyme in a number of aspects, fulfill similar roles in regulated disulfide production, but also display distinctive features. While recent work has begun to link these features to isoform-specific *in vivo* functions, there is certainly more room for discovery regarding the physiological roles of Ero1α and Ero1β. An eminent question for the future is how redundant these roles are in mammals. Given the viability of *ERO1L/ERO1LB* gene trap mice that still harbor detectable levels of the stress oxidase Ero1β [16], it is possible that Ero1β can largely substitute for Ero1α deficiency. Motivated by the finding that cardiomyocytes show decreased excitability due to lowered calcium transients in *ERO1L* mutant mice [18], however, it will be important to look more closely at e.g. ER-stress-induced apoptosis or the secretion of ERp44 substrates in these mice. Moreover, the question whether *ERO1L/ERO1LB* knockout mice are also viable remains to be answered.

Since the reduction of O_2 by Ero1 oxidases produces cytotoxic H_2O_2 in the ER, the function of ER-resident H_2O_2-degrading peroxidases and their crosstalk with the PDI family are likely to be fundamental [2,50]. For instance, the activity of peroxiredoxin IV can produce disulfides and channel them into oxidative folding [17]. As for Ero1-derived H_2O_2, it will be most interesting to carry out loss-of-function analyses with two other PDI peroxidases, GPx7 and GPx8, which physically interact with Ero1α [54].

Many additional features of mammalian Ero1 enzymes still require further investigation. The functional significance of covalent Ero1 dimerization [55] that apparently involves Cys^{166} in Ero1α [29] is completely obscure. Likewise, the molecular basis of membrane association of Ero1α is not known, and it remains to be clarified whether its ER retention/MAM localization is mostly mediated by interaction with the ER membrane [14,15] or with ERp44 and other PDI family members [30]. In addition, the conservation among metazoans of the N-terminal segment including two disulfides in Ero1α (but not Ero1β, Fig. 26) suggests some as yet enigmatic function for this stretch of amino acids. It will also be instrumental to molecularly describe the mode(s) of interaction between Ero1α and ERp44 including the cysteine connectivities and subcellular localization of the complex (ER, ERGIC, or MAM) and compare it to the complex involving PDI [31]. Since the catalytic Ero1α–PDI interaction plays a critical role during the

PDI-assisted translocation of the cholera toxin A1 subunit from the ER to the cytosol [56], it also remains to be explored, if endogenous ER-associated degradation substrates require this interplay. Furthermore, the mechanism of redox-driven activation of Ero1α/β remains to be elucidated, which – in conjunction with the aforementioned – will set the stage for more exciting Ero1 news in the future.

Acknowledgements

We thank Lars Ellgaard for comments on the manuscript. Work in the authors' laboratory is funded by the Swiss National Science Foundation, the University of Basel, and the August Collin-Fonds. T.R. is a recipient of a PhD fellowship by the Boehringer Ingelheim Fonds.

6.10.References

[1] C. Appenzeller-Herzog, L. Ellgaard, The human PDI family: versatility packed into a single fold, Biochim Biophys Acta 1783 (2008) 535-548.
[2] N.J. Bulleid, L. Ellgaard, Multiple ways to make disulfides, Trends Biochem Sci 36 (2011) 485-492.
[3] K. Araki, K. Inaba, Structure, mechanism and evolution of Ero1 family enzymes, Antioxid Redox Signal in press (2012).
[4] A.R. Frand, C.A. Kaiser, The ERO1 gene of yeast is required for oxidation of protein dithiols in the endoplasmic reticulum, Mol Cell 1 (1998) 161-170.
[5] M.G. Pollard, K.J. Travers, J.S. Weissman, Ero1p: a novel and ubiquitous protein with an essential role in oxidative protein folding in the endoplasmic reticulum, Mol Cell 1 (1998) 171-182.
[6] E. Gross, D.B. Kastner, C.A. Kaiser, D. Fass, Structure of Ero1p, source of disulfide bonds for oxidative protein folding in the cell, Cell 117 (2004) 601-610.
[7] B.P. Tu, S.C. Ho-Schleyer, K.J. Travers, J.S. Weissman, Biochemical basis of oxidative protein folding in the endoplasmic reticulum, Science 290 (2000) 1571-1574.
[8] E. Gross, C.S. Sevier, N. Heldman, E. Vitu, M. Bentzur, C.A. Kaiser, C. Thorpe, D. Fass, Generating disulfides enzymatically: reaction products and electron acceptors of the endoplasmic reticulum thiol oxidase Ero1p, Proc Natl Acad Sci U S A 103 (2006) 299-304.
[9] C.S. Sevier, C.A. Kaiser, Disulfide transfer between two conserved cysteine pairs imparts selectivity to protein oxidation by Ero1, Mol Biol Cell 17 (2006) 2256-2266.
[10] A.R. Frand, C.A. Kaiser, Ero1p oxidizes protein disulfide isomerase in a pathway for disulfide bond formation in the endoplasmic reticulum, Mol Cell 4 (1999) 469-477.
[11] A.R. Frand, C.A. Kaiser, Two pairs of conserved cysteines are required for the oxidative activity of Ero1p in protein disulfide bond formation in the endoplasmic reticulum, Mol Biol Cell 11 (2000) 2833-2843.
[12] C.S. Sevier, H. Qu, N. Heldman, E. Gross, D. Fass, C.A. Kaiser, Modulation of cellular disulfide-bond formation and the ER redox environment by feedback regulation of Ero1, Cell 129 (2007) 333-344.
[13] N. Heldman, O. Vonshak, C.S. Sevier, E. Vitu, T. Mehlman, D. Fass, Steps in reductive activation of the disulfide-generating enzyme Ero1p, Protein Sci 19 (2010) 1863-1876.
[14] M. Pagani, M. Fabbri, C. Benedetti, A. Fassio, S. Pilati, N.J. Bulleid, A. Cabibbo, R. Sitia, Endoplasmic reticulum oxidoreductin 1-lbeta (ERO1-Lbeta), a human gene induced in the course of the unfolded protein response, J Biol Chem 275 (2000) 23685-23692.
[15] A. Cabibbo, M. Pagani, M. Fabbri, M. Rocchi, M.R. Farmery, N.J. Bulleid, R. Sitia, ERO1-L, a human protein that favors disulfide bond formation in the endoplasmic reticulum, J Biol Chem 275 (2000) 4827-4833.
[16] E. Zito, K.T. Chin, J. Blais, H.P. Harding, D. Ron, ERO1-beta, a pancreas-specific disulfide oxidase, promotes insulin biogenesis and glucose homeostasis, J Cell Biol 188 (2010) 821-832.
[17] E. Zito, E.P. Melo, Y. Yang, A. Wahlander, T.A. Neubert, D. Ron, Oxidative protein folding by an endoplasmic reticulum-localized peroxiredoxin, Mol Cell 40 (2010) 787-797.
[18] K.T. Chin, G. Kang, J. Qu, L.B. Gardner, W.A. Coetzee, E. Zito, G.I. Fishman, D. Ron, The sarcoplasmic reticulum luminal thiol oxidase ERO1 regulates cardiomyocyte excitation-coupled calcium release and response to hemodynamic load, FASEB J 25 (2011) 2583-2591.
[19] C. Appenzeller-Herzog, J. Riemer, B. Christensen, E.S. Sorensen, L. Ellgaard, A novel disulphide switch mechanism in Ero1alpha balances ER oxidation in human cells, EMBO J 27 (2008) 2977-2987.
[20] A.M. Benham, A. Cabibbo, A. Fassio, N. Bulleid, R. Sitia, I. Braakman, The CXXCXXC motif determines the folding, structure and stability of human Ero1-Lalpha, EMBO J 19 (2000) 4493-4502.
[21] A.C. Tien, A. Rajan, K.L. Schulze, H.D. Ryoo, M. Acar, H. Steller, H.J. Bellen, Ero1L, a thiol oxidase, is required for Notch signaling through cysteine bridge formation of the Lin12-Notch repeats in Drosophila melanogaster, J Cell Biol 182 (2008) 1113-1125.
[22] M. Pagani, S. Pilati, G. Bertoli, B. Valsasina, R. Sitia, The C-terminal domain of yeast Ero1p mediates membrane localization and is essential for function, FEBS Lett 508 (2001) 117-120.
[23] K.M. Baker, S. Chakravarthi, K.P. Langton, A.M. Sheppard, H. Lu, N.J. Bulleid, Low reduction potential of Ero1alpha regulatory disulphides ensures tight control of substrate oxidation, EMBO J 27 (2008) 2988-2997.
[24] L. Wang, L. Zhu, C.C. Wang, The endoplasmic reticulum sulfhydryl oxidase Ero1beta drives efficient oxidative protein folding with loose regulation, Biochem J 434 (2011) 113-121.
[25] L. Wang, S.J. Li, A. Sidhu, L. Zhu, Y. Liang, R.B. Freedman, C.C. Wang, Reconstitution of human Ero1-Lalpha/protein-disulfide isomerase oxidative folding pathway in vitro. Position-dependent differences in role between the a and a' domains of protein-disulfide isomerase, J Biol Chem 284 (2009) 199-206.

[26] K. Araki, K. Nagata, Functional in vitro analysis of ERO1 and protein-disulfide isomerase (PDI) pathway, J Biol Chem 286 (2011) 32705-32712.
[27] J.E. Chambers, T.J. Tavender, O.B. Oka, S. Warwood, D. Knight, N.J. Bulleid, The reduction potential of the active site disulfides of human protein disulfide isomerase limits oxidation of the enzyme by Ero1alpha, J Biol Chem 285 (2010) 29200-29207.
[28] C. Appenzeller-Herzog, J. Riemer, E. Zito, K.T. Chin, D. Ron, M. Spiess, L. Ellgaard, Disulphide production by Ero1alpha-PDI relay is rapid and effectively regulated, EMBO J 29 (2010) 3318-3329.
[29] K. Inaba, S. Masui, H. Iida, S. Vavassori, R. Sitia, M. Suzuki, Crystal structures of human Ero1alpha reveal the mechanisms of regulated and targeted oxidation of PDI, EMBO J 29 (2010) 3330-3343.
[30] M. Otsu, G. Bertoli, C. Fagioli, E. Guerini-Rocco, S. Nerini-Molteni, E. Ruffato, R. Sitia, Dynamic retention of Ero1alpha and Ero1beta in the endoplasmic reticulum by interactions with PDI and ERp44, Antioxid Redox Signal 8 (2006) 274-282.
[31] S. Masui, S. Vavassori, C. Fagioli, R. Sitia, K. Inaba, Molecular Bases of Cyclic and Specific Disulfide Interchange between Human ERO1{alpha} Protein and Protein-disulfide Isomerase (PDI), J Biol Chem 286 (2011) 16261-16271.
[32] E. Vitu, S. Kim, C.S. Sevier, O. Lutzky, N. Heldman, M. Bentzur, T. Unger, M. Yona, C.A. Kaiser, D. Fass, Oxidative activity of yeast Ero1p on protein disulfide isomerase and related oxidoreductases of the endoplasmic reticulum, J Biol Chem 285 (2010) 18155-18165.
[33] G. Bertoli, T. Simmen, T. Anelli, S.N. Molteni, R. Fesce, R. Sitia, Two conserved cysteine triads in human Ero1alpha cooperate for efficient disulfide bond formation in the endoplasmic reticulum, J Biol Chem 279 (2004) 30047-30052.
[34] C.E. Jessop, R.H. Watkins, J.J. Simmons, M. Tasab, N.J. Bulleid, Protein disulphide isomerase family members show distinct substrate specificity: P5 is targeted to BiP client proteins, J Cell Sci 122 (2009) 4287-4295.
[35] S. Schulman, B. Wang, W. Li, T.A. Rapoport, Vitamin K epoxide reductase prefers ER membrane-anchored thioredoxin-like redox partners, Proc Natl Acad Sci U S A 107 (2010) 15027-15032.
[36] C. Khoo, J. Yang, G. Rajpal, Y. Wang, J. Liu, P. Arvan, D.A. Stoffers, Endoplasmic Reticulum Oxidoreductase-1-Like {beta} (ERO1l{beta}) Regulates Susceptibility to Endoplasmic Reticulum Stress and Is Induced by Insulin Flux in {beta}-Cells, Endocrinology 152 (2011) 2599-2608.
[37] Y. Adachi, K. Yamamoto, T. Okada, H. Yoshida, A. Harada, K. Mori, ATF6 is a transcription factor specializing in the regulation of quality control proteins in the endoplasmic reticulum, Cell Struct Funct 33 (2008) 75-89.
[38] S. Nadanaka, T. Okada, H. Yoshida, K. Mori, Role of disulfide bridges formed in the luminal domain of ATF6 in sensing endoplasmic reticulum stress, Mol Cell Biol 27 (2007) 1027-1043.
[39] D. May, A. Itin, O. Gal, H. Kalinski, E. Feinstein, E. Keshet, Ero1-L alpha plays a key role in a HIF-1-mediated pathway to improve disulfide bond formation and VEGF secretion under hypoxia: implication for cancer, Oncogene 24 (2005) 1011-1020.
[40] B. Gess, K.H. Hofbauer, R.H. Wenger, C. Lohaus, H.E. Meyer, A. Kurtz, The cellular oxygen tension regulates expression of the endoplasmic oxidoreductase ERO1-Lalpha, Eur J Biochem 270 (2003) 2228-2235.
[41] L. Qiang, H. Wang, S.R. Farmer, Adiponectin secretion is regulated by SIRT1 and the endoplasmic reticulum oxidoreductase Ero1-L alpha, Mol Cell Biol 27 (2007) 4698-4707.
[42] S.J. Marciniak, C.Y. Yun, S. Oyadomari, I. Novoa, Y. Zhang, R. Jungreis, K. Nagata, H.P. Harding, D. Ron, CHOP induces death by promoting protein synthesis and oxidation in the stressed endoplasmic reticulum, Genes Dev 18 (2004) 3066-3077.
[43] S.Y. Gilady, M. Bui, E.M. Lynes, M.D. Benson, R. Watts, J.E. Vance, T. Simmen, Ero1alpha requires oxidizing and normoxic conditions to localize to the mitochondria-associated membrane (MAM), Cell Stress Chaperones 15 (2010) 619-629.
[44] T. Anelli, L. Bergamelli, E. Margittai, A. Rimessi, C. Fagioli, A. Malgaroli, P. Pinton, M. Ripamonti, R. Rizzuto, R. Sitia, Ero1alpha Regulates Ca2+ Fluxes at the Endoplasmic Reticulum-Mitochondria Interface (MAM), Antioxid Redox Signal in press (2012).
[45] J.P. Decuypere, G. Monaco, G. Bultynck, L. Missiaen, H. De Smedt, J.B. Parys, The IP(3) receptor-mitochondria connection in apoptosis and autophagy, Biochim Biophys Acta 1813 (2011) 1003-1013.
[46] G. Li, M. Mongillo, K.T. Chin, H. Harding, D. Ron, A.R. Marks, I. Tabas, Role of ERO1-alpha-mediated stimulation of inositol 1,4,5-triphosphate receptor activity in endoplasmic reticulum stress-induced apoptosis, J Cell Biol 186 (2009) 783-792.
[47] T. Higo, M. Hattori, T. Nakamura, T. Natsume, T. Michikawa, K. Mikoshiba, Subtype-specific and ER lumenal environment-dependent regulation of inositol 1,4,5-trisphosphate receptor type 1 by ERp44, Cell 120 (2005) 85-98.

[48] T. Anelli, M. Alessio, A. Bachi, L. Bergamelli, G. Bertoli, S. Camerini, A. Mezghrani, E. Ruffato, T. Simmen, R. Sitia, Thiol-mediated protein retention in the endoplasmic reticulum: the role of ERp44, EMBO J 22 (2003) 5015-5022.
[49] G. Li, C. Scull, L. Ozcan, I. Tabas, NADPH oxidase links endoplasmic reticulum stress, oxidative stress, and PKR activation to induce apoptosis, J Cell Biol 191 (2010) 1113-1125.
[50] C. Appenzeller-Herzog, Glutathione- and non-glutathione-based oxidant control in the endoplasmic reticulum, J Cell Sci 124 (2011) 847-855.
[51] Z.V. Wang, T.D. Schraw, J.Y. Kim, T. Khan, M.W. Rajala, A. Follenzi, P.E. Scherer, Secretion of the adipocyte-specific secretory protein adiponectin critically depends on thiol-mediated protein retention, Mol Cell Biol 27 (2007) 3716-3731.
[52] M. Mariappan, K. Radhakrishnan, T. Dierks, B. Schmidt, K. von Figura, ERp44 mediates a thiol-independent retention of formylglycine-generating enzyme in the endoplasmic reticulum, J Biol Chem 283 (2008) 6375-6383.
[53] A. Fraldi, E. Zito, F. Annunziata, A. Lombardi, M. Cozzolino, M. Monti, C. Spampanato, A. Ballabio, P. Pucci, R. Sitia, M.P. Cosma, Multistep, sequential control of the trafficking and function of the multiple sulfatase deficiency gene product, SUMF1 by PDI, ERGIC-53 and ERp44, Hum Mol Genet 17 (2008) 2610-2621.
[54] V.D. Nguyen, M.J. Saaranen, A.R. Karala, A.K. Lappi, L. Wang, I.B. Raykhel, H.I. Alanen, K.E. Salo, C.C. Wang, L.W. Ruddock, Two endoplasmic reticulum PDI peroxidases increase the efficiency of the use of peroxide during disulfide bond formation, J Mol Biol 406 (2011) 503-515.
[55] S. Dias-Gunasekara, J. Gubbens, M. van Lith, C. Dunne, J.A. Williams, R. Kataky, D. Scoones, A. Lapthorn, N.J. Bulleid, A.M. Benham, Tissue-specific expression and dimerization of the endoplasmic reticulum oxidoreductase Ero1beta, J Biol Chem 280 (2005) 33066-33075.
[56] P. Moore, K.M. Bernardi, B. Tsai, The Ero1alpha-PDI redox cycle regulates retro-translocation of cholera toxin, Mol Biol Cell 21 (2010) 1305-1313.

7. Discussion II: Destroy and Exploit: Catalyzed Removal of Hydroperoxides from the Endoplasmic Reticulum

Hindawi Publishing Corporation
International Journal of Cell Biology
Volume 2013, Article ID 180906, 13 pages
http://dx.doi.org/10.1155/2013/180906

Review Article

Destroy and Exploit: Catalyzed Removal of Hydroperoxides from the Endoplasmic Reticulum

Thomas Ramming and Christian Appenzeller-Herzog

Division of Molecular and Systems Toxicology, Department of Pharmaceutical Sciences, University of Basel, Klingelbergstr. 50, 4056 Basel, Switzerland

Correspondence should be addressed to Christian Appenzeller-Herzog; christian.appenzeller@unibas.ch

Received 23 July 2013; Accepted 5 September 2013

Academic Editor: Kenji Inaba

Peroxidases are enzymes that reduce hydroperoxide substrates. In many cases, hydroperoxide reduction is coupled to the formation of a disulfide bond, which is transferred onto specific acceptor molecules, the so-called reducing substrates. As such, peroxidases control the spatiotemporal distribution of diffusible second messengers such as hydrogen peroxide (H_2O_2) and generate new disulfides. Members of two families of peroxidases, peroxiredoxins (Prxs) and glutathione peroxidases (GPxs), reside in different subcellular compartments or are secreted from cells. This review discusses the properties and physiological roles of PrxIV, GPx7, and GPx8 in the endoplasmic reticulum (ER) of higher eukaryotic cells where H_2O_2 and—possibly—lipid hydroperoxides are regularly produced. Different peroxide sources and reducing substrates for ER peroxidases are critically evaluated. Peroxidase-catalyzed detoxification of hydroperoxides coupled to the productive use of disulfides, for instance, in the ER-associated process of oxidative protein folding, appears to emerge as a common theme. Nonetheless, *in vitro* and *in vivo* studies have demonstrated that individual peroxidases serve specific, nonoverlapping roles in ER physiology.

1. Introduction

Hydrogen peroxide (H_2O_2) is an intracellular metabolite, which serves important roles as a second messenger in redox signaling [1]. However, since elevated levels of H_2O_2 (and of other reactive oxygen species, ROS) can damage proteins, nucleic acids, and lipids by peroxidation, temporal and spatial limitation of H_2O_2 levels is critically important. Thus, half-life and spatial distribution of H_2O_2 in the cell are tightly regulated by nonenzymatic antioxidants as well as by specific scavenging enzymes, including the so-called peroxidases of the peroxiredoxin (Prx) or glutathione peroxidase (GPx) families [2]. Prx and GPx isoforms reside in different subcellular compartments where they catalyze the reduction of H_2O_2 to H_2O [2]. The most relevant producers of intracellular ROS/H_2O_2 are the transmembrane enzyme complexes of the nicotinamide adenine dinucleotide oxidase (NOX) family, various enzymes and the respiratory chain in mitochondria, peroxisomal enzymes, and sulfhydryl oxidases in the endoplasmic reticulum (ER) [3–7]. Due to the presence of specific aquaporin channels in cellular membranes, the local diffusion of H_2O_2 is usually not restricted by organelle boundaries [8, 9].

There are a total of six isoforms of Prx in mammals, all of which form distinct types of antiparallel homooligomers [10]. H_2O_2-mediated oxidation of the active site peroxidatic cysteine (C_P) to a cysteine sulfenic acid is a common feature of Prxs. However, only so-called 2-Cys Prxs possess a resolving cysteine (C_R), which attacks the C_P sulfenic acid, leading to the formation of a C_R–C_P disulfide bond. In typical 2-Cys Prxs, the C_R–C_P disulfide connects antiparallel dimers, whereas in atypical 2-Cys Prxs, it forms intramolecularly. In order to complete the catalytic cycle, these disulfide bonds are reduced by a thioredoxin-type oxidoreductase [10–12]. In contrast, 1-Cys Prxs (such as human PrxVI) lack a C_R and instead form a mixed disulfide heterodimer with π glutathione S-transferase, which catalyzes the glutathione-driven reductive regeneration of the Prx [13, 14].

A remarkable feature of Prxs is their susceptibility to oxidative inactivation. Thus, C_P sulfenic acid can react with

7.1. Abstract

Peroxidases are enzymes that reduce hydroperoxide substrates. In many cases, hydroperoxide reduction is coupled to the formation of a disulfide bond, which is transferred onto specific acceptor molecules, the so-called reducing substrates. As such, peroxidases control the spatio-temporal distribution of diffusible second messengers such as hydrogen peroxide (H_2O_2) and generate new disulfides. Members of two families of peroxidases, peroxiredoxins (Prxs) and glutathione peroxidases (GPxs), reside in different subcellular compartments or are secreted from cells. This review discusses the properties and physiological roles of PrxIV, GPx7, and GPx8 in the endoplasmic reticulum (ER) of higher eukaryotic cells where H_2O_2 and – possibly – lipid hydroperoxides are regularly being produced. Different peroxide sources and reducing substrates for ER peroxidases are critically evaluated. Peroxidase-catalyzed detoxification of hydroperoxides coupled to the productive use of disulfides, for instance in the ER-associated process of oxidative protein folding, appears to emerge as a common theme. Nonetheless, in vitro and in vivo studies have demonstrated that individual peroxidases serve specific, non-overlapping roles in ER physiology.

7.2. Introduction

Hydrogen peroxide (H_2O_2) is an intracellular metabolite, which serves important roles as a second messenger in redox signaling [1]. However, since elevated levels of H_2O_2 (and of other reactive oxygen species, ROS) can damage proteins, nucleic acids, and lipids by peroxidation, temporal and spatial limitation of H_2O_2 levels is critically important. Thus, half-life and spatial distribution of H_2O_2 in the cell are tightly regulated by non-enzymatic antioxidants as well as by specific scavenging enzymes, including the so-called peroxidases of the peroxiredoxin (Prx) or glutathione peroxidase (GPx) families [2]. Prx and GPx isoforms reside in different subcellular compartments where they catalyze the reduction of H_2O_2 to H_2O [2]. The most relevant producers of intracellular ROS/H_2O_2 are the transmembrane enzyme complexes of the nicotinamide adenine dinucleotide oxidase (NOX) family, various enzymes and the respiratory chain in mitochondria, peroxisomal enzymes, and sulfhydryl oxidases in the endoplasmic reticulum (ER) [3,4,5,6,7].

Due to the presence of specific aquaporin channels in cellular membranes, the local diffusion of H_2O_2 is usually not restricted by organelle boundaries [8,9].
There are a total of six isoforms of Prx in mammals, all of which form distinct types of antiparallel homooligomers [10]. H_2O_2-mediated oxidation of the active site peroxidatic cysteine (C_P) to a cysteine sulfenic acid is a common feature of Prxs. However, only so-called 2-Cys Prxs possess a resolving cysteine (C_R), which attacks the C_P sulfenic acid, leading to the formation of a C_R–C_P disulfide bond. In typical 2-Cys Prxs, the C_R–C_P disulfide connects antiparallel dimers, whereas in atypical 2-Cys Prxs, it forms intramolecularly. In order to complete the catalytic cycle, these disulfide bonds are reduced by a thioredoxin-type oxidoreductase [10,11,12]. In contrast, 1-Cys Prxs (such as human PrxVI) lack a C_R and instead form a mixed disulfide heterodimer with π glutathione S-transferase, which catalyzes the glutathione-driven reductive regeneration of the Prx [13,14].

A remarkable feature of Prxs is their susceptibility to oxidative inactivation. Thus, C_P sulfenic acid can react with a second molecule of H_2O_2, which gives rise to C_P sulfinic acid. This leads to Prx inactivation, stabilization of decameric over dimeric configuration, and, in some cases, to an increase in chaperone activity [15,16,17]. At least in cytoplasmic and mitochondrial typical 2-Cys Prxs, sulfinic acid formation can be reversed by the action of sulfiredoxin at the expense of ATP [18,19]. Under highly oxidizing conditions, C_P sulfinic acid can further and irreversibly react with a third molecule of H_2O_2 to form C_P sulfonic acid [15].

The GPx family is phylogenetically unrelated to Prxs but shares the ability to reduce hydroperoxide substrates [2]. A total of eight mammalian GPxs are known. They are sub-classified into two groups according to the amino acid tetrad in their catalytic center. In SecGPxs (human GPx1-4, and 6) or CysGPxs, (GPx5, 7, and 8), the common constituents Gln, Trp and Asn are supplemented with a peroxidatic selenocysteine (Sec) or Cys, respectively [20]. Furthermore, GPxs differ with regard to their oligomeric state, with GPx1-3, 5, and 6 constituting homotetramers and GPx4, 7, and 8 monomers [21].

Upon hydroperoxide-mediated oxidation of the active-site selenocysteine, SecGPxs typically react with two molecules of glutathione (GSH) yielding glutathione disulfide (GSSG), which historically accounted for the generalized family name glutathione peroxidases [2,21]. However, the use of GSH as reductant is not a common feature of GPxs nor is it strictly conserved within

the SecGPx subgroup [2,21,22,23,24,25]. In invertebrates and plants, monomeric CysGPxs harbor a C_R and exhibit an identical reaction mechanism as atypical 2-Cys Prxs (see above) [20,26,27]. In contrast, no typical C_R is present in the human monomeric CysGPxs GPx7 and 8.
The ER serves many distinct cellular functions [28]. One of these is chaperone-mediated folding of nascent polypeptide chains, which often involves the introduction of disulfide bonds via oxidation of two adjacent cysteines. This process termed oxidative protein folding is driven by a number of distinct pathways, the most conserved of which involves the sulfhydryl oxidase endoplasmic oxidoreductin 1 (Ero1) as disulfide donor [29]. Since Ero1 can utilize molecular oxygen (O_2) as terminal electron acceptor, it generates stoichiometric amounts of H_2O_2 for every disulfide bond produced, as demonstrated in vitro [30]. In addition, H_2O_2 sources other than the paralogs Ero1α and Ero1β exist within the mammalian ER. Although initially assigned to phagocytic cells only, more recent findings have shown that NOX family members are expressed in various cell types [3] where they produce H_2O_2 at different subcellular sites including the ER [31,32,33]. Likewise, the secreted quiescin-sulfhydryl oxidases were identified as producers of H_2O_2 [34], although these enzymes function in the extracellular space [35] and their contribution to intracellular oxidative protein folding is uncertain [36,37]. It has also been suggested that ROS produced by mitochondrial respiration could impact on disulfide-bond formation in secretory compartments including the ER [38]. Leakage of the mitochondrial electron transport chain, predominantly at complex III, releases superoxide and H_2O_2 into the intermembrane space of mitochondria [39,40]. The close apposition of ER and mitochondria [41] could enable these ROS to contribute to ER-associated oxidative protein folding.

This review will focus on PrxIV, GPx7, and GPx8, which reside in the ER of vertebrates, lancelets, ascidians, and – in case of PrxIV – echinoderms and arthropods [42]. As detailed further below, all ER-resident peroxidases can use protein disulfide isomerases (PDIs; the "thioredoxins of the ER") as reducing substrates, allowing them to exploit the oxidizing power of ER peroxide sources for oxidative protein folding. However, reducing substrates other than PDIs may also participate in the reaction cycle of ER peroxidases.

7.3. H_2O_2 in the ER: Bulk metabolite or locally restricted messenger?

Reliable detection of the cellular distribution of H_2O_2 is a challenging task. The recent development of genetically encoded sensors, which can be expressed in different subcellular compartments, significantly facilitated the monitoring of spatial and temporal changes in H_2O_2/ROS concentration though [43]. For instance, targeted expression of the yellow fluorescent protein-based, ratiometric, and H_2O_2-sensitive HyPer sensor was used to record the oxidizing environment in the mammalian ER [33,44,45,46]. On the basis of the predominantly oxidized state of ER-localized HyPer ($HyPer_{ER}$) and the predominantly reduced state of HyPer on the cytoplasmic surface of the ER, a high $[H_2O_2]_{ER}$, which is strictly confined to the lumen of the organelle, has been inferred [44]. Several lines of evidence argue against this interpretation though. First, as detailed in the following paragraph, numerous examples for signaling roles of ER-derived H_2O_2 are known, which suggest analogy to the critical involvement of Nox-derived H_2O_2 in receptor tyrosine kinase (RTK) signal transduction at the cell surface [47,48,49,50] (Fig. 30). Second, the presence of peroxidases in the ER lumen (see below) appears incompatible with a high steady-state $[H_2O_2]_{ER}$. Third, the demonstration of aquaporin 8-facilitated entry of H_2O_2 into the ER [8] suggests that aquaporin 8 can also facilitate exit of ER-derived H_2O_2 (see also Fig. 30). Forth, since the ratiometric readout of HyPer is based on the formation of an intramolecular disulfide bond [51], oxidation of HyPer in the ER could be catalyzed by resident oxidoreductases independently of H_2O_2. Consistent with this assumption, no effect on $HyPer_{ER}$ oxidation was observed upon overexpression of PrxIV or of ER-targeted catalase in pancreatic beta-cells [46]. The increased oxidation of $HyPer_{ER}$ observed in response to higher levels of Ero1α [44,52] can therefore reflect both enhanced oxidation of PDIs and a rise in $[H_2O_2]_{ER}$. Thus, the Ero1α-induced increase in oxidation of $HyPer_{ER}$ can only be partially reversed by addition of the H_2O_2 scavenger butylated hydroxyanisole (our unpublished observations). Conversely, increased oxidation of $HyPer_{ER}$ in response to NOX4 induction is blunted by co-expression of catalase in the ER [33].

The role of H_2O_2 as signaling molecule typically manifests in the formation of short-lived microdomains of elevated $[H_2O_2]$ [49,53]. For instance, ligand binding to RTKs at the cell surface such as platelet-derived growth factor receptor, epidermal growth factor receptor (EGFR), or insulin receptor stimulates the local production of H_2O_2 via crosstalk with NOX enzymes

[47,49,54,55]. This leads to oxidative inactivation of protein tyrosine phosphatases (PTPs), which prolongs RTK signaling until cytosolic ROS scavengers such as Prxs have cleared H_2O_2 [56,57,58,59,60] (Fig. 30a). At least in certain contexts, such H_2O_2-dependent signal amplification is mediated by ER-resident NOX4 and PTP1B [31] (Fig. 30b). Thus, activated EGFR is internalized into endosomes and transported close to the ER [61] where its PTP1B-dependent dephosphorylation is negatively regulated by NOX4-derived H_2O_2 [31]. In the case of the granulocyte-colony stimulating factor receptor pathway, also ER-resident PrxIV (see next section) can modulate the signaling amplitude [62] (Fig. 30b).

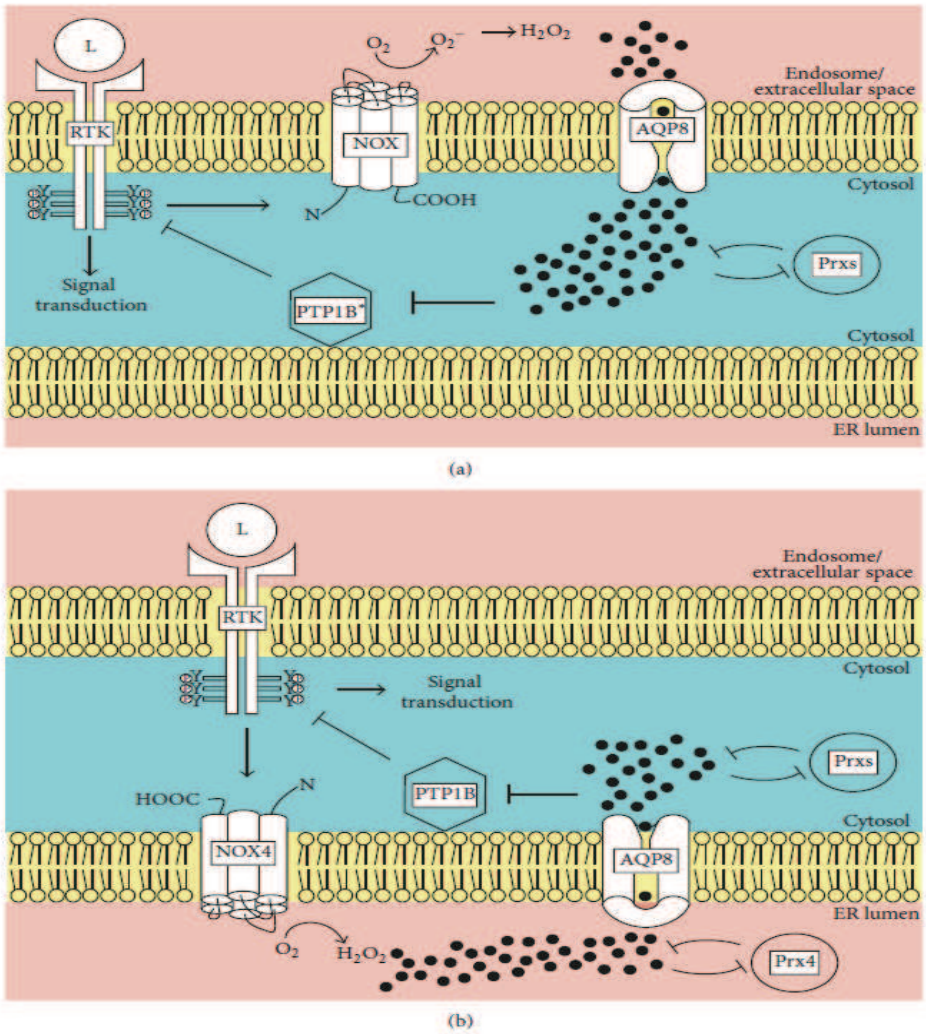

Figure 30: RTK signaling involves NOX-derived H_2O_2 as second messenger. (a) Binding of ligand (L) to receptor tyrosine kinases (RTK) on the cell surface activates NADPH oxidases (NOX) and leads to the generation of extracellular or, following endocytosis, endosomal superoxide (O_2^-), which can be dismutated to H_2O_2. Upon aquaporin 8 (AQP8)-facilitated diffusion across the plasma/endosomal membrane, H_2O_2 locally inactivates the intracellular negative regulators phospho tyrosine phosphatases (PTPs) and peroxiredoxins (Prxs), which prolongs RTK signal transduction. This step mostly, but not exclusively (as depicted by an asterisk) involves the endoplasmic reticulum (ER)-associated PTP1B. Spatial restriction of H_2O_2 is achieved by cytosolic ROS scavengers like Prxs. **(b)** An ER-centered route of RTK-mediated signal transduction involves NOX4 in the ER membrane and PTP1B. In this context, ER-luminal build-up of H_2O_2 is controlled by ER-resident PrxIV.

NOX4-initiated signal transduction is linked to the adaptive/apoptotic output of the ER stress response – a conglomeration of ER-derived signaling cascades known as the unfolded protein response (UPR) [63]. In the context of atherosclerosis, oxysterol-stimulated smooth muscle cell apoptosis depends on NOX4, which is upregulated through the ER stress sensor Ire1α to produce H_2O_2 [32]. Similarly, NOX4 is induced in endothelial cells in response to a subset of ER stressors, leading to presumably locally restricted H_2O_2 signaling [33]. In both cases, proper activation of UPR pathways requires NOX4-derived H_2O_2. Of note, NOX4-dependent, ER-associated oxidative signaling through the RAS–ERK pathway in endothelial cells promotes pro-survival autophagy rather than cell death [33]. A related link operates in smooth muscle cells where NOX4-derived H_2O_2 stimulates autophagy by inhibiting authophagy-related gene 4B activity, which antagonizes ER stress and cell death [64].

Little is known about signaling roles of H_2O_2 sources other than NOX4 in the ER. Nevertheless, the available data on NOX4 strongly suggest that – in analogy to the situation in other compartments – H_2O_2 operates in the ER as a spatially restricted second messenger rather than a bulk metabolite.

7.4. Peroxiredoxin IV

PrxIV is the only ER-resident representative of the Prx family. Its predominant isoform harbors a classical signal peptide, which is cleaved upon co-translational entry into the ER, but no ER retrieval motif to ensure its retention in the early secretory pathway (ESP) [65,66]. Instead, similar to the ER retention mechanism of Ero1α, physical interactions with the ESP oxidoreductases ERp44 and PDI inhibit PrxIV secretion from cells [67]. Therefore, cell-specific differences and/or saturation of the retrieval machinery, e.g. following exogenous overexpression, might explain the ambiguity in the literature on the intracellular or secreted nature of PrxIV [68,69,70,71,72]. This review will focus on the role of the ER-resident fraction of PrxIV.

PrxIV belongs to the subclass of typical 2-Cys Prxs and predominantly exists in decameric configuration. The toroid shaped pentamer of antiparallel dimers (Fig. 31) is stabilized by hydrophobic interactions at dimer-dimer interfaces. In contrast to other family members [73], PrxIV does not show significant transition from the decameric to the dimeric state upon disulfide-

bond formation between C_P and C_R, even though this process is associated with local unfolding [74]. Furthermore, PrxIV harbors a unique N-terminal extension. As judged from the positions of the truncated N-termini in the crystal structure, these flexible extensions protrude into the center of the decameric assembly of full length PrxIV protomers (Fig. 31). In addition to hydrophobic interactions, neighboring antiparallel dimers are linked by Cys^{51}–Cys^{51} interchain disulfide bonds between N-terminal regions (Fig. 31), but mutagenesis to serine or alanine neither affected decamerization nor the catalytic parameters of PrxIV [74,75,76]. The impact of the N-terminal extensions for correct quaternary structure is still unclear. In an N-terminal truncation mutant, Wang et al. observed a significant transition from the decameric to the dimeric state upon oxidation. In contrast to this, Ikeda et al. reported a shift from decameric to higher oligomeric forms [76,77].

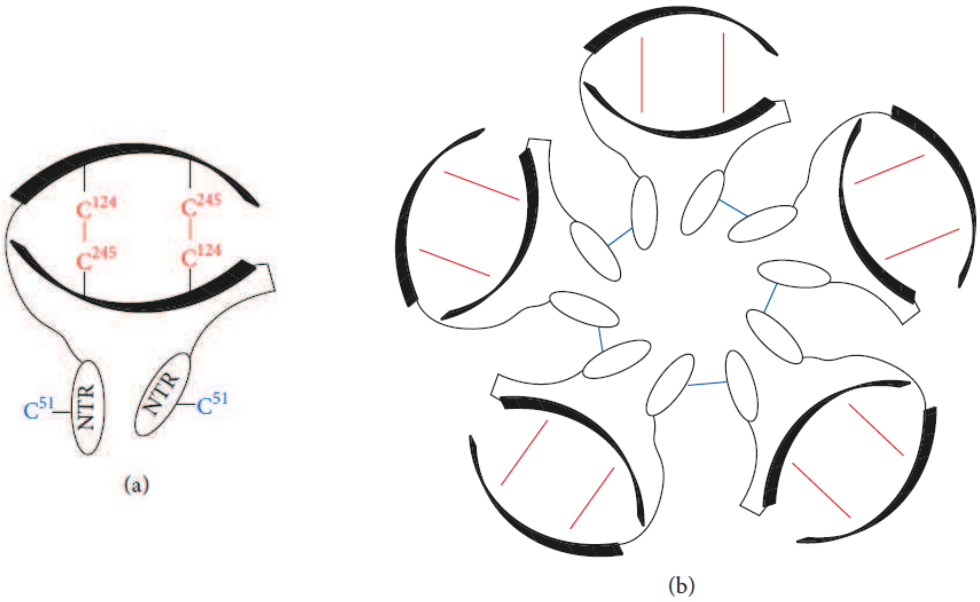

Figure 31: Oligomeric structure of PrxIV. (a) Upon peroxide-mediated oxidation, antiparallel PrxIV dimers are transiently linked by disulfide bonds between C_P (C^{124}) on one subunit and C_R (C^{245}) on the other subunit (depicted in red), which is the characteristic feature of typical 2-Cys Prxs. However, dimer formation relies on hydrophobic interactions and is redox state-independent. The flexible N-terminal region (NTR) of PrxIV is oriented towards the center of the toroid-shaped, decameric complex **(b)**. The role of the disulfide bonds linking adjacent dimers via Cys^{51} in the NTR (depicted in blue) is currently unclear.

Like other Prxs, PrxIV exhibits an exceptionally fast reactivity towards H_2O_2 (2.2×10^7 M^{-1} s^{-1}) [76]. As data on PrxIV reacting with peroxide substrates other than H_2O_2 is scarce, PrxIV may exclusively react with H_2O_2 *in vivo* (Table 2). PrxIV knockout cells stained with H_2O_2-reactive dye showed a bright signal, which was blunted upon reconstitution of PrxIV (Fig. S10 in [62]).

Where does this H_2O_2 come from? A popular model implicates Ero1α-derived H_2O_2, a regular byproduct of oxidative protein folding [78], as oxidizing substrate of PrxIV [79]. This model is based on the finding that activation of Ero1α in cells by dithiothreitol (DTT)-mediated reduction of its regulatory disulfide bonds increased the hyperoxidized fraction of PrxIV [80]. In further support, DTT-triggered hyperoxidation of PrxIV was inhibited by knockdown of Ero1α (Neil Bulleid, personal communication), and Ero1α-dependent accumulation of H_2O_2 in response to DTT treatment was increased by PrxIV knockdown and decreased by PrxIV overexpression (our unpublished observations). However, in contrast to GPx8 (see below), this crosstalk between Ero1α-derived H_2O_2 and PrxIV was only observed in the presence of DTT (our unpublished observations), which likely does not reflect normal physiology. Experiments with murine or fungal loss-of-function models of Ero1 strongly suggested that PrxIV can be coupled to (an) Ero1-independent source(s) of H_2O_2: ectopic expression of PrxIV rescues the thermosensitive ero1-1 yeast strain by Ero1-independent oxidative protein folding [81] (see below) and PrxIV is required to protect Ero1-deficient mice against H_2O_2-mediated ascorbate depletion [82]. The H_2O_2 source(s) targeted by PrxIV remain(s) to be identified [12].

Following disulfide-bond formation between C_P and C_R, PrxIV acts as PDI peroxidase by using several different PDIs as electron donors [75,83] (Table 2). As discussed further below, these PDIs can subsequently shuttle the disulfide onto various substrate proteins, implicating PrxIV as an important element of oxidative protein folding.

It is intriguing that despite the fact that the ER is devoid of sulfiredoxin activity, PrxIV has retained specific structural features to support H_2O_2-mediated hyperoxidation [74,76]. Accordingly, sulfinylation of C_P in PrxIV could potentially serve a specific function. It has been speculated that hyperoxidized PrxIV could operate as a molecular chaperone or as a secreted damage associated molecular pattern [65].

7.5. GPx7 and GPx8

GPx7 and 8 are closely related ER-luminal members of the GPx family. Whereas GPx7 possesses a cleavable N-terminal signal sequence, GPx8 is a transmembrane protein with a short N-terminal cytoplasmic tail. Retention in the ESP is mediated by exposed, C-terminal motifs, –Arg-Glu-Asp-

Leu and –Lys-Glu-Asp-Leu in GPx7 and 8, respectively, which are recognized in the Golgi by KDEL retrieval receptors [84]. This ESP-retention mechanism is noteworthy for GPx8, since ER membrane proteins are usually retrieved to the ER via cytosolic interactions with retrograde coat proteins [85]. The physiological implications of this peculiarity are currently unclear.

Whereas no other peroxide substrate besides H_2O_2 has been documented for GPx8 yet, GPx7 (also known as non-selenocysteine containing phospholipid hydroperoxide glutathione peroxidase, NPGPx) can efficiently react with phospholipid hydroperoxides in vitro ($k > 10^3$ M^{-1} s^{-1}, Table 2) [86]. Although speculative at present, we consider it possible that also in its native context, GPx7 can reduce lipid peroxidation products in the luminal leaflet of the ER membrane. As to GPx8, which largely shares the active-site architecture with GPx7 (Fig. 32), the short linker between the transmembrane anchor and the catalytic domain might not confer enough flexibility for the active site to interact with the lipid bilayer. Accordingly, both GPxs (together with PrxIV) could protect ER-oriented lipids against peroxidation by scavenging ER-luminal H_2O_2, but only soluble GPx7, in analogy to GPx4 [87], would be able to directly reverse lipid peroxidation by enzymatic reduction.

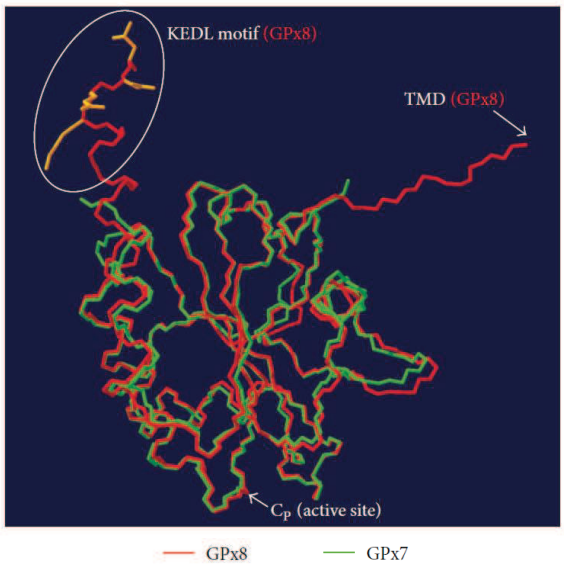

Figure 32: Superimposition of GPx7 and GPx8. Overlay of the carbon-nitrogen backbones of GPx7 (green; PDB ID 2KIJ) and GPx8 (red; PDB ID 2P31) was done using the Swiss PDB viewer software (available at www.expasy.ch). The close resemblance of the two three-dimensional structures is particularly appreciable in the peptide loops surrounding the active-site Cys (C_P). The ESP retention signal (KEDL motif) and the location of the transmembrane domain (TMD) of GPx8 (not part of the crystal structure) are indicated.

Another prevailing model implicates Ero1 activity to provide H_2O_2 as oxidizing substrate for GPx7 and 8 [21,88]. Using a split YFP complementation approach, Ero1α and GPx7 or 8 were found to associate within the ER, and addition of GPx7 increased the oxidase activity of Ero1α in vitro [88]. While the mechanistic basis for the latter finding remains to be elucidated, these data point to a functional interaction between GPxs and Ero1α. In line with this, knockdown of GPx8 but not PrxIV aggravated the accumulation of H_2O_2 induced by a deregulated Ero1α mutant (our unpublished observations). Therefore, despite their lower reactivity towards peroxide, the physical interaction with Ero1α likely places the GPxs in a privileged position relative to PrxIV to detoxify Ero1α-derived H_2O_2.

Irrespective of the peroxide source, the catalytic mechanism for the reductive regeneration of GPx7/8 remains controversial. Despite the absence of a canonical C_R, GPx7 and 8 harbor an additional cysteine in a conserved Pro-$Cys^{86/108}$-Asn-Gln-Phe motif [86]. Studies with GPx7 have highlighted two possible mechanisms of peroxidase reduction [86,89,90] (Fig. 33a). Of note, one of the possibilities features Cys^{86} as a non-canonical C_R. However, since C_P and Cys^{86} are ~11 Å apart in the crystal structure (PDB ID 2P31; Fig. 33b), this implies a major conformational change. Indeed upon H_2O_2 addition, the intrinsic fluorescence of Trp^{142}, which, in reduced GPx7, is particularly solvent-exposed and in close proximity to C_P (Fig. 33b), readily resumes in the time scale of 2-3 sec after initial decline [88,89]. This likely indicates the translocation of Trp^{142} away from the fluorescence-quenching C_P sulfenic acid. In this connection, we note the adjacent aromatic side chain of Phe^{89}, which is part of the conserved motif surrounding Cys^{86} (see above), and speculate that stacking of Phe^{89} and Trp^{142} upon C_P oxidation could promote formation of the C_P–Cys^{86} disulfide (Fig. 33b). Interestingly, in addition to the Pro-Cys-Asn-Gln-Phe motif, the exposed Trp residue is conserved throughout the GPx family [86].

If GPx7 (and likely GPx8) can oxidize reducing substrates in the absence of $Cys^{86/108}$, what could be the reason for its conservation? We suggest that the function of C_R-dependent intramolecular disulfide-bond formation is to prevent the accumulation of sulfenylated GPxs, which may display reactivity towards non-native thiol substrates. Rapid reaction with Cys^{86} largely prevents the accumulation of the C_P-sulfenylated form of purified GPx7 in presence of H_2O_2 [89]. It will be interesting to assay the oxidation state of GPx7 and 8 in living cells. At all events, evidence for a possible toxic gain-of-function of sulfenylated GPxs came from experiments with an engineered H_2O_2-sensing fluorescent protein [91]. This protein is a fusion of redox-sensitive GFP (roGFP2)

and Orp1, which is yeast GPx3. Mutation of C_R in Orp1 accelerated disulfide-bond formation in roGFP2 in response to H_2O_2 in vitro. In living cells, however, the C_R-mutant sensor failed to respond to H_2O_2 addition, which was due to competing reactions with reducing substrates other than roGFP2 including glutathione [91].

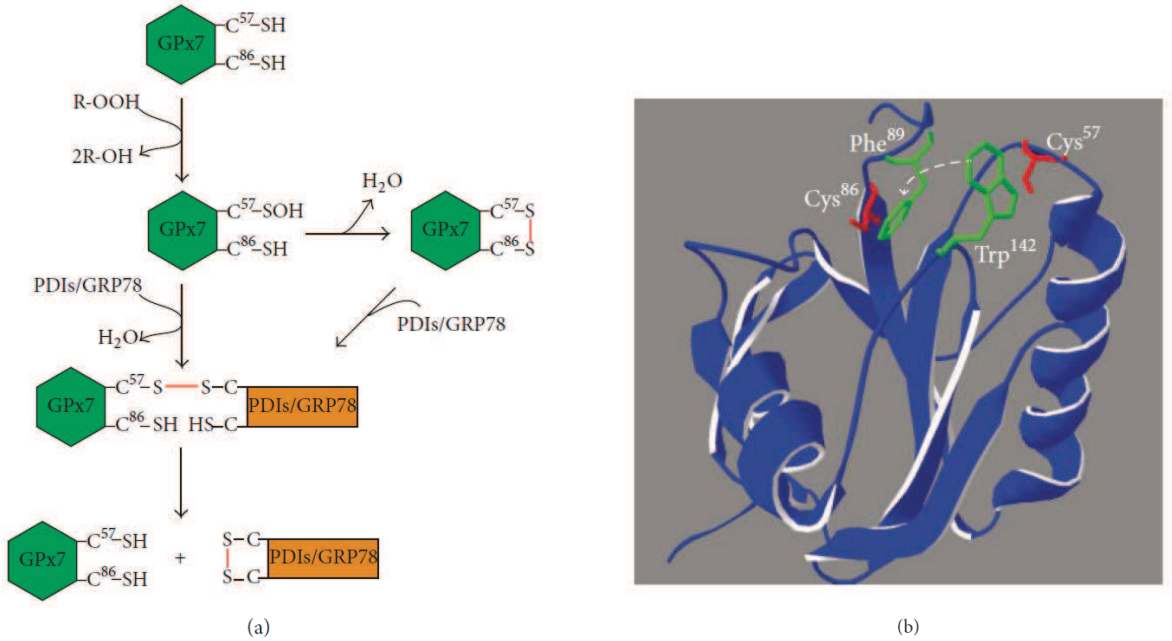

Figure 33: Suggested reaction mechanisms of GPx7. (a) Following peroxide-mediated oxidation of the active-site Cys (C^{57}), sulfenylated C^{57} is either directly subjected to nucleophilic attack by a (deprotonated) Cys in the reducing substrate (PDIs/GRP78) or attacked by (deprotonated) Cys^{86}, which results in formation of an intramolecular disulfide bond. In a second step, this intramolecular disulfide is attacked by a Cys in the reducing substrate. Both pathways converge in the formation of an intermolecular disulfide-bonded intermediate between GPx7 and the reducing substrate prior to the completion of the reaction cycle, which gives rise to regenerated, reduced GPx7 and oxidized PDIs/GRP78. **(b)** Hypothesized conformational change prior to formation of a Cys^{57}–Cys^{86} disulfide bond in GPx7 is depicted on the structure of reduced GPx7 (PDB ID 2KIJ). Active-site rearrangement upon oxidation of Cys^{57} might involve a stacking interaction between the conserved aromatic side chains of Phe^{89} and Trp^{142} (green), which would embed Trp^{142} into a more hydrophobic environment (dashed white arrow).

7.6. Reducing substrates of ER-resident GPxs

In analogy to PrxIV, oxidized GPx7 and 8 were demonstrated to act as PDI peroxidases by using several different PDIs as electron donors [88] (Table 2). The utility of disulfide transfer onto PDIs shall be discussed in the next section. Here, we will touch upon alternative reducing substrates, which have been found to interact with GPx7 (Table 2). For instance, although glutathione reduces sulfenylated GPx7 at a far lower rate compared to PDI, it has been calculated to potentially represent a competing substrate taking into account its millimolar concentration in

vivo [86]. However, since the reaction of glutathione with oxidized PDI is very fast [92], the physiological relevance of direct glutathione-mediated reduction of GPx7 is questionable.

In contrast, disulfide transfer from GPx7 to the abundant ER chaperone and UPR target GRP78/BiP – as evidenced by cysteine-dependent co-immunoprecipitation from H_2O_2-treated cells – appears to have critical influence on ER physiology [90]. GRP78/BiP carrying the resulting Cys^{41}–Cys^{420} disulfide exhibits increased chaperone activity towards misfolded clients, arguing for a role of GPx7 as oxidative stress sensor and positive regulator of GRP78/BiP [90]. Consistently, cells lacking active GPx7 were more susceptible to H_2O_2 and ER-stress-induced toxicity than wild-type control cells [90]. Very much like PrxIV knockout cells (see above), they also displayed increased staining with a H_2O_2-reactive dye compared to wild-type [90].

Non-targeting siRNA-transfected GPx7 knockout cells displayed harmfully elevated levels of siRNA compared to transfected wild-type cells, indicating a potential link between ER-resident GPx7 and the degradation machinery of non-targeting cytoplasmic siRNA [93]. This link was proposed to involve thiol-disulfide transfer between GPx7 and the nuclear exoribonuclease XRN2, although this reaction appears topologically prohibited [93]. Irrespective of this paradox but consistent with a role of GPx7 in the processing of small RNAs, non-targeting siRNA selectively induced GPx7 expression in wild-type fibroblasts [93], a process mediated by the nuclear protein nucleolin and its activity as transactivator of the GPx7 promoter [94]. It is interesting to note that the cytosolic membrane leaflet of the rough ER is emerging as a central nucleation site of miRNA-/siRNA processing in plants and animals [95,96], and the interplay between the RNA silencing machinery and GPx7 (and possibly other ER-resident peroxidases) deserves further attention.

Table 2: Published peroxide and reducing substrates of ER-resident peroxidases

	Peroxide substrates	Reducing substrates
PrxIV	H_2O_2 [76]	PDIs (ERp46, P5, PDI) [75, 83]
GPx7	H_2O_2 [88] phospholipid hydroperoxide [86]	PDIs (PDI, ERp46, ERp57, ERp72, P5) [86, 88, 89], GRP78/BiP [90], GSH [86], XRN2 [93]
GPx8	H_2O_2 [88]	PDIs (PDI, ERp46, ERp57, ERp72, P5) [88]

Compared to GPx7, the enzymatic characterization of GPx8 including the identification of its reducing substrates is far less developed. However, since the structures of their active sites are nearly superimposable (Fig. 32), GPx7 and 8 are likely to share many of their catalytic properties.

7.7. The two-disulfides-out-of-one-O_2 concept

Oxidative protein folding relies on *de novo* disulfide generating enzymes and on oxidants, which accept the electrons derived from thiol oxidation. While several such electron transfer cascades exist in the mammalian ER, resulting in a certain degree of redundancy, Ero1 oxidases (using O_2 as oxidant) and PrxIV (using H_2O_2 as oxidant) are evidently the dominant disulfide sources [29,36,81]. The fact that both enzymes can oxidize PDIs [75,78,81,83,97,98] has led to the intriguing concept that the four oxidizing equivalents in O_2 can be exploited by the consecutive activity of Ero1 and PrxIV to generate two disulfides for oxidative protein folding [79,99] (Fig. 34). Along the same lines, the PDI peroxidase activity of GPx7 constitutes a pathway for the productive use of Ero1α-derived H_2O_2 in the biosynthesis of disulfides [88,89].

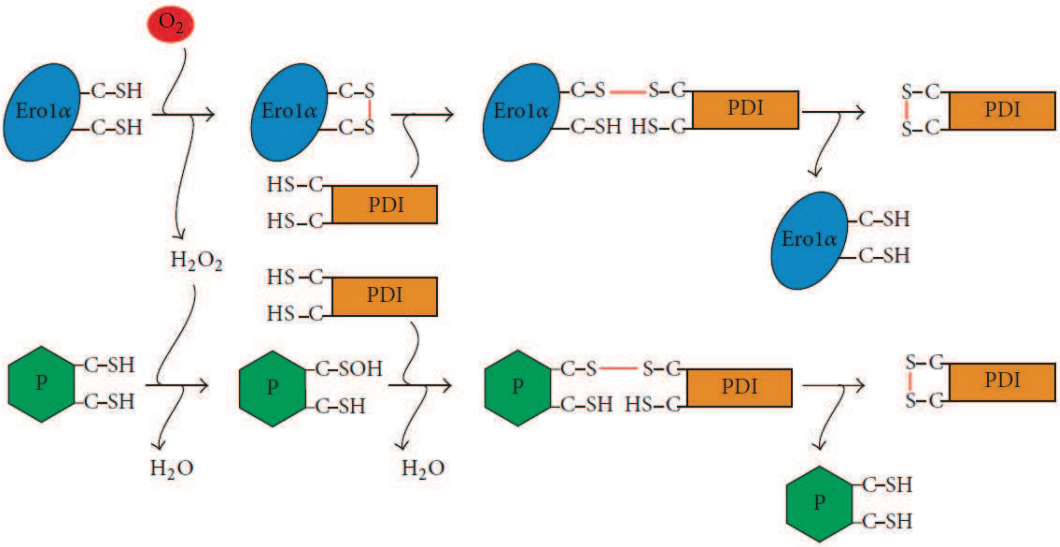

Figure 34: The two-disulfides-out-of-one-O_2 concept. O_2 (red)-mediated oxidation of Ero1α results in the generation of one disulfide bond (red), which is transferred to a reduced PDI, and of one molecule of H_2O_2. ER-resident peroxidases (P) – probably exclusively of the GPx family (see main text for details) – can couple the reduction of Ero1α-derived H_2O_2 to H_2O with the introduction of a second disulfide bond (red) into a PDI family member, thereby exploiting the oxidizing capacity of H_2O_2.

Evidence for a contribution of ER-resident peroxidases to oxidative protein folding is manifold. Mixed disulfide reaction intermediates between peroxidase and PDI were isolated from cells [75,81,89], and in the case of PrxIV, interactions with the PDI family members ERp46 and P5 were also reported [75,83]. Interestingly, of the two Cys-X-X-Cys active sites in PDI, PrxIV preferentially oxidizes the **a´** and GPx7 the **a** domain active site [75,89]. Since the mixed-disulfide complexes were stabilized by a Cys-X-X-Ala active site configuration in PDI [75], they must have resulted from the reaction of reduced PDI with oxidized peroxidase [100]. Accordingly, consumed peroxidase molecules can be activated/recycled by PDIs. It is possible that the availability of reduced PDIs actively adjusts the activation state of ER peroxidases. Thus, peroxidases could be kept in an inactive state unless new disulfides are needed, as indicated by the accumulation of reduced PDIs. In a very related manner, the intramolecular disulfides, which shut off Ero1α, are feedback-regulated by the availability of reduced PDI [101]. In contrast to Ero1α, however, the redox state of PrxIV appears to be predominantly reduced in cells at steady state [83].

Peroxidase/PDI-catalyzed oxidative protein folding can be reconstituted. Refolding of reduced RNase A, a process requiring introduction of four disulfides, occurs in the presence of PDI together with PrxIV or GPx7 [81,89]. It is important to note though that PrxIV-driven refolding appears to depend on the addition of H_2O_2, whereas GPx7-driven refolding readily works in presence of Ero1α, which generates H_2O_2 by reducing ambient O_2 [81,89]. This difference parallels the evidence discussed above for a preference of GPx7 or 8 over PrxIV to detoxify Ero1α-derived H_2O_2.

The role of PrxIV as a source of disulfide bonds is also strongly supported by genetics. Ero1-deficient mouse embryonic fibroblasts are hypersensitive to the loss of PrxIV, which causes hypooxidation of an ER-targeted thiol-disulfide sensor, ER dilation, and decreased cell viability [81]. Somewhat counterintuitively, compound loss of Ero1α/β and PrxIV also leads to oxidative phenotypes such as glutathione depletion and cell senescence [82]. These phenotypes are attributed to the failure to reduce H_2O_2 from as yet unidentified origin, which causes shortage of intracellular ascorbate (vitamin C) associated with defects in collagen synthesis and scurvy [82]. Last but not least, co-depletion of PrxIV in hepatocytes exacerbates the cytotoxic phenotype of Ero1α/β depletion and further slows ER re-oxidation after reductive challenge [36].

Taken together, a role in oxidative protein folding is particularly well documented for PrxIV, but is also shared by the ER-resident GPxs. Still, although appealing, we consider it likely that the concept of peroxidase-dependent exploitation of Ero1α-derived H_2O_2 (Fig. 34) only applies to GPxs (see above).

7.8. Organismal roles of ER peroxidases

For PrxIV and GPx7, in vivo studies have been performed in different model organisms. One striking conclusion of these studies is that whole-body loss-of-function of GPx7 in mice shows a stronger organismal phenotype compared to PrxIV deficiency. No in vivo characterization of the role of GPx8 has been published so far.

Male mice lacking a functional X-chromosomal *PRDX4* gene ($PrxIV^{-/y}$) display a mild phenotype, which manifests predominantly by testicular atrophy accompanied by increased DNA fragmentation and peroxidation of lipids and proteins [69]. The number of sperms is markedly decreased in the epididymis of $PrxIV^{-/y}$ mice, which, however, does not affect their fertility [69]. These phenotypes are likely attributed to loss of the testis-specific transmembrane isoform of PrxIV [65].

Similarly, in fruit flies a decrease in PrxIV expression to 10-20% of wild-type levels is associated with increased [H_2O_2] and lipid peroxidation in membrane preparations from whole animals [102]. However, negative impact on longevity was only observed under oxidative stress conditions induced by H_2O_2 or paraquat treatment. Strikingly, 6-10 fold, global overexpression of PrxIV in flies, which shifted its subcellular distribution from predominantly ER-resident to cytosolic and secreted, resulted in dramatically shortened lifespan under non-stress conditions and increased apoptosis in thoracic muscle and fat body tissue [102]. Since this proapoptotic phenotype upon PrxIV overexpression was not reproducible in cultured fly cells, non-cell autonomous and/or fly-specific in vivo effects of secreted PrxIV need further consideration.

In contrast to this, overexpression of PrxIV in mice has beneficial effects in the context of metabolic diseases. For instance, elevated levels of PrxIV in apolipoprotein E negative mice, which were fed a high cholesterol diet, have anti-atherogenic effects with less oxidative stress, a decrease in apoptosis, and suppressed T-lymphocyte infiltration [103]. In addition, cytoprotective

effects of overexpressed PrxIV were evident in non-genetic mouse models of both type 1 and type 2 diabetes mellitus (T1DM and T2DM) [104,105]. Specifically, autoimmune-induced apoptosis of pancreatic β-cells (in T1DM) and fatty liver phenotypes and peripheral insulin resistance (in T2DM) were diminished upon PrxIV overexpression. It is possible that more efficient clearance of inflammatory ROS is the underlying reason for the ameliorated phenotypes of these mice [104,105]. However, one has to bear in mind that overexpression of PrxIV above a certain threshold exceeds ERp44-mediated ESP retrieval [67] and therefore may result in abnormally high levels of secreted peroxidase. Overexpression studies therefore need careful evaluation, before implications on normal physiology can be conclusively deduced.

Interestingly, endogenous PrxIV is dramatically upregulated during terminal B-cell differentiation [106], a process accompanied by increased ROS levels but not by discernible hyperoxidation of the ER lumen [107,108]. PrxIV knockout splenocytes, however, develop normally and do not show a defect in antibody secretion, arguing for redundancy among different oxidant control mechanisms [106].

In contrast to the relatively mild PrxIV knockout phenotype [69], quite dramatic changes including a shortened lifespan were documented for GPx7$^{-/-}$ compared to control mice [90]. Besides induction of UPR hallmarks in different organs, these mice exhibited oxidative DNA damage and apoptosis predominantly in the kidney. Furthermore, multiple organ dysfunctions including glomerulonephritis, spleno- and cardiomegaly, fatty liver, and multiple malignant neoplasms were diagnosed [90]. Carcinogenesis and premature death were concluded to reflect systemic oxidative stress [90].

Along this line, Peng and coworkers proposed a tumor-suppressive role for GPx7 in oesophageal epithelial cells [109]. Progression from healthy tissue to premalignant Barrett's oesophagus (BO) and further to malignant oesophageal adenocarcinoma (OAC) is associated with gastro-oesophageal reflux, leading to ROS accumulation and increased oxidative DNA damage. BO/OAC neoplastic transformation is accompanied by decreased expression of GPx7 [110]. The diminished levels of GPx7 in BO and OAC tissues are due to DNA-hypermethylation within the respective promoter region. Bile acid-mediated intracellular and extracellular ROS accumulation in oesophageal epithelial cell culture was also responsive to overexpression or downregulation of GPx7 [111]. Furthermore, reconstitution of GPx7 expression suppressed growth and promoted

cellular senescence in both *in vitro* and *in vivo* OAC models [109]. Therefore, inactivation of GPx7 is a crucial step in BO/OAC formation. Despite these conclusive links between oxidative injury and GPx7 expression in vivo, it is important to emphasize that the actual source of peroxide that causes ROS accumulation in absence of GPx7 remains to be identified. A possible involvement of Ero1α [112] remains to be experimentally verified.

7.9. Conclusions and perspectives

The reaction cycle of a peroxidase is split into an oxidizing part, which uses a source of hydroperoxide, and a reductive part, which uses a dithiol substrate. As such, available data highlight a two-fold function of ER-resident peroxidases; on the one hand, they can reduce and spatially restrict local H_2O_2 or lipid hydroperoxides and on the other hand, they are net producers of disulfide bonds.

The model, which has probably generated the highest resonance, holds that ER peroxidases eliminate the obligatory and potentially harmful side product of Ero1-catalyzed disulfide-bond formation, H_2O_2, by exploiting its oxidizing power to generate a second disulfide in PDI for oxidative protein folding (Fig. 34). The fact that all ER peroxidases – PrxIV, GPx7, and GPx8 – can catalyze steps of this pathway in vitro [75,81,88,89] has led to the understanding that they basically perform the same function [65]. But do ER peroxidases really all do the same? Are their functions redundant? We believe that this is clearly not the case. For instance, the prominent phenotype of the $GPx7^{-/-}$ mouse strongly suggests that neither PrxIV nor GPx8 can broadly substitute for the loss of GPx7 [90]. This could be due to the fact that GPx7 uses unique reducing substrates (other than PDI family members) or metabolizes phospholipid hydroperoxides in the ER-facing membrane leaflet in vivo. Alternatively, tissue-specific expression levels might prohibit functional compensation between ER peroxidases. These questions are exciting subjects for future research. Clearly, it will also be interesting to learn about the phenotypes of $GPx8^{-/-}$ and GPx7/8 double knockout animals. Whether or not other human GPx isoforms like e.g. the ubiquitously secreted GPx3 [21] have an additional intracellular function in the ER is another open question.

Differences between ER peroxidases also manifest in terms of the source of hydroperoxide. There is clear proof for PrxIV reacting with Ero1-independent H_2O_2 [81,82], and unpublished data from our laboratory has demonstrated that this peroxidase does not react with Ero1α-derived H_2O_2 in cells under steady-state conditions. In this respect, one of the most urgent questions is, which is the H_2O_2 source that drives PrxIV-dependent oxidative protein folding [36,81,82]. Identification of this source will likely provide major new insights into the diffusion pathways of this metabolite.

Another area for future investigation concerns potential signaling roles of H_2O_2 in the ER lumen and beyond. For instance, the interplay of ER-resident NOX family members and peroxidases is largely unexplored. Likewise, it is currently unclear whether or not the known proapoptotic role of Ero1α during ER stress [113,114,115] is mediated by diffusion of Ero1α-derived H_2O_2 into the cytoplasm, as is suggested [7]. It is foreseeable that aquaporins will be found to play a central function in these processes at the ER membrane [8]. As every discovery arouses further interest and curiosity, we are expecting new insights and again new questions to come.

Acknowledgements

CAH is a recipient of an Ambizione grant by the Swiss National Science Foundation and TR of a Ph.D. fellowship by the Boehringer Ingelheim Fonds.

7.10. References

[1] A. Bindoli, M.P. Rigobello, Principles in redox signaling: from chemistry to functional significance, Antioxidants & redox signaling 18 (2013) 1557-1593.
[2] L. Flohe, S. Toppo, G. Cozza, F. Ursini, A comparison of thiol peroxidase mechanisms, Antioxidants & redox signaling 15 (2011) 763-780.
[3] D.I. Brown, K.K. Griendling, Nox proteins in signal transduction, Free radical biology & medicine 47 (2009) 1239-1253.
[4] T. Finkel, Signal transduction by reactive oxygen species, The Journal of cell biology 194 (2011) 7-15.
[5] R.B. Hamanaka, N.S. Chandel, Mitochondrial reactive oxygen species regulate cellular signaling and dictate biological outcomes, Trends in biochemical sciences 35 (2010) 505-513.
[6] Y. Shimizu, L.M. Hendershot, Oxidative folding: cellular strategies for dealing with the resultant equimolar production of reactive oxygen species, Antioxidants & redox signaling 11 (2009) 2317-2331.
[7] B.P. Tu, J.S. Weissman, Oxidative protein folding in eukaryotes: mechanisms and consequences, The Journal of cell biology 164 (2004) 341-346.
[8] M. Bertolotti, S. Bestetti, J.M. Garcia-Manteiga, I. Medrano-Fernandez, A. Dal Mas, M.L. Malosio, R. Sitia, Tyrosine kinase signal modulation: a matter of H2O2 membrane permeability?, Antioxidants & redox signaling (2013).
[9] G.P. Bienert, A.L. Moller, K.A. Kristiansen, A. Schulz, I.M. Moller, J.K. Schjoerring, T.P. Jahn, Specific aquaporins facilitate the diffusion of hydrogen peroxide across membranes, The Journal of biological chemistry 282 (2007) 1183-1192.
[10] Z.A. Wood, E. Schroder, J. Robin Harris, L.B. Poole, Structure, mechanism and regulation of peroxiredoxins, Trends in biochemical sciences 28 (2003) 32-40.
[11] E.M. Hanschmann, M.E. Lonn, L.D. Schutte, M. Funke, J.R. Godoy, S. Eitner, C. Hudemann, C.H. Lillig, Both thioredoxin 2 and glutaredoxin 2 contribute to the reduction of the mitochondrial 2-Cys peroxiredoxin Prx3, The Journal of biological chemistry 285 (2010) 40699-40705.
[12] E. Zito, PRDX4, an endoplasmic reticulum-localized peroxiredoxin at the crossroads between enzymatic oxidative protein folding and nonenzymatic protein oxidation, Antioxidants & redox signaling 18 (2013) 1666-1674.
[13] A.B. Fisher, Peroxiredoxin 6: a bifunctional enzyme with glutathione peroxidase and phospholipase A(2) activities, Antioxidants & redox signaling 15 (2011) 831-844.
[14] L.A. Ralat, Y. Manevich, A.B. Fisher, R.F. Colman, Direct evidence for the formation of a complex between 1-cysteine peroxiredoxin and glutathione S-transferase pi with activity changes in both enzymes, Biochemistry 45 (2006) 360-372.
[15] W.T. Lowther, A.C. Haynes, Reduction of cysteine sulfinic acid in eukaryotic, typical 2-Cys peroxiredoxins by sulfiredoxin, Antioxidants & redox signaling 15 (2011) 99-109.
[16] S.G. Rhee, H.A. Woo, Multiple functions of peroxiredoxins: peroxidases, sensors and regulators of the intracellular messenger H(2)O(2), and protein chaperones, Antioxidants & redox signaling 15 (2011) 781-794.
[17] S.G. Rhee, H.A. Woo, I.S. Kil, S.H. Bae, Peroxiredoxin functions as a peroxidase and a regulator and sensor of local peroxides, The Journal of biological chemistry 287 (2012) 4403-4410.
[18] W. Jeong, S.H. Bae, M.B. Toledano, S.G. Rhee, Role of sulfiredoxin as a regulator of peroxiredoxin function and regulation of its expression, Free radical biology & medicine 53 (2012) 447-456.
[19] Y.H. Noh, J.Y. Baek, W. Jeong, S.G. Rhee, T.S. Chang, Sulfiredoxin Translocation into Mitochondria Plays a Crucial Role in Reducing Hyperoxidized Peroxiredoxin III, The Journal of biological chemistry 284 (2009) 8470-8477.
[20] S.C. Tosatto, V. Bosello, F. Fogolari, P. Mauri, A. Roveri, S. Toppo, L. Flohe, F. Ursini, M. Maiorino, The catalytic site of glutathione peroxidases, Antioxidants & redox signaling 10 (2008) 1515-1526.
[21] R. Brigelius-Flohe, M. Maiorino, Glutathione peroxidases, Biochimica et biophysica acta 1830 (2013) 3289-3303.
[22] M. Bjornstedt, J. Xue, W. Huang, B. Akesson, A. Holmgren, The thioredoxin and glutaredoxin systems are efficient electron donors to human plasma glutathione peroxidase, The Journal of biological chemistry 269 (1994) 29382-29384.
[23] C. Godeas, F. Tramer, F. Micali, A. Roveri, M. Maiorino, C. Nisii, G. Sandri, E. Panfili, Phospholipid hydroperoxide glutathione peroxidase (PHGPx) in rat testis nuclei is bound to chromatin, Biochemical and molecular medicine 59 (1996) 118-124.

[24] M. Maiorino, A. Roveri, L. Benazzi, V. Bosello, P. Mauri, S. Toppo, S.C. Tosatto, F. Ursini, Functional interaction of phospholipid hydroperoxide glutathione peroxidase with sperm mitochondrion-associated cysteine-rich protein discloses the adjacent cysteine motif as a new substrate of the selenoperoxidase, The Journal of biological chemistry 280 (2005) 38395-38402.
[25] F. Ursini, S. Heim, M. Kiess, M. Maiorino, A. Roveri, J. Wissing, L. Flohe, Dual function of the selenoprotein PHGPx during sperm maturation, Science 285 (1999) 1393-1396.
[26] M. Maiorino, F. Ursini, V. Bosello, S. Toppo, S.C. Tosatto, P. Mauri, K. Becker, A. Roveri, C. Bulato, L. Benazzi, A. De Palma, L. Flohe, The thioredoxin specificity of Drosophila GPx: a paradigm for a peroxiredoxin-like mechanism of many glutathione peroxidases, Journal of molecular biology 365 (2007) 1033-1046.
[27] S. Toppo, S. Vanin, V. Bosello, S.C. Tosatto, Evolutionary and structural insights into the multifaceted glutathione peroxidase (Gpx) superfamily, Antioxidants & redox signaling 10 (2008) 1501-1514.
[28] M. Schuldiner, B. Schwappach, From rags to riches - The history of the endoplasmic reticulum, Biochimica et biophysica acta (2013).
[29] N.J. Bulleid, L. Ellgaard, Multiple ways to make disulfides, Trends in biochemical sciences 36 (2011) 485-492.
[30] E. Gross, C.S. Sevier, N. Heldman, E. Vitu, M. Bentzur, C.A. Kaiser, C. Thorpe, D. Fass, Generating disulfides enzymatically: reaction products and electron acceptors of the endoplasmic reticulum thiol oxidase Ero1p, Proceedings of the National Academy of Sciences of the United States of America 103 (2006) 299-304.
[31] K. Chen, M.T. Kirber, H. Xiao, Y. Yang, J.F. Keaney, Jr., Regulation of ROS signal transduction by NADPH oxidase 4 localization, The Journal of cell biology 181 (2008) 1129-1139.
[32] E. Pedruzzi, C. Guichard, V. Ollivier, F. Driss, M. Fay, C. Prunet, J.C. Marie, C. Pouzet, M. Samadi, C. Elbim, Y. O'Dowd, M. Bens, A. Vandewalle, M.A. Gougerot-Pocidalo, G. Lizard, E. Ogier-Denis, NAD(P)H oxidase Nox-4 mediates 7-ketocholesterol-induced endoplasmic reticulum stress and apoptosis in human aortic smooth muscle cells, Molecular and cellular biology 24 (2004) 10703-10717.
[33] R.F. Wu, Z. Ma, Z. Liu, L.S. Terada, Nox4-derived H2O2 mediates endoplasmic reticulum signaling through local Ras activation, Molecular and cellular biology 30 (2010) 3553-3568.
[34] V.K. Kodali, C. Thorpe, Oxidative protein folding and the Quiescin-sulfhydryl oxidase family of flavoproteins, Antioxidants & redox signaling 13 (2010) 1217-1230.
[35] T. Ilani, A. Alon, I. Grossman, B. Horowitz, E. Kartvelishvily, S.R. Cohen, D. Fass, A Secreted Disulfide Catalyst Controls Extracellular Matrix Composition and Function, Science (2013).
[36] L.A. Rutkevich, D.B. Williams, Vitamin K epoxide reductase contributes to protein disulfide formation and redox homeostasis within the endoplasmic reticulum, Molecular biology of the cell 23 (2012) 2017-2027.
[37] C.S. Sevier, Erv2 and quiescin sulfhydryl oxidases: Erv-domain enzymes associated with the secretory pathway, Antioxidants & redox signaling 16 (2012) 800-808.
[38] Y. Yang, Y. Song, J. Loscalzo, Regulation of the protein disulfide proteome by mitochondria in mammalian cells, Proceedings of the National Academy of Sciences of the United States of America 104 (2007) 10813-10817.
[39] R.S. Balaban, S. Nemoto, T. Finkel, Mitochondria, oxidants, and aging, Cell 120 (2005) 483-495.
[40] M. Giorgio, E. Migliaccio, F. Orsini, D. Paolucci, M. Moroni, C. Contursi, G. Pelliccia, L. Luzi, S. Minucci, M. Marcaccio, P. Pinton, R. Rizzuto, P. Bernardi, F. Paolucci, P.G. Pelicci, Electron transfer between cytochrome c and p66Shc generates reactive oxygen species that trigger mitochondrial apoptosis, Cell 122 (2005) 221-233.
[41] A.A. Rowland, G.K. Voeltz, Endoplasmic reticulum-mitochondria contacts: function of the junction, Nature reviews. Molecular cell biology 13 (2012) 607-625.
[42] K. Araki, K. Inaba, Structure, mechanism, and evolution of Ero1 family enzymes, Antioxidants & redox signaling 16 (2012) 790-799.
[43] A.J. Meyer, T.P. Dick, Fluorescent protein-based redox probes, Antioxidants & redox signaling 13 (2010) 621-650.
[44] B. Enyedi, P. Varnai, M. Geiszt, Redox state of the endoplasmic reticulum is controlled by Ero1L-alpha and intraluminal calcium, Antioxidants & redox signaling 13 (2010) 721-729.
[45] M. Malinouski, Y. Zhou, V.V. Belousov, D.L. Hatfield, V.N. Gladyshev, Hydrogen peroxide probes directed to different cellular compartments, PloS one 6 (2011) e14564.
[46] I. Mehmeti, S. Lortz, S. Lenzen, The H2O2-sensitive HyPer protein targeted to the endoplasmic reticulum as a mirror of the oxidizing thiol-disulfide milieu, Free radical biology & medicine 53 (2012) 1451-1458.
[47] D.R. Gough, T.G. Cotter, Hydrogen peroxide: a Jekyll and Hyde signalling molecule, Cell death & disease 2 (2011) e213.

[48] G. Groeger, C. Quiney, T.G. Cotter, Hydrogen peroxide as a cell-survival signaling molecule, Antioxidants & redox signaling 11 (2009) 2655-2671.
[49] N.M. Mishina, P.A. Tyurin-Kuzmin, K.N. Markvicheva, A.V. Vorotnikov, V.A. Tkachuk, V. Laketa, C. Schultz, S. Lukyanov, V.V. Belousov, Does cellular hydrogen peroxide diffuse or act locally?, Antioxidants & redox signaling 14 (2011) 1-7.
[50] M.B. Toledano, A.G. Planson, A. Delaunay-Moisan, Reining in H(2)O(2) for safe signaling, Cell 140 (2010) 454-456.
[51] V.V. Belousov, A.F. Fradkov, K.A. Lukyanov, D.B. Staroverov, K.S. Shakhbazov, A.V. Terskikh, S. Lukyanov, Genetically encoded fluorescent indicator for intracellular hydrogen peroxide, Nature methods 3 (2006) 281-286.
[52] J. Birk, T. Ramming, A. Odermatt, C. Appenzeller-Herzog, Green fluorescent protein-based monitoring of endoplasmic reticulum redox poise, Frontiers in genetics 4 (2013) 108.
[53] C.C. Winterbourn, Reconciling the chemistry and biology of reactive oxygen species, Nature chemical biology 4 (2008) 278-286.
[54] Y.S. Bae, S.W. Kang, M.S. Seo, I.C. Baines, E. Tekle, P.B. Chock, S.G. Rhee, Epidermal growth factor (EGF)-induced generation of hydrogen peroxide. Role in EGF receptor-mediated tyrosine phosphorylation, The Journal of biological chemistry 272 (1997) 217-221.
[55] M. Sundaresan, Z.X. Yu, V.J. Ferrans, K. Irani, T. Finkel, Requirement for generation of H2O2 for platelet-derived growth factor signal transduction, Science 270 (1995) 296-299.
[56] K. Mahadev, A. Zilbering, L. Zhu, B.J. Goldstein, Insulin-stimulated hydrogen peroxide reversibly inhibits protein-tyrosine phosphatase 1b in vivo and enhances the early insulin action cascade, The Journal of biological chemistry 276 (2001) 21938-21942.
[57] T.C. Meng, T. Fukada, N.K. Tonks, Reversible oxidation and inactivation of protein tyrosine phosphatases in vivo, Molecular cell 9 (2002) 387-399.
[58] M. Reth, Hydrogen peroxide as second messenger in lymphocyte activation, Nature immunology 3 (2002) 1129-1134.
[59] N.K. Tonks, Protein tyrosine phosphatases: from genes, to function, to disease, Nature reviews. Molecular cell biology 7 (2006) 833-846.
[60] H.A. Woo, S.H. Yim, D.H. Shin, D. Kang, D.Y. Yu, S.G. Rhee, Inactivation of peroxiredoxin I by phosphorylation allows localized H(2)O(2) accumulation for cell signaling, Cell 140 (2010) 517-528.
[61] F.G. Haj, P.J. Verveer, A. Squire, B.G. Neel, P.I. Bastiaens, Imaging sites of receptor dephosphorylation by PTP1B on the surface of the endoplasmic reticulum, Science 295 (2002) 1708-1711.
[62] K. Palande, O. Roovers, J. Gits, C. Verwijmeren, Y. Iuchi, J. Fujii, B.G. Neel, R. Karisch, J. Tavernier, I.P. Touw, Peroxiredoxin-controlled G-CSF signalling at the endoplasmic reticulum-early endosome interface, Journal of cell science 124 (2011) 3695-3705.
[63] C. Hetz, The unfolded protein response: controlling cell fate decisions under ER stress and beyond, Nature reviews. Molecular cell biology 13 (2012) 89-102.
[64] C. He, H. Zhu, W. Zhang, I. Okon, Q. Wang, H. Li, Y.Z. Le, Z. Xie, 7-Ketocholesterol Induces Autophagy in Vascular Smooth Muscle Cells through Nox4 and Atg4B, The American journal of pathology (2013).
[65] T. Kakihana, K. Nagata, R. Sitia, Peroxides and peroxidases in the endoplasmic reticulum: integrating redox homeostasis and oxidative folding, Antioxidants & redox signaling 16 (2012) 763-771.
[66] T.J. Tavender, A.M. Sheppard, N.J. Bulleid, Peroxiredoxin IV is an endoplasmic reticulum-localized enzyme forming oligomeric complexes in human cells, The Biochemical journal 411 (2008) 191-199.
[67] T. Kakihana, K. Araki, S. Vavassori, S.I. Iemura, M. Cortini, C. Fagioli, T. Natsume, R. Sitia, K. Nagata, Dynamic regulation of Ero1alpha and Prx4 localization in the secretory pathway, The Journal of biological chemistry in press (2013) doi: 10.1074/jbc.M1113.467845.
[68] V. Haridas, J. Ni, A. Meager, J. Su, G.L. Yu, Y. Zhai, H. Kyaw, K.T. Akama, J. Hu, L.J. Van Eldik, B.B. Aggarwal, TRANK, a novel cytokine that activates NF-kappa B and c-Jun N-terminal kinase, Journal of immunology 161 (1998) 1-6.
[69] Y. Iuchi, F. Okada, S. Tsunoda, N. Kibe, N. Shirasawa, M. Ikawa, M. Okabe, Y. Ikeda, J. Fujii, Peroxiredoxin 4 knockout results in elevated spermatogenic cell death via oxidative stress, The Biochemical journal 419 (2009) 149-158.
[70] D.Y. Jin, H.Z. Chae, S.G. Rhee, K.T. Jeang, Regulatory role for a novel human thioredoxin peroxidase in NF-kappaB activation, The Journal of biological chemistry 272 (1997) 30952-30961.
[71] A. Matsumoto, A. Okado, T. Fujii, J. Fujii, M. Egashira, N. Niikawa, N. Taniguchi, Cloning of the peroxiredoxin gene family in rats and characterization of the fourth member, FEBS letters 443 (1999) 246-250.

[72] A. Okado-Matsumoto, A. Matsumoto, J. Fujii, N. Taniguchi, Peroxiredoxin IV is a secretable protein with heparin-binding properties under reduced conditions, Journal of biochemistry 127 (2000) 493-501.
[73] S. Barranco-Medina, J.J. Lazaro, K.J. Dietz, The oligomeric conformation of peroxiredoxins links redox state to function, FEBS letters 583 (2009) 1809-1816.
[74] Z. Cao, T.J. Tavender, A.W. Roszak, R.J. Cogdell, N.J. Bulleid, Crystal structure of reduced and of oxidized peroxiredoxin IV enzyme reveals a stable oxidized decamer and a non-disulfide-bonded intermediate in the catalytic cycle, The Journal of biological chemistry 286 (2011) 42257-42266.
[75] T.J. Tavender, J.J. Springate, N.J. Bulleid, Recycling of peroxiredoxin IV provides a novel pathway for disulphide formation in the endoplasmic reticulum, The EMBO journal 29 (2010) 4185-4197.
[76] X. Wang, L. Wang, F. Sun, C.C. Wang, Structural insights into the peroxidase activity and inactivation of human peroxiredoxin 4, The Biochemical journal 441 (2012) 113-118.
[77] Y. Ikeda, R. Ito, H. Ihara, T. Okada, J. Fujii, Expression of N-terminally truncated forms of rat peroxiredoxin-4 in insect cells, Protein expression and purification 72 (2010) 1-7.
[78] T. Ramming, C. Appenzeller-Herzog, The physiological functions of mammalian endoplasmic oxidoreductin 1: on disulfides and more, Antioxidants & redox signaling 16 (2012) 1109-1118.
[79] D. Fass, Hunting for alternative disulfide bond formation pathways: endoplasmic reticulum janitor turns professor and teaches a lesson, Molecular cell 40 (2010) 685-686.
[80] T.J. Tavender, N.J. Bulleid, Peroxiredoxin IV protects cells from oxidative stress by removing H2O2 produced during disulphide formation, Journal of cell science 123 (2010) 2672-2679.
[81] E. Zito, E.P. Melo, Y. Yang, A. Wahlander, T.A. Neubert, D. Ron, Oxidative protein folding by an endoplasmic reticulum-localized peroxiredoxin, Molecular cell 40 (2010) 787-797.
[82] E. Zito, H.G. Hansen, G.S. Yeo, J. Fujii, D. Ron, Endoplasmic reticulum thiol oxidase deficiency leads to ascorbic acid depletion and noncanonical scurvy in mice, Molecular cell 48 (2012) 39-51.
[83] Y. Sato, R. Kojima, M. Okumura, M. Hagiwara, S. Masui, K. Maegawa, M. Saiki, T. Horibe, M. Suzuki, K. Inaba, Synergistic cooperation of PDI family members in peroxiredoxin 4-driven oxidative protein folding, Scientific reports 3 (2013) 2456.
[84] I. Raykhel, H. Alanen, K. Salo, J. Jurvansuu, V.D. Nguyen, M. Latva-Ranta, L. Ruddock, A molecular specificity code for the three mammalian KDEL receptors, The Journal of cell biology 179 (2007) 1193-1204.
[85] A. Spang, Retrograde traffic from the Golgi to the endoplasmic reticulum, Cold Spring Harbor perspectives in biology 5 (2013).
[86] V. Bosello-Travain, M. Conrad, G. Cozza, A. Negro, S. Quartesan, M. Rossetto, A. Roveri, S. Toppo, F. Ursini, M. Zaccarin, M. Maiorino, Protein disulfide isomerase and glutathione are alternative substrates in the one Cys catalytic cycle of glutathione peroxidase 7, Biochimica et biophysica acta 1830 (2013) 3846-3857.
[87] H. Imai, Y. Nakagawa, Biological significance of phospholipid hydroperoxide glutathione peroxidase (PHGPx, GPx4) in mammalian cells, Free radical biology & medicine 34 (2003) 145-169.
[88] V.D. Nguyen, M.J. Saaranen, A.R. Karala, A.K. Lappi, L. Wang, I.B. Raykhel, H.I. Alanen, K.E. Salo, C.C. Wang, L.W. Ruddock, Two endoplasmic reticulum PDI peroxidases increase the efficiency of the use of peroxide during disulfide bond formation, Journal of molecular biology 406 (2011) 503-515.
[89] L. Wang, L. Zhang, Y. Niu, R. Sitia, C.C. Wang, Glutathione peroxidase 7 utilizes hydrogen peroxide generated by Ero1alpha to promote oxidative protein folding, Antioxidants & redox signaling doi: 10.1089/ars.2013.5236 (2013).
[90] P.C. Wei, Y.H. Hsieh, M.I. Su, X. Jiang, P.H. Hsu, W.T. Lo, J.Y. Weng, Y.M. Jeng, J.M. Wang, P.L. Chen, Y.C. Chang, K.F. Lee, M.D. Tsai, J.Y. Shew, W.H. Lee, Loss of the oxidative stress sensor NPGPx compromises GRP78 chaperone activity and induces systemic disease, Molecular cell 48 (2012) 747-759.
[91] M. Gutscher, M.C. Sobotta, G.H. Wabnitz, S. Ballikaya, A.J. Meyer, Y. Samstag, T.P. Dick, Proximity-based protein thiol oxidation by H2O2-scavenging peroxidases, The Journal of biological chemistry 284 (2009) 31532-31540.
[92] A.K. Lappi, L.W. Ruddock, Reexamination of the role of interplay between glutathione and protein disulfide isomerase, Journal of molecular biology 409 (2011) 238-249.
[93] P.C. Wei, W.T. Lo, M.I. Su, J.Y. Shew, W.H. Lee, Non-targeting siRNA induces NPGPx expression to cooperate with exoribonuclease XRN2 for releasing the stress, Nucleic acids research 40 (2012) 323-332.
[94] P.C. Wei, Z.F. Wang, W.T. Lo, M.I. Su, J.Y. Shew, T.C. Chang, W.H. Lee, A cis-element with mixed G-quadruplex structure of NPGPx promoter is essential for nucleolin-mediated transactivation on non-targeting siRNA stress, Nucleic acids research 41 (2013) 1533-1543.

[95] S. Li, L. Liu, X. Zhuang, Y. Yu, X. Liu, X. Cui, L. Ji, Z. Pan, X. Cao, B. Mo, F. Zhang, N. Raikhel, L. Jiang, X. Chen, MicroRNAs inhibit the translation of target mRNAs on the endoplasmic reticulum in Arabidopsis, Cell 153 (2013) 562-574.
[96] L. Stalder, W. Heusermann, L. Sokol, D. Trojer, J. Wirz, J. Hean, A. Fritzsche, F. Aeschimann, V. Pfanzagl, P. Basselet, J. Weiler, M. Hintersteiner, D.V. Morrissey, N.C. Meisner-Kober, The rough endoplasmatic reticulum is a central nucleation site of siRNA-mediated RNA silencing, The EMBO journal 32 (2013) 1115-1127.
[97] A.R. Frand, C.A. Kaiser, Ero1p oxidizes protein disulfide isomerase in a pathway for disulfide bond formation in the endoplasmic reticulum, Molecular cell 4 (1999) 469-477.
[98] B.P. Tu, S.C. Ho-Schleyer, K.J. Travers, J.S. Weissman, Biochemical basis of oxidative protein folding in the endoplasmic reticulum, Science 290 (2000) 1571-1574.
[99] C. Appenzeller-Herzog, Glutathione- and non-glutathione-based oxidant control in the endoplasmic reticulum, Journal of cell science 124 (2011) 847-855.
[100] F. Hatahet, L.W. Ruddock, Substrate recognition by the protein disulfide isomerases, The FEBS journal 274 (2007) 5223-5234.
[101] C. Appenzeller-Herzog, J. Riemer, B. Christensen, E.S. Sorensen, L. Ellgaard, A novel disulphide switch mechanism in Ero1alpha balances ER oxidation in human cells, The EMBO journal 27 (2008) 2977-2987.
[102] S.N. Radyuk, V.I. Klichko, K. Michalak, W.C. Orr, The effect of peroxiredoxin 4 on fly physiology is a complex interplay of antioxidant and signaling functions, FASEB journal : official publication of the Federation of American Societies for Experimental Biology 27 (2013) 1426-1438.
[103] X. Guo, S. Yamada, A. Tanimoto, Y. Ding, K.Y. Wang, S. Shimajiri, Y. Murata, S. Kimura, T. Tasaki, A. Nabeshima, T. Watanabe, K. Kohno, Y. Sasaguri, Overexpression of peroxiredoxin 4 attenuates atherosclerosis in apolipoprotein E knockout mice, Antioxidants & redox signaling 17 (2012) 1362-1375.
[104] Y. Ding, S. Yamada, K.Y. Wang, S. Shimajiri, X. Guo, A. Tanimoto, Y. Murata, S. Kitajima, T. Watanabe, H. Izumi, K. Kohno, Y. Sasaguri, Overexpression of peroxiredoxin 4 protects against high-dose streptozotocin-induced diabetes by suppressing oxidative stress and cytokines in transgenic mice, Antioxidants & redox signaling 13 (2010) 1477-1490.
[105] A. Nabeshima, S. Yamada, X. Guo, A. Tanimoto, K.Y. Wang, S. Shimajiri, S. Kimura, T. Tasaki, H. Noguchi, S. Kitada, T. Watanabe, J. Fujii, K. Kohno, Y. Sasaguri, Peroxiredoxin 4 Protects Against Nonalcoholic Steatohepatitis and Type 2 Diabetes in a Nongenetic Mouse Model, Antioxidants & redox signaling (2013).
[106] M. Bertolotti, S.H. Yim, J.M. Garcia-Manteiga, S. Masciarelli, Y.J. Kim, M.H. Kang, Y. Iuchi, J. Fujii, R. Vene, A. Rubartelli, S.G. Rhee, R. Sitia, B- to plasma-cell terminal differentiation entails oxidative stress and profound reshaping of the antioxidant responses, Antioxidants & redox signaling 13 (2010) 1133-1144.
[107] R. Vene, L. Delfino, P. Castellani, E. Balza, M. Bertolotti, R. Sitia, A. Rubartelli, Redox remodeling allows and controls B-cell activation and differentiation, Antioxidants & redox signaling 13 (2010) 1145-1155.
[108] R.E. Hansen, M. Otsu, I. Braakman, J.R. Winther, Quantifying changes in the cellular thiol-disulfide status during differentiation of B cells into antibody-secreting plasma cells, International journal of cell biology this issue (2013).
[109] D. Peng, T. Hu, M. Soutto, A. Belkhiri, A. Zaika, W. El-Rifai, Glutathione peroxidase 7 has potential tumour suppressor functions that are silenced by location-specific methylation in oesophageal adenocarcinoma, Gut (2013).
[110] D.F. Peng, M. Razvi, H. Chen, K. Washington, A. Roessner, R. Schneider-Stock, W. El-Rifai, DNA hypermethylation regulates the expression of members of the Mu-class glutathione S-transferases and glutathione peroxidases in Barrett's adenocarcinoma, Gut 58 (2009) 5-15.
[111] D. Peng, A. Belkhiri, T. Hu, R. Chaturvedi, M. Asim, K.T. Wilson, A. Zaika, W. El-Rifai, Glutathione peroxidase 7 protects against oxidative DNA damage in oesophageal cells, Gut 61 (2012) 1250-1260.
[112] D.M. Battle, S.D. Gunasekara, G.R. Watson, E.M. Ahmed, C.G. Saysell, N. Altaf, A.L. Sanusi, P.C. Munipalle, D. Scoones, J. Walker, Y. Viswanath, A.M. Benham, Expression of the endoplasmic reticulum oxidoreductase ero1alpha in gastro-intestinal cancer reveals a link between homocysteine and oxidative protein folding, Antioxidants & redox signaling 19 (2013) 24-35.
[113] J. Han, S.H. Back, J. Hur, Y.H. Lin, R. Gildersleeve, J. Shan, C.L. Yuan, D. Krokowski, S. Wang, M. Hatzoglou, M.S. Kilberg, M.A. Sartor, R.J. Kaufman, ER-stress-induced transcriptional regulation increases protein synthesis leading to cell death, Nature cell biology 15 (2013) 481-490.
[114] G. Li, M. Mongillo, K.T. Chin, H. Harding, D. Ron, A.R. Marks, I. Tabas, Role of ERO1-alpha-mediated stimulation of inositol 1,4,5-triphosphate receptor activity in endoplasmic reticulum stress-induced apoptosis, The Journal of cell biology 186 (2009) 783-792.

[115] S.J. Marciniak, C.Y. Yun, S. Oyadomari, I. Novoa, Y. Zhang, R. Jungreis, K. Nagata, H.P. Harding, D. Ron, CHOP induces death by promoting protein synthesis and oxidation in the stressed endoplasmic reticulum, Genes & development 18 (2004) 3066-3077.